

Scattering and Gravitational Effective Field Theory

Thesis by
Nabha Shah

In Partial Fulfillment of the Requirements for the
Degree of
Doctor of Philosophy

The logo for the California Institute of Technology (Caltech), featuring the word "Caltech" in a bold, orange, sans-serif font.

CALIFORNIA INSTITUTE OF TECHNOLOGY
Pasadena, California

2024
Defended May 29, 2024

© 2024

Nabha Shah

ORCID: 0000-0003-0458-7163

All rights reserved except where otherwise noted

ACKNOWLEDGEMENTS

I would like to thank my advisor, Clifford Cheung, for his invaluable guidance and for sharing his infectious excitement for physics, my collaborators on the projects included in this thesis, Cliff, Jordan Wilson-Gerow, James Mangan, Julio Parra-Martinez, Ira Rothstein, Mikhail Solon, whose understanding of physics has helped shape my own, and Sudarshan Ananth for setting me on this path.

I would also like to thank my fellow students, Maria Derda, Joonhwi Kim, James, Zander Moss, who have not just made being part of this group academically engaging but also lively and entertaining, and my officemates, Ashmeet Singh, for welcoming me to the floor and making me feel at home here, and Mrunmay Jagadale, for always lending an ear and for his sage insights. I am grateful to Jordan, Andreas Helset, Julio, Allic Sivaramakrishnan for providing glimpses into and counsel regarding life as a postdoc, to Mark Wise for our conversations and his advice, to my committee members, Zvi Bern, David Simmons-Duffin, Mark, and to Carol Silberstein for all her help through the years.

I would like to acknowledge the support I have received from the Dominic Orr Graduate Fellowship in Physics, the Kip Thorne Graduate Fellowship, the Walter Burke Institute for Theoretical Physics, and the Department of Energy (Grant No. DE-SC0011632).

My time at Caltech has allowed me to meet some wonderful people that I feel privileged to add to all the lifelong friends and family whose love and support have been important anchors in this journey.

ABSTRACT

Advances in the methodologies developed in quantum field theory and in the scattering amplitudes program have led to their application to questions pertaining to the classical physics of gravitationally interacting binary systems. The perturbative and relativistic nature of the quantum field theoretic setup is perfectly suited for obtaining results in an expansion in the gravitational constant, also known as the post-Minkowskian (PM) expansion. However, there are several practical scenarios where the gravitational waves produced by the inspiral or interaction of two massive bodies arise from dynamics in the strong field regime and the PM expansion breaks down. Extreme mass ratio inspirals, where a lighter body interacts with a much heavier black hole, are examples of such systems.

In contrast, classical solutions, such as the Schwarzschild metric, and the geodesic trajectories of test bodies traversing in these nontrivial backgrounds encode information to all orders in the gravitational constant. In fact, these solutions can be viewed as the summation of certain infinite sets of Feynman diagrams from the perspective of point particle effective field theory (EFT). Alternatively, metrics and related geodesic trajectories can be seen as performing enormous simplifications of the tensor structures arising in these equivalent sets of Feynman integrals. We describe how the all order in PM information present in classical solutions can be utilized to simplify PM calculations in point particle EFT and set up a systematic framework for studying the classical dynamics of binary systems as an expansion in their mass ratio.

We also delve into questions about the origin and scope of validity of color-kinematics duality and the double copy relation, which can be used to generate amplitudes of one theory from another. For example, graviton amplitudes can be obtained from gluon amplitudes. Unveiling the underlying structure that gives rise to these relations would not only deepen our understanding of the properties of these theories but could also serve in streamlining their application to computations of practical interest such as those showing up in the study of the gravitational two-body problem using field theory techniques. Specifically, we analyze a toy system in two dimensions where we find a Lagrangian-level manifestation of the duality in a classical equivalent of the nonlinear sigma model. We unpack the implications of an off-shell formulation of the color-kinematics duality and double copy in order to understand the possible wider implications for these relations in other theories.

PUBLISHED CONTENT AND CONTRIBUTIONS

Chapters in this thesis reproduce results and content from the publications listed below.

- [1] Clifford Cheung, Nabha Shah, and Mikhail P. Solon. Mining the geodesic equation for scattering data. *Phys. Rev. D*, 103:024030, Jan 2021. doi: 10.1103/PhysRevD.103.024030.
URL <https://link.aps.org/doi/10.1103/PhysRevD.103.024030>.
N.S. contributed to the calculation of results in the paper and the preparation of the manuscript.
- [2] Clifford Cheung, James Mangan, Julio Parra-Martinez, and Nabha Shah. Nonperturbative double copy in flatland. *Phys. Rev. Lett.*, 129:221602, Nov 2022. doi: 10.1103/PhysRevLett.129.221602.
URL <https://link.aps.org/doi/10.1103/PhysRevLett.129.221602>.
N.S. contributed to the results in the paper and helped in the preparation of the manuscript.
- [3] Clifford Cheung, Julio Parra-Martinez, Ira Z. Rothstein, Nabha Shah, and Jordan Wilson-Gerow. Effective field theory for extreme mass ratio binaries. *Phys. Rev. Lett.*, 132:091402, Feb 2024. doi: 10.1103/PhysRevLett.132.091402.
URL <https://link.aps.org/doi/10.1103/PhysRevLett.132.091402>.
N.S. contributed towards the results in the paper.
- [4] Clifford Cheung, Julio Parra-Martinez, Ira Z. Rothstein, Nabha Shah, and Jordan Wilson-Gerow. Backreacting on the background field method. (*in preparation*).
N.S. contributed towards the results in the paper and the preparation of the manuscript.

TABLE OF CONTENTS

Acknowledgements	iii
Abstract	iv
Published Content and Contributions	v
Table of Contents	vi
List of Illustrations	viii
List of Tables	xi
Chapter I: Introduction	1
Chapter II: Mining the Geodesic Equation for Scattering Data	9
2.1 Introduction	9
2.2 Test-Particle Dynamics	11
2.3 Leading Order in	15
2.4 All Orders in	27
2.5 Conclusions	34
Chapter III: Effective Field Theory for Extreme Mass Ratio Binaries	36
3.1 Introduction	36
3.2 Basic Setup	38
3.3 Background Field Theory as Resummation	39
3.4 Black Hole Recoil	41
3.5 Self-Energy and Regularization	42
3.6 Gravitational Scattering with Additional Fields	43
3.7 Calculation of the Radial Action	44
3.8 Conclusions	45
Chapter IV: Backreacting on the Background Field Method	47
4.1 Introduction	47
4.2 Electromagnetism	50
4.3 General Relativity	75
4.4 Conclusions	99
Chapter V: Color-Kinematics Duality and the Double Copy in Two Dimensions	101
5.1 Introduction	101
5.2 Color Algebra	103
5.3 Kinematic Algebra	103
5.4 Lagrangian Double Copy	104
5.5 Masses and Higher-Dimension Operators	107
5.6 Fundamental BCJ Relation	107
5.7 Integrable Models	108
5.8 Nonperturbative Solutions	110
5.9 Generalization Using the Moyal Algebra	113
5.10 Future Directions	114
Appendix A: Derivation of Eq. (2.19)	115

Appendix B: Electric and Magnetic Weyl Tensors	117
Appendix C: Feynman Rules	118
Appendix D: Time-Domain Trajectories	121
D.1 Electromagnetism	121
D.2 Gravity	128
Appendix E: Probe Radial Actions	132
E.1 On-shell Action and Radial Action	132
E.2 General Perturbative Radial Action Integral	133
E.3 Electromagnetism	134
E.4 Gravity	135
Bibliography	137

LIST OF ILLUSTRATIONS

<i>Number</i>	<i>Page</i>
1.1 A depiction of the bound system of two inspiraling black holes. . . .	1
1.2 The classical dynamics the gravitational two-body problem is studied using a scattering problem in effective field theory.	2
1.3 Examples of diagrams contributing to the quantum scattering of interacting masses. The diagram on the left, which involves a graviton-mediated long range force, will contribute classically but the diagram on the right will not.	2
1.4 The Schwarzschild metric can be viewed as a compact expression for the sum of an infinite class of flat space Feynman diagrams that induce corrections to the Minkowski metric. The circles represent a static or inertial massive scalar source and the squiggly lines denote flat space graviton propagators.	4
1.5 The propagator of a massive scalar particle in curved space is composed of the flat space propagator and an infinite set of tree-level Feynman diagrams where gravitons sourced by a static, heavy point particle self-interact and eventually land on the propagating particle.	5
2.1 At leading PM order, tidal corrections to the scattering amplitude arise from fan diagrams. For an operator composed of ϵ curvature tensors, this contribution corresponds to an $\epsilon^2 = \epsilon^0$ -loop diagram. Thick and thin lines denote matter and graviton lines while the black dots denote tidal operator insertions.	15
2.2 To all orders in PM, contributions to the scattering amplitude of a tidally distorted test particle are generated by fan diagrams. Shown here are examples at one-, two-, and three-loop orders.	28
3.1 Background-field Feynman diagrams contributing to the 1SF radial action. The circles denote the light geodesic source (!) and the heavy recoil operator (). The double lines denote background field propagators for the graviton (wavy) and the scalar or vector fields (straight).	43

4.1	The series expansion of the Schwarzschild metric, δ_{ab} , in the gravitational constant, κ , corresponds to a perturbative computation, in flat space, of the graviton one-point function in the presence of a massive scalar point particle source.	48
4.2	Feynman rules for computing the 1SF electromagnetic radial action.	67
4.3	Diagram encoding the 1SF electromagnetic on-shell radial action in the potential region. The L.H.S. is composed of the source probe trajectory, photon propagators, and the 1SF electromagnetic recoil operator and the R.H.S. depicts contributions from the diagram at 2PL and 3PL orders.	71
4.4	The curved space graviton propagator can be thought of as a sum of the flat space propagator and corrections involving interactions with the background. These interactions, depicted as insertions on the flat space propagator, are organized in a PM expansion of the background gravitational field.	85
4.5	Feynman rules for the flat space graviton propagator, recoil vertex, and graviton source that are required to compute the 1SF gravitational radial action.	87
4.6	Diagrams showing up at 1SF when computing the gravitational effective action are shown on the left and the contributions relevant to 3PM are depicted to the right of the arrows. In actuality, the diagram with a 2PM metric insertion does not contribute at this order (see footnote 4).	95
4.7	Flat space diagram topologies that contribute to the 1SF action to 3PM order. The dotted straight lines depict static massive sources and the solid straight lines represent matter propagators.	96
4.8	Diagrams necessary for computing the 2SF gravitational radial action to 3PM order. The first diagram involves cubic graviton vertices in a Schwarzschild background, the second makes use of the 2SF recoil operator, and the third diagram uses the 1SF recoil operator in combination with the cubic graviton vertex.	96

- 4.9 The contribution to the 1SF radial action from a field which couples to the light body but not the heavy body, so there is no recoil operator insertion. The doubled line is the propagator of this additional field (scalar or vector) in the Schwarzschild background. Its nontrivial contributions to 3PM order when expanded in terms of flat space diagrams are shown on the right. 97
- 5.1 We numerically solve the SG equations of motion in Eq. (5.19) for a pair of colliding Gaussian wave packets. The discrete Fourier transform of this solution, defined in Eq. (5.36), is inserted into Eq. (5.37) to obtain a putative matrix-valued solution of ZM theory. The above density plots characterize this ZM configuration, where the horizontal (vertical) axes denote space (time) and lighter (darker) colors denote positive (negative) field values. Each panel depicts a different matrix-valued, spacetime-dependent operator, $\mathcal{O} = q - q_{cc} - q_{GG}$, etc., where the subscripts denote derivatives. Each operator is visualized by plotting its projection onto a single component, $\text{tr}^1 \mathcal{O} Z_0^0$, where $Z_0 = \sum_{\alpha} Z_{\alpha}$. Each term in the ZM equations of motion in Eq. (5.13) is nonzero, but they nevertheless cancel to high precision in the final panel. These results were obtained for $\epsilon^1 \neq 0$ with $\# = 499$. See <https://bit.ly/30dGI04> for an animation of this scattering process. 112
- D.1 Diagram topology corresponding to Eq. (D.23) 127

LIST OF TABLES

<i>Number</i>	<i>Page</i>
2.1 Tidal operators evaluated on a background Schwarzschild metric in isotropic coordinates. As discussed in the text, since we are working at linear order in the tidal coefficients we have set the energy component of the test-particle momentum to be the Hamiltonian \mathcal{H}_0 in the absence of tidal corrections.	30
2.2 Coefficients specifying the diffeomorphism in Eq. (2.59) that goes to isotropic coordinates.	31
2.3 Contribution to the isotropic Hamiltonian \mathcal{H}_1 from tidal operators at all PM orders.	32
2.4 Contribution to the scattering amplitude \mathcal{M}_1 from tidal operators at all PM orders.	33
2.5 Contribution to the scattering angle j_1 from tidal operators at several PM orders.	34

Chapter 1

INTRODUCTION

Quantum field theory (QFT) has proven to be a highly successful formulation for describing the quantum mechanical and relativistic properties of fundamental particles. Beginning in the 1920s with the birth of quantum electrodynamics from attempts to quantize the electromagnetic field [1], the past century has seen major advances in the tools and techniques emerging from the quantum theoretical framework with applications reaching beyond the boundaries of elementary particle physics to areas such as the study of condensed matter systems. In recent years, methodologies developed in QFT and in the computation of scattering amplitudes for perturbative processes have found an unexpected yet fruitful application: the calculation of classical observables for a gravitational binary system, Fig. 1.1 [2–29].

The exact solution to the two-body problem in general relativity remains an unsolved problem. However, a vast amount of work, spanning several decades, has been done to determine the gravitational forces, potentials, and waveforms predicted by Einstein’s equations and other theories of gravity using approximations that range from the post-Minkowskian (PM) expansion [30–42], an expansion in the gravitational constant, G , the post-Newtonian (PN) expansion [43–57], an expansion in velocity, v/c , to the self force (SF) expansion [58, 59], an expansion in the mass ratio, $m_1/m_2 \ll 1$, of the lighter body to that of the heavier body. These formalisms are supplemented with methods such as the effective one-body theory [60, 61], numerical relativity [62–64], and effective field theory [65–74]. In particular, point particle effective theory allows the import of many useful computational

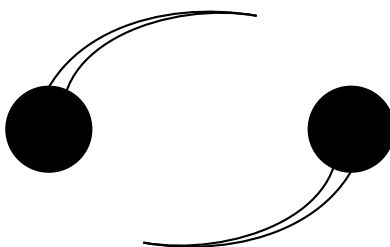


Figure 1.1: A depiction of the bound system of two inspiraling black holes.

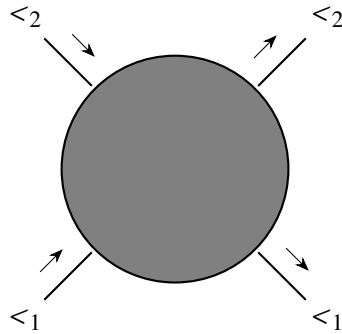


Figure 1.2: The classical dynamics the gravitational two-body problem is studied using a scattering problem in effective field theory.



Figure 1.3: Examples of diagrams contributing to the quantum scattering of interacting masses. The diagram on the left, which involves a graviton-mediated long range force, will contribute classically but the diagram on the right will not.

schemes, such as recursion relations, generalized unitarity, double copy relations, and dimensional regularization, from the quantum world to a classical problem [65, 75–94]. While the field theory is geared for studying scattering, Fig. 1.2, results relevant to the bound scenario can be extracted via the computation of a Hamiltonian [95–97] or by analytical continuation from the scattering state to the bound state [98, 99]. It may seem as though we are trading the benefit of remaining in a classical limit for the use of these tools but not all quantum contributions to the final answer need actually be calculated. They can be dropped along the way by only including the desired Feynman diagrams (see Fig. 1.3) and from the terms in the integrands of such diagrams.

The landmark measurements of gravitational waves produced by the inspiral and merger of a pair of black holes made by the Laser Interferometer Gravitational-Wave Observatories (LIGO) [100], followed by the detection of several subsequent events, steadily improving experimental precision, and plans for future gravitational wave detectors, have made it essential for theoretical predictions from general relativity or other modified theories of gravity to meet certain necessary levels of accuracy. The adoption of the Laser Interferometer Space Antenna (LISA) [101] as a flight project

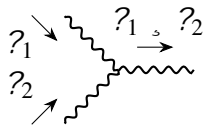
by the European Space Agency (ESA), in partnership with the National Aeronautics and Space Administration (NASA), opens a pathway to exploring new regimes of parameter space in the detection of binary mergers. Unlike LIGO, LISA is expected to detect waves produced by the inspiral of much lighter bodies around heavy black holes, events known as *extreme mass ratio inspirals* (EMRIs) [102], at the order of about a hundred per year [103, 104]. In the region of interest, where the mass ratio of the interacting bodies is 10^{-4} - 10^{-7} , gravitational effects become extremely strong with dynamics reaching relativistic speeds and we can no longer study the system using a perturbative expansion in v/c or as a weak field, nonrelativistic system using further expansion in the relative velocity of the bodies. However, we still have a perturbative parameter: the mass ratio of the two bodies. Can we tailor QFT methods to address this regime and improve the accuracy of the predicted values of observables?

Currently, only self force theory and numerical relativity, which solves the equations nonperturbatively, can be applied to EMRIs. The advances made in calculations using tools developed for computing quantum scattering amplitudes [2–29] suffer in the strong field regime for the same reason that they are so well suited for the PM expansion: the formulation of the theory as an expansion in v/c with gravitons mediating the scattering of relativistic massive particles in flat space. QFT computations of this type are inherently perturbative in v/c .

On the other hand, known solutions to the classical gravitational equations, such as the Schwarzschild solution, carry information to all orders in the gravitational constant. While this is obvious from the perspective of classical general relativity, it is highly nontrivial when considered from the point of view of perturbative computations in QFT. As shown in [105] and verified to all orders in [106], the Schwarzschild metric can be computed, albeit with considerable difficulty, from tree-level Feynman diagrams that contribute to the one-point function for a graviton sourced by a massive scalar point particle (see Fig. 1.4). A straightforward computation, using Feynman rules dictated by the Einstein-Hilbert Lagrangian when expanding around flat space, would naively require the use of graviton vertices that get increasingly complicated and cumbersome. For example, the three-point graviton vertex has the form [79, 107],

$$\delta_{ab} = \Gamma_{ab} + \text{[diagrams]}$$

Figure 1.4: The Schwarzschild metric can be viewed as a compact expression for the sum of an infinite class of flat space Feynman diagrams that induce corrections to the Minkowski metric. The circles represent a static or inertial massive scalar source and the squiggly lines denote flat space graviton propagators.



$$\begin{aligned}
 = \text{Sym} & \left[\frac{1}{2} \%_3^1 \?_1 \?_2 [\cdot d [a _ [f g^0 \right. \left. \frac{1}{2} \%_6^1 \?_1 a \?_1 _ [\cdot d [f g^0 \right. \\
 & \left. \frac{1}{2} \%_3^1 \?_1 \?_2 [\cdot a [d _ [f g^0 \right. \left. \%_6^1 \?_1 \?_2 [\cdot d [f a [_ g^0 \right. \quad (1.1) \\
 & \left. \left. 2 \%_3^1 \?_1 a \?_1 g [\cdot d [_ f^0 \right. \left. \%_3^1 \?_1 _ \?_2 a [d a [f g^0 \right. \\
 & \left. \left. \%_3^1 \?_1 f \?_2 a [\cdot a [d _ ^0 \right. \left. \%_6^1 \?_1 f \?_1 g [\cdot a [d _ ^0 \right. \\
 & \left. \left. 2 \%_6^1 \?_1 a \?_2 g [_ \cdot [d f^0 \right. \left. 2 \%_3^1 \?_1 a \?_2 \cdot [_ f [g d^0 \right. \\
 & \left. \left. 2 \%_3^1 \?_1 \?_2 [d a [_ f [g \cdot ^0 \right. \right.
 \end{aligned}$$

where Sym stands for symmetrizing over each index pair, $\cdot d - a - f g$, and $\%_\ell$ stands for permutations involving the three graviton legs producing an ℓ number of terms. The graviton four-point vertex contains more than a thousand terms. In practice, the computations are considerably simplified using alternate procedures for calculating amplitudes, but there are still an appreciable number of steps involved in getting to the final answer. The expansion of the Schwarzschild solution in \hbar trivially provides the answers to the evaluation of a certain set of Feynman diagrams, containing complex tensor structures in their vertices, at any order in \hbar .

The metric is not the only piece of classical data that we can leverage in this manner to trivialize or simplify large swathes of structures that appear in the field theoretic approach to gravitational interactions between massive scalar bodies. In the limit where the mass of one body is negligible compared to the other, i.e., when $m \ll M$, the lighter body traverses a geodesic trajectory in the background produced by the heavier body. From the perspective of point particle effective field theory, the propagation of a massive scalar in curved space encodes another infinite set of Feynman diagrams as shown in Fig. 1.5. Once again, diagrams, at all orders in \hbar

Figure 1.5: The propagator of a massive scalar particle in curved space is composed of the flat space propagator and an infinite set of tree-level Feynman diagrams where gravitons sourced by a static, heavy point particle self-interact and eventually land on the propagating particle.

and at the leading order in the mass ratio, for the classical scattering of a particle off of another with a much higher mass are resummed.

It is therefore worthwhile to ask whether we can tackle the question of determining all order results using effective field theory or increase the efficiency of the perturbative EFT computational pipeline by leveraging the all order data provided by classical solutions for metrics and geodesic trajectories. More generally, it would be interesting to examine how quantum and classical approaches can be applied to a problem in a way that harnesses and combines the strengths and power of both.

In Chapter 2, we take the first steps in utilizing the resummation in provided by the metric to obtain amplitudes for systems that are perturbatively away from the interaction of two nonspinning black holes. Using an identity known as the *impetus formula* [96, 97, 99, 108], which was observed in the process of determining a Hamiltonian for the classical interaction of two massive scalars using quantum amplitude techniques, we *algebraically* obtain amplitudes for systems where one of the massive bodies experiences tidal distortions or other perturbative corrections such as those coming from higher derivative modifications to the Einstein-Hilbert action or from the presence of charge on one of the black holes. Here, the synergy resulting from the combination of classical and amplitudes-based perspectives is highlighted since all order amplitude computations can be done, without the need to

perform integration, using classical information in a formula obtained from effective field theoretic studies.

Metrics and geodesic trajectories encode information in the limit where the mass ratio approaches zero. However, two generic bodies participating in a gravitational process will have a larger mass ratio. Even in a regime where the PM expansion is a valid approximation and we can make use of the simplification of diagrams provided by the classical solutions, we would need data that accounts for these larger mass ratios. Can we continue to take advantage of classical solutions while systematically moving beyond the $\epsilon \rightarrow 0$ limit? This is the subject of Chapter 3 and Chapter 4. The former consists of a short letter laying out the key ideas in building an effective field theory as a systematic expansion in the mass ratio. When we perturb away from the extremal limit of a test body moving in a Schwarzschild background, the mass of the light body also affects the geometry of spacetime and the dynamics of the heavy black hole sourcing the background. The corrections act back on the motion of the lighter mass in an effect known as the *self force*. Therefore, the system cannot be solely described by the background field method where fluctuations of gravitons about a nontrivial classical background interact with a particle and affect its motion while leaving the background unchanged. In our formalism, the additional effects are accounted for by *recoil operators* which acquire their name by enforcing the backreaction experienced by the heavy particle sourcing the background. Such a setup allows for the use of simplifications provided by the metric and geodesic trajectories when computing results in a PM expansion. The details of the effective field theory and applications to a variety of systems are presented in Chapter 4. The setup is first tested in a simpler theory where charged massive scalar particles interact electromagnetically and then applied to the gravitational case which differs from the former due to the nonlinearity of Einstein's field equations.

In Chapter 5, we take a detour to look into a relation between graviton and gluon amplitudes known as the *double copy* [75, 77–79]. Through the color-kinematics or Bern-Carrasco-Johansson (BCJ) duality present in the structure of the kinematic dependent parts and the color factors of the numerators in suitably rearranged gluon amplitudes, graviton amplitudes can be obtained from gluon amplitudes by a simple replacement of the color factors by another copy of the associated kinematic numerators. This relationship has been proven to all orders for tree-level diagrams and poses an intriguing question about potential hidden properties of these theories

This is the reason why an expansion in the mass ratio is also referred to as the self force expansion.

while also serving a practical purpose in calculations involving gravitons such as the ones encountered in deriving results for the classical gravitational binary problem [96, 97]. As such, revealing the underlying structure giving rise to the duality and the double copy relation may elucidate novel symmetries in these theories, lead to a deeper understanding of the constraints placed on field theories that are realized in the natural world, and expand the scope and ease of application of the relations in computations of practical interest.

The discovery of the color-kinematics duality is a product of the modern incarnation of S-matrix theory, the scattering amplitudes program. The standard perturbative approach to calculating observables, such as the scattering cross-sections of subatomic particles, starting with a Lagrangian and through the use of the resulting Feynman rules becomes increasingly complex at higher orders in the perturbative expansion in several theories of interest. Due to the *off-shell* nature of the formulation, the simplicity of the final *on-shell* results is hidden by gauge redundancies and the freedom in choosing a field basis for describing relevant physics. The Parke-Taylor formula [109] for maximum helicity violating gluon amplitudes serves as a quintessential example of a simple structure that is obscured by a proliferation of terms in the intermediate steps towards its derivation. The amplitudes program sidesteps these complexities by using a first principles based, on-shell approach to calculating observables in QFT. This is achieved by imposing necessary conditions such as unitarity, analyticity, and factorization to constrain expressions and determine amplitudes using the physical properties and symmetries of a theory. This perspective has not only led to a speed up of calculations necessary for experimental situations, such as those arising in collider physics, but has also spurred on research into the fundamental structures and properties of scattering amplitudes. New techniques arising from such studies feed back into increasing computational efficiency with the aforementioned color-kinematics duality and the double copy being examples of such discoveries.

Given their origin from an on-shell approach and otherwise, there are several open questions regarding the basis for these relations and their scope of validity. Is the duality a property of loop amplitudes at all orders in the perturbation constant? Is it valid off-shell? And, if so, can it be made manifest at the level of the Lagrangian or equations of motion? Do classical solutions possess the duality? Do the duality and double copy point to an as yet unknown symmetry in these theories? In fact, color-kinematics duality and double copy relations exist in a plethora of theories

beyond Yang-Mills and pure gravity. Could their presence indicate some wider principle regarding these theories?

In order to investigate these questions, we examine color-kinematics duality and the double copy in the context of scalar effective field theories. The nonlinear sigma model exhibits a duality of the same type between the flavor and kinematic components of its amplitudes . Applying the double copy by replacing flavor with another copy of the kinematics dependent numerators produces the amplitudes of the special Galileon theory. For our purposes, we can treat these theories as simpler analogs to Yang-Mills theory and gravity.

In Chapter 5, we boil down to an even simpler setup by studying a theory that is classically equivalent to the nonlinear sigma model in two dimensions. Here, for the first time, we are able to manifest the duality at the level of the Lagrangian in a theory with interactions. This implies that, for this theory, the duality holds off-shell, at the level of the Feynman rules, and is therefore present in the integrands of loop amplitudes to all orders. In addition, we explore several interesting consequences of this explicit duality. We hope to export the insights gained from this specific setup to uncover answers regarding color-kinematics duality in the context of Yang-Mills theory and beyond.

Since flavor acts as the analog to color, these terms are used interchangeably.

Chapter 2

MINING THE GEODESIC EQUATION FOR SCATTERING DATA

This chapter reproduces the contents of the publication: Clifford Cheung, Nabha Shah, and Mikhail P. Solon. Phys. Rev. D 103, 024030 – Published 14 January 2021.

2.1 Introduction

In recent years, powerful tools from the modern amplitudes program [75–84] and effective field theory have [65, 85–94] been unified to derive new results [95–97, 110] of relevance to the search for gravitational waves at the LIGO/Virgo experiment [100, 111]. These efforts have spurred a resurgence of interest in post-Minkowskian (PM) perturbation theory [30–42], which organizes dynamics in powers of the gravitational constant while retaining all orders in velocity. This approach lies in contrast with post-Newtonian (PN) perturbation theory [43–57], which further expands in velocity as appropriate for a virialized system. The PM and PN formalisms, together with methods from numerical relativity [62–64], effective one-body theory [60, 61], self-force [58, 59], and effective field theory [65–74] form a vital ecosystem of ideas and tools for solving the binary inspiral problem. Many recent developments have benefited immensely from a genuine cross-pollination of ideas between classical general relativity and quantum field theory [2–29], culminating in new results pertaining to spinning black holes [112–128], orbital mechanics [98, 99, 108, 129], and radiation [130, 131].

The preponderance of work in this area has centered on black holes in general relativity. There are, however, many reasons to consider perturbations away from this minimal scenario. A prime example of this is tidal distortion, which is central to disentangling the inspiral dynamics of neutron binary systems that will hopefully shed light on the underlying nuclear properties of dense matter [132, 133]. Indeed, gravitational waves from neutron binaries should place substantive constraints on the nuclear equation of state [111, 134–150]. For these reasons, tidal phenomena have been modeled with a variety of methods [135, 151–174], including, very recently, PM perturbation theory [175–180].

Deviations from the minimal scenario also arise in theories of modified gravity.

In the absence of additional light degrees of freedom such dynamics are encoded at long distances by higher derivative corrections to general relativity [181–184]. While these effects will be exceedingly small in any sensible ultraviolet completion of gravity it is still worth understanding their influence on the dynamics of the binary inspiral [185–189].

In this paper we explore how the geodesic equation encodes conservative dynamics in the presence of an arbitrary perturbative correction away from a nonspinning black hole binary system in general relativity. We will be interested in computing the perturbed scattering amplitudes and Hamiltonians which characterize these effects. Our main application will be tidal interactions. However, given the generality of our approach we will also study other examples, including higher derivative corrections to Einstein-Maxwell theory and their effects on gravitationally and electrically interacting bodies. While it is straightforward to derive analogous results for spin-dependent effects from geodesic motion in a Kerr background, we leave this interesting possibility for future study.

As is well-known, the test-particle limit—and corrections away from it [190–194]—encode critical information about scattering in the PM approximation [127, 195]. More trivially, this limit completely fixes the dynamics of spinning and nonspinning black holes at low PM orders and offers a useful consistency check at higher orders [95–97, 110, 128, 177, 196]. At a practical level, the test-particle regime is attractive since in many cases it is analytically tractable to all PM orders. While this observation is somewhat trivial it is tantalizing in the context of scattering amplitudes, where it implies that the geodesic equation effectively resums certain infinite towers of loop diagrams. An enticing possibility then emerges of bootstrapping certain multi-loop scattering calculations directly from geodesic motion.

Here we present two methods, each with its own advantages and target applications. The first applies at leading nontrivial PM order and linear order in some additional perturbative parameter. Our method is based on the connection between PM Hamiltonians and scattering amplitudes [95], and derives the tidal Hamiltonian in isotropic coordinates from the geodesic equation through a set of trivial algebraic operations. A key simplification is that at leading PM order, the canonical transformation from nonisotropic to isotropic coordinates is encapsulated by a replacement rule shown in Eq. (2.19). In the context of tidal interactions, this approach elaborates on the essential insight of [175] that such contributions are

encoded entirely by the geodesic dynamics of a tidally distorted test particle in a Schwarzschild background. We demonstrate the simplicity of our approach by deriving analytic formulas for scattering amplitudes and Hamiltonians at arbitrary mass ratio for certain infinite classes of tidal operators, including electric Weyl and magnetic Weyl to any power, as shown in Eq. (2.27) and Eq. (2.33). We also apply this method to other types of perturbative corrections, e.g., which arise for electrically charged bodies or from higher derivative corrections to Einstein-Maxwell theory.

Our second method is a mechanical procedure for deriving closed-form expressions for the scattering amplitude in the test-particle limit at all orders in the PM expansion. We systematically perform a general diffeomorphism on the metric and then constrain it to eliminate non-isotropic terms in the geodesic equation. A general formula for the isotropic Hamiltonian induced by any tidal moment operator is presented in Eq. (2.61). From this Hamiltonian we then derive expressions for the corresponding scattering amplitudes at all PM orders in Eq. (2.64). As an application of these general formulas, we derive all orders in PM expressions for the isotropic Hamiltonian and scattering amplitude for a set of tidal operators, as presented in Table. 2.3 and Table. 2.4. These results may provide useful data for checking future higher order PM calculations.

2.2 Test-Particle Dynamics

In this section we present some basic tools for deriving scattering amplitudes from the geodesic equation. For concreteness we describe this formalism in the context of tidal effects, but as we will see later on our essential approach is trivially generalized to any scenario in which the geodesic equation is perturbatively corrected.

To begin, we consider the scattering amplitude of a tidally distorted body of mass m_1 interacting with a black hole of mass m_2 in the test-particle limit $m_1 \ll m_2$. In the rest frame of the black hole, the dynamics are described by the geodesic motion of a nonminimally coupled test particle of three-momentum \vec{p} propagating on a Schwarzschild background. An arbitrary tidal moment is represented by the field theoretic operator,

$$\mathcal{O} = \frac{1}{2} \int d^3x \sqrt{-g} \delta g_{\mu\nu} \mathcal{O}^{\mu\nu} q - \quad (2.1)$$

where \mathcal{O} is some operator that involves the metric tensor g , the matter field q , and their derivatives. We work at linear order in the tidal parameter ϵ throughout.

In order to make contact with known results, we express \mathcal{O} in a basis of operators composed of products of the electric and magnetic Weyl tensors and their derivatives. Note, however, that these tensors are defined with respect to the four-momentum of a propagating body and so one naively encounters an ambiguity in Eq. (2.1): should the four-momentum be associated with \hat{r}^{\otimes} or \hat{r}° ? As it turns out, this choice is actually irrelevant since the difference is suppressed by the momentum transfer carried away by gravitons relative to the momentum of the bodies. This suppression factor is infinitesimal, scaling inversely with the angular momentum of the scattering process in units of \sim , as expected for a quantum correction to the dynamics [95–97].

2.2.1 Geodesic to Hamiltonian

In the presence of tidal distortion the geodesic equation is [168]

$$0 = \delta^a \cdot \%_a \cdot \%_a \cdot \delta^2 \cdot \mathcal{O}^1 \delta \cdot \%^0 \cdot \quad (2.2)$$

in mostly plus signature and where as discussed earlier we identify Γ with the four-momentum $\%$ of the test particle. For maximum generality we assume an arbitrary static, spherically symmetric metric whose line element is

$$3B^2 = \delta_{\ell\ell}^1 A^0 3\ell^2 \cdot \delta_{AA}^1 A^0 3A^2 \cdot \delta^1 A^0 A^2 1 3 \setminus^2 \cdot \sin^2 \setminus 3q^2 \cdot \quad (2.3)$$

This form of the metric will accommodate all our scenarios of interest, i.e., black holes in general relativity and beyond in various coordinate systems.

The four-momentum of the test particle is

$$\% \cdot = 1 \cdot \delta_A \cdot \delta \setminus \cdot \delta q^0 = \frac{q}{\mathcal{P}^2} \frac{2}{A^2} \cdot 0 \cdot \quad (2.4)$$

where \mathcal{H} is the test-particle Hamiltonian and $\delta_A = \delta A \cdot A$ is the radial momentum. In the last equality we have assumed a trajectory on the equatorial plane at $\setminus = c \cdot 2$, so $\delta \setminus = 0$ and $\delta q =$ is the angular momentum of the particle. We have also used $\delta_A^2 = \mathcal{P}^2 \frac{2}{A^2}$ to relate the radial momentum to the total momentum \mathcal{P} and angular momentum δ .

To derive the Hamiltonian we first expand to linear order in the tidal coefficient, $\mathcal{O} = \mathcal{O}^0 \cdot \mathcal{O}^1 \cdot \mathcal{O}^2$, and then solve the geodesic equation order by order in \mathcal{O} . At zeroth order in the tidal coefficients, the Hamiltonian is

$$\mathcal{H}^0 = \frac{\mathcal{P}^2}{\delta_{\ell\ell}^1 A^0} \cdot \frac{\delta^2}{\delta_{AA}^1 A^0} \cdot \frac{2}{\delta^1 A^0 A^2} \cdot \quad (2.5)$$

From Eq. (2.2) we see that the tidal operator manifestly enters as a shift of the mass term. Thus in the presence of tidal distortion the Hamiltonian becomes

$$H_0 = \frac{p^2}{2m} + \frac{1}{2} \frac{\partial^2 \gamma_{\mu\nu}}{\partial x^\alpha \partial x^\beta} x^\alpha x^\beta + \dots \quad (2.6)$$

Let us elaborate on the appearance of $\frac{1}{2} \frac{\partial^2 \gamma_{\mu\nu}}{\partial x^\alpha \partial x^\beta} x^\alpha x^\beta$ in the above expression. *A priori*, the tidal operator is of the form $\frac{1}{2} \frac{\partial^2 \gamma_{\mu\nu}}{\partial x^\alpha \partial x^\beta} x^\alpha x^\beta$, which depends on the radius A through the background metric γ , and on \dot{x}^α , \dot{x}^β and x^α through the four-momentum p^α . However, the tidal operator can be approximated by $\frac{1}{2} \frac{\partial^2 \gamma_{\mu\nu}}{\partial x^\alpha \partial x^\beta} x^\alpha x^\beta = \frac{1}{2} \frac{\partial^2 \gamma_{\mu\nu}}{\partial x^\alpha \partial x^\beta} x^\alpha x^\beta + \dots$ up to corrections subleading in ϵ . Further linearizing Eq. (2.6) in ϵ we obtain the tidal Hamiltonian,

$$H_0 = \frac{p^2}{2m} + \frac{1}{2} \frac{\partial^2 \gamma_{\mu\nu}}{\partial x^\alpha \partial x^\beta} x^\alpha x^\beta + \dots \quad (2.7)$$

While the focus of the present work is the leading correction in ϵ , it is of course straightforward to solve Eq. (2.2) at any arbitrary order in ϵ , yielding the corresponding tidal Hamiltonian at that order.

We will often be interested in corrections at the leading nontrivial PM order, in which case Eq. (2.7) simplifies since $\frac{\partial^2 \gamma_{\mu\nu}}{\partial x^\alpha \partial x^\beta} x^\alpha x^\beta = \frac{p^2}{2m} + \dots$ is the energy of a free particle, so

$$H_0 = \frac{p^2}{2m} + \dots \text{ higher order in PM} \quad (2.8)$$

We thus conclude that the Hamiltonian at leading order in ϵ and leading PM order is literally the tidal operator evaluated on the Newtonian metric with all momenta taken to be on-shell.

As we will see, it is often convenient to study the dynamics in isotropic gauge, i.e., coordinates in which the Hamiltonian is a function $H^{\text{iso}}(x, p)$ which depends only on x and p but not \dot{x} . At zeroth order in tidal corrections, i.e., for bodies with minimal gravitational coupling, $H^{\text{iso}}(x, p)$ is trivially obtained by choosing isotropic coordinates for the black hole metric,

$$\begin{aligned} \gamma_{\mu\nu}^{\text{iso}} &= \frac{1}{1 - \frac{2M}{r}} \delta_{\mu\nu} \\ \gamma_{AA}^{\text{iso}} &= \gamma^{\text{iso}}_{AA} = \left(1 - \frac{2M}{r}\right)^{-2} \end{aligned} \quad (2.9)$$

where $r = 2M$ is the Schwarzschild radius. Plugging Eq. (2.9) into Eq. (2.5), we obtain the isotropic Hamiltonian for a point-like test particle [197],

$$H_0^{\text{iso}}(x, p) = \frac{p^2}{2m} + \frac{1}{2} \frac{\partial^2 \gamma_{\mu\nu}^{\text{iso}}}{\partial x^\alpha \partial x^\beta} x^\alpha x^\beta + \dots \quad (2.10)$$

which we will use frequently for the remainder of the paper.

2.2.2 Hamiltonian to Amplitude

Starting from an arbitrary Hamiltonian it is straightforward to compute the scattering amplitude for elastic scattering via effective field theory methods [95]. This approach requires the tedious albeit mechanical computation of loop diagrams order by order in the PM expansion. On the other hand, for a Hamiltonian which is already in isotropic gauge there exists an extraordinarily simple procedure which bypasses loop integration in favor of solving an algebraic equation. First discovered in the 3PM calculation of [96, 97] and later proven in [98, 108], this map exploits an elegant algebraic relation between the amplitude \mathcal{M} and the isotropic gauge Hamiltonian \mathcal{H}^{iso} . In the test-particle limit this relation is

$$\mathcal{M}^1(\mathbf{p}, A^0) = \frac{1}{2} \mathcal{H}^1(A^0) \mathcal{H}^2(\mathbf{p}, A^0) \dots \text{iterations} \quad (2.11)$$

where $\mathcal{H}^1(A^0)$ is the local momentum at a position A dictated by the conservation of energy equation,

$$\mathcal{H}^{\text{iso}}(\mathbf{p}, A^0) = 0 \quad (2.12)$$

The iteration contributions in Eq. (2.11) are infrared divergent terms defined in the prescription of [95]. These contributions always cancel in any effective field theory matching to extract coefficients in the Hamiltonian.

Note that in the scattering amplitude $\mathcal{M}^1(\mathbf{p}, A^0)$ we should interpret the quantities $\mathbf{p} = \sqrt{2E^2 - A^2}$ and E as the asymptotic energy and momentum of the test particle and the variable A as the Fourier transform of the three-momentum transfer \mathcal{Q} . This differs from $\mathcal{H}^{\text{iso}}(\mathbf{p}, A^0)$, where \mathbf{p} and A should be interpreted as the time-dependent phase space coordinates of the test particle.

The upshot here is that the isotropic Hamiltonian and scattering amplitude are trivially related. In particular, we expand the scattering amplitude as $\mathcal{M} = \mathcal{M}_0 + \mathcal{M}_1 + \mathcal{O}(\epsilon^2)$ and solve Eq. (2.11) and Eq. (2.12) order by order in ϵ . This procedure yields the tidally corrected scattering amplitude in the test-particle limit,

$$\begin{aligned} \mathcal{M}_0^1(\mathbf{p}, A^0) &= \frac{1}{2} \mathcal{H}^1(A^0) \mathcal{H}^2(\mathbf{p}, A^0) \dots \text{iterations} \\ \mathcal{M}_1^1(\mathbf{p}, A^0) &= \frac{\mathcal{H}^{\text{iso}}(\mathbf{p}, A^0)}{\mathcal{H}^1(A^0)} \mathcal{H}^1(A^0) \mathcal{H}^2(\mathbf{p}, A^0) \dots \text{iterations} \end{aligned} \quad (2.13)$$

where in the first line we have solved Eq. (2.12) at zeroth order in the tidal coefficient using \mathcal{H}^{iso} from Eq. (2.10). In the second line we have the leading tidal correction

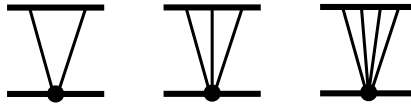


Figure 2.1: At leading PM order, tidal corrections to the scattering amplitude arise from fan diagrams. For an operator composed of \mathcal{R} = curvature tensors, this contribution corresponds to an $\mathcal{O}(1)$ -loop diagram. Thick and thin lines denote matter and graviton lines while the black dots denote tidal operator insertions.

to the amplitude in terms of an abstract $\mathcal{M}_1^{\text{iso}}$ which we will compute explicitly later on.

At leading PM order, the tidal correction to the amplitude is

$$\mathcal{M}_1^{\text{iso}} \mathcal{A}^0 = \mathcal{M}_1^{\text{iso}} \mathcal{A}^0 + \text{higher order in PM} \quad (2.14)$$

so as expected the amplitude is exactly the Feynman vertex defined by the isotropic Hamiltonian.

2.3 Leading Order in M

In this section we consider the dynamics at leading PM order and leading order in some additional perturbative correction. Our aim is to compute the perturbed scattering amplitude and Hamiltonian. In such a regime the test-particle limit encodes complete information about the dynamics at arbitrary mass ratio. This fact is obvious from the point of view of scattering amplitudes. Consider, for example, tidal corrections at leading PM order. These contributions are generated by the lowest order loop diagrams which induce classical scattering [96, 97] and enter at linear order in the tidal coefficient, corresponding to the “fan diagrams” depicted in Fig. 2.1. By definition, fan diagrams do not include matter propagators of the tidally distorted particle. More generally, we will henceforth refer to any diagram in which all matter propagators are on one side as a fan diagram. As discussed in [95–97, 110], all fan diagrams are free from infrared divergences or iterations of lower order contributions. In the classical limit we are thus permitted to drop all recoil effects on the other particle, which can then be represented by a static background. This connection has been made in the context of the effective one-body theory as well as the mass dependence of the scattering angle, and we refer the reader to [39, 127, 195] for further discussions.

2.3.1 Lifting to Arbitrary Mass Ratio

At leading PM order the test-particle limit encodes sufficient data to reconstruct the perturbed scattering amplitude for arbitrary mass ratio in an arbitrary reference frame. To do this start we start with the test-particle amplitude and boost away from the rest frame by sending

$$|_{<_1} f \quad \text{and} \quad ? \quad |_{<_1} \frac{\rho}{f^2 - 1} \quad \text{where} \quad f = \frac{\%_1 \cdot \%_2}{<_1 <_2}. \quad (2.15)$$

Here $\%_1 = |_{<_1} \cdot ?_1^0$ and $\%_2 = |_{<_2} \cdot ?_2^0$ are the four-momenta of the scattering bodies in a boosted frame where $|_{<_2} = \frac{?_{1-2}^2}{<_{1-2}^2}$. At the same time, we also continue away from the test-particle limit to accommodate arbitrary masses $<_1$ and $<_2$.

Applying the replacement in Eq. (2.15), we derive the leading PM tidal correction to the scattering amplitude for arbitrary mass ratio and in a general frame

$$M_{|_{<_1} \%_1 - \%_2 - A^0} = \frac{<_1 <_2 f}{|_{<_1} <_2} M_{|_{<_1} \frac{\rho}{f^2 - 1} - A^0} \quad (2.16)$$

where the left-hand side of Eq. (2.16) is the amplitude for arbitrary mass ratio in a general frame and the right-hand side is the amplitude in the test-particle limit in the rest frame of the heavy body, as defined in Eq. (2.13). Here the prefactor accounts for proper nonrelativistic normalization after applying the replacement in Eq. (2.15). Note that if both bodies are tidally deformed then one should sum over Eq. (2.16) with particle labels swapped.

This procedure similarly applies to the isotropic Hamiltonian,

$$|_{\text{iso } 1} \%_1 - \%_2 - A^0 = \frac{<_1 <_2 f}{|_{\text{iso } 1} <_1} |_{\text{iso } 1} \frac{\rho}{f^2 - 1} - A^0 \quad (2.17)$$

where the left-hand side of Eq. (2.17) is the Hamiltonian for arbitrary mass ratio in an arbitrary frame and the right-hand side is the isotropic gauge test-particle Hamiltonian in the rest frame of the heavy body.

While we have presented Eq. (2.16) and Eq. (2.17) in the context of tidal corrections, we emphasize that this basic procedure can be applied to any perturbation that deviates from the standard scenario of black holes interacting in general relativity.

2.3.2 Fourier Transform

Eq. (2.16) is an explicit formula for the leading PM scattering amplitude of tidally interacting bodies at arbitrary mass ratio written in terms of the amplitude in the test-particle limit. According to Eq. (2.14) the latter is essentially the isotropic

gauge Hamiltonian in the test-particle limit. Consequently, our only task is to map the test-particle Hamiltonian in Eq. (2.8) to isotropic coordinates. Typically, this is achieved by explicitly constructing a coordinate transformation from $\mathcal{H}_1^1 \mathcal{H} \mathcal{A}^{-\circ}$ to $\mathcal{H}_1^{\text{iso}1} \mathcal{H} \mathcal{A}^0$, as we will do in Sec. 2.4. In this section, we derive a much simpler procedure applicable at the leading PM order.

Our basic idea is to take $\mathcal{H}_1^1 \mathcal{H} \mathcal{A}^{-\circ}$ and Fourier transform to momentum space to obtain $\mathcal{E}_1^1 \mathcal{H} \mathcal{A}^{\circ}$. As discussed at length in [95–97] one can compute the scattering amplitude mediated by the tidal corrections, treating $\mathcal{E}_1^1 \mathcal{H} \mathcal{A}^{\circ}$ as a Feynman vertex. Crucially, at leading PM order, the contribution to the amplitude is exactly proportional to $\mathcal{E}_1^1 \mathcal{H} \mathcal{A}^{\circ}$ albeit evaluated at on-shell kinematics. For a scattering particle with momentum \mathcal{H} and momentum transfer \mathcal{A} , the on-shell condition implies that $\mathcal{H} \mathcal{A} \mathcal{A}^2$, which is subleading in classical counting and can thus be dropped. From Eq. (2.14) we also know that the amplitude is given by the isotropic gauge Hamiltonian, so

$$\mathcal{E}_1^1 \mathcal{H} \mathcal{A}^{\circ} \Big|_{\mathcal{H} \mathcal{A}=0} = \mathcal{E}_1^{\text{iso}1} \mathcal{H} \mathcal{A}^{\circ} \quad (2.18)$$

where the replacement drops quantum contributions which are irrelevant to the classical dynamics. We can then Fourier transform $\mathcal{E}_1^{\text{iso}1} \mathcal{H} \mathcal{A}^{\circ}$ to obtain the isotropic Hamiltonian in position space, $\mathcal{H}_1^{\text{iso}1} \mathcal{H} \mathcal{A}^0$.

Conveniently, we can perform this procedure—Fourier transforming to momentum space, dropping terms that vanish on-shell, and Fourier transforming back to position space—in a single step. This is encapsulated by the replacement,

$$\frac{\mathcal{H}^2}{\mathcal{A}^2} \rightarrow \frac{\mathcal{H}^2 \mathcal{A}^2}{\mathcal{A}^2} \frac{\text{Poch} \frac{\mathcal{H}}{2} \frac{1}{2} \mathcal{H} \mathcal{A}}{\text{Poch} \frac{\mathcal{H}}{2} \mathcal{H} \mathcal{A}} \quad (2.19)$$

where $\text{Poch} \mathcal{H} \mathcal{A} = \frac{\Gamma(\mathcal{H} \mathcal{A})}{\Gamma(\mathcal{H}) \Gamma(\mathcal{A})}$ is a ratio of Gamma functions and the left- and right-hand sides are exactly equal up to terms that Fourier transform to objects proportional to $\mathcal{H} \mathcal{A}$ which can be discarded on-shell. See App. A for details. Also, note that this replacement must be used with care: it can only be applied after first expanding an expression fully in \mathcal{H} and $\mathcal{H} \mathcal{A}$, since Fourier transform and multiplication do not commute.

The upshot here is that Eq. (2.19) maps any non-isotropic Hamiltonian $\mathcal{H}_1^1 \mathcal{H} \mathcal{A}^{-\circ}$ to a physically equivalent isotropic Hamiltonian $\mathcal{H}_1^{\text{iso}1} \mathcal{H} \mathcal{A}^0$ at leading PM order. After deriving $\mathcal{H}_1^{\text{iso}1} \mathcal{H} \mathcal{A}^0$ we can then obtain the scattering amplitude via Eq. (2.14) and lift to arbitrary mass ratio via Eq. (2.16) and Eq. (2.17).

2.3.3 Tidal Operators

Let us now utilize the tools derived above to compute the leading PM tidal corrections to the isotropic gauge Hamiltonian. We emphasize that our procedure is purely algebraic and thus implemented with ease. In particular, for a tidal operator given by a product of traces of matrices built from electric and magnetic Weyl, i.e., $O = \text{tr}_1 E - B^o \text{tr}_2 E - B^o \text{tr}_3 E - B^o$, we simply calculate O using Eq. (2.23) and Eq. (2.29) below, plug into Eq. (2.8), and apply the replacement rule in Eq. (2.19) to derive the isotropic Hamiltonian at arbitrary mass ratio in Eq. (2.17). As we will see, this procedure yields closed form results for certain infinite classes of tidal operators. We have verified that our results can also be obtained by the method of Ref. [175], and that we agree with all results collected in the Appendix of [198] up to the choice of normalization.

2.3.3.1 Kretschmann Scalar to a Power: $O = \text{tr} R^2$

As a first trivial example let us consider a tidal operator given by the Kretschmann scalar to a power. Computing $\text{tr} R^2 = \frac{12 r'^2}{A^6}$ in Schwarzschild coordinates and plugging into Eq. (2.8), we obtain the test-particle Hamiltonian,

$$\text{tr}_1 R^2 - A^o = \text{tr}_1^{\text{iso}} R^2 - A^o = \frac{1}{2} \frac{12 r'^2}{A^6} \quad (2.20)$$

which is automatically in isotropic form. Boosting to an arbitrary frame via Eq. (2.17), we obtain the isotropic Hamiltonian at arbitrary mass ratio,

$$\text{tr}_1^{\text{iso}} R^2 - A^o = \frac{1}{2} \frac{48 r'^2}{A^6} \quad (2.21)$$

For $\alpha = 1$, this agrees with previous results [175–177, 180]. Note the relative factor of $1 \cdot 2$ in the normalization of the tidal coefficient here as compared to [177].

2.3.3.2 Electric Weyl to a Power: $O = \text{tr} E^n$

Next, consider a tidal operator given by the trace of a power of the electric Weyl tensor,

$$E_{UV} = \frac{1}{2} E^a_{UV} \quad (2.22)$$

where at leading order in tidal coefficients, E is defined as in Eq. (2.4) with an energy component equal to ϵ_0 . The choice of coordinates for the metric will not affect

our answer at leading PM order since need only be evaluated on the Newtonian background. The mixed index electric Weyl tensor at leading PM order is

$$E^U_V = \frac{1}{\langle^2 A^3} \begin{pmatrix} \frac{3}{2} \frac{1}{A^2} & 0 & 0 & 0 \\ \frac{1}{A^2} & \frac{1}{2} \frac{1}{A^2} & 0 & 0 \\ 0 & 0 & \frac{1}{2} \frac{1}{A^2} & 0 \\ \frac{1}{2} \frac{1}{A^2} & 0 & 0 & \frac{1}{2} \frac{1}{A^2} \end{pmatrix} \quad (2.23)$$

and its eigenvalues are

$$\text{eig } E^U_V = 0, \frac{1}{2A^3}, \frac{1}{2A^3}, \frac{1}{2A^3} \quad (2.24)$$

See App. B for these expressions at all orders in the PM expansion. Thus the electric Weyl tensor to the power $\mathcal{O}(v^2)$ is

$$\mathbb{E}^{\text{iso}} = \text{Tr}^1 \mathbb{E} \quad \mathbb{E}^0 = \frac{1}{2A^3} \begin{pmatrix} 1 & 0 & 0 & 0 \\ 0 & 1 & 0 & 0 \\ 0 & 0 & 1 & 0 \\ 0 & 0 & 0 & 1 \end{pmatrix} \quad (2.25)$$

We then apply a binomial expansion and then eliminate \mathbb{E}^0 via the replacement in Eq. (2.19). Resumming terms analytically, we obtain the test-particle Hamiltonian in isotropic gauge,

$$\mathbb{H}_1^{\text{iso}} = \frac{1}{2} \frac{1}{A^3} \left(1 + \frac{3}{2} \frac{1}{A^2} + \frac{3}{2} \frac{1}{A^4} + \frac{3}{2} \frac{1}{A^6} + \dots \right) \quad (2.26)$$

Applying Eq. (2.17), we derive a closed form expression for the isotropic

Hamiltonian at arbitrary mass ratio,

$$\begin{aligned}
 {}_1^{iso} \rho_1 - \rho_2 - A^0 &= \frac{\langle 2}{2} \frac{\langle 2}{A^3} = \frac{1}{2} \frac{3}{2} - \frac{3}{2} - 3^1 f^2 \quad 1^0 \\
 &= \frac{1}{2} \frac{3}{2} - \frac{3}{2} - \frac{3}{2} \frac{1}{2} f^2 \quad 1^0 \\
 &= 0 \\
 &= \frac{\langle 2}{2} \frac{3^1 \langle 2^{02} 35 f^4 \quad 30 f^2 \quad 11}{8A^6} \\
 &= \frac{\langle 2}{2} \frac{6^1 \langle 2^{03} 40 f^4 \quad 36 f^2 \quad 7}{11A^9} \\
 &= \frac{\langle 2}{2} \frac{9^1 \langle 2^{04} 12155 f^8 \quad 22880 f^6 \quad 18590 f^4 \quad 7304 f^2 \quad 1231}{896A^{12}} \\
 &\vdots
 \end{aligned} \tag{2.27}$$

The case of $n = 2$ agrees with [175–177, 180] while $n = 3$ agrees with [175]. We can similarly compute arbitrary products of traces of electric Weyl, noting that due to the simple form of the eigenvalues a trace of any product can be reduced to products of $\text{tr} E^2$ and $\text{tr} E^3$.

2.3.3.3 Magnetic Weyl to a Power: $O = \text{tr} B^n$

We can repeat the same procedure for a tidal operator given by the trace of a power of magnetic Weyl,

$$B_{UV} = \frac{1}{2} \rho^a \rho^b \sim_{UV} \tag{2.28}$$

where $\sim_{UV} = \frac{1}{2} n_{UV}$ is the dual Weyl tensor. The mixed index magnetic Weyl tensor is

$$B^U_V = \frac{1}{2A^3} \begin{pmatrix} 0 & 0 & \frac{3}{2} \frac{1}{A^2} & 0 \\ 0 & 0 & \frac{3}{2} & 0 \\ \frac{3}{2A^2} & \frac{1}{A^2} & \frac{3}{2A^2} & 0 \\ 0 & 0 & 0 & 0 \end{pmatrix} \tag{2.29}$$

and its eigenvalues are

$$\text{eig } B^U_V = \left\{ 0, 0, \frac{3}{2} \frac{1}{A^2}, \frac{3}{2} \frac{1}{A^2} \right\} \tag{2.30}$$

with expressions at all PM orders in App. B. Any trace of an odd power of B will vanish. The tidal operator is then

$$\text{Tr}^1 B B^2 = 2 \frac{9 \langle 2^1 2^1 1 \rangle \langle 2^2 \rangle_0}{4 \langle 2^2 \rangle^8} \quad (2.31)$$

Expanding and replacing via Eq. (2.19), we obtain

$$\text{Tr}^1 B^3 = \frac{1}{2} \frac{\langle 3^1 \rangle}{\langle 2^3 \rangle} = \frac{13 \langle 2^0 \rangle \langle 1^2 \rangle_2}{12 \langle 2^0 \rangle \langle 1^2 \rangle_2} = \frac{1}{2} \frac{\langle 2^0 \rangle \langle 1^2 \rangle_2}{\langle 2^0 \rangle \langle 1^2 \rangle_2} \quad (2.32)$$

Again applying Eq. (2.17), we obtain

$$\begin{aligned} \text{Tr}^1 B^4 &= \frac{\langle 2 \rangle}{1^2} \frac{3 \langle 2^0 \rangle \langle 1^2 \rangle_2}{A^3} = \frac{13 \langle 2^0 \rangle \langle 1^2 \rangle_2}{12 \langle 2^0 \rangle \langle 1^2 \rangle_2} \\ &= \frac{\langle 2 \rangle}{1^2} \frac{15 \langle 2^0 \rangle \langle 1^2 \rangle_2}{16 A^6} \\ &= \frac{\langle 2 \rangle}{1^2} \frac{1287 \langle 2^0 \rangle \langle 1^2 \rangle_2}{1792 A^{12}} \\ &\vdots \end{aligned} \quad (2.33)$$

The case of $\ell = 2$ agrees with previous results [175–177, 180], and is consistent with the relation $\text{Tr}^1 B^2 = 8 \text{Tr}^1 E^2 = \text{Tr}^1 B^2$. Due to the simple form of the eigenvalues of magnetic Weyl, any product of its traces can be reduced to a single trace $\text{Tr}^1 B^2 = 2 \text{Tr}^1 B^2$.

2.3.4 Beyond Schwarzschild

Our method for extracting kinematic data from the geodesic equation applies quite generally. The only prerequisite for this approach is that the leading perturbative correction arises from a fan diagram in which the matter propagators are only on one side. For the remainder of this section we study scenarios in which the tidal interactions may be absent but the system still has some small perturbative correction that deviates from a binary system of Schwarzschild black holes in general relativity.

In the examples below we will assume a static, spherically symmetric metric that is a function of some small perturbative parameter. Plugging into Eq. (2.6), we then expand to linear order in the perturbative coefficient. Applying the replacement in Eq. (2.19), we obtain the test-particle Hamiltonian in isotropic coordinates, from

which we derive the associated scattering amplitude and Hamiltonian for arbitrary mass ratio via Eq. (2.16) and Eq. (2.17).

2.3.4.1 Higher Derivative Corrections

As a concrete example let us consider a modification to general relativity given by the leading higher derivative correction to graviton self-interactions,

$$\mathcal{L} = \frac{b}{16c} \int d^4x \sqrt{-g} \left[\frac{1}{2} \partial_\mu g_{\alpha\beta} \partial^\mu g^{\alpha\beta} + \frac{1}{2} \partial_\mu g^{\alpha\beta} \partial^\mu g_{\alpha\beta} - \frac{1}{2} \partial_\mu g^{\alpha\beta} \partial_\nu g^{\gamma\delta} \partial^\nu g_{\alpha\beta} \partial^\mu g_{\gamma\delta} \right]. \quad (2.34)$$

In four dimensions this operator is the leading correction to Einstein gravity which depends solely on the metric and cannot be eliminated by a field redefinition. Indeed, Eq. (2.34) is radiatively generated at two-loop order by graviton self-interactions in the Einstein-Hilbert term [199–202], albeit with a tiny coefficient.

It is clear that at linear order in b and leading PM order this correction contributes via a fan diagram which is accounted for by the geodesic equation. In the presence of Eq. (2.34) the perturbed metric is [188]

$$\begin{aligned} g_{\mu\nu}^1 A^0 &= \left(1 - \frac{5b}{A^7} \right) \delta_{\mu\nu} - \frac{27}{A^6} \partial_\mu \partial_\nu \mathcal{F}^2, \\ g_{AA}^1 A^0 &= \left(1 - \frac{54b}{A^6} \right) \frac{49b}{A^7} \mathcal{F}^2, \\ g^{-1} A^0 &= 1. \end{aligned} \quad (2.35)$$

Next, we plug Eq. (2.35) into Eq. (2.5) and expand $\mathcal{H} = \mathcal{H}_0 + b \mathcal{H}_1$. Solving to linear order in b , we derive the perturbed Hamiltonian,

$$\mathcal{H}_1^{\text{PN}} A^0 = \frac{27}{A^6} \mathcal{F}^2 \frac{1}{A^2}. \quad (2.36)$$

where we have truncated to leading PM order. Transforming to isotropic gauge via Eq. (2.19) yields

$$\mathcal{H}_1^{\text{iso}} A^0 = \frac{9}{2} \frac{\mathcal{F}^2}{A^6}. \quad (2.37)$$

We then boost to an arbitrary frame via Eq. (2.17) and sum over the exchange of bodies 1 and 2 since Eq. (2.34) generates contributions from fan diagrams as well as their flipped partners. We thus obtain

$$\mathcal{H}_1^{\text{iso}} \mathcal{H}_1^{\text{PN}} A^0 = \frac{18}{1} \frac{\langle \mathcal{F}_1^2 \rangle \langle \mathcal{F}_2^2 \rangle}{2A^6} \mathcal{F}^2 \frac{1}{A^2} \mathcal{H}_1^{\text{PN}} \mathcal{H}_1^{\text{PN}} \quad (2.38)$$

which agrees with known results in the PN [185, 186] and PM [185, 187, 198] expansions.

2.3.4.2 Electric Charge

Another application of our approach is the scattering of electrically charged bodies. While this is obviously irrelevant to astrophysical black holes, we can still derive scattering amplitudes of more formal interest. To begin, we consider the interactions of a neutral body of mass $m_1 = m$ and charge $q_1 = 0$ with an electrically charged body of mass $m_2 = M$ and charge $q_2 = Q$ in the test-particle limit, $m \ll M$. We can define a charge-to-mass ratio parameter,

$$f = \frac{Q^2}{4C M^2} \quad (2.39)$$

for which $0 \leq f \leq 1$. We take $f \ll 1$ to be perturbatively small, i.e., corresponding to a millicharged body.

To compute the geodesic motion we use the Reissner-Nördstrom metric in standard coordinates where

$$\begin{aligned} g_{CC}^{-1} A^0 &= 1 - \frac{f}{A} + \frac{f^2}{4A^2} \\ g_{AA}^{-1} A^0 &= 1 - \frac{f}{A} + \frac{f^2}{4A^2} \\ g^{-1} A^0 &= 1 \end{aligned} \quad (2.40)$$

We then expand the Hamiltonian up to linear order in the charge-to-mass ratio, $f \ll 1$, and solve the geodesic equation in Eq. (2.2) order by order in f . At zeroth order in f , H_0 is obtained by inserting the metric for an uncharged black hole in Schwarzschild coordinates into Eq. (2.5). Meanwhile, at first order we obtain

$$H_1^{-1} A^0 = \frac{f^2}{8A^2} \quad (2.41)$$

again truncating to leading PM order. Applying the replacement rule in Eq. (2.19), we trivially obtain the isotropic test-particle Hamiltonian,

$$H_1^{\text{iso}} A^0 = \frac{f^2}{8A^2} \quad (2.42)$$

Boosting to a general frame and lifting to arbitrary mass ratio we obtain

$$H_1^{\text{iso}} q_1 - q_2 A^0 = \frac{f^2}{4M^2} \quad (2.43)$$

which describes a neutral body interacting with a charged body at lowest order in the charge. The static limit of this expression agrees exactly with [203–206] after

including the charge-to-mass ratio $l = \frac{q^2}{4c^2}$ as defined in Eq. (2.39). This result is trivially generalized to include multiple electric and magnetic charges simply by inserting the sum of all charges squared into l .

We can verify Eq. (2.42) by mapping to isotropic coordinates at the very beginning of the calculation. In particular, we can apply the diffeomorphism,

$$A^{\mu\nu} \rightarrow \delta^{\mu\nu} A^0 = A^0 \left(1 - \frac{l}{2A} - \frac{l^2}{16A^2} \right) \quad (2.44)$$

which sends the metric components to

$$\begin{aligned} g_{\mu\nu}^{\text{iso}} A^0 &= \frac{1 - \frac{l^2}{16A^2}}{1 - \frac{l}{2A} - \frac{l^2}{16A^2}} A^0 \\ g_{AA}^{\text{iso}} A^0 &= g^{\text{iso}} A^0 = \left(1 - \frac{l}{2A} - \frac{l^2}{16A^2} \right)^{-2} A^0 \end{aligned} \quad (2.45)$$

Plugging into the geodesic equation and solving for $\gamma^{\text{iso}} = \gamma_0^{\text{iso}} + l \gamma_1^{\text{iso}}$ perturbatively in l we obtain exactly Eq. (2.42).

2.3.4.3 Electric Charge and Higher Derivative Corrections

Last but not least, we consider the case of a neutral body interacting with a charged body in the presence of both tidal distortion and higher derivative corrections to the Einstein-Maxwell system,

$$\begin{aligned} \mathcal{L} = & \frac{b}{2} \int d^4x \sqrt{-g} \left[O_1 \delta^{ab} \delta_{ab} + O_2 \delta^{ab} \delta_{ab} + O_3 \delta^{abcd} \delta_{abcd} + O_4 \delta^{ab} \delta_{ab} \delta_{ab} \delta_{ab} \right. \\ & + b \int d^4x \sqrt{-g} \left[2_1 \delta^{ab} \delta_{ab} + 2_2 \delta^{ab} \delta_{ab} + 2_3 \delta^{abcd} \delta_{abcd} + 2_4 \delta^{ab} \delta_{ab} \delta_{ab} \delta_{ab} \right. \\ & + 2_5 \delta^{abcd} \delta_{abcd} + 2_6 \delta^{abcd} \delta_{abcd} \delta_{ab} \delta_{ab} + 2_7 \delta^{abcd} \delta_{abcd} \delta_{ab} \delta_{ab} \\ & \left. \left. + 2_8 \delta^{abcd} \delta_{abcd} \delta_{ab} \delta_{ab} \delta_{ab} \delta_{ab} \right] \right] \end{aligned} \quad (2.46)$$

where the global prefactor b characterizes the overall size of the perturbations. Here we have included tidal corrections on the neutral body, so the geodesic equation is Eq. (2.2) where $\gamma = b$ and the tidal operator is

$$\mathcal{O} = O_1 \delta^{ab} \delta_{ab} + O_2 \delta^{ab} \delta_{ab} + O_3 \delta^{abcd} \delta_{abcd} + O_4 \delta^{ab} \delta_{ab} \delta_{ab} \delta_{ab} \quad (2.47)$$

Of course, tidal interactions of this form can be eliminated with a field redefinition, but this fact will provide a useful consistency check of our final answer. Finally, let

us define natural dimensionless coefficients,

$$\begin{aligned} 1_{1-2} &= 0_{1-2} & 1_{3-4} &= {}^18C^0 \cdot {}^10_{3-4} & 3_{1-2-3} &= {}^18C^0 \cdot {}^02_{1-2-3} \\ 3_{4-5-6} &= 2_{4-5-6} & 3_{7-8} &= {}^18C^0 \cdot {}^12_{7-8} \end{aligned} \quad (2.48)$$

for later convenience.

In this setup we consider the dynamics for arbitrary charge-to-mass ratio l but treating the the overall scale of the higher derivative corrections b as a small parameter. Since the \mathcal{Z}_β coefficients modify the extremality condition for large black holes they are intimately linked to the weak gravity conjecture [207], which mandates the instability of such objects to avoid remnant pathologies. Motivated by these connections, the linear in \mathcal{Z}_β corrections to the Reissner-Nördstrom metric were computed in [208], and were later used to demonstrate the equivalence of the weak gravity conjecture to certain positivity conditions on black hole entropy [209, 210] that are valid in any tree-level ultraviolet completion of Eq. (2.46). The corrected metric from [208] is

$$\begin{aligned} \delta_{CC} {}^1A^0 &= 1 - \frac{l'}{A} + \frac{l'^2}{4A^2} + b {}^1A^0 \\ \delta_{AA} {}^1A^0 &= 1 - \frac{l'}{A} + \frac{l'^2}{4A^2} + b {}^1A^0 \\ \delta {}^1A^0 &= 1 \end{aligned} \quad (2.49)$$

where the perturbation functions to leading PM order are

$$\begin{aligned} {}^1A^0 &= \frac{l'^2}{A^4} ({}^1\mathcal{Z}_2 + 4\mathcal{Z}_3 + 2\mathcal{Z}_4 + \mathcal{Z}_6^0) \\ {}^1A^0 &= \frac{l'^2}{A^4} ({}^2\mathcal{Z}_2 + 8\mathcal{Z}_3 + 8\mathcal{Z}_4 + 3\mathcal{Z}_5 + 4\mathcal{Z}_6^0) \end{aligned} \quad (2.50)$$

We again expand the Hamiltonian as $\mathcal{H} = \mathcal{H}_0 + b \mathcal{H}_1$, this time inserting Eq. (2.47) into Eq. (2.2) for $\mathcal{H} = b$ and solving order by order in b . At zeroth order in b we obtain the Hamiltonian for a test-particle in the Reissner-Nördstrom background while at linear order we find

$$\begin{aligned} {}^1\mathcal{H} &= \frac{l'^2}{A^4} \left(\frac{1}{8} \frac{l_1}{4} \frac{l_3}{4} \frac{l_4}{2} \frac{\mathcal{Z}_2}{2} + 2\mathcal{Z}_3 + \mathcal{Z}_4 + \frac{\mathcal{Z}_6^0}{2} \right. \\ &\quad \left. + \frac{\mathcal{Z}_2^2}{2} + \frac{3\mathcal{Z}_3}{2} + 6\mathcal{Z}_3 + 3\mathcal{Z}_4 + \frac{3\mathcal{Z}_5}{2} + \frac{5\mathcal{Z}_6^0}{2} \right) \\ &\quad + \frac{2}{A^2} \left(\frac{l_1}{4} \frac{l_3}{4} + \mathcal{Z}_2 + 4\mathcal{Z}_3 + 4\mathcal{Z}_4 + \frac{3\mathcal{Z}_5}{2} + 2\mathcal{Z}_6^0 \right) \end{aligned} \quad (2.51)$$

at leading PM order. Again applying Eq. (2.19), we obtain the isotropic gauge Hamiltonian in the test-particle limit,

$$\begin{aligned} \text{iso}_1 \mathcal{H}^0 = \frac{l'^2}{A^4} & \left[\frac{1}{8} \frac{1_1}{4} \frac{1_3}{4} \frac{1_4}{2} \frac{3_2}{2} \frac{2_3}{3} \frac{3_4}{2} \frac{3_6^0}{2} \right. \\ & \left. + \frac{3_1}{16} \frac{3_3}{16} \frac{3_5}{4} \frac{3_7}{4} \frac{3_9}{8} \frac{3_{10}^0}{2} \right]. \end{aligned} \quad (2.52)$$

Lifting to arbitrary mass ratio and inserting $l = \frac{e_2^2}{4c \langle_2^2}$, we obtain

$$\begin{aligned} \text{iso}_1 \mathcal{H}^0 = \frac{\langle_1^2 \langle_2^2}{4c \langle_1^2 A^4} & \left[\frac{3_1}{4} \frac{3_3}{4} \frac{3_5}{2} \frac{3_7}{2} \frac{3_9}{2} \frac{3_{11}^0}{2} \right. \\ & \left. + \frac{1_1}{4} \frac{1_3}{4} \frac{1_5}{2} \frac{1_7}{2} \frac{1_9}{2} \frac{1_{11}^0}{2} \right] f^2 \end{aligned} \quad (2.53)$$

which describes the dynamics of a neutral and charged body interacting via higher derivative corrections. A similar exercise can be done in the presence of electric and magnetic charges using the perturbed metric computed in [210].

A useful consistency check of Eq. (2.53) comes from invariance of physical quantities under field redefinitions of the graviton in the effective field theory defined by Eq. (2.46). In particular, we consider a redefinition of the metric [209, 211],

$$\begin{aligned} \delta_{ab} & \rightarrow \delta_{ab} + \chi \delta_{ab} \quad \text{where} \\ \chi \delta_{ab} & = A_1 \delta_{ab} + A_2 \delta_{ab} + 8c^{-1} A_3 \delta_{ab} + A_4 \delta_{ab} \quad (2.54) \end{aligned}$$

which corresponds to a shift of the tidal coefficients by

$$\begin{aligned} T_1 & \rightarrow T_1 + A_1 \\ T_2 & \rightarrow T_2 + A_2 \\ T_3 & \rightarrow T_3 + A_3 \\ T_4 & \rightarrow T_4 + A_4 \end{aligned} \quad (2.55)$$

and a shift of the higher dimension operator coefficients by

$$\begin{aligned}
3_1 & ! \quad 3_1 \quad A_1 \cdot 4 \quad A_2 \cdot 2 \\
3_2 & ! \quad 3_2 \quad A_1 \cdot 2 \\
3_3 & ! \quad 3_3 \\
3_4 & ! \quad 3_4 \quad A_1 \cdot 8 \quad A_3 \cdot 4 \quad A_4 \cdot 2 \\
3_5 & ! \quad 3_5 \quad A_1 \cdot 2 \quad A_3 \cdot 2 \\
3_6 & ! \quad 3_6 \\
3_7 & ! \quad 3_7 \quad A_3 \cdot 8 \\
3_8 & ! \quad 3_8 \quad A_3 \cdot 2 \cdot
\end{aligned} \tag{2.56}$$

We then find that Eq. (2.53) is invariant under Eq. (2.55) and Eq. (2.56), as expected since the isotropic Hamiltonian is proportional to the physical scattering amplitude at leading PM order.

2.4 All Orders in M

Test-particle dynamics can offer useful consistency checks for higher order PM calculations. In this section we present a prescription for analytically deriving the isotropic gauge Hamiltonian in the test-particle limit for a general tidal moment at all PM orders. From this quantity we then derive closed form expressions for the corresponding scattering amplitudes at all PM orders.

2.4.1 Diffeomorphism to Isotropic Coordinates

To begin, we apply a radius-dependent diffeomorphism $A \rightarrow \tilde{A}^0$ to an initial metric of the form in Eq. (2.3). The transformed line element is

$$3B^2 = 6c^1 5^1 A^{00} 3c^2 \quad 6_{AA}^1 5^1 A^{00} 5^0 1 A^{02} 3A^2 \quad 6 \quad 1 5^1 A^{00} 5^1 A^{02} 3 \quad \cdot \tag{2.57}$$

Any diffeomorphism of the metric will produce a new set of coordinates that automatically preserves the usual Poisson bracket structure of the corresponding phase space variables. Crucially, \tilde{A}^0 can be an implicit function of constants of motion such as the energy and the angular momentum, so we define

$$5^1 A^0 = A \quad _ _ 2^1 A \quad _ _ \circ _ \quad 2^1 A \quad _ _ \circ _ = \quad \tilde{\Theta} \quad \tilde{\Theta} \quad 20 1^1 A^0 \quad 20 \quad 2^1 \cdot \tag{2.58}$$

$0=0 \quad 1=0$

By construction, the nontrivial component of the diffeomorphism starts at linear order in the tidal coefficients so it only modifies tidal corrections to the Hamiltonian.

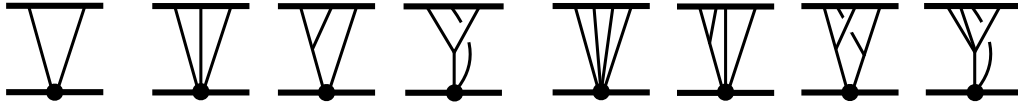


Figure 2.2: To all orders in PM, contributions to the scattering amplitude of a tidally distorted test particle are generated by fan diagrams. Shown here are examples at one-, two-, and three-loop orders.

For our purposes $Z^1 A^-$ will be a polynomial and only a finite number of the Z_{0l} coefficients will be nonzero. Note that since \mathbf{r} and \mathbf{p} are constants of motion, derivatives with respect to A yield $\delta^{01} A^0 = 1 \dots Z^1 A^-$, where we define

$$Z^1 A^- = \sum_{l=0}^{\infty} \sum_{m=0}^{\infty} Z_{0l}^m A^0 \dots \quad (2.59)$$

i.e., derivatives do not act on \mathbf{r} or \mathbf{p} .

Earlier, we solved the geodesic equation in Eq. (2.2) to obtain the Hamiltonian at zeroth order in the tidal coefficients \mathcal{H}^0 in Eq. (2.5). Since the tidal operator enters algebraically as a mass deformation, we can solve Eq. (2.2) at linear order in the tidal coefficient to obtain

$$\mathcal{H}^1 = \frac{\mathbf{p}^2}{6c^2 \delta^{00}} \dots \frac{\mathbf{r}^2}{6 A A^1 \delta^{00} \delta^{01} A^0} \dots \frac{\mathbf{r}^2}{6 \delta^{01} \delta^{00} \delta^{01} A^0} \dots \quad (2.60)$$

Noting the implicit δ dependence in $\delta^{01} A^0$, we then decompose Eq. (2.60) as $\mathcal{H}^1 = \mathcal{H}^1_{\delta} + \mathcal{H}^1_{\delta^2}$ and expand to linear order in δ . Similar to before, any term entering with an explicit factor of δ can be simplified since any appearance of δ can be replaced with the point-particle Hamiltonian in the absence of tidal effects, \mathcal{H}^0 . So concretely, the tidal operator should be evaluated as $\mathcal{H}^1_{\delta} = \mathcal{H}^1_{\delta^0}$ and the diffeomorphism functions should be evaluated as $Z^1 A^- = Z^1 A^-_{\delta^0}$ and $Z^1 A^- = Z^1 A^-_{\delta^0}$.

While $\mathcal{H}^1_{\delta^0}$ will in general have δ dependence we can simplify our calculation by using the isotropic coordinates in Eq. (2.9) for the initial metric before applying the diffeomorphism. We will assume this for the remainder of this section. By contrast, the tidal Hamiltonian $\mathcal{H}^1_{\delta^2}$ has δ^2 dependence even if the initial metric is in isotropic coordinates. Since $\mathcal{H}^1_{\delta^2}$ is quite complicated we do not write it explicitly here, but the procedure for computing it is completely mechanical and described above.

In the final step, we solve for the coefficients $2_{01}^1 A^0$ of the diffeomorphism to exactly cancel all r dependence in $g_{11}^1 A^0$. We immediately find that $g_{11}^1 A^0$ is a polynomial in r of finite degree, so only a finite number of terms are needed in the diffeomorphism in Eq. (2.58). Demanding that the coefficient of every positive power of r is zero then produces a set of differential equations for the coefficients $2_{01}^1 A^0$ in Eq. (2.58). These equations can be solved analytically, yielding closed form expressions for $2_{01}^1 A^0$, which turn out to be rational functions of the radius A .

Inserting the solved-for diffeomorphism back into $g_{11}^1 A^0$ yields the tidal Hamiltonian in isotropic coordinates,

$$g_{11}^{\text{iso}} A^0 = \frac{\delta_{cc}^{\text{iso}} A^0}{2} g_{11}^{\text{iso}} - \frac{\delta_{00}^{\text{iso}}}{2} \quad (2.61)$$

$$\approx \frac{\delta_{cc}^{\text{iso}} A^0}{2} - \frac{\delta_{AA}^{\text{iso}} A^0}{2} \frac{\delta_{cc}^{\text{iso}} A^0}{\delta_{AA}^{\text{iso}} A^0} \quad (2.62)$$

$$\approx \frac{\delta_{cc}^{\text{iso}} A^0}{2} - \frac{\delta_{AA}^{\text{iso}} A^0}{2} \quad (2.63)$$

where $2^1 A^0$ and $2^0 A^0$ are defined in Eq. (2.58) and Eq. (2.59), and must be solved for to eliminate all r dependence in $g_{11}^1 A^0$. Explicit expressions for these quantities will be presented in the examples given below. We again emphasize that all components of the initial metric are evaluated in isotropic coordinates. Importantly, every step of this procedure can be performed at all PM orders.

Following the procedure described in Sec. 2.2.2, we obtain the scattering amplitude in the test-particle limit,

$$\begin{aligned} M_{11}^1 A^0 &= \frac{1}{2} \delta_{AA}^{\text{iso}} A^0 g_{11}^{\text{iso}} - \frac{1}{2} M_0 \delta_{AA}^{\text{iso}} A^0 \\ &\approx \frac{1}{2} \delta_{AA}^{\text{iso}} A^0 - \frac{1}{2} \frac{\delta_{AA}^{\text{iso}} A^0}{\delta_{cc}^{\text{iso}} A^0} \frac{\delta_{cc}^{\text{iso}} A^0}{\delta_{AA}^{\text{iso}} A^0} \quad (2.64) \\ &\approx \frac{1}{2} \delta_{AA}^{\text{iso}} A^0 - \frac{1}{2} \delta_{cc}^{\text{iso}} A^0 \quad \text{iteration} \end{aligned}$$

together with $M_0^1 A^0$ as defined in Eq. (2.13). These results are in the test-particle limit and at all orders in PM, and are equivalent to the resummation of the Feynman diagrams shown in Fig. 2.2.

It is straightforward to compute the scattering angle to arbitrarily high PM order from either the Hamiltonian or the scattering amplitude (see for example [97, 98,

The constants of integration are fixed so that the coefficients $2_{01}^1 A^0$ do not blow up at large A .

$\gg E^{2\frac{1}{4}}$ $\gg B^{2\frac{1}{4}}$	$2_{00} = \frac{16}{5005d^1 d_1^{1011} \llcorner^{2,3}} 15015d^7, 7865d^6, 429d^5, 2405d^4, 1755d^3, 605d^2, 105d, 7$ $2_{01} = \frac{512d}{715^1 d_1^{1015} \llcorner^{4,5}} 6435d^7, 5005d^6, 3003d^5, 1365d^4, 455d^3, 105d^2, 15d, 1$ $2_{10} = \frac{16}{5005^1 d_1^{102} d_1^{109} \llcorner^{4,3}} 105105d^7, 43615d^6, 9009d^5, 17615d^4, 6825d^3, 695d^2, 105d, 7$
$\gg E^{3\frac{1}{4}}$	$2_{00} = \frac{1536}{1616615d^1 d_1^{1017} \llcorner^{2,5}} 1175720d^{10}, 764218d^9, 239666d^8, 98192d^7, 180880d^6, 124355d^5, 53599d^4, 15428d^3, 2884d^2, 315d, 15$ $2_{01} = \frac{147456d}{323323^1 d_1^{1021} \llcorner^{4,7}} 352716d^{10}, 293930d^9, 203490d^8, 116280d^7, 54264d^6, 20349d^5, 5985d^4, 1330d^3, 210d^2, 21d, 1$ $2_{10} = \frac{1536}{1616615^1 d_1^{102} d_1^{105} \llcorner^{4,5}} 11757200d^{10}, 6995534d^9, 1406342d^8, 1547816d^7, 1718360d^6, 870485d^5, 253897d^4, 38836d^3, 1372d^2, 315d, 15$
$\gg 3E^{2\frac{1}{4}}$	$2_{00} = \frac{768}{1616615d^1 d_1^{1017} \llcorner^{2,5}} 4849845d^{11}, 4555915d^{10}, 352716d^9, 388892d^8, 339796d^7, 226100d^6, 113050d^5, 41762d^4, 11039d^3, 1967d^2, 210d, 10$ $2_{01} = \frac{49152d}{323323^1 d_1^{1021} \llcorner^{4,7}} 1939938d^{11}, 1587222d^{10}, 293930d^9, 203490d^8, 116280d^7, 54264d^6, 20349d^5, 5985d^4, 1330d^3, 210d^2, 21d, 1$ $2_{10} = \frac{768}{1616615^1 d_1^{102} d_1^{105} \llcorner^{4,5}} 121246125d^{11}, 140351575d^{10}, 6113744d^9, 7795928d^8, 12684856d^7, 9405760d^6, 4318510d^5, 1262702d^4, 219051d^3, 17927d^2, 210d, 10$

Table 2.2: Coefficients specifying the diffeomorphism in Eq. (2.59) that goes to isotropic coordinates.

four-momentum that defines electric and magnetic Weyl. Our results in terms of $d = 4A \cdot '$ are shown in Table. 2.1.

As discussed, by setting all dependence in $_{1}^1 \text{?}-A-^{\circ}$ to zero we derive a system of differential equations which can be solved to obtain the $2_{01}^1 A^{\circ}$ coefficients in Table. 2.2, where all coefficients not shown are vanishing. The solutions for $\gg E^{4\frac{1}{4}}$ are too cumbersome to display here but are included in the supplemental material. Note that the solutions for $\gg E^{2\frac{1}{4}}$ and $\gg B^{2\frac{1}{4}}$ are the same since the difference of these operators is the Kretschmann scalar, which is independent of .

$\gg E^{2\frac{1}{4}}$	$\frac{64}{5005 \langle^{41} d, 1^{022} \cdot 4 \rangle_{\text{iso}}^0} 520 \langle^{41} d \ 1^0 d \ 462 d^6 \ 198 d^4 \ 33 d^3 \ 77 d^2 \ 33 d \ 5 \ 1 d \ 1^0 \rangle^8$ $\ 2 \langle^{22} \mathcal{P}^1 d \ 1^0 d^3 \ 300300 d^8 \ 49335 d^7 \ 160875 d^6 \ 143 d^5 \ 29965 d^4$ $\ 6955 d^3 \ 2465 d^2 \ 965 d \ 21 \ 1 d \ 1^0 \ 1^4 \ 7^4 \ 1 d \ 1^0 d^6 \ 525525 d^9 \ 53625 d^8$ $\ 226512 d^7 \ 16952 d^6 \ 26598 d^5 \ 4090 d^4 \ 3240 d^3 \ 464 d^2 \ 231 d \ 21$
$\gg E^{3\frac{1}{4}}$	$\frac{6144}{1616615 \langle^{41} d, 1^{028} \cdot 6 \rangle_{\text{iso}}^0} 2128 \langle^{41} d \ 1^0 d \ 12155 d^9 \ 7293 d^7 \ 1547 d^6 \ 1547 d^5 \ 1785 d^4 \ 935 d^3$ $\ 289 d^2 \ 51 d \ 4 \ 1 d \ 1^0 \rangle^8 \ 2 \langle^{22} \mathcal{P}^1 d \ 1^0 d^3 \ 51731680 d^{11} \ 13873496 d^{10}$ $\ 24043474 d^9 \ 7746186 d^8 \ 1224816 d^7 \ 2568496 d^6 \ 1146327 d^5$ $\ 164787 d^4 \ 48412 d^3 \ 23548 d^2 \ 3073 d \ 45 \ 1 d \ 1^0 \ 1^4$ $\ 7^4 \ 1 d \ 1^0 d^6 \ 94057600 d^{12} \ 42854994 d^{11} \ 33404014 d^{10} \ 12290150 d^9$ $\ 341734 d^8 \ 2042329 d^7 \ 875273 d^6 \ 38437 d^5 \ 73675 d^4 \ 17703 d^3$ $\ 1193 d^2 \ 765 d \ 45$
$\gg 3E^{2\frac{1}{4}}$	$\frac{3072}{1616615 \langle^{41} d, 1^{028} \cdot 6 \rangle_{\text{iso}}^0} 1064 \langle^{41} d \ 1^0 d \ 364650 d^{10} \ 875160 d^9 \ 838695 d^8 \ 376805 d^7$ $\ 13923 d^6 \ 23205 d^5 \ 17255 d^4 \ 7905 d^3 \ 2295 d^2 \ 391 d \ 30 \ 1 d \ 1^0 \rangle^8$ $\ 2 \langle^{22} \mathcal{P}^1 d \ 1^0 d^3 \ 484984500 d^{12} \ 1168812645 d^{11} \ 1130895675 d^{10}$ $\ 492156392 d^9 \ 23740500 d^8 \ 31407228 d^7 \ 20575100 d^6 \ 7936110 d^5$ $\ 1617546 d^4 \ 43225 d^3 \ 49959 d^2 \ 7350 d \ 30 \ 1 d \ 1^0 \ 1^4$ $\ 7^4 \ 1 d \ 1^0 d^6 \ 848722875 d^{13} \ 2214027725 d^{12} \ 2178109479 d^{11}$ $\ 849478049 d^{10} \ 32687600 d^9 \ 37685056 d^8 \ 22228214 d^7 \ 7028518 d^6$ $\ 558467 d^5 \ 421925 d^4 \ 157773 d^3 \ 19637 d^2 \ 510 d \ 30$
$\gg B^{2\frac{1}{4}}$	$\frac{64}{5005 \langle^{41} d, 1^{022} \cdot 4 \rangle_{\text{iso}}^0} 520 \langle^{41} d \ 1^0 d \ 462 d^6 \ 198 d^4 \ 33 d^3 \ 77 d^2 \ 33 d \ 5 \ 1 d \ 1^0 \rangle^8$ $\ 2 \langle^{22} \mathcal{P}^1 d \ 1^0 d^3 \ 300300 d^8 \ 49335 d^7 \ 160875 d^6 \ 143 d^5 \ 29965 d^4$ $\ 6955 d^3 \ 2465 d^2 \ 965 d \ 21 \ 1 d \ 1^0 \ 1^4 \ 7^4 \ 1 d \ 1^0 d^6 \ 525525 d^9 \ 53625 d^8$ $\ 226512 d^7 \ 16952 d^6 \ 26598 d^5 \ 4090 d^4 \ 3240 d^3 \ 464 d^2 \ 231 d \ 21$

Table 2.3: Contribution to the isotropic Hamiltonian \mathcal{H}_1 from tidal operators at all PM orders.

From our results in Table. 2.1 and Table. 2.2, we assemble the isotropic test-particle Hamiltonian from Eq. (2.61) as well as the scattering amplitude from Eq. (2.64). The tidal corrections to the isotropic Hamiltonian and the scattering amplitude (modulo iterations) are summarized in Table. 2.3 and Table. 2.4. We emphasize again that these results are valid at all PM orders in the test-particle limit. However, we have verified that our expressions for $\gg E^{2\frac{1}{4}}$ and $\gg B^{2\frac{1}{4}}$ are consistent with the 3PM results of [177] in the test-particle limit.

Last but not least, as a check of our results we compute the tidal corrections to the scattering angle at several PM orders for both $\mathcal{A}_1^1 \mathcal{P}^1 \mathcal{A}^0$ and $\mathcal{A}_1^{\text{iso}1} \mathcal{P}^1 \mathcal{A}^0$ and find that they agree, thus establishing their physical equivalence at that order. These

»E ^{2¼}	$\frac{64}{5005} \langle^4 1 d \rangle_{1^{05} d^6 1 d, 1^{08} \cdot 4}$ ${}^4 1 d, 1^{04} 525525 d^9 \quad 53625 d^8, 226512 d^7, 16952 d^6$ $26598 d^5 \quad 4090 d^4, 3240 d^3, 464 d^2 \quad 231 d \quad 21$ $\langle^4 165165 d^8, 12870 d^7, 20592 d^6, 20098 d^5, 13390 d^4$ $, 6050 d^3, 1760 d^2, 294 d, 21 \rangle 1 d \quad 1^{05}$ $2 \quad 2 \langle^2 1 d, 1^{02} 225225 d^9 \quad 102960 d^8, 65637 d^7, 16809 d^6$ $, 3367 d^5, 2865 d^4, 775 d^3 \quad 501 d^2 \quad 252 d \quad 21 \rangle 1 d \quad 1^{02}$
»E ^{3¼}	$\frac{6144}{1616615} \langle^4 1 d \rangle_{1^{05} d^6 1 d, 1^{014} \cdot 6}$ ${}^4 1 d, 1^{04} 94057600 d^{12} \quad 42854994 d^{11}, 33404014 d^{10}$ $, 12290150 d^9, 341734 d^8 \quad 2042329 d^7 \quad 875273 d^6 \quad 38437 d^5$ $, 73675 d^4, 17703 d^3 \quad 1193 d^2 \quad 765 d \quad 45$ $\langle^4 16460080 d^{11}, 1352078 d^{10}, 2188648 d^9, 2278442 d^8$ $, 1777792 d^7, 1073975 d^6, 501676 d^5, 177821 d^4, 46144 d^3$ $, 8239 d^2, 900 d, 45 \rangle 1 d \quad 1^{05} \quad 2 \quad 2 \langle^2 1 d, 1^{02} 42325920 d^{12}$ $28981498 d^{11}, 9360540 d^{10}, 4543964 d^9, 1566550 d^8$ $, 526167 d^7, 271054 d^6, 126350 d^5, 25263 d^4 \quad 5845 d^3$ $4266 d^2 \quad 810 d \quad 45 \rangle 1 d \quad 1^{02}$
»3E ^{2¼}	$\frac{3072}{1616615} \langle^4 1 d \rangle_{1^{05} d^6 1 d, 1^{014} \cdot 6}$ ${}^4 1 d, 1^{04} 848722875 d^{13} \quad 2214027725 d^{12}, 2178109479 d^{11}$ $849478049 d^{10}, 32687600 d^9, 37685056 d^8, 22228214 d^7$ $, 7028518 d^6, 558467 d^5 \quad 421925 d^4 \quad 157773 d^3 \quad 19637 d^2$ $510 d \quad 30 \rangle \langle^4 266741475 d^{11} \quad 274089725 d^{10}$ $6231316 d^9 \quad 4458692 d^8 \quad 2665396 d^7 \quad 1311380 d^6$ $520030 d^5 \quad 161462 d^4 \quad 37639 d^3 \quad 6167 d^2 \quad 630 d$ $30 \rangle 1 d \quad 1^{06} \quad 2 \quad 2 \langle^2 1 d, 1^{02} 363738375 d^{13}$ $1045215080 d^{12}, 1047213804 d^{11} \quad 357321657 d^{10}$ $, 8947100 d^9, 6277828 d^8, 1653114 d^7 \quad 907592 d^6$ $1059079 d^5 \quad 465150 d^4 \quad 107814 d^3 \quad 12287 d^2$ $540 d \quad 30 \rangle 1 d \quad 1^{02}$
»B ^{2¼}	$\frac{64}{5005} \langle^4 1 d \rangle_{1^{05} d^6 1 d, 1^{08} \cdot 4}$ ${}^4 1 d, 1^{04} 525525 d^9 \quad 53625 d^8, 226512 d^7, 16952 d^6$ $26598 d^5 \quad 4090 d^4, 3240 d^3, 464 d^2 \quad 231 d \quad 21$ $\langle^4 75075 d^7, 62205 d^6, 41613 d^5, 21515 d^4, 8125 d^3$ $, 2075 d^2, 315 d, 21 \rangle 1 d \quad 1^{06} \quad 2 \quad 2 \langle^2 1 d, 1^{02} 225225 d^9$ $102960 d^8, 65637 d^7, 16809 d^6, 3367 d^5, 2865 d^4, 775 d^3$ $501 d^2 \quad 252 d \quad 21 \rangle 1 d \quad 1^{02}$

Table 2.4: Contribution to the scattering amplitude M_1 from tidal operators at all PM orders.

$\gg E^{2\frac{1}{4}}$	$\frac{45cD^4 \cdot 135D^4 \cdot 40D^2 \cdot 16^0 <^4 \cdot 2}{512^6} \gg \frac{12D^3 \cdot 160D^6 \cdot 288D^4 \cdot 168D^2 \cdot 35^0 <^5 \cdot 3}{35^7}$ $\gg \frac{63cD^2 \cdot 19009D^8 \cdot 20790D^6 \cdot 16800D^4 \cdot 5600D^2 \cdot 640^0 <^6 \cdot 4}{8192^8}$ $\gg \frac{4 \cdot 14336D^{11} \cdot 39424D^9 \cdot 40128D^7 \cdot 18480D^5 \cdot 3696D^3 \cdot 231D^0 <^7 \cdot 5}{77^9} \gg \mathbb{O}1 \cdot 6_0$
$\gg E^{3\frac{1}{4}}$	$\frac{96D^7 \cdot 140D^4 \cdot 44D^2 \cdot 11^0 <^7 \cdot 3}{385^9} \gg \frac{189cD^6 \cdot 13861D^6 \cdot 7128D^4 \cdot 3960D^2 \cdot 640^0 <^8 \cdot 4}{32768^{10}}$ $\gg \frac{8D^5 \cdot 140320D^8 \cdot 98280D^6 \cdot 82940D^4 \cdot 27885D^2 \cdot 3003^0 <^9 \cdot 5}{1001^{11}} \gg \mathbb{O}1 \cdot 6_0$
$\gg E^{4\frac{1}{4}}$	$\frac{891cD^{10} \cdot 12155D^8 \cdot 25740D^6 \cdot 22880D^4 \cdot 9856D^2 \cdot 1792^0 <^{10} \cdot 4}{1048576^{12}}$ $\gg \frac{192D^9 \cdot 12903040D^{10} \cdot 8273664D^8 \cdot 9550464D^6 \cdot 5697720D^4 \cdot 1763580D^2 \cdot 230945^0 <^{11} \cdot 5}{1616615^{13}} \gg \mathbb{O}1 \cdot 6_0$
$\gg 3E^{2\frac{1}{4}}$	$\frac{1575cD^6 \cdot 135D^4 \cdot 40D^2 \cdot 16^0 <^6 \cdot 2}{1024^8} \gg \frac{96D^5 \cdot 13680D^6 \cdot 7392D^4 \cdot 4752D^2 \cdot 1155^0 <^7 \cdot 3}{385^9}$ $\gg \frac{1701cD^4 \cdot 121593D^8 \cdot 56760D^6 \cdot 53040D^4 \cdot 21120D^2 \cdot 3200^0 <^8 \cdot 4}{32768^{10}}$ $\gg \frac{8D^3 \cdot 1469440D^{10} \cdot 4615520D^8 \cdot 5479760D^6 \cdot 3045900D^4 \cdot 786786D^2 \cdot 75075^0 <^9 \cdot 5}{1001^{11}} \gg \mathbb{O}1 \cdot 6_0$
$\gg B^{2\frac{1}{4}}$	$\frac{225cD^6 \cdot 17D^2 \cdot 8^0 <^4 \cdot 2}{512^6} \gg \frac{24D^5 \cdot 180D^4 \cdot 144D^2 \cdot 63^0 <^5 \cdot 3}{35^7} \gg \frac{1323cD^4 \cdot 4 \cdot 1429D^6 <^6 \cdot 990D^4 <^6 \cdot 720D^2 <^6 \cdot 160 <^6 \cdot 0}{8192^8}$ $\gg \frac{32D^3 \cdot 1792D^8 \cdot 4928D^6 \cdot 4752D^4 \cdot 1848D^2 \cdot 231^0 <^7 \cdot 5}{77^9} \gg \mathbb{O}1 \cdot 6_0$

Table 2.5: Contribution to the scattering angle j_1 from tidal operators at several PM orders.

scattering angles are presented in Table. 2.5. The Hamiltonian, amplitude, and scattering angle for $\gg E^{4\frac{1}{4}}$ are included in the supplementary material.

2.5 Conclusions

Geodesic motion encodes all the kinematic data needed to reconstruct any scattering process mediated by fan diagrams, i.e., topologies in which only propagators of one of the bodies is present. In this work we have exploited this fact to derive the complete conservative dynamics—in the form of amplitudes and isotropic Hamiltonians—at leading PM order in various scenarios which deviate perturbatively from the minimal setup of a black hole binary system in general relativity. As we have demonstrated, our approach only entails simple algebraic manipulations and can be applied to a wide range of examples such as tidal operators and higher derivative corrections to gravitational or electromagnetic interactions. Furthermore, we have derived a method for computing the test-particle scattering amplitude to all PM orders, which could offer a useful check of higher PM calculations.

Note: During the completion of this project we learned of the interesting concurrent

work of Ref. [198], which has similar results at leading PM order obtained via direct evaluation of multi-loop scattering amplitudes. Their approach is nicely complementary to our own and where our results overlap they agree completely. We thank the authors of Ref. [198] for sharing their work with us before submission.

Chapter 3

EFFECTIVE FIELD THEORY FOR EXTREME MASS RATIO BINARIES

This chapter reproduces the contents of the publication: Clifford Cheung, Julio Parra-Martinez, Ira Z. Rothstein, Nabha Shah, and Jordan Wilson-Gerow. Phys. Rev. Lett. 132, 091402 – Published 29 February 2024.

3.1 Introduction

The landmark observation of gravitational waves by LIGO and Virgo [100] has sparked a scientific revolution in the fields of astrophysics and gravitation. The recent discovery of a stochastic gravitational wave background by NANOGrav [212] has added fuel to this fire.

In parallel with these longstanding experimental efforts is a decades-long theoretical program to derive the *ab initio* predictions of general relativity (GR). This endeavor has generated numerous lines of attack, including numerical relativity (NR) [62, 213, 214], effective one body (EOB) theory [60], self-force (SF) methods [215–217], and perturbative post-Newtonian (PN) calculations using traditional methods in GR [218] and effective field theory (EFT) [65]. More recently, the modern scattering amplitudes program [15, 219–223] has been retooled towards these efforts in what is known as the post-Minkowskian (PM) expansion [20, 32, 34, 37, 40, 94–96, 176, 224–236]. Of course, all of these approaches are highly complementary (see, e.g., [41, 190, 191, 237–251]).

Looking to the future, we can expect new insights into the physics of ultra-compact binaries and extreme mass ratio inspirals (EMRIs) from the proposed LISA experiment [252, 253]. However, the EMRI problem is intractable in the vast majority of theoretical approaches, including NR, PN, and PM. The only extant theoretical approach to the EMRI problem is SF theory, which uses a hybrid of analytical and numerical approaches to calculate the motion of a small companion orbiting a much heavier body, as an expansion in their mass ratio,

$$\text{---} = \frac{\llcorner}{\llcorner} \cdot \tag{3.1}$$

In SF theory, the light body induces a perturbation of the black hole spacetime, which then reacts back onto the light body, and so on and so forth (cf. some

reviews [215–217] and state of the art computations at $\mathcal{O}^1_{\text{SF}}$, or 1SF, for generic bound orbits in Kerr [254, 255] and at $\mathcal{O}^1_{\text{2SF}}$, or 2SF, for quasicircular orbits in Schwarzschild [256–258]).

In this letter we revisit the classic problem of describing the dynamics of a heavy and light body as a systematic expansion in their mass ratio, μ . Notably, in the limit of vanishing μ , many physical systems are analytically *solvable*. For example, in the textbook solution to the Rutherford scattering problem, high-energy alpha particles impinge on a gold nucleus described entirely by a rigid $1 \cdot A$ background. Of course, this description is only valid in the limit that the gold nucleus is infinitely heavy—which begs the question, how does one systematically compute the leading nontrivial correction in μ ? Can this effect be encoded as an *operator* added to the theory of a $1 \cdot A$ background?

Analogous logic holds for gravity. The limit of vanishing mass ratio corresponds to the 0SF dynamics of a probe particle in geodesic motion on a Schwarzschild background. These background dynamics are understood analytically to all orders in perturbation theory. But is there an *operator* that encodes the 1SF order corrections, and so on and so forth?

Here we offer an affirmative answer to this question in the context of massive, gravitationally interacting *point particles*. At 1SF order, the dynamics are described by a standard background field theory of a light particle worldline coupled to graviton fluctuations in a Schwarzschild background, supplemented by a “recoil operator” encoding the wobble of the background black hole induced by its interactions with the light particle:

$$\mathcal{O}_{\text{recoil}} = \frac{\kappa^2}{2} \int d\tau \sqrt{-g} \chi^{\mu\nu} \frac{1}{m_g^2} \chi_{\mu\nu} \quad (3.2)$$

Here we have defined $\chi^{\mu\nu} = g^{\mu\alpha} g^{\beta\nu} \chi_{\alpha\beta}$ and $\chi_{\mu\nu} = \chi_{\mu\nu} - \bar{\chi}_{\mu\nu}$ is the difference between the connection and its background value. Physically, Eq. (3.2) is generated by integrating out the fluctuations of the heavy body trajectory at 1SF. In our framework, the 2SF and higher order analogs of the recoil operator can be systematically computed as well.

The key insight in our analysis is to reinterpret the known analytic formulas of classical GR for the Schwarzschild metric and the geodesics of probe particles as implicit resummations of an infinite class of Feynman diagrams in *flat space* graviton perturbation theory [94, 105, 259]. In particular, the Schwarzschild background,

$\delta_a^1 G^0 = \int_a \mathbb{W}_a^1 G^0$, is given by the infinite sum of flat-space Feynman diagrams that compute the graviton one-point function induced by a heavy particle:

$$\mathbb{W}_a = \begin{array}{c} \text{[Diagram 1]} \\ \text{[Diagram 2]} \\ \text{[Diagram 3]} \\ \text{[Diagram 4]} \end{array} \quad (3.3)$$

Similarly, the trajectories of geodesics implicitly encode an infinite set of flat-space Feynman diagrams describing interactions of light and heavy particles.

Of course, it is far easier to manipulate known analytic solutions in classical GR than to build them order by order in point particle perturbation theory. For this reason, we exactly invert the sequence of logic of [105], and use the Schwarzschild metric and geodesic trajectories to extract perturbative information. In doing so, we can perform PM calculations in a streamlined way that should pay dividends at high PM orders.

Crucially, having ascertained which flat space Feynman diagrams are resummed by the dynamics of a classical probe, we immediately see that there are missing contributions—and at 1SF order these are entirely accounted for by the recoil operator in Eq. (3.2). Furthermore, by explicitly framing classical GR in terms of flat space perturbation theory, we can use standard tools such as dimensional regularization to deal with point-like or self-energy divergences.

Applying our framework—which at 1SF is simply the background field method plus a recoil operator—we derive old and new results governing conservative gravitational dynamics up to 3PM accuracy. In particular, we compute the radial action for two massive, gravitationally interacting particles without spin, including the effects of scalar or vector fields which are coupled directly to the light body. While the results of the present work are limited to 1SF gravity, a longer forthcoming work (see Chapter 4), will contain many technical details on the systematic derivation of the EFT at 1SF, 2SF, and beyond, as well as applications to non-gravitational theories.

3.2 Basic Setup

We begin with the Einstein-Hilbert action coupled to a pair of massive particles [20, 176, 260],

$$S = \frac{1}{16c} \int d^4x \sqrt{-g} \left(R - \sum_{\beta=1}^D \frac{1}{2} \partial_\mu \tilde{\phi}_\beta \partial^\mu \tilde{\phi}_\beta - \sum_{\beta=1}^D m_\beta^2 \tilde{\phi}_\beta^2 \right) \quad (3.4)$$

where we work in mostly minus metric throughout. Here we have gauge fixed the einbein to unity, so $\tilde{\theta}_\beta^2 = 1$.

Our construction is based on expanding the trajectories and metric about their OSF values,

$$G_{\hat{g}} = \hat{G}_{\hat{g}} + \chi G_{\hat{g}} \quad \text{and} \quad \hat{g}_{\hat{a}} = \hat{g}_{\hat{a}} + \chi \hat{g}_{\hat{a}}. \quad (3.5)$$

Here $\hat{G}_{\hat{g}} = \hat{g}_{\hat{a}} \in \mathcal{O}^1_{-00}$ are *explicit functions* describing OSF dynamics of a probe in a Schwarzschild background. Meanwhile, $\chi G_{\hat{g}} = \chi \hat{g}_{\hat{a}} \in \mathcal{O}^1_{-10}$ are *dynamical modes* controlling all contributions at 1SF and higher. In particular, $\chi G_{\hat{g}}$ is the deviation from geodesic motion, while $\chi \hat{g}_{\hat{a}}$ is the graviton perturbation propagating in a Schwarzschild background. Inserting Eq. (3.5) into Eq. (3.4), the action becomes literally that of the background field method, so $\mathcal{I} = \mathcal{I}_{\text{BF}}[\hat{g}, \chi \hat{g}, \chi G_{\hat{g}}]$.

An important conceptual point now arises. In standard SF theory, the totality of the dynamics is described by a background field action $\mathcal{I}_{\text{BF}}[\hat{g}, \chi \hat{g}, \chi G_{\hat{g}}]$ in which the only degrees of freedom are the geodesic deviation of the light worldline, $\chi G_{\hat{g}}$, and the fluctuation graviton, $\chi \hat{g}_{\hat{a}}$. How can such a theory emerge from our starting point of a pair of gravitationally interacting point particles, which we have just shown is described by $\mathcal{I}_{\text{BF}}[\hat{g}, \chi \hat{g}, \chi G_{\hat{g}}]$? What happened to the heavy particle? Furthermore, how do we make sense of singular self-force contributions in background field method such as $\hat{g}_{\hat{a}}^1 \hat{g}^0$? As we will see, while the standard SF theory is perfectly fine, these naive confusions can be explained and handled quite simply in our setup.

3.3 Background Field Theory as Resummation

Let us first consider the dynamics at OSF order, corresponding to an infinite mass ratio between the heavy and light particles. In this limit the heavy particle is undeflected, so it travels on an inertial trajectory,

$$\hat{g}^{\hat{a}} = D^{\hat{a}} g. \quad (3.6)$$

while serving as a point source for the background gravitational field, which is the boosted Schwarzschild metric.

Famously, this metric can be computed order by order using graviton perturbation theory about flat space [105]. Concretely, the Feynman diagrams shown in Eq. (3.3) form the one-point function of the flat space graviton, which is equal to the difference between the Schwarzschild metric and the flat metric. The precise choice of coordinates for the resulting metric are dictated by the choice of field basis and

Note that the action itself can have explicit powers of χ , e.g., in the contribution to Eq. (3.4) from the light particle.

gauge fixing in the original flat space perturbative formulation. This essential procedure has been refined and reformulated in many contexts, for instance using modern amplitudes methods [94, 259]. In the present work, we will use the boosted Schwarzschild metric in isotropic gauge,

$$\tilde{g}_{ab} = \frac{5^{-1}A^0}{5^{-1}A^0} \left[-\frac{5^{-1}A^0}{5^{-1}A^0} dt^2 - \frac{5^{-1}A^0}{5^{-1}A^0} D^i D^j a^i a^j \right] \quad (3.7)$$

where $5^{-1}A^0 = 1 - \frac{A_\zeta}{4A}$. Here $A = \sqrt{D^2 G^2 + G^2}$ is the boosted radial distance from the black hole center and $A_\zeta = 2r_s$ is the Schwarzschild radius. Expanding the metric in powers of Newton's constant,

$$\begin{aligned} \tilde{g}_{ab} &= \frac{A_\zeta}{A} \left[-dt^2 - 2D^i D^j a^i a^j \right] \\ &+ \frac{1}{8} \frac{A_\zeta^2}{A^2} \left[-3D^i D^j a^i a^j \right] + \dots \end{aligned} \quad (3.8)$$

we obtain the one-point function of the flat space graviton at all orders in the PM expansion.

Note that none of this implies that the Schwarzschild solution of GR is not a *vacuum* solution. Rather, the claim is that the PM expansion of the Schwarzschild metric coincides order by order with the gravitational field of an inertial point source.

Now, let us move on to the light particle, whose OSF trajectory is a probe geodesic in a Schwarzschild spacetime. While these trajectories are analytically soluble [247, 261], their closed-form expressions are better known in parametric form, i.e., $A^1 \lambda^0$, rather than in explicit time domain, i.e., $A^1 g^0$ and $\lambda^1 g^0$. Nevertheless, starting from the known parametric solutions one can mechanically extract the time domain expression for the probe trajectory order by order in the PM expansion, $\tilde{G}_I = \sum_{I=0}^{\infty} \tilde{G}_I$, where the first few terms in isotropic coordinates are

$$\begin{aligned} \tilde{G}_0 &= 1 - D^i D^j g^i g^j \\ \tilde{G}_1 &= \frac{A_\zeta \operatorname{arcsinh} \frac{Eg}{f} - f^2 E^2 - 1^0 D^i D^j g^i g^j}{A_\zeta^2 E^2 + 1^0 \sqrt{f^2 + E^2 g^2} - 1} \quad (3.9) \\ &\quad \frac{2E^3}{2f^2 E^2} \end{aligned}$$

Here $f = D^i D^j g^i g^j$, $E = \sqrt{f^2 + 1^0 g^2}$, $1 = \frac{1}{\sqrt{1 + \frac{1^0}{f^2}}}$ is the impact parameter, and the trajectories have been computed with time-symmetric boundary conditions. As we will see, the above 0PM and 1PM expressions are sufficient to compute up to 3PM in the conservative dynamics. As described in App. C, these geodesic trajectories can

be used to directly extract data about corresponding perturbative Feynman diagrams in flat space.

In summary, background metrics and geodesic trajectories can be straightforwardly distilled into remarkably simple PM integrands for perturbative calculations at higher orders. This will be explained in detail in Chapter 4.

3.4 Black Hole Recoil

The last puzzle piece is the *recoil* of the black hole background. When we center a static Schwarzschild black hole at the origin, it stays there for all eternity, past and future. As a result, the background metric is secretly defined in the *rest frame* of the physical black hole, which need not be an inertial frame. Indeed, at 1SF order, the light particle should induce a nonzero deflection of the heavy particle.

In the context of standard SF theory, this subtle effect is accounted for by the nonradiating part of the metric perturbations, captured in the low multipole moments [262, 263] whose computation requires imposing suitable boundary conditions at the event horizon.

Since our starting point is a point particle effective field theory, there is an easier way: simply compute the path integral over the geodesic deviation of the heavy particle, χG . At 1SF order this is a Gaussian integral which can be done exactly, yielding exactly the recoil operator in Eq. (3.2). The corrections at 2SF order and higher are similarly computed in a mechanical fashion.

To summarize, the background field theory defined by a light particle worldline interacting with fluctuation gravitons in a Schwarzschild background is *not* equivalent to a theory of heavy and light particles interacting gravitationally. To match the latter, one must supplement the former with the recoil operator. Doing so yields our main result, which is the action for our EFT of extreme mass ratios at 1SF order,

$$\Gamma_{\text{EFT}} = \Gamma_{\text{BF}} + \delta\Gamma - \mathcal{G}_I - \chi G_I + \Gamma_{\text{recoil}} \quad (3.10)$$

This quantity is precisely the standard background field action for the light particle interacting with fluctuating gravitons in a Schwarzschild background, plus the recoil operator in Eq. (3.2). See App. C for a summary of the Feynman rules in this EFT. Note that a key advantage of the recoil operator is that it obviates the need to iteratively solve for the deflection of the heavy particle and its concomitant corrections to the background spacetime.

Since the recoil operator has a $1/m_G^2$ pole, it requires a choice of boundary conditions, which corresponds to an δn prescription for the χG propagator. For the present work, we only consider conservative scattering, for which the propagator for the heavy particle fluctuation never goes on-shell and the choice of δn is thus immaterial (see Chapter 4 for details). Here we use the Feynman prescription for simplicity, but more generally one should deploy the recoil operator with the δn prescription appropriate to the physical process in question.

From the viewpoint of traditional EFT, it is somewhat peculiar to integrate out states to generate a *nonlocal* operator. One usually restricts consideration to a kinematic regime in which such effects becomes effectively local—and indeed for the conservative region this is the case. Still, one might reasonably worry about power counting ambiguities stemming from these nonlocal interactions. Nevertheless, since the masses of particles are effectively coupling constants in the worldline formalism, higher order insertions of nonlocal operators such as the recoil operator are suppressed in the SF expansion.

3.5 Self-Energy and Regularization

Our derivation of the recoil operator in Eq. (3.2) actually entails a critical subtlety involving self-energy and its regularization. Strictly speaking, the equation for the heavy particle geodesic in its own Schwarzschild background is

$$\delta^{\mu\nu} \partial_\mu \partial_\nu \mathcal{G}^0 + \delta^{\mu\nu} \Gamma_{\mu\nu}^{\alpha\beta} \mathcal{G}^0 = 0. \quad (3.11)$$

The second term is singular because it involves the background connection at the position of the heavy particle.

In traditional SF theory, self-energy divergences of this type afflict the light particle dynamics. However, in the present context of point particle effective field theory, all such divergences are trivially eliminated using dimensional regularization. In particular, any self-energy divergence ultimately arises in perturbation theory as a self-energy diagram. For example, the self-energy contribution from the Newton potential arises from the $A \rightarrow 0$ limit of $1/A \sim 3^{3/2} n @ \ell^{\delta @ A} @^2$. However, taking the limit inside the integral yields a scaleless integrand that vanishes *by definition* in dimensional regularization.

The upshot here is that we can simply drop all PM corrections involving the background metric evaluated at \mathcal{G} , so dimensional regularization effectively sets $\delta^{\mu\nu} \partial_\mu \partial_\nu \mathcal{G}^0 = \Gamma_{\mu\nu}^{\alpha\beta} \mathcal{G}^0 = 0$. While these equations may appear

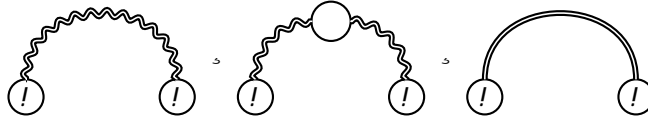


Figure 3.1: Background-field Feynman diagrams contributing to the 1SF radial action. The circles denote the light geodesic source (!) and the heavy recoil operator (\ominus). The double lines denote background field propagators for the graviton (wavy) and the scalar or vector fields (straight).

at odds with general covariance, they are not. Rather, the statement is that formally $\delta_{\cdot a}^{\cdot 1} \mathcal{G}^{\cdot 0}$ is generally covariant, but its difference from $\Gamma_{\cdot a}$ at the point \mathcal{G} is zero in dimensional regularization. Note that numerous terms have been dropped in the recoil operator in Eq. (3.2) on account of dimensional regularization. Furthermore, the indices of the recoil operator are implicitly contracted with flat space metrics, rather than the divergent background metric. As we will see later on, this prescription exactly yields known correct results for the conservative dynamics.

3.6 Gravitational Scattering with Additional Fields

Our effective field theory can also be used to compute new results at 1SF order. As it turns out, the SF theory community has a particular interest in a model in which the gravitational action in Eq. (3.4) is supplemented with a massless scalar or vector which couple directly to the light particle but interact only gravitationally with the heavy particle [e.g. 247, 264]. This is a well-known toy model for the full gravitational SF problem. Thus we add to Eq. (3.4) the additional scalar and vector contributions,

$$\begin{aligned} \mathcal{L} = & \int^4 \mathcal{G}^{\cdot 0} \left[\frac{1}{2} \dot{r}^{\cdot 2} + \frac{1}{2} b^{\cdot 2} - \frac{1}{4} \dot{a}^{\cdot 2} \right. \\ & \left. + \int_I 3g H_I \cdot {}^1 G_I^{\cdot 0} + \int_I \cdot {}^1 G_I^{\cdot 0} \theta_I^{\cdot} \right]. \end{aligned} \quad (3.12)$$

For generality we have included a nonminimal coupling of the scalar to gravity.

Since the heavy particle does not couple directly to the new fields, the recoil operator is unaffected. However, new contributions to scattering are induced by the gravitational interactions of the scalar and vector fields sourced by the light particle. At 1SF these arise solely from the background field diagrams.

3.7 Calculation of the Radial Action

As a consistency check of our formalism, we will calculate the radial action for conservative dynamics at 1SF order. The radial action is a convenient gauge-invariant quantity encoding the conservative scattering dynamics. Moreover, it is a generating function for the time-delay and scattering angle. Common approaches to the PM radial action involve applying simple maps to scattering amplitudes [224, 225] or to momentum impulses [98, 99]. Here, we will instead directly calculate the radial action by evaluating the “on-shell” value of the EFT action in Eq. (3.10), which physically corresponds to plugging in the solutions to the classical equation of motion. The resulting object is the radial action, which takes the form

$$A_{\text{EFT on-shell}}^{\text{radial}} = \sum_{l=0}^{\infty} \mathcal{A}_l \quad (3.13)$$

where l labels the order in the SF expansion and each \mathcal{A}_l contains all orders in ϵ . In what follows we perturbatively expand the 1SF contribution \mathcal{A}_1 in powers of ϵ .

In the language of quantum field theory, Eq. (3.13) is calculated by evaluating the path integral over all the particle and graviton degrees of freedom. At 1SF order, the radial action is equal to the sum of connected tree diagrams in which the light body sources a graviton, which propagates in the full Schwarzschild background, has an arbitrary number of recoil operator insertions, and then returns to the light body. These manipulations are equivalent to the Feynman rules in App. C.

Notably, the resulting tree diagrams effectively generate loop integrals arising from Fourier transforms in the worldline trajectories. These integrals can be easily evaluated in dimensional regularization using integration-by-parts (IBP) identities [222] and canonical differential equations [223], as explained, e.g., in [25]. Since we are focusing on conservative dynamics, and up to 3PM order, there are no tail effects to handle; we can expand all loop momenta in the potential region. Diagrams with more than one recoil operator insertion vanish in the potential region, and thus the 1SF dynamics up to 3PM order are computed by the first two diagrams in Fig. 3.1. At higher PM orders tail effects mandate that we supplement these diagrams by the appropriate number of recoil operator insertions while extending the loop integration to include contributions from the ultrasoft region.

The final result for the 1SF-3PM radial action, including scalar and vector

contributions, is

$$\begin{aligned}
1 = & \frac{A_C}{7} \frac{3C}{16} \frac{5f^2}{f^2-1} \frac{1}{1} \\
& + \frac{A_C^2}{7^2} \frac{f}{12} \frac{36f^6}{f^2-1} \frac{114f^4 + 132f^2 + 55}{1^{5 \cdot 2}} + \frac{4f^4 + 12f^2 + 3 \operatorname{arccosh} f}{2(f^2-1)} \\
& + \frac{A_C}{7} \frac{3f^2}{8} \frac{1}{f^2-1} \frac{A_C}{7^2} \frac{f}{12} \frac{8f^4 + 28f^2 + 23}{f^2-1} \frac{2f^2 + 1 \operatorname{arccosh} f}{f^2-1} \\
& + \frac{A_C}{7} \frac{C}{8} \frac{f^2}{f^2-1} \frac{1 + 4b}{1} \frac{A_C}{7^2} \frac{f}{6} \frac{2f^4 + f^2 + 1 + b}{f^2-1} \frac{6f^2 + 3}{1^{3 \cdot 2}}
\end{aligned} \tag{3.14}$$

where we have introduced the scalar and vector charge radii, $A = R_I^2 < \cdot^{14} C^0$, $A = R_I^2 < \cdot^{14} C^0$.

This is in agreement with the radial action inferred from scattering angles previously reported in the literature [96, 244]. The 3PM scalar result with $b = 0$ agrees with the recently reported result derived via scattering amplitudes [248], while the 3PM vector result is new. The 2PM results pass an additional check, which is that taking $_ = 1$ gives the 2PM radial action in the probe limit for trajectories in certain charged black hole backgrounds (see Chapter 4).

A highly nontrivial check of our EFT is that the 2SF-3PM radial action must agree with the 0SF-3PM radial action [195]. Although we have not presented the 2SF Feynman rules, they are straightforwardly derived by expanding the action one further order in the mass ratio. To check consistency, we have indeed carried out this expansion and computed the complete 2SF-3PM radial action for the model above, including gravitation as well as the toy scalar and photon. The result exactly matches the probe limit in the appropriate background as required for consistency of our approach (see Chapter 4).

3.8 Conclusions

Our EFT framework leaves numerous avenues for future exploration. First and foremost, it is of utmost importance to see if there is a direct relation, if any, to current approaches to black hole recoil in standard SF theory, which involve a so-called ‘‘matter-mediated’’ force [265]. Perhaps by connecting our results with those ideas, our EFT can have a more direct application to existing SF results. Secondly, it would be interesting to generalize our results beyond the case of Schwarzschild, which corresponds to a heavy, spinless, minimally coupled particle. Here a natural

extension would be to include spin by considering a Kerr background. Another option would be to study a background sourced by a neutron star, or an electrically charged particle. In all of these cases, the recoil operator will change, simply because the propagation of the heavy particle will be modified.

Third, it should be relatively straightforward to apply our EFT to the nonconservative sector, i.e., to the dynamics of gravitational radiation. Since the recoil operator is simply a nonlocal in time correction to the graviton propagator, it can be readily included in any PM calculation for graviton emission.

Last but not least, we should note that the general approach of this work—that we can systematically derive corrections to background field method from flat space perturbation theory—can also be applied outside the context of gravity. Here a natural target is the study of fluid mechanics. In this case, the long-range force carrier is the fluid velocity, the backgrounds are classical solutions to the Navier-Stokes equations, and the probe particles are worldlines that are minimally coupled to the fluid.

Note: While this paper was at a late stage we learned of the upcoming work [266] on a framework for self-force using scattering amplitudes in curved space. We thank the authors for coordinating release of their work.

Chapter 4

BACKREACTING ON THE BACKGROUND FIELD METHOD

Contents of this chapter are adapted from an upcoming publication: Clifton Cheung, Julio Parra-Martinez, Ira Z. Rothstein, Nabha Shah, and Jordan Wilson-Gerow (in preparation).

4.1 Introduction

Perturbative quantum field theory typically describes a sparse collection of particles evolving dynamically atop a quiescent vacuum state. As these degrees of freedom begin to pile up, however, this naive picture breaks down. Eventually, their collective behavior is better described by an ambient coherent *background*, for instance, as characterized by the Coulomb potential or the Schwarzschild metric.

In this condensed regime, one usually adopts a background field method in which each degree of freedom is split between a rigid classical background value and the fluctuations about it. However, it is obvious that such a description will ultimately break down as well, as soon as the field fluctuations carry charge or energy-momentum of the order of the background field itself.

At what point does quantum field theory on the vacuum “end” and quantum field theory on a background “begin”? Here, an important clue can be gleaned from the seminal work of [105], who showed how the Schwarzschild metric can be constructed perturbatively—that is, order by order in the gravitational constant, κ ,—using the standard, expanded Einstein-Hilbert field theory of gravitons interacting in a *flat space background*. Specifically, the metric is computed from the one-point function of the graviton sourced by a massive scalar point particle. The relevant Feynman diagrams for this calculation are shown in Fig. 4.1. Crucially, this procedure is viable only because the Schwarzschild metric has a regular series expansion in κ .

The broader takeaway of [105] is that certain classical solutions can be computed, albeit with considerable difficulty, using perturbation theory in a trivial background [267]. Conversely, it is natural to ask whether the reverse procedure—extracting perturbative data from classical solutions—can be systematically leveraged to reorganize and simplify perturbative calculations in a trivial background. After all, the Schwarzschild metric is known explicitly and it manifestly encodes perturbative

$$\delta_{ab} = \Gamma_{ab} + \dots$$

Figure 4.1: The series expansion of the Schwarzschild metric, δ_{ab} , in the gravitational constant, κ , corresponds to a perturbative computation, in flat space, of the graviton one-point function in the presence of a massive scalar point particle source.

information at arbitrarily high orders in κ . The geodesic motion of particles in a nontrivial background also carries all orders information in κ .

Thus, we naturally land on the same question encountered earlier, here framed more sharply: what portion of flat space Feynman diagrams are completely accounted for by a known nontrivial background and the geodesics followed by a test body within it? More importantly, what are the *additional* contributions not accounted for?

In this paper, we derive a systematic effective field theory that rigorously delineates these contributions and maximally exploits classical backgrounds and trajectories which resum large swaths of perturbation theory. Our system of study will be a light and a heavy point particle of masses, m_l and m_h , interacting via a long-range force carrier. We will apply our methods to both electromagnetism (EM) and general relativity (GR), though we will describe our results here in terms of the latter. The expansion parameter of this effective field theory is the ratio of masses of two interacting bodies,

$$\epsilon = \frac{m_l}{m_h}. \quad (4.1)$$

In the parlance of existing classical GR approaches to the black hole binary inspiral problem for extreme mass ratios, we refer to the expansion in ϵ as the self-force (SF) expansion.

Let us briefly describe the structure of this effective field theory. We begin by decomposing the graviton field, together with the light and heavy particle trajectories, into its background values and higher order in SF contributions. At 0SF order, we use the well-known result that the full gravitational dynamics of the heavy and light particles are described by a probe evolving in a Schwarzschild background. Here, we implicitly view the Schwarzschild background as the 0SF one-point function of the graviton built perturbatively from the heavy particle, whose 0SF trajectory is that of a static or inertial source. Meanwhile, the 0SF trajectory of the light particle is dictated by the geodesic equation. Our effective field theory allows for an intriguing reorganization of flat space perturbation theory in the language of

classical solutions. Perhaps the most interesting calculational tool is the extraction of multiloop integrands *directly* from the time-domain geodesic trajectories of probe particles and from the Schwarzschild solution.

To determine higher SF orders, we simply expand the action in terms of the background and fluctuation contributions to the appropriate order. In this way, we can systematically calculate to any arbitrary order in the SF expansion. At 1SF order, the fluctuations of the heavy particle become important. However, they enter quadratically into the action so we can integrate them out exactly. The resulting effective action is literally the action for a probe particle interacting with fluctuation gravitons in a Schwarzschild background—plus an additional operator describing the *recoil* of the heavy particle.

At a technical level, the recoil operator is simply a correction to the two-point function of the graviton. It is nonlocal in time, precisely because the heavy particle is actually a dynamical degree of freedom. Physically, the recoil operator describes how graviton propagation is modified by wobbles of the heavy particle that is sourcing the Schwarzschild background. It must be supplemented to any background field calculation in order to correctly reproduce the results of perturbation theory in a flat background.

A convenient benefit of our approach is a trivial prescription for eliminating well-known divergences that appear in SF theory. In particular, classical EM and GR are famously plagued by self-energy contributions coming from the electromagnetic or gravitational energy of a source induced by its own field. As we will show explicitly, since all classical dynamics are secretly resummations of perturbative diagrams in a trivial background, we can regulate these annoying divergences using dimensional regularization. While this prescription is standard in treatments of point particle effective theory [65–74], our framework allows us to apply these ideas to dynamics in a nontrivial background.

As a demonstration of the power of our formalism, we present a number of old and new calculations describing the elastic scattering of particles in EM and GR. In particular, we show how the conservative dynamics—as encoded by the on-shell radial action [224, 268, 269]—can be computed more easily in explicit examples at 0SF, 1SF, and 2SF. The radial action encodes the exact same dynamical information as more familiar on-shell scattering amplitudes. For EM and GR, we work in the post-Lorentzian (PL) and post-Minkowskian (PM) expansions, which simply correspond to perturbation theory in the fine structure constant, \mathcal{U} , and the

gravitational constant, κ , respectively. In the language of quantum field theory, all of our calculations include contributions up to and including two-loop order and our results match exactly with known results [5, 11, 95, 96, 270, 271]. Note that this agreement relies crucially on the inclusion of the recoil operator—the background field method alone does not yield the correct expression. Afterwards, we present new calculations of the radial action for dyonic scattering at 3PL, and for massive particle scattering in GR where the light particle couples to a scalar or vector field that itself interacts gravitationally. The latter theories are of particular relevance to previous SF studies [247, 248, 265].

A brief outline of our paper is as follows. We begin with an extensive derivation of our effective field theory in the context of EM in Sec. 4.2. This discussion includes the derivation of the effective action at 0SF, 1SF, and 2SF orders, followed by a presentation of the Feynman rules for perturbation theory. We describe the physics of classical resummation, whereby expressions for EM trajectories can be used to extract perturbative multi-loop integrands. We then present a calculation of the radial action for scattering charged particles and dyons. Afterwards, in Sec. 4.3, we generalize all of these results to the case of gravity and perturbative multi-loop integrands are extracted from the Schwarzschild metric and its geodesic trajectories. Furthermore, we present explicit calculations for the radial action for scattering massive particles in GR, with and without the additional scalar and vector fields.

Notation and Conventions: We choose mostly minus metric signature and fix units such that $2 = \sim = 1$. We also make use of the notation, $\hat{\chi}^1 \mathcal{G}^0 = 2c\chi^1 \mathcal{G}^0$. Where we are not explicitly working in d dimensions, divergent integrals are defined via dimensional regularization. We use the integral notation $\int_{1, \dots, d} = \frac{3}{12c^0} = \frac{3}{12c^0}$, and will occasionally take the $d = 4$ limit implicitly after integration when the context is unambiguous.

4.2 Electromagnetism

In this section, we construct an effective field theory for electromagnetism in which the expansion parameter is the ratio of masses of the interacting particles. Let us briefly outline our plan of attack.

Our starting point is the worldline action for a pair of charged massive scalar particles interacting via an electromagnetic field. Crucially, there are exact expressions governing the 0SF dynamics which corresponds to the limit where the mass of the lighter particle is negligible compared to that of the heavier particle. In this case,

the latter moves in a straight line trajectory, forming a background Coulomb field that governs the orbital motion of the former.

At 1SF, the fluctuations of the heavy particle away from its inertial motion must be taken into account, while the fluctuations of the light particle away from its 0SF orbital motion can be ignored. By integrating out the heavy particle fluctuations, we derive a 1SF recoil operator encoding the backreaction of the heavy particle. This recoil operator is a nonlocal-in-time correction to the propagation of the electromagnetic field. It literally encodes the leading correction to Rutherford scattering in the ratio of masses of the light and heavy particles. This approach generalizes systematically to higher orders. Power counting in the mass ratio, we integrate out fluctuations to the heavy trajectories at higher orders, and explicitly derive the 2SF recoil operator.

To check our formalism, we compute the radial action for scattering at 0SF, 1SF, and 2SF—up to 3PL order. The 0SF radial action is a known quantity [271] to all PL orders, which we present in generality in App. E. Meanwhile, we compute the 1SF radial action at 2PL and 3PL order and find that it agrees with known results [270, 271]. The first appearance of 2SF contributions are at 3PL order and they match the 0SF-3PL terms upon exchanging the l - labels.

As another simple application, we compute the 1SF radial action for the scattering of dyonically charged particles at 2PL and 3PL which is a new result.

4.2.1 Effective Theory

To begin, let us consider the action describing a pair of charged particles interacting via an electromagnetic field. As described in App. D, we fix the worldline einbein so that the action takes the simple form,

$$S = \int_{\mathcal{C}_\ell} \left[\frac{1}{2} m_\ell \dot{G}_\ell^\mu \dot{G}_\ell^\mu - \frac{1}{2} \frac{q_\ell^2}{m_\ell} \mathcal{G}_\ell^{\mu\nu} \mathcal{G}_\ell^{\mu\nu} \right] d\tau_\ell + \int_{\mathcal{C}_a} \left[\frac{1}{2} m_a \dot{G}_a^\mu \dot{G}_a^\mu - \frac{1}{2} \frac{q_a^2}{m_a} \mathcal{G}_a^{\mu\nu} \mathcal{G}_a^{\mu\nu} \right] d\tau_a - \int_{\mathcal{C}_\ell} \int_{\mathcal{C}_a} \frac{q_\ell q_a}{4\pi r} d\tau_\ell d\tau_a \quad (4.2)$$

where G_ℓ^μ are the worldline trajectories and $\mathcal{G}^{\mu\nu}$ is the photon field. Our worldline gauge fixing enforces the on-shell condition, $\mathcal{G}_\ell^{\mu\nu} \mathcal{G}_\ell^{\mu\nu} = 1$, for physical solutions. Here Eq. (4.2) is written in terms of the charge-to-mass ratios, $l_\ell = q_\ell/m_\ell < \ell$, which we assume throughout to be of similar size. This is, of course, not generically true. For example, the charge-to-mass ratios of the electron and proton are very different in magnitude. However, for our purposes, we assume l_ℓ of the same magnitude so that the electric forces scale proportionally to mass and the dynamics more closely parallel that of gravity.

The equations of motion for the particles and fields derived from Eq. (4.2) are

$$\mathbb{D}_\mu \left(I_{\mu\nu} \dot{x}^\nu \right) = 0 \quad \text{and} \quad m \dot{x}^\mu = \dot{x}^\mu \quad (4.3)$$

where the electromagnetic current is

$$\dot{x}^\mu = \tilde{O} \quad \dot{x}^\mu = \tilde{O} \quad I_{\mu\nu} = 3g \dot{x}^\mu \dot{x}^\nu \quad (4.4)$$

There are two very different approaches to solving these equations of motion, which we now discuss. As we will see, these different approaches will yield different intermediate expressions on the way to computing physical observables.

4.2.1.1 Post-Lorentzian Expansion about Electromagnetic Vacuum

The most common way to proceed in solving these equations of motion is to expand around the $\dot{x}^\mu = 0$ (or $I_{\mu\nu} = 0$) solutions to Eq. (4.3), i.e., straight line trajectories and the electromagnetic vacuum,

$$\begin{aligned} \dot{x}^\mu &= D^\mu g_\nu \dot{x}^\nu, \quad X \dot{x}^\mu = \\ \dot{x}^\mu &= D^\mu g_\nu \dot{x}^\nu, \quad X \dot{x}^\mu = \\ \dot{x}^\mu &= 0, \quad X \dot{x}^\mu = \end{aligned} \quad (4.5)$$

The deviations $X \dot{x}^\mu - X \dot{x}^\mu - X \dot{x}^\mu$, are then suppressed by powers of $I_{\mu\nu}$ and their expressions as a perturbative series in $I_{\mu\nu}$ can be determined by iteratively solving the equations of motion. For example, at leading order, one has

$$\begin{aligned} X \dot{x}^\mu &= I_{\mu\nu} \frac{1}{m} \dot{x}^\nu, \quad D_\mu \dot{x}^\mu = 0 \\ m X \dot{x}^\mu &= I_{\mu\nu} \dot{x}^\nu \quad 3g \dot{x}^\mu \dot{x}^\nu \quad D_\mu \dot{x}^\mu = \end{aligned} \quad (4.6)$$

and higher orders are obtained by expanding the equations of motion yet further about these deviated solutions.

There is nothing intrinsically flawed in this approach. However, since it amounts to building solutions from scratch, it does not leverage any known information about the dynamics. For example, in the limit that one charged particle can be treated as a fixed background, it is known that the exact dynamics of the other particle is Keplerian. The integrability of the dynamics in this limit is not at all obvious from the perturbative expansion described above, let alone being used to

simplify computations. In what follows, we instead build an effective field theory that encodes the solutions to these equations of motion organized in powers of λ . A crucial ingredient is that many of our manipulations will be all orders in the PL expansion.

4.2.1.2 Mass Ratio Expansion in a Background Coulomb Field

The key observation is that we can solve the equations of motion exactly in the limit where $\lambda \rightarrow 0$, describing the so called OSF dynamics. In this limit, the light particle decouples from the electromagnetic current in Eq. (4.4). Hence, there are no forces in play and the heavy particle moves in an inertial, straight line trajectory,

$$\dot{G}^{\mu\nu} g^{\nu\rho} = D^\mu g^\rho \quad (4.7)$$

where D^μ is the heavy particle velocity. At the same time, the heavy particle sources an ambient boosted Coulomb field as per the equation of motion,

$$m \dot{a}^\mu = \dot{a}^\mu = \dot{a}^\mu = \int d^3x \sqrt{-g} \dot{G}^{\mu\nu} g^{\nu\rho} \quad (4.8)$$

written here in Lorenz gauge $\partial_\mu \dot{G}^{\mu\nu} = 0$. This has a well-known solution,

$$\dot{G}^{\mu\nu} = \frac{I^\mu \dot{a}^\nu - I^\nu \dot{a}^\mu}{4cA} \quad (4.9)$$

where $A = \sqrt{D^\mu D^\mu} = \frac{1}{\lambda}$ is the boosted radius.

Meanwhile, the light particle equation of motion at OSF is

$$\partial_\mu \dot{G}^{\mu\nu} g^{\nu\rho} = 0 \quad (4.10)$$

The 1SF corrections induce fluctuations away from the OSF solutions,

$$\dot{G}^{\mu\nu} = \dot{G}_0^{\mu\nu} + \delta \dot{G}^{\mu\nu} \quad \text{and} \quad g^{\mu\nu} = g_0^{\mu\nu} + \delta g^{\mu\nu} \quad (4.11)$$

Since $\dot{G}_0^{\mu\nu}$ and $g_0^{\mu\nu}$ are exact OSF solutions valid at $\lambda \rightarrow 0$, we know that the fluctuation degrees of freedom are effectively 1SF objects and scale as

$$\delta \dot{G}^{\mu\nu} \sim \delta g^{\mu\nu} \sim \lambda^2 \quad (4.12)$$

when they are set to their on-shell configurations.

¹The fluctuations here are not to be confused with those in Eq. (4.5) as, here, we are expanding about nontrivial background solutions rather than the free theory solutions. Henceforth, the fluctuations we refer to will always be about this nontrivial background.

Why we even want the OSF trajectory for the light particle may not be apparent. However, as we will shortly see, the 1SF action only depends on the light particle via this OSF trajectory. In particular, we will show how the OSF trajectory secretly encodes the 1SF, all PL order dynamics.

4.2.1.3 Self Force Divergences and Dimensional Regularization

At this point, let us comment on the subtlety of self-energy contributions to the heavy particle. Consider the heavy particle action at OSF,

$$S = \int dt \left[-\frac{1}{2} \dot{\mathbf{x}}^2 - \frac{1}{2} \mathbf{G}^0 \right] \quad (4.13)$$

with the corresponding equation of motion,

$$\ddot{\mathbf{x}} + \mathbf{G}^0 = 0 \quad (4.14)$$

If we attempt to evaluate the heavy particle action on the solution to the OSF equations of motion, we find singular terms. Equivalently, in the equation of motion we have \mathbf{G}^0 being evaluated at $\mathbf{x} = 0$, corresponding to the effect on the heavy particle from its own Coulomb field.

In the usual approach to classical dynamics, one must devise a regularization scheme to subtract this self-energy or self-force contribution. In our setup, we view the background trajectories and field configurations to literally be a repackaging of flat space dynamics. In this picture, \mathbf{G}^0 corresponds precisely to a potential photon mode that is emitted and then reabsorbed by the heavy worldline. As usual, such terms yield self-energy contributions which are absorbed through the mass counterterm. Effectively, we can discard \mathbf{G}^0 wherever it appears. More generally, we are permitted to drop any contributions which arise in the flat space theory from potential photons emitted and reabsorbed by the heavy particle. The upshot is that the heavy particle equation of motion essentially becomes $\ddot{\mathbf{x}} = 0$, with the solution, Eq. (4.7).

To explain our choice of regularization scheme it is instructive to pedantically recall how the solution in Eq. (4.9) arises using the language of Feynman diagrams. In Lorenz gauge, the solution to Eq. (4.8) is given by the single Feynman diagram which equals the propagator integrated against the source,

$$\mathbf{G}^0 = \int d^4x' \mathbf{H}(\mathbf{x} - \mathbf{x}') \mathbf{H}(\mathbf{x}') \quad (4.15)$$

As is customary, we can evaluate this in momentum space, where the heavy source is simply

$$\delta^4(x) = \int \frac{d^4k}{(2\pi)^4} e^{ikx} \quad (4.16)$$

and the Lorenz gauge propagator is

$$D_{\mu\nu}(k) = \frac{-i}{k^2} \left(\eta_{\mu\nu} - \frac{k_\mu k_\nu}{k^2} \right) \quad (4.17)$$

The solution to the equations of motion is then simply,

$$A_\mu(x) = \int \frac{d^4k}{(2\pi)^4} e^{ikx} \frac{-i}{k^2} \left(\eta_{\mu\nu} - \frac{k_\mu k_\nu}{k^2} \right) j^\nu(k) \quad (4.18)$$

whose Fourier transform yields Eq. (4.9). In the language of Feynman diagrams, the singular term in Eq. (4.13) is a contribution to the classical self-energy,

$$\begin{aligned} \text{self-energy} &= \frac{e^2}{2} \int \frac{d^4k}{(2\pi)^4} \frac{1}{k^2} \left(\eta_{\mu\nu} - \frac{k_\mu k_\nu}{k^2} \right) j^\mu(k) j^\nu(k) \\ &= \frac{e^2}{2} \int \frac{d^4k}{(2\pi)^4} \frac{1}{k^2} \left(\eta_{\mu\nu} - \frac{k_\mu k_\nu}{k^2} \right) j^\mu(k) j^\nu(k) \end{aligned} \quad (4.19)$$

where $\int d^4k = 2cX^0 \int d^3k$ is the total time integral. The coefficient of $\int d^3k$, i.e., the energy, is indeed ultraviolet divergent due to the integration over large values of k . For instance, a cutoff regularization gives

$$E_{\text{self}} = \frac{e^2}{2} \int \frac{d^3k}{(2\pi)^3} \frac{1}{k^2} \left(\eta_{\mu\nu} - \frac{k_\mu k_\nu}{k^2} \right) j^\mu(k) j^\nu(k) \quad (4.20)$$

This linear divergence corresponds to the $k=0$ singularity in Eq. (4.13). Of course, this can be explicitly reabsorbed by a mass counterterm. However, note that the divergence is power-like, so we can instead use a dimensional regulator in which the integral is analytically continued to general dimension. The great advantage of this choice is that by definition, dimensional regularization sets all power divergences to zero,

$$\int \frac{d^d k}{(2\pi)^d} \frac{1}{k^2} \left(\eta_{\mu\nu} - \frac{k_\mu k_\nu}{k^2} \right) j^\mu(k) j^\nu(k) = 0 \quad (4.21)$$

In other words, in dimensional regularization we find that

$$E_{\text{self}} = 0 \quad (4.22)$$

²The choice of ϵ -prescription is immaterial for this computation.

This is an important simplification which will become crucial when we study the gravitational case. To reiterate, the renormalized heavy particle action at OSF is simply that of a free particle,

$$S = \int dt \left[\frac{1}{2} m \dot{\mathbf{x}}^2 - \frac{1}{2} \frac{1}{m} \mathbf{p}^2 \right] \quad (4.23)$$

and we will end up dropping this contribution as it contains no dynamical information.

4.2.1.4 OSF Dynamics

In this work we will focus on conservative scattering dynamics, for which the gauge invariant quantity of interest is the scattering angle. Practically though, we will actually just compute the on-shell action from which the scattering angle follows by simple differentiation.

Inserting the SF expanded trajectories and fields in Eq. (4.11) into the action in Eq. (4.2), we now compute

$$S = \int dt \left[\frac{1}{2} m \dot{\mathbf{x}}^2 - \frac{1}{2} \frac{1}{m} \mathbf{p}^2 \right] \quad (4.24)$$

where $\int dt$ denotes the SF order and is simply the action evaluated on the O_{1-00} solutions. The renormalized OSF action is

$$S = \int dt \left[\frac{1}{2} m \dot{\mathbf{x}}^2 - \frac{1}{2} \frac{1}{m} \mathbf{p}^2 \right] + \int dt \left[\frac{1}{2} \frac{1}{m} \mathbf{p}^2 - \frac{1}{2} \frac{1}{m} \mathbf{p}^2 \right] \quad (4.25)$$

and all dependence on the dynamical fluctuation modes are contained in the O_{1-00} solutions. Note the suppression of the probe particle action by a factor $\frac{1}{m}$ compared to that of the heavy particle and background Coulomb field. Thus, the leading nontrivial SF contribution \mathcal{O}_{1-20} , starts at \mathcal{O}_{1-20} .

Let us first focus on the OSF dynamics in $d = 4$ dimensions. The heavy particle is nondynamical in this limit, and all dynamics are governed by the single-particle action,

$$S = \int dt \left[\frac{1}{2} m \dot{\mathbf{x}}^2 - \frac{1}{2} \frac{1}{m} \mathbf{p}^2 \right] \quad (4.26)$$

in a background Coulomb electric field, Eq. (4.9). The equation of motion is just the Lorentz force equation. Rather than working in Cartesian components explicitly, one naturally uses the fact that the background is static and isotropic to focus only on planar motion. One also uses the conserved energy and angular momentum,

$$E = \frac{1}{2} m \dot{\mathbf{x}}^2 + \frac{1}{2} \frac{1}{m} \mathbf{p}^2 \quad \text{and} \quad \mathbf{L} = \mathbf{x} \times \mathbf{p} \quad (4.27)$$

to simplify down to a one-dimensional central force problem. The remaining radial equation of motion is also a first-order ordinary differential equation coming simply from the on-shell condition,

$$A^2 = \frac{2\mu \dot{r}^2}{2\mu} - \frac{2\mu}{r} + \frac{L^2}{2\mu r^2} \quad (4.28)$$

In $\ell = 0$, one can write exact solutions for the orbital trajectory $r(\phi)$, as this is just Keplerian motion [268, 272]. For general ℓ , we outline how to solve these equations perturbatively in App. D. In practice, depending on the observable one is interested in, the explicit solutions need not be computed.

In upcoming sections on higher SF corrections, we will need to make use of explicit trajectory solutions in order to compute the on-shell action. However, while we restrict to OSF in this section, we can use textbook classical mechanics to evaluate the on-shell action as a straightforward radial action integral (see App. D),

$$S = 2 \int_{r_{\min}}^r \sqrt{2\mu \left(E - \frac{2\mu}{r} + \frac{L^2}{2\mu r^2} \right)} dr \quad (4.29)$$

The radial conjugate momentum is readily solved for from the on-shell condition, giving

$$p_r = \sqrt{2\mu \left(E - \frac{2\mu}{r} + \frac{L^2}{2\mu r^2} \right)} \quad (4.30)$$

Passing to orbital parameters more convenient for scattering,

$$f = \frac{r}{2\mu} \quad \text{and} \quad 1 = \frac{1}{f^2} - \frac{1}{f^2} \quad (4.31)$$

we evaluate the radial action integral to 3PM order (see App. E),

$$\begin{aligned} S = & \frac{2\mu}{f^2} \log \frac{1}{f^2} - \frac{1}{f^2} \\ & + \frac{c}{21} \frac{A^2}{f^2} + \frac{c}{312} \frac{A^3 f}{f^2} - \frac{3}{1^{5/2}} \end{aligned} \quad (4.32)$$

where \tilde{m} is a reference mass scale, and the infrared divergence $\ln 4$ is the familiar Coulomb logarithm it is a physical divergence in the time delay, but does not affect the scattering angle.

As we generalize to higher SF orders, we no longer know the exact expression for the radial momentum. However, we will still be able to compute the on-shell action

in terms of diagrammatics, and the symmetries of the problem ensure that the radial action still serves as a generating function for the scattering angle. Since we wish to fix the energy and angular momentum of the solutions but do not a priori know the interaction potential, we must be sure to use causal propagators so that the integrals of motion can be specified by their values in the asymptotic past when the particles are decoupled.

4.2.1.5 1SF Dynamics

Considering that the OSF action was secretly $\mathcal{O}(\epsilon^0)$ due to the light particle terms, let us now consider the various contributions to the action up to $\mathcal{O}(\epsilon^2)$ which requires expanding only up to quadratic order in the fluctuations. First, the action for the electromagnetic field becomes

$$3^4 G \frac{1}{4} \dot{a}^a \dot{a}^a = 3^4 G \frac{1}{4} \dot{a}^a \dot{a}^a, \frac{1}{2} X^a \dot{a}^a, \frac{1}{4} X^a X^a \dot{a}^a - \quad (4.33)$$

where $X^a = m X^a - m X^a$ and the second term on the R.H.S. $\frac{1}{2} X^a \dot{a}^a$, will cancel with other terms in the action because it satisfies its equation of motion.

Next, consider the contributions to the action from the worldlines,

$$\begin{aligned} & 3g \frac{1}{2}, \frac{1}{2} \mathcal{G}, \mathcal{I} \mathcal{G}, \mathcal{I} \mathcal{G}^0 \\ = & 3g \frac{1}{2}, \frac{1}{2} \mathcal{G}, \mathcal{I} \mathcal{G}, \mathcal{I} \mathcal{G}^0 \\ & , X \mathcal{G}, \mathcal{I} X \mathcal{G} \mathcal{G}^a \mathcal{I} \mathcal{G}^0, \mathcal{I} X \mathcal{G}^a \mathcal{I} \mathcal{G}^0 \\ & , \frac{1}{2} X \mathcal{G}, \mathcal{I} X \mathcal{G} \mathcal{G}^a \mathcal{I} \mathcal{G}^0, \frac{1}{2} \mathcal{I} X \mathcal{G} X \mathcal{G}^a \mathcal{I} \mathcal{G}^0 \\ & , \frac{1}{2} \mathcal{I} X \mathcal{G} X \mathcal{G} \mathcal{G}^a \mathcal{I} \mathcal{G}^0, \quad - \end{aligned} \quad (4.34)$$

where the ellipses are higher than quadratic order in the fluctuation. It will be useful to look at the contributions from the heavy and light worldlines separately since they will be treated differently. In particular, for the heavy particle and light particle we

Putting together the terms in Eq. (4.33) and Eq. (4.35) that are relevant to the leading 1SF dynamics, the fluctuation action is

$$\begin{aligned} \delta S^{(1)} = & \int d^4x \left[-\frac{1}{2} \delta X^\mu \delta G_{\mu\nu} \delta X^\nu + \int d^3x \delta X^\mu \delta G_{\mu\nu} \delta X^\nu \right] \\ & + \int d^4x \delta X^\mu \delta G_{\mu\nu} \delta X^\nu \end{aligned} \quad (4.36)$$

We note again that the light particle's coupling to the gauge field had an explicit factor of ϵ , so we only needed to expand that term to linear order in fluctuations. Typically, when expanding an action about a background solution, the terms which are linear in fluctuations vanish simply because we are expanding about a solution. However, in our situation, we must emphasize that this is a solution in the $\epsilon \rightarrow 0$ limit, i.e., it did not account for the light particle source, and we have to keep a term that is linear in δX^μ .

The interactions in $\delta S^{(1)}$ all have a very simple physical interpretation. In particular, this action describes a fluctuation photon that is dynamical and couples to two sources. The first source is the OSF trajectory of the light particle. The second source is the heavy particle, which also is dynamical.

With this interpretation in mind, let us write the fluctuation action as

$$\begin{aligned} \delta S^{(1)} = & \int d^4x \left[-\frac{1}{2} \delta X^\mu \delta G_{\mu\nu} \delta X^\nu + \int d^3x \delta X^\mu \delta G_{\mu\nu} \delta X^\nu \right] \\ & + \int d^4x \delta X^\mu \delta G_{\mu\nu} \delta X^\nu \end{aligned} \quad (4.37)$$

where the light particle OSF current is

$$\int d^3x \delta X^\mu \delta G_{\mu\nu} \delta X^\nu = \int d^3x \delta X^\mu \delta G_{\mu\nu} \delta X^\nu \quad (4.38)$$

We emphasize again that, for the 1SF dynamics, we can completely ignore the light particle fluctuations away from geodesic motion.

It would be perfectly fine to simply compute observables using δX^μ . However, provided that we are not interested in heavy body observables and are instead interested in light body deflection, the conservative scattering angle, or radiated waveforms/fluxes, it will be more convenient to derive an even simpler effective theory by integrating out the heavy particle fluctuations completely. The resulting theory will then describe a light particle worldline and a photon fluctuation field propagating in a background electromagnetic field. At OSF, such a procedure

trivially generates the action for a charged probe evolving in the field of the inertial heavy source. However, with our 1SF corrections, there is an additional effect encoded in a term we dub the recoil operator which accounts for the underlying dynamical propagation of the heavy particle.

Conveniently, at 1SF order, \mathcal{H}^{10} is quadratic in $X^{\dot{a}}$ and we can integrate out this mode exactly. Performing the path integral over $X^{\dot{a}}$ we obtain, up to constant normalization,

$$\begin{aligned} & \int \mathcal{D}X^{\dot{a}} \exp \left[- \int dt \left(\frac{1}{2} \dot{X}^{\dot{a}} \dot{X}_{\dot{a}} + \mathcal{H}^{10} \right) \right] \\ & = \exp \left[- \int dt \mathcal{H}_{\text{recoil}}^{10} \right] \end{aligned} \quad (4.39)$$

where $\mathcal{H}_{\text{recoil}}^{10}$ is the electromagnetic recoil operator with the superscript denoting the SF order. To compute this operator, we use the fact that, for a Gaussian integral, we can simply set the fluctuation to its solution under the equations of motion. Variation of Eq. (4.37) with respect to the heavy particle fluctuation gives,

$$\dot{X}^{\dot{a}} + \mathcal{H}_{\text{recoil}}^{10} \dot{X}^{\dot{a}} = 0 \quad (4.40)$$

which, as expected, is simply the equation for the heavy worldline expanded to 1SF. Plugging this back into Eq. (4.37) we obtain the recoil operator,

$$\mathcal{H}_{\text{recoil}}^{10} = \frac{1}{2} \dot{X}^{\dot{a}} \dot{X}_{\dot{a}} + \frac{1}{m_H^2} \mathcal{H}^{10} \dot{X}^{\dot{a}} \dot{X}_{\dot{a}} \quad (4.41)$$

This gauge invariant operator encodes the dynamical propagation of the heavy particle as a nonlocal-in-time correction to photon propagation localized exactly at the position of the heavy particle. Note that, since $\mathcal{H}_{\text{recoil}}^{10} \propto \dot{X}^{\dot{a}} \dot{X}_{\dot{a}}$, we can view the recoil operator as a polarizability operator on the heavy worldline that is nonlocal in time. The nonlocality makes this operator sufficiently different from true polarizability operators that we will not push on this analogy further. However, we note that, while a photon does not scatter off a fixed 1A Coulomb potential, it will scatter off the recoil operator.

The utility of the recoil operator is that we no longer need to track the heavy degree of freedom. The only explicit source of photons is the light particle OSF current and the recoil of the heavy body appears only in a modification to the fluctuation photon's propagator. This allows us to use background field method, a very powerful organizational tool, albeit with this modified propagator. The advantage of this will be more apparent in gravity where the graviton fluctuations couple to the background.

Note that, in Eq. (4.41), we have not been careful about the boundary conditions for the Green's function \mathcal{G}^2 . For the case of conservative dynamics, time reversal symmetry implies that quantities like the scattering angle or radial action can be computed using either retarded or advanced boundary conditions. For these computations it will then not matter if we use a retarded or advanced prescription for the propagator. However, more generally one must properly specify the boundary prescription for \mathcal{G}^2 appropriate to the calculation at hand.

In conclusion, we have obtained the effective action encoding all 1SF dynamics,

$$\Gamma_e^{(1)} = \Gamma_{\text{recoil}}^{(1)} + 3^4 G \frac{1}{4} X_a X^a X_b X^b \cdot \quad (4.42)$$

This describes photon fluctuations about the background electromagnetic field sourced by the probe motion of the light particle and augmented by the recoil of the heavy particle via $\Gamma_{\text{recoil}}^{(1)}$. For example, for the case of Rutherford scattering, this would account for the wobble of the nucleus upon scattering.

4.2.1.6 2SF Dynamics

To study the 2SF dynamics we must continue the expansion of the action to $\mathcal{O}(\hbar^2)$. This will involve terms of the schematic form $X_a X^a X_b X^b$, as well as $X_a X^a X_b X^b$. The contributions involving the light particle were already worked out in Eq. (4.35),

$$\begin{aligned} \Gamma_l^{(2)} = & \langle \dots \rangle + 3g \frac{1}{2} X_a X^a X_b X^b + \dots \\ & + \frac{1}{2} \int X_a X^a X_b X^b + \frac{1}{2} \int X_a X^a X_b X^b \cdot \end{aligned} \quad (4.43)$$

The two terms on the first line are completely analogous to the terms at 1SF which generated the recoil operator for the heavy particle. That is, they describe how fluctuation photons can nudge the light particle off its 0SF trajectory. The two terms on the second line have no analog at 1SF since they involve the value of the background field, X_a , at the 0SF position of the light particle. The analogous terms at 1SF were self-energy and therefore discarded. Here, these terms describe the fact that while the light particle is nudged off its 0SF trajectory by fluctuation photons it still propagates in the background X_a . As a preview, we note that in gravity these types of terms at 2SF, involving the light particle, describe geodesic deviation caused by the fluctuation gravitons.

The contributions to the heavy worldline action which are cubic in fluctuations are straightforwardly worked out,

$$\begin{aligned}
 \Gamma^{(12)} = & \int d^4x \left[3g \frac{1}{2} X^i X^j \mathcal{E}_a^i X^k \mathcal{E}_a^k \right. \\
 & + \frac{1}{2} X^i X^j \mathcal{E}_a^i \mathcal{E}_a^j m_a \left. \right] \mathcal{E}_a^i X^k \mathcal{E}_a^k \\
 & + \frac{1}{3} X^i X^j X^k \mathcal{E}_a^i \mathcal{E}_a^j \mathcal{E}_a^k m_a \\
 & + \frac{1}{6} X^i X^j X^k X^l \mathcal{E}_a^i \mathcal{E}_a^j \mathcal{E}_a^k \mathcal{E}_a^l m_a \left. \right] \mathcal{E}_a^i X^k \mathcal{E}_a^k \cdot
 \end{aligned} \quad (4.44)$$

The last two terms are self-energy and can be dropped. The first two terms give rise to a double-recoil operator, i.e., an effective cubic photon operator which contains two iterated matter propagators.

To see this, we combine all terms in the effective action which involve the heavy particle fluctuation through 2SF order,

$$\begin{aligned}
 \Gamma^{(11)}, \Gamma^{(12)} = & \int d^4x \left[3g \frac{1}{2} X^i X^j \mathcal{E}_a^i X^k \mathcal{E}_a^k \right. \\
 & + \frac{1}{2} \int d^4y X^i X^j \mathcal{E}_a^i X^k \mathcal{E}_a^k \\
 & + \frac{1}{2} \int d^4y X^i X^j X^k \mathcal{E}_a^i \mathcal{E}_a^j m_a X^l \mathcal{E}_a^l \left. \right] \mathcal{E}_a^i X^k \mathcal{E}_a^k -
 \end{aligned} \quad (4.45)$$

and integrate out the heavy particle as before to get recoil operators,

$$\exp \left[\Gamma^{(11)}, \Gamma^{(12)} \right] = \exp \left[\Gamma_{\text{recoil}}^{(11)}, \Gamma_{\text{recoil}}^{(12)} \right] \cdot \quad (4.46)$$

Since Eq. (4.45) now contains terms which are cubic in fluctuations, i.e., power counting as λ^3 , when we integrate out the heavy particle fluctuations we generate terms at arbitrarily high SF order. Given that we started with a 2SF accurate action we are only, however, permitted to trust the obtained recoil operators up to 2SF order.

The new recoil operator showing up at 2SF order is

$$\begin{aligned}
 \Gamma_{\text{recoil}}^{(12)} = & \frac{\lambda^3}{2} \int d^4x \left[3g \int d^4y \int d^4z X^i X^j \mathcal{E}_a^i X^k \mathcal{E}_a^k \frac{1}{m_a^2} X^l \mathcal{E}_a^l \frac{1}{m_a} X^m \mathcal{E}_a^m \right. \\
 & + \int d^4y \int d^4z X^i X^j \mathcal{E}_a^i X^k \mathcal{E}_a^k \frac{1}{m_a^2} X^l \mathcal{E}_a^l \frac{1}{m_a} X^m \mathcal{E}_a^m \left. \right] \mathcal{E}_a^i X^k \mathcal{E}_a^k -
 \end{aligned} \quad (4.47)$$

where the electric field felt by the heavy particle $X^i \mathcal{E}_a^i = \mathcal{E}_a^i X^i \mathcal{E}_a^i$.

All together then, the effective action describing the dynamics through 2SF order is

$$\begin{aligned}
 \langle e^{iS} \rangle = \langle e^{iS_{\text{recoil}}} \rangle &= \langle e^{iS_{\text{recoil}}} \rangle \langle e^{iS_{\text{photon}}} \rangle \langle e^{iS_{\text{heavy}}} \rangle \\
 &= \langle e^{iS_{\text{recoil}}} \rangle \langle e^{iS_{\text{photon}}} \rangle \langle e^{iS_{\text{heavy}}} \rangle \langle e^{iS_{\text{photon}}} \rangle \langle e^{iS_{\text{recoil}}} \rangle \\
 &= \langle e^{iS_{\text{recoil}}} \rangle \langle e^{iS_{\text{photon}}} \rangle \langle e^{iS_{\text{heavy}}} \rangle \langle e^{iS_{\text{photon}}} \rangle \langle e^{iS_{\text{recoil}}} \rangle \langle e^{iS_{\text{photon}}} \rangle \langle e^{iS_{\text{heavy}}} \rangle \langle e^{iS_{\text{photon}}} \rangle \langle e^{iS_{\text{recoil}}} \rangle \dots
 \end{aligned} \tag{4.48}$$

This action is still quadratic in fluctuations and can, in principle, be evaluated exactly. In studying conservative scattering dynamics, the light particle fluctuations do not actually contribute until 4PL order, and the two terms involving X_{photon} do not contribute until 5PL. Thus, for the 3PL computations performed later in this work, only the recoil operators $\langle e^{iS_{\text{recoil}}} \rangle$ and $\langle e^{iS_{\text{recoil}}} \rangle$ are needed.

4.2.2 Feynman Rules

Any physical observable computed from the 1SF effective action $\langle e^{iS_{\text{photon}}} \rangle$, in Eq. (4.42) will involve computing the path integral over the one remaining degree of freedom which is the photon fluctuation. From Eq. (4.42), it is straightforward to derive the Feynman rules governing these photon fluctuations. We first describe the Feynman rules for the propagator and vertex for the photon, and then move on to describe its source.

4.2.2.1 Photon Propagators and Vertices

To begin, we choose Feynman gauge for the photon fluctuation

$$\begin{aligned}
 \overline{\text{wavy line}} &= \frac{8 \delta_{ab}}{q^2} \cdot
 \end{aligned} \tag{4.49}$$

Next, we can easily derive the two-point vertex for the photon fluctuation induced by the recoil operator $\langle e^{iS_{\text{recoil}}} \rangle$ in Eq. (4.41),

$$\begin{aligned}
 \overline{\text{wavy line}} &= 8i^2 \int \frac{d^4q}{(2\pi)^4} \frac{e^{iq \cdot x} \delta_{ab}}{q^2} \langle e^{iS_{\text{recoil}}} \rangle \\
 &= 8i^2 \int \frac{d^4q}{(2\pi)^4} \frac{e^{iq \cdot x} \delta_{ab}}{q^2} \langle e^{iS_{\text{recoil}}} \rangle \delta_{ab} \int \frac{d^4q'}{(2\pi)^4} \frac{e^{iq' \cdot x}}{q'^2} \langle e^{iS_{\text{recoil}}} \rangle \delta_{ab} \dots
 \end{aligned} \tag{4.50}$$

where $\langle e^{iS_{\text{recoil}}} \rangle = \int \frac{d^4q}{(2\pi)^4} \frac{e^{iq \cdot x}}{q^2} \langle e^{iS_{\text{recoil}}} \rangle$. The denominator factor is simply the nonlocal-in-time worldline propagator $\frac{1}{m^2}$, while the delta function encodes that the heavy

Since we are focused on conservative dynamics one should understand a prescription here, but only the the time reflection symmetric part of the result is to be retained.

particle trajectory is invariant under translations in the direction and momentum is conserved in that direction.

Note that the 1SF action in Eq. (4.42) does not contain any explicit dependence on the background gauge field. This is not an accident since electromagnetism is a linear theory, the interactions of fluctuations decouple from the background upon which we expand. The same will not be true, however, for gravity. Nevertheless, for future reference let us restate

$$\vec{A} = \int d^3x \frac{\vec{X} \cdot \vec{D}}{c} \quad \text{and} \quad \vec{A} = \int d^3x \frac{\vec{X} \cdot \vec{D}}{c} \quad (4.51)$$

which are the background electromagnetic gauge field and field strength in momentum space.

4.2.2.2 Photon Sources

Meanwhile, at 1SF the photon can only terminate on the light particle source in Eq. (4.38) which, transformed into momentum space and to all PL orders, is

$$\vec{A} = \int d^3x \frac{\vec{X} \cdot \vec{D}}{c} \quad (4.52)$$

In practice, we will be interested in a perturbative PL expansion. To define this we first define the length scale,

$$A_2 = \frac{|q_1 q_2|}{4c} \quad (4.53)$$

which is positive if the particles are oppositely charged, i.e., attracting. This is simply the classical charge radius of a particle with charge q_j , and mass m_j .

The PL expansion is then in powers of the dimensionless ratio $\frac{A_2}{b}$, where b is the characteristic length scale of the relevant dynamics, e.g., the impact parameter in scattering. To compute to any given PL order, we expand the expression for the light particle trajectory,

$$\vec{G} = \sum_{n=0}^{\infty} \vec{G}^{(n)} \quad (4.54)$$

where $\vec{G}^{(n)}$ is the n th PL order contribution. In such an expansion, we get

$$\begin{aligned} \vec{A} &= \int d^3x \frac{\vec{X} \cdot \vec{D}}{c} = \int d^3x \frac{\vec{X} \cdot \vec{D}}{c} + \int d^3x \frac{\vec{X} \cdot \vec{D}}{c} + \dots \\ &= \int d^3x \frac{\vec{X} \cdot \vec{D}}{c} + \int d^3x \frac{\vec{X} \cdot \vec{D}}{c} + \int d^3x \frac{\vec{X} \cdot \vec{D}}{c} + \dots \end{aligned} \quad (4.55)$$

where in the last line we have expanded up to 2PL order in terms of Eq. (4.54). Here, we have integrated by parts to make some terms look more uniform and the ellipses denote contributions that enter beyond 2PL order. For concreteness, let us consider the light particle current at 1PL order which can be written more compactly as

$$\dot{\mathbf{r}}_l^{(1)} = -\frac{1}{c} \mathbf{E} + \frac{1}{2c} \mathbf{v} \times \mathbf{B} + \mathcal{O}(\beta^2) \quad (4.56)$$

where we have defined the trajectories in frequency space $\mathbf{r}_l^{(1)}(\omega) = \int dt e^{i\omega t} \dot{\mathbf{r}}_l^{(1)}(t)$.

At this point we can use any method we like to compute the light particle trajectory in frequency space $\mathbf{r}_l^{(1)}(\omega)$. As will be described in Sec. 4.2.3, we can either compute these probe trajectories perturbatively from the second-order equation of motion or extract them from first-order differential equations by making use of conserved quantities and integrals of motion. If we take the former approach, we simply expand Eq. (4.10) to leading PL order and transform to frequency space,

$$\dot{\mathbf{r}}_l^{(1)}(\omega) = \frac{1}{c} \frac{\mathbf{D}_a}{\omega^2} + \frac{3}{2c^3} \frac{\mathbf{D}_a \times \mathbf{D}_a}{\omega^4} + \mathcal{O}(\beta^2) \quad (4.57)$$

where the background electromagnetic field strength in momentum space is defined in Eq. (4.51).

In summary, the Feynman rule for the photon source is

$$\begin{aligned} \text{?} \uparrow \text{?} &= \text{?} \uparrow \text{?} + \text{?} \uparrow \text{?} \\ &= \frac{1}{c} \frac{\mathbf{D}_a}{\omega^2} + \frac{3}{2c^3} \frac{\mathbf{D}_a \times \mathbf{D}_a}{\omega^4} + \mathcal{O}(\beta^2) \end{aligned} \quad (4.58)$$

where, for $\mathbf{r}_l^{(1)}(\omega)$, we can choose either the expression in Eq. (4.57) or any other representation of the trajectory.

For ease of use, we have presented a table summarizing all of the 1SF Feynman rules for electromagnetism in Fig. 4.2.

4.2.3 Classical Resummation

4.2.3.1 Expansion of the Second-order Differential Equation of Motion

The most straightforward approach to solving Eq. (4.10) is perturbatively in the PL expansion. In this picture, we plug Eq. (4.54) into the light particle equations of motion in Eq. (4.10) to obtain the perturbative equations of motion at 0PL, 1PL, and

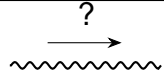
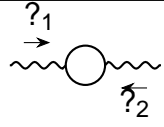

 Photon propagator	$\frac{8[_a}{?^2}$
 Recoil vertex	$8P < \frac{X^1 D ?_1, D ?_2^0}{1D ?_1^0 1D ?_2^0} O^{U, 11D} - ?^0 O_U ?^2 1D - ?^0$
 Photon source	$8_l < 4^{8?1} D_l X^1 D_l ?^0 8O_U ?^1 1D_l - ?G^U 1D_l ?^0,$

Figure 4.2: Feynman rules for computing the 1SF electromagnetic radial action.

2PL order,

$$\begin{aligned}
 \mathcal{E}_0 &= 0 - \\
 \mathcal{E}_1 &= l! \quad \text{\textasciitilde}^a 1 G_0^0 \mathcal{E}_a - \\
 \mathcal{E}_2 &= l! \quad \text{\textasciitilde}^a 1 G_0^0 \mathcal{E}_a, G^d m \text{\textasciitilde}^a 1 G_0^0 \mathcal{E}_a -
 \end{aligned}
 \tag{4.59}$$

and so on and so forth. The solution to the 0PL equation is just the straight line trajectory,

$$\hat{G}_0 = 1 \text{\textasciitilde} , D_l \hat{g} - \tag{4.60}$$

where D_l is the light particle velocity and \textasciitilde is a space-like vector defining the impact parameter. Plugging this back into the 1PL equation, we obtain

$$\hat{G}_1^1 g^0 = \frac{1}{m_g^2} l! \quad \text{\textasciitilde}^a 1 1 \text{\textasciitilde} , D_l g^0 D_l a - \tag{4.61}$$

expressed formally in terms of the light particle propagator \hat{G}_1^1 .

In this perturbative expansion, one solves the Lorentz force equation as well as Maxwell's equations, for the particle trajectory and field configuration, order by order in the PL expansion. Since Maxwell's equations are linear, the latter step truncates at leading order,

$$m \text{\textasciitilde}^a = \text{\textasciitilde}^a = \text{\textasciitilde}^a = l < 3g^D X^4 1 \hat{G} \text{\textasciitilde} D g^0 \bullet \tag{4.62}$$

In nonlinear field theories, like gravity, the low PM order solutions of the field are themselves sources for higher order perturbations and the perturbative series for the field configuration does not truncate leading, in principle, to more and more complicated perturbative computations.

4.2.3.2 Expansion Utilizing Integrals of Motion

An alternative approach to computing \dot{G} is to extract it from a solution to the orbital problem which manifests all of the symmetries. The orbital equations are most naturally written in $C-A$ coordinates. On the outward branch of the scattering trajectory $A=0$ and in d dimensions, we then have

$$\begin{aligned} \dot{C} &= f - \frac{\dot{A}}{A^3} \\ \dot{A} &= \frac{1}{r} \frac{1 - f^2 - \frac{1}{A^2}}{1 - \frac{A^2}{A^2} - \frac{1 - f^2}{A^2}} \end{aligned} \quad (4.63)$$

By the integrability of the probe motion, the equations of motion have reduced to three first-order differential equations. Given their structure, these equations can be perturbatively solved very straightforwardly. One may wonder whether there is any advantage over the approach of expanding the second-order differential equations of motion if we will solve Eq. (4.63) perturbatively anyway. As we will see, the solutions extracted this way have a much simplified structure when compared with the other approach. The comparison is best articulated in the language of Feynman loop integrals the trajectories extracted from this method have many pinches manifested, leading to simpler denominators, and come with considerable tensor reduction already performed, leading to simpler numerators. In App. D, we provide details on this procedure in general dimensions which illustrate that this method effectively performs integral-by-parts reduction on the Feynman integrals which comprise the trajectories.

It is convenient to combine the equations of motion $\dot{A}-\dot{C}$ into equations of motion for the Cartesian components $\dot{G}-\dot{H}$

$$\begin{aligned} \dot{H} &= \frac{H}{A} \dot{A} + \frac{G}{A^2} \dot{A} \\ \dot{G} &= \frac{G}{A} \dot{A} + \frac{H}{A^2} \dot{A} \end{aligned} \quad (4.64)$$

where, here and in the equation above we understand A as a function of $G-H$. From this, the Lorentz covariant solution is trivially obtained,

$$\dot{G}^1 g^0 = \dot{C} g^0 \dot{D} + \dot{G} g^0 \frac{1}{1} + \dot{H} g^0 \frac{D_1}{1 - f^2} \frac{f D}{1 - f^2} \quad (4.65)$$

Details on how to solve these equations perturbatively in PL are provided in the appendix. Integrating them is very straightforward, however, the utility for later PL

computations comes from our ability to rewrite the time domain solutions in terms of iterated time integrals of powers of $g^0 = \frac{1}{1^2 + f^2 + 1^{0 \cdot 2} g^2}$. This rewriting can be done mechanically at each order. The solutions we extract, to 2PL order in four dimensions, are

$$\begin{aligned} G &= A_2 \frac{1}{m_g} \dots \\ G_1 &= A_2 f \frac{1}{m_g^2} \dots \\ H_1 &= A_2 \frac{f}{1 f^2 + 1^{0 \cdot 2}} \frac{1}{m_g} \dots \end{aligned} \tag{4.66}$$

and

$$\begin{aligned} G_2 &= A_2^2 \frac{f \frac{1}{m_g} \frac{1}{f^2 + 1}}{\dots} \\ G_2 &= A_2^2 \left[\frac{1 f^2 \frac{1}{m_g} \frac{1}{f^2 + 1}}{\dots} + \frac{1 f^2 \frac{1}{m_g} \frac{1}{f^2 + 1}}{\dots} + \frac{1}{m_g^2} \frac{1}{f^2 + 1} \dots \right] \\ H_2 &= A_2^2 \left[\frac{1}{21^2} \frac{1}{m_g} \frac{1}{f^2 + 1} \dots + \frac{1}{2} \frac{1}{m_g} \frac{1}{f^2 + 1} \dots + \frac{f^2 \frac{1}{m_g} \frac{1}{f^2 + 1}}{1^2} \dots \right] \end{aligned} \tag{4.67}$$

This now has a structure resembling elements of a Feynman diagram. Upon Fourier transform the powers of f will be simple powers of spatial momenta (as is the case for the 1•A Coulomb potential) and the $\frac{1}{m_g}$ will be mapped to linearized matter propagators, i.e. $\frac{1}{D^2 + p^2}$ for some momentum p . For example,

$$\frac{1}{m_g} \frac{1}{f^2 + 1} = 168 c^2 \frac{4}{1^2} \frac{8 A_{1, 2} \hat{X}^1 D_{1, 2} \hat{X}^1 D_{2, 1}}{1^2} \dots \tag{4.68}$$

The mapping to Feynman integrals is straightforward, the powers of f and 1^3 correspond to background photon insertions, and the powers of $\frac{1}{m_g}$ correspond to matter propagators. Using this, one can inspect and see which Feynman integral topologies are contained in the solutions. As mentioned above, the advantage of this approach in electromagnetism is minor. However, we will see later that the structure of the solutions in gravitation, namely the resulting integral topologies, is nearly identical to electromagnetism.

4.2.4 Results and Checks

To compute the on-shell radial action, we simply perform the path integral over the fluctuation degrees of freedom. In particular, the radial action \mathcal{I}_{EM} is defined up to a constant normalization by

$$\exp\left(\frac{i}{\hbar} \mathcal{I}_{EM}\right) = \int \mathcal{D}X \mathcal{D}\tilde{X} \mathcal{D}\tilde{X} \exp\left(\frac{i}{\hbar} \mathcal{I}(\tilde{X}, \tilde{X}, X)\right). \quad (4.69)$$

As we are interested only in classical physics, we always take the saddle-point approximation and the path integral serves only as an organizational tool for our perturbation theory. Working up to 0SF and 1SF, we can ignore the fluctuations of the light particle, X . Meanwhile, doing the path integral over the heavy particle fluctuations, \tilde{X} , simply yields the recoil operator which appears in the effective action, $\mathcal{I}_e^{(1)}$, as defined in Eq. (4.42). Thus, we obtain

$$\exp\left(\frac{i}{\hbar} \mathcal{I}_{EM}\right) = \int \mathcal{D}\tilde{X} \exp\left(\frac{i}{\hbar} \mathcal{I}(\tilde{X}, \tilde{X}, 0)\right) \exp\left(\frac{i}{\hbar} \mathcal{I}_e^{(1)}\right) \quad (4.70)$$

where the ellipses denote contributions beyond 1SF. Decomposing the radial action according to the SF expansion,

$$\mathcal{I}_{EM} = \mathcal{I}_{EM}^{(0)} + \mathcal{I}_{EM}^{(1)} + \dots \quad (4.71)$$

where the superscripts denote the SF order of a given contribution, we find that

$$\begin{aligned} \mathcal{I}_{EM}^{(0)} &= \left(- \right. \\ \mathcal{I}_{EM}^{(1)} &= \left. \log \int \mathcal{D}\tilde{X} \exp\left(\frac{i}{\hbar} \mathcal{I}(\tilde{X}, \tilde{X}, 0)\right) \right) \end{aligned} \quad (4.72)$$

The above manipulations imply, as is well-known, that the 0SF radial action, $\mathcal{I}_{EM}^{(0)}$, is simply the action evaluated on the probe solution, as given in Sec. 4.2.1.4, Eq. (4.32). Furthermore, the 1SF radial action, $\mathcal{I}_{EM}^{(1)}$, is computed by summing all tree-level connected 1SF Feynman diagrams that arise from integrating out the photon fluctuation.

In what follows, we compute the 0SF and 1SF actions in $d=4$ spacetime dimensions, expanded in the PL expansion. Concretely, we express

$$\mathcal{I}_{EM}^{(1)} = \sum_{\substack{\delta=0 \\ \delta=1}}^{\infty} \tilde{\mathcal{O}}_{EM}^{(1-\delta)} \quad (4.73)$$

where δ and $\tilde{\mathcal{O}}$ denote the SF and PL orders of a given contribution. Remarkably, to compute to arbitrarily high orders in PL, it suffices to simply expand the light particle

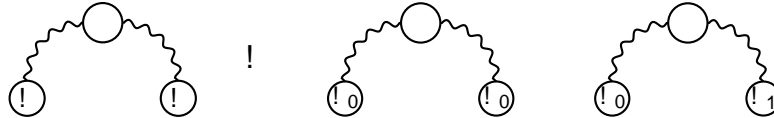


Figure 4.3: Diagram encoding the 1SF electromagnetic on-shell radial action in the potential region. The L.H.S. is composed of the source probe trajectory, photon propagators, and the 1SF electromagnetic recoil operator and the R.H.S. depicts contributions from the diagram at 2PL and 3PL orders.

trajectory to the appropriate order. We will focus on scattering dynamics, in which case the kinematic data is the asymptotic impact parameter, b , and the relative boost factor, $f = D/D_1$. It follows from dimensional analysis that the SF+PL expansion of the radial action has the form,

$$I_{EM}^{18-09} = -\frac{8}{\pi} A_2 \frac{A_2}{1} \int_{EM}^{18-09} f^{0-} \quad (4.74)$$

which is the electromagnetic analog of the good mass polynomiality in gravity [195].

4.2.4.1 Scattering Electric Charges

At last, we are equipped to compute the 1SF radial action for the scattering of electrically charged particles in electromagnetism. This is computed by summing Feynman diagrams in our 1SF order effective theory.

We are interested in only the conservative contributions to the scattering dynamics, leaving a treatment of radiative losses for future work. Through 3PL order, these conservative contributions to the radial action are entirely accounted for by the diagram in Fig. 4.3. Beyond 3PL order, but still at 1SF, one must also consider multi-insertions of the recoil operator, however such diagrams vanish in the potential region.

The leading, 2PL, contribution evaluates to

$$I_{EM}^{11-20} = \frac{2}{\pi} \int_{EM}^{11-20} |^2|^2 <^3 \frac{4 \int_{EM}^{81} \int_{EM}^{201} \int_{EM}^{00} \int_{EM}^{01} \int_{EM}^{20}}{1^{-2} \frac{2}{1} \frac{2}{2}} 1, \frac{f^{21} \int_{EM}^{1} \int_{EM}^{20}}{1D \int_{EM}^{01} D \int_{EM}^{20}} \quad (4.75)$$

$$= -\frac{8}{\pi} A_2 \frac{A_2}{1} \frac{c}{f^2} \frac{1}{1}$$

where, when unspecified, the matter propagators are understood to have a principal value pole prescription. The two integrations correspond to a one-loop integral

over the internal photon momentum, followed by a Fourier transform to impact parameter space. As expected, $\langle A_2^2 \rangle_{EM}^{11-20}$ is the same as the probe result $\langle A_2^2 \rangle_{EM}^{10-20}$, upon swapping $k_1 \leftrightarrow k_2$, where $\langle A_2^2 \rangle_{EM}^{10-20}$ is given by Eq. (4.32).

As a check, we have also performed the 2PL calculation in general spacetime dimension, d ,

$$\langle A_2^2 \rangle_{EM}^{11-20} = \frac{1}{12} \frac{A_2^2}{7} \frac{1}{c} \frac{7 \cdot 2^{d-1} \cdot 2 \cdot 3 \cdot 2^{d-2} \cdot 12}{3^d} \frac{7 f^2}{21 f^2} \frac{1}{103 \cdot 2} \quad (4.76)$$

and verified that it is consistent with all known results. We point the reader to App. E for technical details.

Moving on to the next order, we compute the 3PL Feynman diagram in Fig. 4.3, integrating via the methods described in [25, 273]. The resulting integrand and final answer is

$$\begin{aligned} \langle A_2^2 \rangle_{EM}^{11-30} &= \frac{1}{12} \frac{A_2^2}{7} \frac{1}{c} \frac{1}{103 \cdot 2} \int \frac{d^3x_1 d^3x_2 d^3x_3}{(2\pi)^9} \frac{e^{i(k_1 x_1 + k_2 x_2 + k_3 x_3)}}{k_1^2 k_2^2 k_3^2} \frac{1}{k_1^2 k_2^2 k_3^2} \frac{1}{k_1^2 k_2^2 k_3^2} \\ &= \frac{1}{12} \frac{A_2^2}{7} \frac{1}{c} \frac{1}{103 \cdot 2} \frac{1}{(2\pi)^9} \int \frac{d^3x_1 d^3x_2 d^3x_3}{(2\pi)^9} \frac{e^{i(k_1 x_1 + k_2 x_2 + k_3 x_3)}}{k_1^2 k_2^2 k_3^2} \frac{1}{k_1^2 k_2^2 k_3^2} \frac{1}{k_1^2 k_2^2 k_3^2} \\ &= \frac{1}{12} \frac{A_2^2}{7} \frac{1}{c} \frac{1}{103 \cdot 2} \frac{1}{(2\pi)^9} \frac{1}{(2\pi)^9} \int \frac{d^3x_1 d^3x_2 d^3x_3}{(2\pi)^9} \frac{e^{i(k_1 x_1 + k_2 x_2 + k_3 x_3)}}{k_1^2 k_2^2 k_3^2} \frac{1}{k_1^2 k_2^2 k_3^2} \frac{1}{k_1^2 k_2^2 k_3^2} \\ &= \frac{1}{12} \frac{A_2^2}{7} \frac{1}{c} \frac{1}{103 \cdot 2} \frac{1}{(2\pi)^9} \frac{1}{(2\pi)^9} \frac{1}{(2\pi)^9} \int \frac{d^3x_1 d^3x_2 d^3x_3}{(2\pi)^9} \frac{e^{i(k_1 x_1 + k_2 x_2 + k_3 x_3)}}{k_1^2 k_2^2 k_3^2} \frac{1}{k_1^2 k_2^2 k_3^2} \frac{1}{k_1^2 k_2^2 k_3^2} \end{aligned} \quad (4.77)$$

which agrees exactly with the calculation from [271].

We also compute the 2SF radial action to 3PM order. The integrand and integration is very simple,

$$\begin{aligned} \langle A_2^2 \rangle_{EM}^{12-30} &= \frac{1}{32} \frac{A_2^2}{c} \frac{1}{103 \cdot 2} \int \frac{d^3x_1 d^3x_2 d^3x_3}{(2\pi)^9} \frac{e^{i(k_1 x_1 + k_2 x_2 + k_3 x_3)}}{k_1^2 k_2^2 k_3^2} \frac{1}{k_1^2 k_2^2 k_3^2} \frac{1}{k_1^2 k_2^2 k_3^2} \\ &= \frac{1}{32} \frac{A_2^2}{c} \frac{1}{103 \cdot 2} \frac{1}{(2\pi)^9} \int \frac{d^3x_1 d^3x_2 d^3x_3}{(2\pi)^9} \frac{e^{i(k_1 x_1 + k_2 x_2 + k_3 x_3)}}{k_1^2 k_2^2 k_3^2} \frac{1}{k_1^2 k_2^2 k_3^2} \frac{1}{k_1^2 k_2^2 k_3^2} \\ &= \frac{1}{32} \frac{A_2^2}{c} \frac{1}{103 \cdot 2} \frac{1}{(2\pi)^9} \frac{1}{(2\pi)^9} \int \frac{d^3x_1 d^3x_2 d^3x_3}{(2\pi)^9} \frac{e^{i(k_1 x_1 + k_2 x_2 + k_3 x_3)}}{k_1^2 k_2^2 k_3^2} \frac{1}{k_1^2 k_2^2 k_3^2} \frac{1}{k_1^2 k_2^2 k_3^2} \end{aligned} \quad (4.78)$$

This agrees with the OSF result, Eq. (4.32), providing a crucial check on the consistency of our mass ratio expansion EFT.

4.2.4.2 Scattering Dyonic Charges

Since our framework is manifestly gauge invariant, it is straightforward to generalize the above results to the scattering of particles with both electric and magnetic charges. The action for the point-particle effective theory is then

$$S_{\text{dyon}} = \int_{\mathcal{M}} \left[-\frac{1}{2} g_{\mu\nu} \dot{x}^\mu \dot{x}^\nu - \frac{1}{2} \frac{e^2}{g^2} \mathcal{G}_{\mu\nu} \dot{x}^\mu \dot{x}^\nu - \frac{1}{2} \frac{g^2}{e^2} \tilde{\mathcal{G}}_{\mu\nu} \dot{x}^\mu \dot{x}^\nu \right] \quad (4.79)$$

where e is the electric charge, g is the magnetic charge, and $\tilde{\mathcal{G}}$ is the dual-photon field [274]. The photon and dual-photon are not independent fields, however, for our purposes, all that needs to be known about their relationship is how, in vacuum, they each relate to the field strength tensor,

$$\begin{aligned} m_{\mu\nu} &= \mathcal{G}_{\mu\nu} \\ m_{\mu\nu} &= \tilde{\mathcal{G}}_{\mu\nu} \end{aligned}$$

where $\tilde{\mathcal{G}}$ denotes the Hodge star operation.

The derivation of the 1SF effective action exactly parallels the purely electric case so we will not repeat all of the details. The upshot of the derivation is that promoting the charged particles to dyons amounts to just a few minor transformations of the 1SF effective action in the purely electric case. The light particle's coupling to the background changes to

$$\int_{\mathcal{M}} \left[\frac{1}{2} g_{\mu\nu} \dot{x}^\mu \dot{x}^\nu - \frac{1}{2} \frac{e^2}{g^2} \mathcal{G}_{\mu\nu} \dot{x}^\mu \dot{x}^\nu - \frac{1}{2} \frac{g^2}{e^2} \tilde{\mathcal{G}}_{\mu\nu} \dot{x}^\mu \dot{x}^\nu \right] = 0 \quad (4.80)$$

and the background field strength, previously given in Eq. (4.51), gets mapped to

$$\mathcal{G}_{\mu\nu} = \frac{1}{2} \epsilon_{\mu\nu\rho\sigma} \tilde{\mathcal{G}}^{\rho\sigma} \quad (4.81)$$

Within the recoil operator, the fluctuation field strength gets mapped to

$$\tilde{\mathcal{G}}_{\mu\nu} = \frac{1}{2} \epsilon_{\mu\nu\rho\sigma} \mathcal{G}^{\rho\sigma} \quad (4.82)$$

In the previous section, we wrote everything in terms of the charge-to-mass ratios, $l_g = \frac{e}{g} <_g$. To do so in this section, and best mirror the form of the previous

expressions, it is convenient to define the electric and magnetic charges in terms of angles,

$$Q_g = \langle g | g \cos \theta_g -$$

$$G_g = \langle g | g \sin \theta_g -$$

so that the total magnitude of each particle's charge is still given by g . An electromagnetic duality rotation rotates these angles simultaneously and a check on our final results is that they depend only on the duality invariant $\theta = \theta_1 - \theta_2$. In terms of these variables, the light particle's equation of motion is mapped to

$$\vec{E} + \vec{v} \times \vec{B} + \vec{a} \cdot \vec{G} = 0 \quad (4.83)$$

where \vec{a} is given by Eq. (4.51), and the fluctuation field strength in the recoil operator is mapped to

$$X_{\vec{a}} = \vec{X} \cdot \vec{a} = |\vec{X}| \cos \theta \sin \theta \vec{X} \cdot \vec{a} \quad (4.84)$$

In summary, the 1SF effective action for the scattering of dyons is

$$X_{\text{dyons}}^{(e)} = \left(\text{recoil}_{\text{dyons}} \right) \quad (4.85)$$

$$= \frac{3^4 G^2}{4} X_{\vec{a}} X_{\vec{a}} \cos \theta \sin \theta \vec{X} \cdot \vec{a} \quad (4.85)$$

with

$$\left(\text{recoil}_{\text{dyons}} \right) = \frac{1}{2} |\vec{J}|^2 < \frac{3g^2}{4} \vec{X} \cdot \vec{a} \frac{1}{n_g^2} \vec{X} \cdot \vec{a} \vec{G} \quad (4.86)$$

where \vec{J} is the point particle vector current given in Eq. (4.38), with the particle following a solution to Eq. (4.83), and $\vec{X}_{\vec{a}}$ is the appropriate duality rotation of the fluctuation photon's field strength, Eq. (4.82).

Naively, when doing perturbative computations, one would need to describe the explicit relationship between the photon and dual-photon but, since the recoil operator is manifestly gauge invariant, such expressions are never required. Concretely, when computing diagrams, we can only ever encounter contractions between gauge potentials and field strengths and never between two gauge potentials. Such contractions are unambiguous and thus, as initially claimed, the manifest gauge-invariance of the recoil operator allows us to straightforwardly compute the radial action for the scattering of dyonic charged particles.

Computing the 1SF radial action for the scattering of two dyonically charged particles, we obtain

$$\begin{aligned} \frac{11-2^0}{EM} \Gamma & \frac{11-2^0}{EM-\lambda} = -\frac{A_2}{1} \frac{c \cos^2 \lambda + \sin^2 \lambda}{2 f^2 + 1} \frac{\cos^2 \lambda + \sin^2 \lambda}{1} - \\ \frac{11-3^0}{EM} \Gamma & \frac{11-3^0}{EM-\lambda} = -\frac{A_2}{1} \frac{2 \cos \lambda + f^2 \cos 2 \lambda + 2f^4 + 7f^2 + 6}{3 f^2 + 1^{5 \cdot 2}} \bullet \end{aligned} \quad (4.87)$$

Notably, the 2PL radial action is exactly the same as for pure electric charge scattering. This agrees with the probe limits computed in [275], wherein pure electric scattering and electric-magnetic scattering at 2PL were identical. Furthermore, notice that the 3PL radial action vanishes for a relative angle, $\lambda = \pi/2$, corresponding to a pure electric charge scattering against a pure magnetic charge. This agrees with general expectations from the all-orders probe computations [275]. The above general 3PL result is new.

4.3 General Relativity

In this section, we derive an effective field theory for gravity in the extreme mass ratio expansion. Our manipulations will exactly parallel all of the steps taken in our analysis of electromagnetism.

In particular, we begin with the worldline action for a pair of massive scalar particles interacting via general relativity. At 0SF, one particle produces a background gravitational field described by the Schwarzschild metric while the other particle, whose mass is comparatively negligible, evolves as a test-body moving in this background.

At 1SF, the heavy particle fluctuates dynamically while, as before, the light particle fluctuations can be conveniently ignored. Integrating out the former, we derive the gravitational recoil operator for the effective field theory. This operator encodes the recoil of the Schwarzschild background against the orbiting mass. An important difference between general relativity and electromagnetism is that gravitons are self-interacting and fluctuations will couple to the background. As we will see, these effects are encoded entirely in the usual framework describing gravitons propagating in a Schwarzschild background. While an analytic expression for the propagator of such gravitons is not known, we can leverage the known background metric to straightforwardly compute this in the PM expansion.

As a crucial test of our framework, we compute the radial action for massive particle scattering at 0SF, 1SF, and 2SF, through 3PM order in general relativity. The 0SF radial action is already known to all PM orders, as recapitulated in App. E, and our results at 1SF and 2SF find exact agreement with known results [5, 11, 95, 96].

To demonstrate the versatility of our framework, we also compute the 2PM and 3PM radial actions for gravitational theories in which the light particle sources a scalar or vector field which itself interacts gravitationally. The former agrees with existing calculations while the latter is a new result.

4.3.1 Effective Theory

As our starting point, we consider the action for a pair of massive, gravitationally interacting scalar particles in general relativity. Once again, as shown in App. D, we can fix the worldline einbein so that the action takes the simple form,

$$S = \int_{\mathcal{C}} d\tau \left[-m \sqrt{-g_{\mu\nu} \dot{x}^\mu \dot{x}^\nu} - \frac{1}{2} \int_{\mathcal{C}} d\tau' \int_{\mathcal{C}} d\tau'' \dot{x}^\mu \dot{x}^\nu g_{\mu\nu}(x) \right] \quad (4.88)$$

where \mathcal{C} and \mathcal{C}' are the particle trajectories and $g_{\mu\nu}$ is the metric field. Our gauge fixing implies the on-shell condition $\dot{x}^\mu \dot{x}_\mu = 1$.

The geodesic equation and Einstein field equations are

$$\ddot{x}^\mu + \Gamma^\mu_{\nu\rho} \dot{x}^\nu \dot{x}^\rho = 0 \quad \text{and} \quad \nabla_\mu \nabla^\mu g_{\nu\rho} - \frac{1}{2} g_{\nu\rho} \nabla_\sigma \nabla^\sigma \ln \Omega = 8\pi G \mathcal{T}_{\nu\rho} \quad (4.89)$$

where the energy-momentum tensor is

$$\mathcal{T}_{\mu\nu} = \int_{\mathcal{C}} d\tau \dot{x}^\alpha \dot{x}^\beta g_{\alpha\beta} \delta^4(x - x(\tau)) \quad (4.90)$$

Our effective field theory will provide an efficient way to solve these equations of motion as an expansion in the mass ratio. As has been noted previously [276], the Schwarzschild metric itself encodes infinite PM orders, simply by virtue of the fact that it is a formula that holds at infinite gravitational coupling. We will describe how the Schwarzschild metric, together with the geodesics of particles within it, can be used to incorporate all orders in PM information into a systematic calculational framework.

4.3.1.1 Mass Ratio Expansion in Curved Space

At $\mathcal{O}(m^0)$, the light particle acts as a nongravitating probe. Consequently, the heavy particle moves in a straight line,

$$\dot{G}^\mu{}_\nu = \dot{D}^\mu g_\nu \quad (4.91)$$

providing a stress-energy density,

$$p \frac{1}{6^{(1)}G} \cdot_a 1G = < 3g^{(1)}G D g^0 D D^a - \quad (4.92)$$

which sources the OSF accurate field equations,

$$\mathcal{E}_{,df} \cdot 1G^0 \mathcal{E}^d \mathcal{E} = 0 \quad \text{and} \quad \cdot_a \frac{1}{2} 6 \cdot_a = 8c \cdot_a \bullet \quad (4.93)$$

Let us comment briefly on the issue of self-energies. Technically, the heavy particle follows a geodesic according to the equation,

$$\mathcal{E}_{,df} \cdot 1G^0 \mathcal{E}^d \mathcal{E} = 0 \bullet \quad (4.94)$$

Since $\cdot_{df} 1G^0$ is the Christoffel symbol for the Schwarzschild metric evaluated at the point, $A = 0$, it is formally divergent. However, just as in the case of electromagnetism, we interpret this as a potential graviton mode that has been emitted and then reabsorbed by the heavy particle. This divergent self-energy contribution can be absorbed by a counterterm, and can effectively be dropped. Consequently, the effective equation of motion for the heavy particle is 0.

As before, one could try to solve the equations of motion perturbatively by PM expanding the trajectory and metric and solving the equations iteratively at each order. Alternatively, thanks to the symmetries of the problem, we can first-order differential equations instead. The gravitational background is just the boosted Schwarzschild metric and \mathcal{G} is a geodesic within it. The solution can be written in isotropic coordinates,

$$6 \cdot_a 1G = 1, \frac{A}{4A} \cdot_a \left[\cdot_a, \frac{1}{1, \frac{A}{4A}} \frac{A}{4A}^2 \cdot_a, \frac{A}{4A} \cdot_a \right] D \cdot D_a - \quad (4.95)$$

where $A = \frac{p}{1D G^2} G$ is the boosted radius and $A = 2 <$ is the Schwarzschild radius. Since we will recast the Schwarzschild background as a resummation of an infinite class of flat space diagrams, it will be useful to define the deviation from flat space,

$$W_a 1G = 6 \cdot_a 1G \left[\cdot_a = \frac{A}{A} \cdot_a - 2D \cdot D_a^0 \right. \\ \left. , \frac{1}{8} \frac{A}{A}^2 \cdot_a \cdot_a, D \cdot D_a^0, O^1 A^3 \cdot_a \right] - \quad (4.96)$$

allowing us to trivially read off PM data order by order. Details on the light particle geodesic will be provided in upcoming sections where we see, once again, that we can read off PM data from simple position space expressions.

At leading nontrivial order in the mass ratio $\mu \ll 1$, the Schwarzschild metric and particle trajectories are perturbed by 1SF corrections,

$$\hat{G}_{\alpha\beta} = \bar{G}_{\alpha\beta} + X\delta\hat{G}_{\alpha\beta} \quad \text{and} \quad \hat{6}_a = \bar{6}_a + X\delta\hat{6}_a \quad (4.97)$$

where $X\delta\hat{6}_a$ is the fluctuation graviton propagating on a Schwarzschild background. Since the OSF solutions $\bar{G}_{\alpha\beta}$ and $\bar{6}_a$ are valid at $\mathcal{O}(1-\mu^0)$, we know that

$$X\delta\hat{G}_{\alpha\beta} = \mathcal{O}(1-\mu^1) \quad (4.98)$$

for on-shell configurations of the fluctuation degrees of freedom.

4.3.1.2 OSF Dynamics

Since our interest is in computing the on-shell action, let us insert the SF expanded trajectories and fields in Eq. (4.97) into the action in Eq. (4.88), and compute

$$\tilde{\mathcal{I}} = \int_{\mathcal{M}} \mathcal{L}(\hat{G}_{\alpha\beta}, \hat{6}_a) \sqrt{-\hat{G}} \, d^4x \quad (4.99)$$

where $\tilde{\mathcal{I}}$ denotes the SF order action and is simply the action evaluated on the $\mathcal{O}(1-\mu^0)$ solutions. The renormalized OSF action is

$$\mathcal{I} = \frac{\hbar}{c^3} \int_{\mathcal{M}} \left[\frac{1}{2} \delta\hat{G}_{\alpha\beta} \delta\hat{G}^{\alpha\beta} - \frac{1}{2} \delta\hat{6}_a \delta\hat{6}^a \right] \sqrt{-\bar{G}} \, d^4x \quad (4.100)$$

and all dependence on the dynamical fluctuation modes are contained in the $\delta\hat{G}$ and $\delta\hat{6}$ terms. Note the suppression of the probe particle action by a factor \hbar/c^3 compared to that of the heavy particle.

Let us first focus on the OSF dynamics in $d = 4$ dimensions. The heavy particle is nondynamical in this limit and the dynamics are governed by the single-particle action,

$$\mathcal{I} = \frac{\hbar}{c^3} \int_{\mathcal{M}} \left[\frac{1}{2} \delta\hat{G}_{\alpha\beta} \delta\hat{G}^{\alpha\beta} - \frac{1}{2} \delta\hat{6}_a \delta\hat{6}^a \right] \sqrt{-\bar{G}} \, d^4x \quad (4.101)$$

where the background metric sourced by the heavy (spinless) particle is just the Schwarzschild solution,

$$\bar{6}_{00} = \frac{5}{5} \frac{1}{A^0} \quad \text{and} \quad \bar{6}_{89} = X_{89} \frac{1}{A^0} \quad (4.102)$$

presented here in isotropic coordinates where we have defined the function,

$$\frac{5}{5} \frac{1}{A^0} = 1 - \frac{A_t}{4A} \quad (4.103)$$

with the Schwarzschild radius $r_s = 2 < .$ Solutions to the equations of motion satisfy the curved space on-shell condition $\epsilon_a \epsilon^a = 1$.

The background is static and isotropic so we can restrict to motion in the equatorial plane with dynamics constrained by the conserved energy and angular momentum. We prefer, again, to label trajectories by (l) , in terms of which we have equations of motion,

$$\epsilon = f \frac{5^1 A^2}{5^1 A^2} \quad \text{and} \quad \dot{\phi} = \frac{1^1 f^2 \quad 1^{0 \cdot 2}}{A^2} 5^1 A^4 - \quad (4.104)$$

with the radial equation of motion coming from the on-shell condition,

$$\dot{r} = 5^1 A^4 \frac{5^1 A^2}{5^1 A^2} f^2 - 1 \quad \frac{1^2 1 f^2 \quad 1^0}{A^2} 5^1 A^8 \quad 1^{\cdot 2} \quad (4.105)$$

As discussed in App. E, with this set of symmetries, the OSF on-shell action is given by a simple radial action integral,

$$S = 2 \int_{A_{\min}}^1 3A j_A^1 A - \quad (4.106)$$

and we can use the equation of motion and conserved quantities to write the exact probe radial momentum,

$$j_A^1 = \frac{5^1 A^4}{5^1 A^2} f^2 - 1 \quad \frac{1^2 1 f^2 \quad 1^0}{A^2} \quad 1^{\cdot 2} \quad (4.107)$$

Integrating j_A^1 to 3PM (see App. E for details) we obtain

$$\begin{aligned} S &= c_1 \int_{r_1}^{r_2} \frac{p}{f^2 - 1} \quad , \quad c_1 < \frac{2 \quad 4f^2 \log \quad 4^{-\frac{1}{4}} \quad , \quad 1}{p \quad f^2 - 1} \\ & , \quad c_2 < \int_{r_1}^{r_2} \frac{3c \quad 5f^2 \quad 1}{41 \quad f^2 - 1} \quad (4.108) \\ & , \quad c_3 < \int_{r_1}^{r_2} \frac{64f^6 \quad 120f^4 \quad 60f^2 \quad 5}{31^2 \quad f^2 - 1 \quad 5^{\cdot 2}} \quad . \end{aligned}$$

4.3.1.3 1SF Dynamics

Next, we discuss the dynamical modes relevant to the 1SF gravitational problem. As before, we will derive a 1SF effective action obtained from integrating out heavy particle fluctuations. Given that the OSF action was actually due to the

suppression of the light particle action by a factor of ω we expand the action up to $\mathcal{O}(\omega^2)$, which requires expanding only up to quadratic order in the fluctuations.

Expanding the Einstein-Hilbert action about the Schwarzschild background, we obtain the usual action for a graviton in curved spacetime,

$$\begin{aligned} \frac{1}{16c} \int d^4x \sqrt{-g} \left(-\frac{1}{2} \partial_\mu h_{\alpha\beta} \partial^\mu h^{\alpha\beta} + \partial_\mu h^\mu{}_\alpha \partial^\alpha h - \frac{1}{2} \partial_\mu h^\mu{}_\alpha \partial^\alpha h + \frac{1}{2} \partial_\mu h^\mu{}_\alpha \partial^\alpha h \right) \\ + \frac{1}{4} \partial_\mu h^\mu{}_\alpha \partial^\alpha h - \frac{1}{8} \partial_\mu h^\mu{}_\alpha \partial^\alpha h \\ + \frac{1}{2} \partial_\mu h^\mu{}_\alpha \partial^\alpha h - \frac{1}{2} \partial_\mu h^\mu{}_\alpha \partial^\alpha h \\ + \frac{1}{4} \partial_\mu h^\mu{}_\alpha \partial^\alpha h - \frac{1}{2} \partial_\mu h^\mu{}_\alpha \partial^\alpha h \end{aligned} \quad (4.109)$$

where $h_{\alpha\beta} = g_{\alpha\beta} + h_{\alpha\beta}$ and we have added a harmonic gauge fixing term for the graviton perturbation defined by $h = g^{\alpha\beta} h_{\alpha\beta}$. All raising, lowering, and contractions of indices are performed with the background metric,

At this point, let us comment on a subtlety in the above action. Normally, when considering fields propagating in a Schwarzschild background, we would set $T_{\mu\nu} = 0$ on account of the fact that the metric satisfies the vacuum Einstein field equations. This would naively suggest that we can simply drop any terms containing $h^\mu{}_\alpha$ or h . However, this is not correct when working in perturbation theory because our equations of motion in Eq. (4.89) describe a source that is not a vacuum but, rather, is composed of worldlines. Consequently, in perturbation theory $T_{\mu\nu}$ are zero except on the support of the heavy worldline. This crucial distinction implies that we must actually keep all such terms in the action in any perturbative calculation. For this reason, $h^\mu{}_\alpha \partial^\alpha h$ in Eq. (4.109) is not identically zero in perturbation theory, but will actually cancel with other terms in the worldline action since the Einstein field equations are sourced by worldlines.

Next, consider the action for the worldlines, which is

$$\begin{aligned} S_{\text{WL}} &= \int d\tau \left(-m \sqrt{-g_{\alpha\beta} \dot{x}^\alpha \dot{x}^\beta} + \frac{1}{2} g_{\alpha\beta} \dot{x}^\alpha \dot{x}^\beta \right) \\ &= \int d\tau \left(-m \sqrt{-g_{\alpha\beta} \dot{x}^\alpha \dot{x}^\beta} + \frac{1}{2} g_{\alpha\beta} \dot{x}^\alpha \dot{x}^\beta \right) \\ &\quad + \int d\tau \left(\frac{1}{2} g_{\alpha\beta} \dot{x}^\alpha \dot{x}^\beta + \frac{1}{2} g_{\alpha\beta} \dot{x}^\alpha \dot{x}^\beta \right) \\ &\quad + \int d\tau \left(\frac{1}{2} g_{\alpha\beta} \dot{x}^\alpha \dot{x}^\beta + \frac{1}{2} g_{\alpha\beta} \dot{x}^\alpha \dot{x}^\beta \right) \\ &\quad + \int d\tau \left(\frac{1}{2} g_{\alpha\beta} \dot{x}^\alpha \dot{x}^\beta + \frac{1}{2} g_{\alpha\beta} \dot{x}^\alpha \dot{x}^\beta \right) \end{aligned} \quad (4.110)$$

where the ellipses denote contributions that are higher than quadratic order in the fluctuations and we have defined the difference of connections $\chi_{ab}^d = \dot{x}_a^d - \dot{x}_a^d = \frac{1}{2} \delta^{df} \Gamma_{ab}^f - \Gamma_{ab}^d$, which is a tensor with respect to the background metric. As before, the worldline actions for the heavy and light particles are treated differently, so

$$\begin{aligned}
 & \langle \dots \rangle = \langle 3g_{\frac{1}{2}} \dots \rangle \\
 & = \langle 3g_{\frac{1}{2}} \dots \rangle \\
 & \quad \langle \dots \rangle \\
 & \quad \langle \dots \rangle \\
 & \quad \langle \dots \rangle \\
 & \quad \langle \dots \rangle
 \end{aligned} \tag{4.111}$$

$$\begin{aligned}
 & \langle \dots \rangle = \langle \dots \rangle \\
 & \quad \langle \dots \rangle \\
 & \quad \langle \dots \rangle \\
 & \quad \langle \dots \rangle
 \end{aligned}$$

where several terms can be dropped. Terms containing the background metric evaluated at the heavy particle position have components which correspond to the emission and reabsorption of potential gravitons from the heavy particle. All terms involving \dot{x}_a^d or Γ_{ab}^d are self-energy contributions. Furthermore, while there are many implicit insertions of \dot{x}_a^d , the components of these which deviate from \dot{x}_a^d at space are again self-energy contributions. As elaborated in Sec. 4.2.1.3, such self-energy contributions can be renormalized away and, in fact, in dimensional regularization they are identically zero. Hence, in this scheme, the metric evaluated on the heavy trajectory \dot{x}_a^d , can be effectively set to the flat metric η_{ab} .

Furthermore χ_{ab}^d vanishes because of the background value of the heavy particle trajectory. $\frac{1}{2} \delta^{df} \Gamma_{ab}^f$ gives zero when combined with terms from the expanded Einstein-Hilbert action, and χ_{ab}^d vanishes because the light trajectory satisfies its background equation of motion. Finally, the terms in the last two lines of the expanded light particle action can be dropped because the light particle action is suppressed by ϵ , so these contributions enter $\mathcal{O}(\epsilon^3)$ and are subleading at 1SF.

Combining the relevant terms from Eq. (4.109) and Eq. (4.111), we obtain the 1SF action for fluctuations,

$$\begin{aligned} \langle S^{(1)} = & \int d^4x \sqrt{-g} \left[\frac{1}{2} \partial_\mu h_{\alpha\beta} \partial^\mu h^{\alpha\beta} - \partial_\mu h^{\alpha\beta} \partial_\nu h^{\gamma\delta} X^{\mu\nu} \partial^\alpha h^{\gamma\delta} + \frac{1}{2} \partial_\mu h^{\alpha\beta} \partial_\nu h^{\gamma\delta} X^{\mu\nu} \partial^\alpha h^{\gamma\delta} \right. \\ & \left. + \frac{3}{32} \partial_\mu h^{\alpha\beta} \partial_\nu h^{\gamma\delta} X^{\mu\nu} \partial^\alpha h^{\gamma\delta} + \frac{1}{4} \partial_\mu h^{\alpha\beta} \partial_\nu h^{\gamma\delta} X^{\mu\nu} \partial^\alpha h^{\gamma\delta} \right] \end{aligned} \quad (4.112)$$

The above action describes a dynamical graviton that is sourced by the light particle geodesic motion, and whose propagator is corrected by the motion of the heavy particle. We rewrite the action as

$$\begin{aligned} \langle S^{(1)} = & \int d^4x \sqrt{-g} \left[\frac{1}{2} \partial_\mu h_{\alpha\beta} \partial^\mu h^{\alpha\beta} - \partial_\mu h^{\alpha\beta} \partial_\nu h^{\gamma\delta} X^{\mu\nu} \partial^\alpha h^{\gamma\delta} \right. \\ & \left. + \frac{3}{32} \partial_\mu h^{\alpha\beta} \partial_\nu h^{\gamma\delta} X^{\mu\nu} \partial^\alpha h^{\gamma\delta} + \frac{1}{4} \partial_\mu h^{\alpha\beta} \partial_\nu h^{\gamma\delta} X^{\mu\nu} \partial^\alpha h^{\gamma\delta} \right. \\ & \left. + \frac{1}{2} \partial_\mu h^{\alpha\beta} \partial_\nu h^{\gamma\delta} X^{\mu\nu} \partial^\alpha h^{\gamma\delta} \right] \end{aligned} \quad (4.113)$$

where the light particle OSF energy-momentum tensor is

$$T_{\alpha\beta} = \frac{1}{\sqrt{-g}} \left[\partial_\alpha h^{\gamma\delta} \partial_\beta h^{\epsilon\zeta} X^{\gamma\delta} \partial^\epsilon h^{\zeta\eta} - \frac{1}{2} g_{\alpha\beta} \partial_\mu h^{\gamma\delta} \partial^\mu h^{\epsilon\zeta} X^{\gamma\delta} \partial^\epsilon h^{\zeta\eta} \right] \quad (4.114)$$

The 1SF action in Eq. (4.113) describes a graviton propagating in a Schwarzschild background, sourced by a light particle geodesic, together with the fluctuations of the heavy particle. Just like in the case of electromagnetism, we see that for general relativity we only need the geodesic for the light particle in order to compute at 1SF order.

Next, let us integrate out the heavy particle fluctuation $h_{\alpha\beta}$, to obtain a 1SF effective action that depends solely on the graviton. The path integral yields

$$\begin{aligned} \int \mathcal{D}h_{\alpha\beta} \exp \left[i \int d^4x \sqrt{-g} \left(\frac{1}{2} \partial_\mu h_{\alpha\beta} \partial^\mu h^{\alpha\beta} - \partial_\mu h^{\alpha\beta} \partial_\nu h^{\gamma\delta} X^{\mu\nu} \partial^\alpha h^{\gamma\delta} \right) \right] \\ = \exp \left[i \int d^4x \sqrt{-g} S_{\text{recoil}}^{(1)} \right] \end{aligned} \quad (4.115)$$

where $S_{\text{recoil}}^{(1)}$ is the gravitational recoil operator. To do the path integral, we plug the solution for the heavy particle back into the action. As a consistency check we see that variation of the action with respect to $h_{\alpha\beta}$ is

$$\partial_\mu h^{\alpha\beta} \partial_\nu h^{\gamma\delta} X^{\mu\nu} \partial^\alpha h^{\gamma\delta} = 0 \quad (4.116)$$

which is the geodesic equation expanded to 1SF. Inserting this solution back into Eq. (4.113) yields the recoil operator,

$$S_{\text{recoil}}^{(1)} = \frac{1}{2} \int d^4x \sqrt{-g} \left[\partial_\mu h^{\alpha\beta} \partial_\nu h^{\gamma\delta} X^{\mu\nu} \partial^\alpha h^{\gamma\delta} - \frac{1}{2} g_{\alpha\beta} \partial_\mu h^{\gamma\delta} \partial^\mu h^{\epsilon\zeta} X^{\gamma\delta} \partial^\epsilon h^{\zeta\eta} \right] \quad (4.117)$$

We emphasize again that this operator is gauge invariant because $X_a^d(i)$ is a difference of connections, and thus a tensor with respect to the background metric at each of the two spacetime points where it is evaluated in Eq. (4.117), and (ii) within our renormalization scheme, the background metric evaluated at the location of the heavy body is effectively flat and the tensor indices are thus unambiguously parallel transported between the two spacetime points without the need for a gravitational Wilson line.

To summarize, we have defined a 1SF effective action for general relativity,

$$\begin{aligned} \Gamma^{10} = & \Gamma_{\text{recoil}}^{10} + 3^4 G^{\text{P}} \frac{1}{6} \frac{1}{32c} \frac{1}{2} r_{\text{d}} X_{6a} r^{\text{d}} X_{6a} - \frac{1}{4} r_{\text{d}} X_{6a} r^{\text{d}} X_{6a} + \dots \\ & \frac{1}{2} X_{6a} \dot{\Gamma}^a - \end{aligned} \quad (4.118)$$

which describes a graviton in a Schwarzschild background, sourced by a light particle geodesic $\dot{\Gamma}^a$, in Eq. (4.114), and perturbed by the recoil operator $\Gamma_{\text{recoil}}^{10}$, defined in Eq. (4.117). This operator encodes the fluctuations of the Schwarzschild metric due to the motion of the orbiting light particle at 1SF.

4.3.1.4 2SF Dynamics

As with electromagnetism, the 2SF dynamics are determined by expanding the action to \mathcal{O}^1_{-30} . Contributions to the light particle worldline were given in Eq. (4.111),

$$\begin{aligned} \Gamma_1^{20} = & 3g \frac{1}{2} \dot{\Gamma}^a \dot{\Gamma}^b r_{\text{d}} X_{6a} r^{\text{d}} X_{6b} + \frac{1}{2} X_{6a} \dot{\Gamma}^a \dot{\Gamma}^b r_{\text{d}} X_{6b} + \dots \\ & X_{6a} \dot{\Gamma}^a X_{6a} \dot{\Gamma}^a + \dots \end{aligned} \quad (4.119)$$

The first two terms describe geodesic deviation of the light particle trajectory caused by fluctuation gravitons which kick the body off its 0SF motion due to the interaction shown in the last term. This interaction of fluctuation gravitons with the light body is analogous to the recoil experienced by the heavy body at 1SF.

Contributions to the heavy particle worldline at 2SF consist of terms of the type, $X_{6a} X_{6a} X_{6a}$ that are cubic in fluctuations,

$$\begin{aligned} \Gamma^{20} = & 3g \frac{1}{2} X_{6a} X_{6a} X_{6a} + X_{6a} \dot{\Gamma}^a X_{6a} \dot{\Gamma}^a + \dots \\ & \frac{1}{2} X_{6a} \dot{\Gamma}^a X_{6a} \dot{\Gamma}^a + \dots \end{aligned} \quad (4.120)$$

such that the total heavy particle effective action to 2SF order is given by

$$\begin{aligned} \Gamma^{(10)}, \Gamma^{(20)} = & \int d^4x \left[\frac{1}{2} \partial_\mu \phi^a \partial^\mu \phi^a + \frac{1}{2} \partial_\mu \phi^a \partial^\mu \phi^a + \frac{1}{2} \partial_\mu \phi^a \partial^\mu \phi^a \right] \\ & + \frac{1}{2} \int d^4x \partial_\mu \phi^a \partial^\mu \phi^a + \frac{1}{2} \int d^4x \partial_\mu \phi^a \partial^\mu \phi^a \quad (4.121) \\ & + \frac{1}{2} \int d^4x \partial_\mu \phi^a \partial^\mu \phi^a \quad \bullet \end{aligned}$$

The additional terms give rise to a new recoil operator at 2SF which is determined, as before, by integrating the heavy particle fluctuations,

$$\int d^4x \exp \left[\Gamma^{(10)}_{\text{recoil}}, \Gamma^{(20)}_{\text{recoil}} \right] \quad (4.122)$$

so that

$$\begin{aligned} \Gamma^{(20)}_{\text{recoil}} = & \int d^4x \left[\frac{1}{2} \partial_\mu \phi^a \partial^\mu \phi^a + \frac{1}{2} \partial_\mu \phi^a \partial^\mu \phi^a + \frac{1}{2} \partial_\mu \phi^a \partial^\mu \phi^a \right] \\ & + \frac{1}{2} \int d^4x \partial_\mu \phi^a \partial^\mu \phi^a + \frac{1}{2} \int d^4x \partial_\mu \phi^a \partial^\mu \phi^a \quad (4.123) \\ & + \frac{1}{2} \int d^4x \partial_\mu \phi^a \partial^\mu \phi^a \quad \bullet \end{aligned}$$

With this new recoil operator, the full effective action at 2SF is

$$\begin{aligned} \Gamma^{(10)}, \Gamma^{(20)} = & \Gamma^{(10)}_{\text{recoil}}, \Gamma^{(20)}_{\text{recoil}} \\ & + \frac{1}{3!} \int d^4x \partial_\mu \phi^a \partial^\mu \phi^a + \frac{1}{3!} \int d^4x \partial_\mu \phi^a \partial^\mu \phi^a \\ & + \frac{1}{2} \int d^4x \partial_\mu \phi^a \partial^\mu \phi^a + \frac{1}{2} \int d^4x \partial_\mu \phi^a \partial^\mu \phi^a \quad (4.124) \\ & + \frac{1}{2} \int d^4x \partial_\mu \phi^a \partial^\mu \phi^a \quad \bullet \end{aligned}$$

where the curved space graviton three-point self-interaction terms are calculated in a PM expansion where necessary.

4.3.2 Feynman Rules

Using the 1SF effective action in Eq. (4.118), we can calculate physical observables by computing the path integral over the graviton fluctuations. In principle, we could choose to work entirely in curved spacetime, in which case we would compute with the graviton propagator in a Schwarzschild background. However, a simple closed form expression for this object does not exist and, furthermore, the absence

Figure 4.4: The curved space graviton propagator can be thought of as a sum of the flat space propagator and corrections involving interactions with the background. These interactions, depicted as insertions on the flat space propagator, are organized in a PM expansion of the background gravitational field.

of momenta for the particles makes technical calculations difficult. Instead, we will further decompose this framework in the PM expansion, which describes perturbative corrections from flat space. In such an approach, we can think of the Schwarzschild graviton propagator as the flat space propagator corrected by terms involving interactions with the background as shown in Fig. 4.4. We also PM expand the background field, treating terms of the form $\frac{1}{M_{\text{Pl}}^2}$, as corrections to flat space. The benefits of determining PM corrections using the known Schwarzschild background will be discussed in Sec. 4.3.3.

4.3.2.1 Graviton Propagator and Vertices

With the choice of harmonic gauge in the background field action for the graviton in Eq. (4.109), the flat space (0PM) graviton propagator is in deDonder gauge,

$$\frac{\overset{?}{\longrightarrow}}{\text{wavy line}} = \frac{32c8}{\text{?}^2} \frac{[\text{?}^d][\text{?}^f]}{2} \frac{[\text{?}^a][\text{?}^b]}{2} \cdot \quad (4.125)$$

Meanwhile, it is trivial to compute the two-point vertex for the graviton from the recoil operator $\mathcal{O}_{\text{recoil}}^{10}$ in Eq. (4.117), giving

$$\frac{\overset{?_1}{\longrightarrow}}{\text{wavy line}} \text{---} \text{---} \overset{?_2}{\longleftarrow} \text{wavy line} = \frac{8}{2} \frac{[\text{?}_1^a][\text{?}_2^b]}{[\text{?}_1^c][\text{?}_2^d]} \mathcal{O}_{\text{recoil}}^{10} = \text{?}^0 \mathcal{O}_{\text{recoil}}^{20} = \text{?}^0 \quad (4.126)$$

where we have defined $\mathcal{O}_{\text{recoil}}^{10} = \frac{1}{2} [\text{?}_1^a][\text{?}_2^b] \mathcal{O}_{\text{recoil}}^{10} = \text{?}^0 \mathcal{O}_{\text{recoil}}^{20}$. Notice the close similarity of the above equation to the corresponding Feynman vertex in electromagnetism in Eq. (4.117).

Since we will be treating the background metric insertions as perturbations about flat space, we perform a PM expansion of the Schwarzschild metric. At leading

nontrivial PM order, the background metric and Christoffel connection are

$$\begin{aligned}
 W_a^{1?0} &= \frac{8c \langle \dots \rangle}{?^2} X^a D^{?0}, \quad - \\
 \Gamma_{UV}^{1?0} &= \frac{8}{2} \langle \dots \rangle, \quad \bullet
 \end{aligned}
 \tag{4.127}$$

These should be inserted into \mathcal{M} at space Feynman diagrams effectively as sources. Notably, at 3PM and lower orders, the background metric insertions beyond 1PM order are not needed. However, starting at 4PM order, these contributions become relevant. Note that the benefits of resumming contributions into the background metric grow exponentially with PM order.

4.3.2.2 Graviton Sources

From the 1SF effective action, we see that gravitons are sourced solely by the light particle geodesic in Eq. (4.114) which in momentum space is

$$\begin{aligned}
 \frac{1}{6} \langle \dots \rangle &= \frac{3^4 G^4}{6^1} \langle \dots \rangle = \dots \\
 &= \dots \\
 &= \dots
 \end{aligned}
 \tag{4.128}$$

where we have expanded up to 1PM order via Eq. (4.54) and reorganized the expression by integrating by parts. In terms of the 1PM light particle trajectory, this expression is

$$\frac{1}{6} \langle \dots \rangle = \dots
 \tag{4.129}$$

where we have again defined the frequency domain trajectory $\mathcal{G}^{1|0} = \frac{3^4 G^4}{12c^0} \mathcal{G}^{1|0}$. The 1PM trajectory can be obtained perturbatively as discussed in Sec. 4.3.3.2,

$$\mathcal{G}^{1|0} = \frac{1}{12} \frac{3^4 @}{12c^0} \langle \dots \rangle
 \tag{4.130}$$

where the background metric and Christoffel symbol in momentum space are defined in Eq. (4.127). Putting everything together, the Feynman vertex for the graviton source is

⁴This follows from the happy accident the 2PM background metric, i.e. the Einstein-Infeld-Ho man correction to the Newtonian potential, enters at 3PM via a two-loop diagram that does not contribute classically. In particular, it arises through diagram #8 in Fig. 14 of [97].

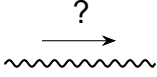
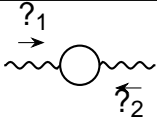

 Graviton propagator	$\frac{32c8}{?^2} \frac{[\cdot d[af, [f [ad]}{2} \frac{[\cdot a[df]}{2}$
 Recoil vertex	$\frac{8< \dot{X}^1 D ?_1, D ?_2^0}{2 \cdot 1 D ?_1^0 1 D ?_2^0} O^{U \cdot 1 a_1 1 D} - ?_1^0 O_U \cdot 2 a_2 1 D - ?_2^0$
 Graviton source	$8_{-< 4^{8?1} \frac{1}{2} D_1 \cdot D_1 \dot{X}^1 D_1 ?^0} 8 O^{U \cdot a_1 D_1} - ? G_U^1 D_1 ?^0,$

Figure 4.5: Feynman rules for the at space graviton propagator, recoil vertex, and graviton source that are required to compute the 1SF gravitational radial action.

$$\begin{aligned}
 \text{?}^\uparrow \text{wavy} \text{!} &= \text{?}^\uparrow \text{wavy} \text{!}_0 + \text{?}^\uparrow \text{wavy} \text{!}_1 + \dots \\
 &= 8_{-< 4^{8?1} \frac{1}{2} D_1 \cdot D_1 \dot{X}^1 D_1 ?^0} 8 O^{U \cdot a_1 D_1} - ? G_U^1 D_1 ?^0, \quad \bullet
 \end{aligned}
 \tag{4.131}$$

See Fig. 4.5 for a convenient table showing the 1 SF Feynman rules for the at space graviton propagator, recoil vertex, and graviton source.

4.3.3 Classical Resummation

4.3.3.1 Background Field Vertices

In order to see the simplifications obtained by calculating using an expansion of the Schwarzschild metric, we can focus on computing the Feynman rules for a gravitationally coupled scalar propagating in a nontrivial background field,

$$\left(= \frac{1}{2} \cdot 3 G^p \frac{1}{66} \cdot a_1 G_{m i m a i} \bullet \tag{4.132}$$

The at space propagator receives corrections,

$$\text{=====} = \text{-----} , \text{---} \otimes \text{---} , \text{---} \otimes \otimes \text{---} ,$$

and the Feynman rules are very simple,

$$\text{---} \xrightarrow{\cdot} \text{---} = \frac{8}{\cdot 2} \tag{4.133}$$

$$\begin{array}{c} \downarrow @ \\ \text{---} \otimes \text{---} \\ \begin{array}{cc} \rightarrow & \leftarrow \\ :1 & :2 \end{array} \end{array} = \frac{g^{\mu\nu} \delta^{\alpha\beta}}{66} \delta^{\alpha\beta} @ \quad [\delta^{\alpha\beta} : 1 : 2 \alpha -] \quad (4.134)$$

with momentum conservation requiring $\delta_{\mu\nu} @ = 0$ on the vertex.

The background-eld Feynman rule above simply encodes the following sum over at-space Feynman diagrams,

$$\text{---} \otimes \text{---} = \text{---} \text{---} \text{---} + \text{---} \text{---} \text{---} + \text{---} \text{---} \text{---} + \text{---} \text{---} \text{---} + \text{---} \text{---} \text{---} + \text{---} \text{---} \text{---} \quad (4.135)$$

which is the perturbative solution of Einstein's equations with a point-like source,

$$\delta^{\alpha\beta} @ = \int d^3x \sqrt{-g} D^{\alpha\beta} X^{\mu\nu} @ \quad (4.136)$$

or, equivalently, in momentum space,

$$\delta^{\alpha\beta} @ = D^{\alpha\beta} X^{\mu\nu} @ \quad (4.137)$$

The crucial observation is that we do not need to compute the sum over diagrams, as we already know that they just compute the metric. One has to choose a gauge to write the background metric, but we do not need to restrict ourselves to traditional perturbative gauges (e.g., harmonic gauge). A convenient choice of background eld gauge is isotropic coordinates, in which,

$$\delta^{\alpha\beta} @ = \int d^3x \sqrt{-g} D^{\alpha\beta} X^{\mu\nu} @ \quad (4.138)$$

where the mass parameter is

$$\mu = \frac{4\pi G}{c^2} \rho \quad (4.139)$$

and

$$|j| = \frac{p}{G} \quad (4.140)$$

with $\tilde{c} = 16c^{-1} \cdot 3^{0 \cdot 1} \cdot 2^0$ defined for later convenience. Expanded perturbatively this yields

$$6_a^{-1} \mathcal{G} = \left[\tilde{c} - \frac{2}{3} D \cdot D_a - \frac{1}{2} \left[\tilde{c} \frac{\cdot}{|rj|} \right]_3 \right] \cdot \quad (4.141)$$

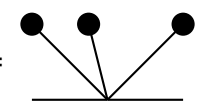
More generally, the position-space background field vertex has an expansion of the form,

$$1 + O_0 \frac{\cdot}{|rj|} + O_1 \frac{\cdot^2}{|rj|^2} + O_2 \frac{\cdot^3}{|rj|^3} + \dots \quad (4.142)$$

The Fourier transform of a given power in this expansion is

$$!_1 q^0 = \int d^3 r \frac{A^{\cdot, 1}}{|rj|^{\cdot, 1}} = \frac{1^{\cdot, 1}}{1 q^{201} \cdot 2^{\cdot 3!}} \frac{1^{\cdot 3!}}{14 c^{0-2!}} \frac{1^{\cdot 3!}}{2^{\cdot 3!}} \cdot \quad (4.143)$$

Let us compare the Fourier transform of a specific power to the fan integral,



$$!_{fan} 1 q^0 = \ddot{O} \frac{3}{8} \frac{X^1 D}{12 c^0} \frac{1^0 X^1 D}{2 \cdot 2} \frac{2^0}{2!} \frac{X^1 D}{8^0} \cdot \quad (4.144)$$

This can be evaluated by going to the rest frame of the heavy object,

$$\begin{aligned} !_{fan} 1 q^0 &= \ddot{O} \frac{3}{8} \frac{1}{12 c^0} \frac{1}{2 \cdot 2} \frac{1}{2! q} \frac{1}{8^0} \quad (4.145) \\ &= \frac{1}{1 p^{200} \cdot 3^{0 \cdot 2}} \frac{1^{\cdot 3!}}{14 c^{0-2!}} \frac{1^{\cdot 3!}}{2^{\cdot 3!}} \cdot \end{aligned}$$

where the last equality is obtained by iteratively using the identity,

$$\begin{aligned} &\frac{3}{12 c^0} \frac{1}{2 \cdot 2} \frac{1}{2! q} \\ &= \frac{1}{1 p^{200} \cdot 3^{0 \cdot 2}} \frac{1^{\cdot 3!}}{14 c^{0-2!}} \frac{0}{10^0} \frac{1^{\cdot 3!}}{2} \frac{0}{0^0} \cdot \quad (4.146) \end{aligned}$$

It is easy to see that

$$!_1 q^0 = 1^{\cdot, 1} !_{fan} 1 q^0 \cdot \quad (4.147)$$

This means that we can rewrite any background field insertion in terms of simple loop integrals without bulk graviton vertices. In particular, noting that

$$\begin{aligned}
 & \rho_{ab} \mathcal{G}^a \mathcal{G}^b \\
 = & \frac{1}{2^1} \frac{4}{3^0} \int \mathcal{G}^a \mathcal{G}^a - \frac{2}{3} D^a D^a \frac{1}{|r|} \\
 & + \frac{1}{16^1} \frac{5^0 2^2}{3^0 2} \int \mathcal{G}^a \mathcal{G}^a + \frac{7}{8^1} \frac{13}{3^0 2} D^a D^a \frac{1}{|r|^2} \\
 & + \frac{1}{96^1} \frac{5^0 1^4}{3^0 3} \int \mathcal{G}^a \mathcal{G}^a + \frac{3^3}{48^1} \frac{26^2}{3^0 3} \frac{93}{100} D^a D^a \frac{1}{|r|^3} \\
 & \dots
 \end{aligned} \tag{4.148}$$

we find that the leading background field insertion on a scalar propagator in isotropic gauge is

$$\begin{aligned}
 & \text{---} \otimes \text{---} \\
 = & \text{---} \otimes_1 \text{---} + \text{---} \otimes_2 \text{---} + \text{---} \otimes_3 \text{---} + \dots \\
 = & \mathcal{G}^2 \frac{1}{2^1} \frac{4}{3^0} : 1 :_2 - \frac{2}{3} D^a : 1^{01} D^a :_2^0 \quad \text{---} \bullet \\
 & + \mathcal{G}^2 \frac{1}{16^1} \frac{5^0 2^2}{3^0 2} : 1 :_2 + \frac{7}{8^1} \frac{13}{3^0 2} D^a : 1^{01} D^a :_2^0 \quad \text{---} \bullet \bullet \\
 & + \mathcal{G}^3 \frac{1}{96^1} \frac{5^0 1^4}{3^0 3} : 1 :_2 + \frac{3^3}{48^1} \frac{26^2}{3^0 3} \frac{93}{100} D^a : 1^{01} D^a :_2^0 \quad \text{---} \bullet \bullet \bullet \\
 & \dots
 \end{aligned} \tag{4.149}$$

As mentioned in the previous sections, we do not have an analytic expression for the propagator of field fluctuations in a Schwarzschild background. Nonetheless, we have demonstrated how one can build such a propagator to a desired perturbative order rather efficiently. Without resorting to summing complicated trees of self-interacting gravitons, we simply extract the perturbative insertions by expanding the exactly known metric. The upshot is that all would-be complicated tree graphs reduce to simple scalar fan integrals which we know to arbitrary loop order. The expansion of the Schwarzschild graviton propagator using the known all-order metric inherits simplifications in the same manner.

4.3.3.2 Expansion of the Second-order Differential Equation of Motion

To perturbatively solve for the trajectory, we expand both the worldline and background field in a PM series,

$$\dot{G} = \sum_{n=0}^{\infty} \tilde{G}^{(n)} \quad \text{and} \quad \dot{UV} = \sum_{n=1}^{\infty} \tilde{UV}^{(n)} \quad (4.150)$$

in which case the equations of motion become

$$\begin{aligned} \xi_0 &= 0 \\ \xi_1 &= \sum_{UV} \tilde{UV}^{(1)} \xi_0 \\ \xi_2 &= \sum_{UV} \tilde{UV}^{(2)} \xi_0 + \sum_{UV} \tilde{UV}^{(1)} \xi_1 + \sum_{UV} \tilde{UV}^{(1)} \xi_1 + \sum_{UV} \tilde{UV}^{(1)} \xi_1 + \sum_{UV} \tilde{UV}^{(1)} \xi_1 + \sum_{UV} \tilde{UV}^{(1)} \xi_1 + \sum_{UV} \tilde{UV}^{(1)} \xi_1 + \sum_{UV} \tilde{UV}^{(1)} \xi_1 + \sum_{UV} \tilde{UV}^{(1)} \xi_1 + \sum_{UV} \tilde{UV}^{(1)} \xi_1 \end{aligned} \quad (4.151)$$

and so on and so forth. Rather quickly, there is a proliferation of the number of derivatives acting on the background metric, the various independent index contractions, and the powers of Λ^2 . When inserting these solutions into Feynman diagrams to compute a quantity such as the radial action, this leads to increasingly complicated numerators and denominators of the loop integrands.

The total loop integrand is often equivalent to infinitely many other integrands, thanks to various linear relations among integrals in dimensional regularization. One could hope to find, without needing to solve complicated linear systems of equations, a simpler form of the integrand via a more direct route. In the above section we showed precisely how this can be done for background field insertions on the propagator of a fluctuation field. In the following section we will show how this can be done for the light particle trajectory. Further details are given in App. D.

4.3.3.3 Expansion Utilizing Integrals of Motion

An alternative approach to computing \dot{G} is to extract it from a solution to the orbital problem which manifests all of the symmetries. The orbital equations are most naturally written in r - A^0 coordinates. On the outward branch of the scattering trajectory $A^0 = 0$, we then have

$$\begin{aligned} \dot{r} &= f \frac{5 \Lambda^2}{5 \Lambda^2} \\ \dot{A}^0 &= \frac{1 f^2}{\Lambda^2} \frac{10 \Lambda^2}{5 \Lambda^2} \frac{4}{3} \\ \dot{A} &= \frac{5 \Lambda^2}{5 \Lambda^2} \frac{4}{3} \frac{5 \Lambda^2}{5 \Lambda^2} f^2 + 1 \frac{12 f^2}{\Lambda^2} \frac{10}{5 \Lambda^2} \frac{8}{3} \frac{1}{2} \end{aligned} \quad (4.152)$$

As in electromagnetism, we will prefer to write the equations of motion for the Cartesian components, now of the form,

$$\begin{aligned} \dot{H} &= \frac{H}{A} + \frac{G}{A^2} \left(5 \frac{1}{f^2} - \frac{4}{3} \frac{1}{f^2} \right) \frac{1}{\gamma^2} - \\ \dot{G} &= \frac{G}{A} + \frac{H}{A^2} \left(5 \frac{1}{f^2} - \frac{4}{3} \frac{1}{f^2} \right) \frac{1}{\gamma^2} \end{aligned} \quad (4.153)$$

The equations of motion have reduced to three first-order differential equations which can be perturbatively solved very straightforwardly. The Lorentz covariant solution is trivially obtained from these solutions,

$$\dot{G} \frac{1}{\gamma^2} = C \dot{g}^0 D, \quad \dot{G} g^0 \frac{1}{\gamma^2}, \quad \dot{H} g^0 \frac{D}{f^2} \frac{f D}{\gamma^2} \quad (4.154)$$

Details on how to solve these equations perturbatively in PM are provided in App. D. Crucially, we can mechanically rewrite the time domain solutions at each order as iterated time integrals of powers of $g^0 = \frac{1}{1 - \frac{1}{f^2} - \frac{1}{\gamma^2} g^2}$. The general expressions are given in the appendix, while here we write the shorter expressions through 2PM order,

$$\begin{aligned} G &= 2^1 < \text{of } \frac{1}{m_g} \frac{1}{\gamma} - \\ G &= 1^1 < \text{o } 1 - 2f^2 \frac{1}{m_g^2} \frac{1}{\gamma^3} - \\ H &= \frac{1 < \text{o } \frac{1}{m_g} \frac{1}{\gamma}}{f^2 - 1} - \end{aligned} \quad (4.155)$$

and

$$\begin{aligned}
 G_2 &= 6 \left(\frac{1}{m_g} \right)^2 \frac{1}{f^2} \frac{1}{1^2} \left(\frac{1}{m_g} \right)^2 \frac{1}{f^2} \frac{1}{1^2} - \\
 &= \frac{1^2 \left(\frac{1}{m_g} \right)^2 \frac{1}{f^2} \frac{1}{1^2} \left(\frac{1}{m_g} \right)^2 \frac{1}{f^2} \frac{1}{1^2}}{f^2 1} \left(\frac{1}{m_g} \right)^2 \frac{1}{f^2} \frac{1}{1^2} - \\
 &= \frac{3}{2} \frac{1^2 \left(\frac{1}{m_g} \right)^2 \frac{1}{f^2} \frac{1}{1^2} \left(\frac{1}{m_g} \right)^2 \frac{1}{f^2} \frac{1}{1^2}}{f^2 1} - \\
 H_2 &= \frac{\frac{1}{m_g} \frac{1}{f^2} \frac{1}{1^2} \left(\frac{1}{m_g} \right)^2 \frac{1}{f^2} \frac{1}{1^2}}{2 \frac{1}{f^2} \frac{1}{1^2} \frac{1}{m_g} \frac{1}{f^2} \frac{1}{1^2}} \left(\frac{1}{m_g} \right)^2 \frac{1}{f^2} \frac{1}{1^2} \left(\frac{1}{m_g} \right)^2 \frac{1}{f^2} \frac{1}{1^2} \\
 &= \frac{1^2 \left(\frac{1}{m_g} \right)^2 \frac{1}{f^2} \frac{1}{1^2} \left(\frac{1}{m_g} \right)^2 \frac{1}{f^2} \frac{1}{1^2}}{f^2 1} \left(\frac{1}{m_g} \right)^2 \frac{1}{f^2} \frac{1}{1^2} \left(\frac{1}{m_g} \right)^2 \frac{1}{f^2} \frac{1}{1^2}
 \end{aligned} \tag{4.156}$$

One can readily identify the structure of a Feynman diagram in these expressions. Upon Fourier transform the powers of f will be simple powers of spatial momenta (as is the case for the Coulomb potential), and the m_g^{-1} will be mapped to linearized matter propagators, i.e. $\frac{1}{k^2}$ for some momentum. For example,

$$\frac{1}{m_g} \frac{1}{f^2} = 168 c^2 \frac{4}{1^{-2}} \frac{8 A_1 \cdot 2^0 \hat{X}^1 D_1 \cdot 1^0 \hat{X}^1 D_2 \cdot 2^0}{2 \frac{2}{2} D_1 \cdot 1 \cdot D_2 \cdot 2^0} \tag{4.157}$$

The mapping to Feynman integrals is straightforward, the powers of f and m_g^{-1} correspond to background photon insertions via fan integrals, and the powers of m_g^{-1} correspond to matter propagators. Using this, one can see which Feynman diagram topologies are contained in the solutions. Note that a great simplification has occurred, as these expressions have the same diagram topologies as the electrodynamics case with no need to manage multi-graviton vertices!

4.3.4 Results and Checks

In order to calculate the radial on-shell action for general relativity, we do the path integral over all graviton perturbations. Following our procedure in electromagnetism, we compute

$$\begin{aligned} \exp^{18} \text{GR}^0 &= \left(\frac{3}{4} \right)^2 \left(\frac{3}{4} \right)^2 \left(\frac{3}{4} \right)^2 \exp^{18}(\dots) \\ &= \left(\frac{3}{4} \right)^2 \exp^{18} \left(\dots, 8X \frac{1^{10}}{\epsilon}, \dots \right) \end{aligned} \quad (4.158)$$

In the SF expansion, the radial action is

$$\text{GR} = \frac{1^0}{\text{GR}} + \frac{1^1}{\text{GR}} + \dots \quad (4.159)$$

with

$$\begin{aligned} \frac{1^0}{\text{GR}} &= \left(- \right. \\ \frac{1^1}{\text{GR}} &= 8 \log \left(\frac{3}{4} \right)^2 \exp^{18} \left(\frac{1^{10}}{\epsilon} \right) - \end{aligned} \quad (4.160)$$

and we will further expand in a PM series,

$$\frac{1^0}{\text{GR}} = \tilde{\mathcal{O}}_{9=8,1} \frac{1^{18-9}}{\text{GR}} \bullet \quad (4.161)$$

We will compute this SF and PM expanded radial action for an array of gravitational theories. Again, dimensional analysis ensures the good mass polynomiality of the expansion [195],

$$\frac{1^{18-9}}{\text{GR}} = - \frac{8}{\epsilon} \left(\frac{A}{1} \right)^{9,1} \frac{1^{18-9}}{\text{GR}} f^0 \bullet \quad (4.162)$$

4.3.4.1 Scattering Masses

Let us now compute the 0SF and 1SF radial actions for general relativity. As reviewed in App. E, the 0SF radial action for gravity is

$$\begin{aligned} \frac{1^0}{\text{GR}} &= \left(\frac{A}{1} \right)^2 \left[\frac{1}{4} \log \left(1 + \frac{1}{f^2} \right) + \frac{1^{0+2}}{f^2} \frac{1^0}{1} + \frac{A}{1} \frac{3c^{15} f^2}{16 f^2} \frac{1^0}{1} \right. \\ &\quad \left. + \frac{A^2}{1^2} \frac{64 f^6}{24 f^2} + \frac{120 f^4}{10^{\frac{5}{2}}} + \frac{60 f^2}{10^{\frac{5}{2}}} \right] \bullet \end{aligned} \quad (4.163)$$

shown here to the first few PM orders.

Using the Feynman rules in Fig. 4.5, we compute $\frac{1^{10}}{\text{GR}}$ from the Feynman diagrams in Fig. 4.6, which at 2PM gives

$$\frac{1^{1-2^0}}{\text{GR}} = - \frac{8}{\epsilon} \left(\frac{A}{1} \right)^2 \frac{3c^{15} f^2}{4 f^2} \frac{1^0}{1} \bullet \quad (4.164)$$

The flat space diagram topologies that need to be evaluated for 1SF, 3PM computations are shown in Fig. 4.7 for comparison. As an additional consistency

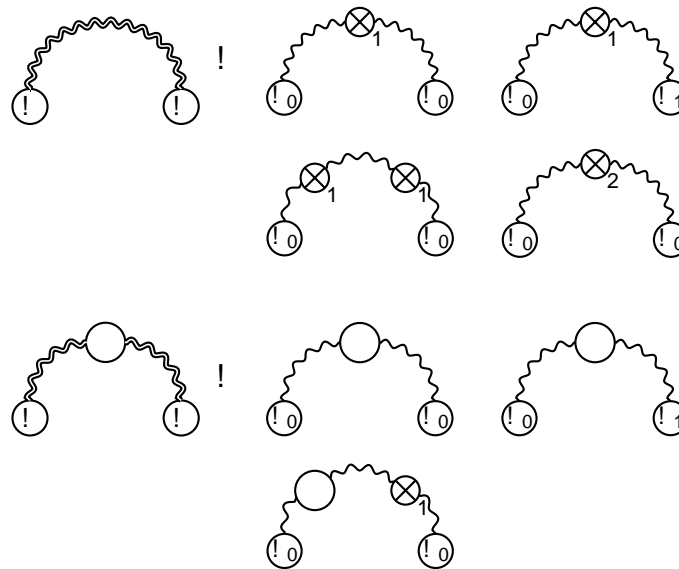


Figure 4.6: Diagrams showing up at 1SF when computing the gravitational effective action are shown on the left and the contributions relevant to 3PM are depicted to the right of the arrows. In actuality, the diagram with a 2PM metric insertion does not contribute at this order (see footnote 4).

check, we have performed the 2PM calculation in an alternative and more general gauge fixing with the choice of $\gamma = Z_1 r^a X_6 a - \frac{1}{2} Z_2 r \cdot X_6$ in Eq. (4.109). For general Z_1 and Z_2 , the flat space graviton propagator deviates from the deDonder form in Eq. (4.125) and, in fact, has spurious s^4 and s^6 poles. Working in this gauge, we find that the contributions from pure background field method diagrams are not gauge invariant nor is the contribution from the recoil operator. However, their sum is gauge invariant and yields the correct 2PM expression.

For yet another check, we have also performed the same calculation in general spacetime dimension, d , in App. E, yielding

$$\begin{aligned}
 \Gamma_{\text{GR}}^{11-20} = & -\frac{1}{2} \frac{A^2}{\Lambda^2} \frac{1}{\epsilon} \left[\frac{c^{\frac{7}{2}}}{1} \frac{12}{2^{02}} \frac{5^0 f^2}{f^2} \frac{12}{1} \frac{3^0 f^2}{1} \frac{6}{3^{*2}} \frac{6}{1} \frac{3}{2^0} \frac{7}{2} - \frac{1}{2} \right]^2 \cdot \\
 & \hspace{15em} (4.165)
 \end{aligned}$$

which agrees with known results [18].

Last, but not least, we compute the 1SF Feynman diagrams at 3PM order, shown in

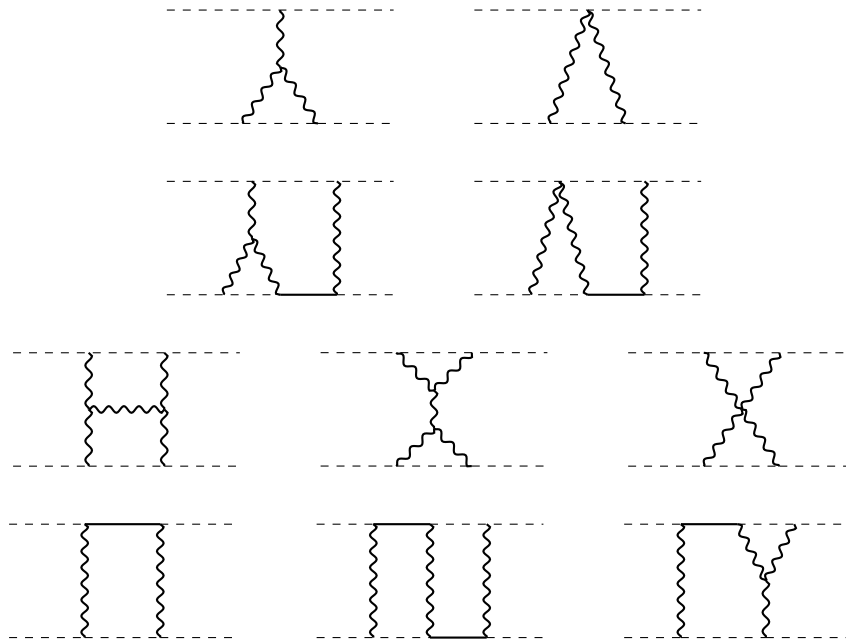


Figure 4.7: Flat space diagram topologies that contribute to the 1SF action to 3PM order. The dotted straight lines depict static massive sources and the solid straight lines represent matter propagators.

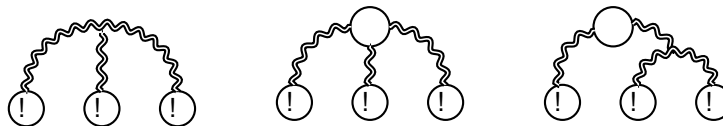


Figure 4.8: Diagrams necessary for computing the 2SF gravitational radial action to 3PM order. The first diagram involves cubic graviton vertices in a Schwarzschild background, the second makes use of the 2SF recoil operator, and the third diagram uses the 1SF recoil operator in combination with the cubic graviton vertex.

Fig. 4.6, to obtain the 3PM radial action,

$$\begin{aligned}
 \frac{11-30}{\text{GR}} = -\frac{1}{2} \frac{A}{1} \frac{2}{1} \frac{f}{1} \frac{36f^6}{12f^2} \frac{114f^4, 132f^2}{1^{5 \cdot 2}} \frac{55}{3 \arccos f} \frac{!}{2f^2 - 1} \quad (4.166)
 \end{aligned}$$

using the integration methods described in [25, 273]. The above results agree exactly with the known 2PM and 3PM expressions [5, 11, 95, 96].

In a similar fashion, contributions to the 2SF, 3PM action, which should match the 0SF, 3PM expression upon switching the μ and ν labels, can be calculated with the relevant diagrams shown in Fig. 4.8.

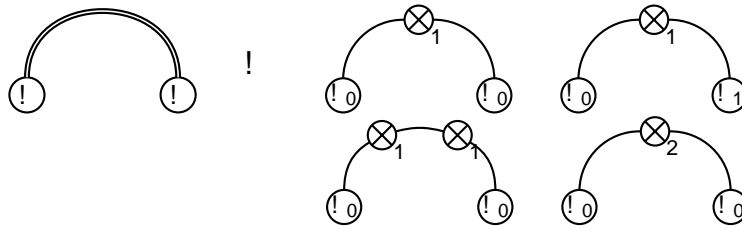


Figure 4.9: The contribution to the 1SF radial action from a field which couples to the light body but not the heavy body, so there is no recoil operator insertion. The doubled line is the propagator of this additional field (scalar or vector) in the Schwarzschild background. Its nontrivial contributions to 3PM order when expanded in terms of space diagrams are shown on the right.

4.3.4.2 Scattering Scalar Charged Masses

It is trivial to incorporate additional fields in our framework. In particular, let us consider an additional scalar field that couples directly to the light particle but only gravitationally to the heavy particle. Such theories have been explored in SF studies [248, 265] as a toy model for full gravity. The additional term in action for this theory is

$$S_{\text{scalar}} = \int d^4x \sqrt{-g} \left[\frac{1}{2} g^{\mu\nu} \partial_\mu \phi \partial_\nu \phi - \frac{1}{2} b^2 \phi^2 \right] \quad (4.167)$$

where, for maximum generality, we have included a nonminimal coupling and the scalar couples to the current,

$$T^{\mu\nu} = H \langle \dots \rangle - \frac{1}{6} \nabla^\mu \phi \nabla^\nu \phi - \frac{1}{6} g^{\mu\nu} \Box \phi^2 \quad (4.168)$$

which only involves the light particle.

Crucially, in this theory the heavy particle does not accrue any additional interactions. Consequently, the gravitational recoil operator in Eq. (4.117) is completely unchanged. Thus, to compute the radial action we need only include the additional background field diagram depicted in Fig. 4.9.

Including this Feynman diagram, we find that the 1SF radial action for the scattering of scalar charged masses is corrected by

$$\begin{aligned} \delta S_{\text{scalar}}^{11-2^0} &= -\langle \dots \rangle A \left[\frac{A}{1} \frac{c f^2}{8} \frac{1}{f^2} + \frac{4b}{1} \right] \quad (4.169) \\ \delta S_{\text{scalar}}^{11-3^0} &= -\langle \dots \rangle A \left[\frac{A}{12} \frac{f^2}{6 f^2} + \frac{2f^4}{1} \frac{f^2}{1} + \frac{1}{3 \cdot 2} \frac{b}{6 f^2} \frac{6f^2}{1} \right] \end{aligned}$$

where we have defined the scalar charge radius,

$$A = \frac{H^2 c}{4c} \cdot \quad (4.170)$$

The above expression agrees with the results of [248]. Note that the contribution from the nonminimal coupling, constitutes a new calculation.

An interesting check of the result can be performed by calculating the probe action in a background given by a solution to Einstein's equations in the presence of a gravitationally coupled massless scalar field [277]. We find that the expressions for the action match under the swap, $\phi \leftrightarrow \psi$. We also compare the contribution from the nonminimal coupling, by computing the probe action in an Einstein-conformal scalar solution where $\psi = 1/\phi$ [278, 279] and find agreement with the above result.

4.3.4.3 Scattering Vector Charged Masses

The exact same procedure can be applied to a theory in which an additional, gravitationally interacting vector field couples directly to the light particle but not to the heavy particle. This theory is described by an additional term in the action,

$$S_{\text{vector}} = \int d^4x \sqrt{-g} \left[-\frac{1}{4} F_{\mu\nu} F^{\mu\nu} - \dots \right] \quad (4.171)$$

where the vector current couples only to the light particle,

$$j^\mu = \frac{1}{\sqrt{-g}} \frac{\delta S_{\text{vector}}}{\delta A_\mu} = \dots \quad (4.172)$$

As before, the recoil operator is unchanged, and now the only additional diagram is a background field loop of the vector field shown in Fig. 4.9. Computing this Feynman diagram and integrating, we obtain the 1SF radial action for the scattering of vector charged masses,

$$\begin{aligned} S_{\text{vector}}^{11-20} &= -\frac{1}{2} A^2 \int d^3x \sqrt{-g} \left[\frac{c}{8} \frac{3f^2 - 1}{f^2 - 1} \right] \\ S_{\text{vector}}^{11-30} &= -\frac{1}{2} A^2 \int d^3x \sqrt{-g} \left[\frac{f}{12} \frac{8f^4 - 28f^2 + 23}{f^2 - 1} + \frac{2f^2 - 1}{f^2 - 1} \arccos f \right] \end{aligned} \quad (4.173)$$

where we have defined the vector charge radius,

$$A = \frac{I^2 c}{4c} \cdot \quad (4.174)$$

The above expression is a new result. We find that the expression for the probe radial action in the Reissner-Nordström metric when it is linearized in the vector charge and under the swap, $\mathcal{L} \rightarrow \mathcal{L}^*$, matches with the expression above.

4.4 Conclusions

In this paper we have derived a systematic effective field theory describing the dynamics of two interacting bodies in an expansion of their mass ratio, $m_1 \ll m_2$.

A key ingredient is the simple fact that classical solutions e.g., the Schwarzschild metric, together with the span of all of probe geodesics carry information that is effectively all orders in perturbation theory from the point of view of the field theory constructed in a trivial background. Consequently, these classical solutions can be directly leveraged as resummations to simplify certain perturbative contributions.

The main technical result of our paper is a precise characterization of those perturbative contributions which are not encoded in the background fields and trajectories that constitute the OSF theory. In particular, these leading corrections to the background field method enter at 1SF and are entirely accounted for by a recoil operator describing describes the wobble of the heavy particle sourcing the background field. The sole effect of this operator is a nonlocal-in-time correction to the two-point function of the force carrier. Importantly, corrections at 2SF or higher orders can be systematically derived.

Applying this effective field theory framework to EM and GR, we compute the conservative radial action for scattering particles in various systems. Here, we have verified that our framework correctly reproduces the conservative dynamics in a number of familiar scenarios. We also present a number of new calculations.

The present work leaves many directions for future study. First and foremost, it would be wonderful to understand to what extent our results can be made technically useful for existing methods in SF theory. Here a crucial caveat which may in the end limit the utility of our framework is that our construction is fundamentally built from an effective field theory of point particles interacting through long range forces. While resumming diagrams reproduces the classical backgrounds such as the Schwarzschild metric, we should nevertheless interpret the resulting background as a fundamentally perturbative field sourced by sources, rather than a vacuum solution to the Einstein field equations. This approach has the unique advantage that we can use dimensional regularization to deal with ultraviolet divergent self-energy contributions. However, in the approach of existing SF methods, there is no heavy

point source. Hence, dimensional regularization is not an option, and self-energy contributions must instead be dealt with in a substantially different way. For this reason, it would be useful to try to port our results to this different approach. For example, it would be interesting to see if our recoil operator, which is defined naturally in dimensional regularization, can be adapted to other regulators.

Second of all, it would be interesting and relatively straightforward to generalize our results to other binary systems relevant to gravitational wave physics. For example, the case of gravitationally interacting spinning particles has a 0SF sector which is described by a spinning probe particle in a Kerr-Newman background. The 1SF sector should also be corrected by a recoil operator corresponding to the back reaction on the heavy spinning source. Another topic of interest would be to generalize our results to include tidal moments, as is relevant for neutron star binaries.

Thirdly, let us note another possible physical application of these ideas: fluid dynamics. Such systems exhibit gapless force carriers in the form of quanta of the fluid velocity field. These degrees of freedom are governed by the Navier-Stokes equation. By introducing a heavy and light body that interact with the fluid medium, we might then attempt to construct an effective field theory in the large mass ratio limit.

Chapter 5

COLOR-KINEMATICS DUALITY AND THE DOUBLE COPY IN TWO DIMENSIONS

This chapter reproduces the contents of the publication: Clifford Cheung, James Mangan, Julio Parra-Martinez, and Nabha Shah. Phys. Rev. Lett. 129, 221602 Published 23 November 2022.

5.1 Introduction

Recent breakthroughs in scattering theory have unveiled an extraordinary hidden structure lying dormant within the fundamental laws of nature. The so-called double copy [75, 77–79] is a mathematical formula, only proven at tree level, that very simply relates perturbative scattering amplitudes of gravitons in Einstein's general relativity (GR) to those of gluons in Yang Mills theory (YM).

At a purely practical level, the double copy is an immensely efficient tool for recycling past results in gauge theory to derive new ones for gravity. This approach has made feasible many previously intractable calculations, for example those relevant to the finiteness of supergravity theories [280–287] and more recently, post-Minkowskian computations for black hole binary dynamics [95–97, 224] which are directly relevant to the LIGO experimental program [41, 246] and are, within the last three years, competing with the state of the art.

At the conceptual level, the double copy remains deeply mysterious. Its structure transcends gauge theory and gravity and applies to a broad web of theories [79]. For example, the exact same double copy also relates all tree-level amplitudes of pions in the chiral limit to those of certain hypothetical scalars known as Galileons, which have been studied independently as viable theories of cosmology and modified gravity.

In broad strokes, the double copy maps gauge theory to gravity by first expressing every gauge theory amplitude as a sum over cubic graphs,

$$= = \sum_{\text{cubic}} \frac{\tilde{\mathcal{O}}_{2_8} \mathcal{N}_{2_8}}{3_8} \quad (5.1)$$

where the 2_8 are color factors (structure constants), the \mathcal{N}_{2_8} are kinematic numerators, and the 3_8 are propagators [77–79, 219, 288]. Color-kinematics duality states that

there exists a rearrangement of terms such that the kinematic numerators obey the same Jacobi identities as the color factors. Gravity as the square of double copy of gauge theory is simply obtained by replacing each color factor with the associated kinematic numerators.

The double copy is an established fact about flat space, perturbative scattering amplitudes but its generality is far from understood. To what extent does it apply on-shell [289–295]? To curved geometries [296–306]? Nonperturbatively? Finding answers to these questions could provide a nonperturbative, background independent mapping between gravity and far simpler quantum field theories.

In this Letter, we present a nonperturbative double copy in two spacetime dimensions. This is the first on-shell Lagrangian level formulation of the double copy for interacting theories¹ Extending the proof of the double copy from tree level to all loop orders has implications for the understanding of all double copy constructions. Our approach is inspired by a remarkable isomorphism between the algebras of unitary transformations and diffeomorphisms [307],

$$\lim_{\hbar \rightarrow 0} \text{Diff}(M) \cong \text{U}(n) \quad (5.2)$$

and applies to an enormous class of scalar theories, including masses and higher-dimension operators.

We apply this construction successively to map bi-adjoint scalar (BAS) theory to Zakharov-Mikhailov (ZM) theory [308] to the special Galileon (SG) [309–311], thus deriving the corresponding and more familiar amplitudes-level double copy at all orders in perturbation theory² Since ZM theory is classically integrable, it furnishes a Lax connection whose Wilson lines define an infinite tower of conserved currents, all of which are shown to double copy into corresponding objects in the SG. An extension of the double copy based on the Moyal algebra is presented where \hbar , the rank of the gauge group, parameterizes an infinite tower of higher-dimension operators.³ Note that at the classical level, ZM theory is very closely related to self-dual Yang-Mills (SDYM) theory [289, 290], which exhibits identical integrable and Moyal structures [314].

¹Remarkably, three-dimensional Chern-Simons theory which topologically automatically manifests on-shell, Lagrangian-level color-kinematics duality [293].

²In relation to the prototypical double copy described above, ZM plays the role of the gauge theory and SG is analogous to gravity. BAS has the same role in both setups.

³The Moyal algebra has appeared before in maps from noncommutative gauge theory to ordinary gauge theory [312, 313]. Gravity is notably missing from this picture so an immediate connection to the double copy is opaque but potentially promising nonetheless. We thank a referee for bringing this to our attention.

Implementing the double copy on nonperturbative, large- ℓ configurations, we show analytically that every classical solution of the SG theory is isomorphic to corresponding dual solutions in ZM and BAS theory. As a highly nontrivial check, we compute an explicit, large- ℓ , numerical solution for soliton scattering in the SG theory, map it to a corresponding configuration in ZM theory⁴ at large ℓ , and verify that it satisfies the ZM equations of motion to high precision.

5.2 Color Algebra

A ℓ in the adjoint of $su(\ell)$ is a Hermitian matrix $\lambda = +^0 Z_0$, where $\mathfrak{Z}_1^2 = 8 \mathfrak{Z}_1^2$ and $\mathfrak{Z}_0 - \mathfrak{Z}_1^2 = 8 \mathfrak{Z}_1^2 Z_2$. For odd ℓ there exists a basis of generators labeled by a two-vector, $Z_{\#} = Z_{\#} [307]$. In this basis $\lambda = +^? Z_?$ where $+^? = +^?$, and

$$\mathfrak{Z}_{?_8} - \mathfrak{Z}_{?_9}^2 = 8 \mathfrak{Z}_{?_9}^? Z_{?_?} - \quad (5.3)$$

with the corresponding color structure constant,

$$\mathfrak{Z}_{?_8 ?_9}^? = \frac{\#}{2c} \sin \frac{2c}{\#} \mathfrak{X}_{?_8 ?_9 ?}^{\#11} = \mathfrak{X}_{?_8 ?_9 ?} \bullet \quad (5.4)$$

Hence, the $\ell \rightarrow 1$ limit literally defines the algebra of volume-preserving diffeomorphisms on the torus [307], or equivalently, the Poisson algebra. The toroidal geometry arises because the generator labels are defined mod ℓ .

5.3 Kinematic Algebra

Eq. (5.2) implies that ℓ in the adjoint of $su(\ell)$ at large ℓ are isomorphic to ℓ -dependent diffeomorphisms,

$$\lambda = n^a m_a = m^+ m^- = \dot{m}^+ m^- \quad (5.5)$$

which are volume-preserving because $m^+ m^- = 0$. This algebra is closed since the commutator of diffeomorphisms yields another diffeomorphism via

$$\dot{\lambda} = \lambda \cdot \dot{\lambda} = m^+ \dot{m}^- - \dot{m}^+ m^- = m / \dot{m}^- \quad (5.6)$$

where $/ = m^+ \dot{m}^-$. Motivated by these structures, we propose a color-kinematic duality replacement,

$$\begin{aligned} & +^0 \quad ! \quad +^- \\ \mathfrak{Z}_{01}^{2+0, 1} \quad ! \quad m^+ \dot{m}^-, - \\ \mathfrak{Z}_{01}^{+0, 1} \quad ! \quad +, \bullet \end{aligned} \quad (5.7)$$

⁴In our conventions, the Minkowski metric and Levi-Civita tensor obey $\eta_{01} = 1$ so that $\eta_a b = 1 [\cdot]_{af} [\cdot]_{ad}$. Furthermore, we define the dual derivative $\dot{m} = n^a \dot{m}_a$ and the antisymmetric product $\mathfrak{X} = n^a ?_8 ?_9 a$.

The first line simply maps any color-adjoint field to a corresponding singlet field. The second line maps the color structure constant to a kinematic structure constant whose momentum space representation is

$$f_{89}^1 = \frac{1}{\sqrt{2}} \delta_{89}^1 \quad (5.8)$$

This is literally the continuum limit of Eq. (5.4), in accordance with the algebra isomorphism in Eq. (5.2). The third line is obtained from the Killing form $\text{tr} \, t^a t^b$ at large N , which effectively defines a Killing form for the Lie algebra [307].

5.4 Lagrangian Double Copy

The color-kinematic replacement rules in Eq. (5.7) can be applied directly at the level of the Lagrangian, thus giving an on-shell, nonperturbative definition of the double copy.

5.4.1 Biadjoint Scalar Theory

The Lagrangian for BAS theory is

$$\mathcal{L}_{\text{BAS}} = \frac{1}{2} m^2 q_{00}^2 + \frac{1}{6} f_{12}^3 f_{12}^3 q^{00} q^{11} q^{22} \quad (5.9)$$

while the corresponding equation of motion is

$$q^{22} - \frac{1}{2} f_{12}^3 f_{12}^3 q^{00} q^{11} = 0 \quad (5.10)$$

The tree-level four-point on-shell BAS amplitude is

$$\mathcal{M}_{\text{BAS}} = \frac{2_B^2}{B} + \frac{2_C^2}{C} + \frac{2_D^2}{D} \quad (5.11)$$

where $B = s_{12}^2$, $C = s_{23}^2$, $D = s_{31}^2$, and the color factors are $2_B = f_{10_2}^1 f_{0_3 0_4}^1$, $2_C = f_{20_3}^1 f_{0_1 0_4}^1$, $2_D = f_{30_1}^1 f_{0_2 0_4}^1$, and likewise for barred color.

Massless on-shell kinematics in two dimensions is famously plagued by infrared singularities since all asymptotic states are either left or right movers. For example, for the case of four-point scattering with color-ordered external states, the external momenta exhibit kinematic configurations which we classify as *split*, where $s_{23} = s_{31}$, $s_{41} = 0$ or $s_{23} = s_{31}$, $s_{41} = 0$, versus *alternating*, where $s_{31} = s_{23}$, $s_{41} = 0$. Since either B , C or D is always zero, there is a vanishing Gram determinant, $BCD = 0$, and propagator exchanges generically exhibit collinear singularities.

The precise method of infrared regulation be it going o-shell, introducing a physical mass term to the theory, or analytically continuing away from two dimensions can yield different answers for nominally classical equivalent theories, and special care must be taken [315]. Nevertheless, the claim of the present paper is that assuming a particular infrared regulator, our construction can be applied to map any given infrared-regulated theory to a corresponding infrared-regulated double copy theory.

5.4.2 Zakharov-Mikhailov Theory

Applying the replacement rules in Eq. (5.7) to the Lagrangian of BAS theory in Eq. (5.9), we obtain the action of ZM theory, whose Lagrangian is [308, 315, 317]

$$L_{\text{ZM}} = \frac{1}{2} m q_0 \dot{m} q^0, \frac{1}{6} \epsilon_{12} q^0 m q^1 \dot{m} q^2. \quad (5.12)$$

The resulting equation of motion is

$$q^2 - \frac{1}{2} \epsilon_{01}{}^2 m q^0 \dot{m} q^1 = 0, \quad (5.13)$$

which can alternatively be obtained from Eq. (5.10) via Eq. (5.7). Note that Eq. (5.13) also encodes the dynamics of SDYM theory [289, 290, 314].

As is well-known [308, 315, 317], ZM theory is classically equivalent to the principal chiral model (PCM), otherwise known as the nonlinear sigma model (NLSM) in two dimensions. In general dimensions, the NLSM is classically defined by

$$m_a \epsilon_{a'1}^2 \epsilon_{01}{}^2 g^0 g_a^1 = 0 \quad \text{and} \quad \dot{m} g^0 = 0, \quad (5.14)$$

where the former is a pure gauge condition implying $\epsilon_{a'1}^2 g^0 g_a^1 = 0$ and the latter is the NLSM equation of motion. By defining $\epsilon^0 = n_a m^a q^0$, we trivially enforce the latter, while the former is equivalent to Eq. (5.13).

The three-point Feynman vertex defined by Eq. (5.12) is

$$= \frac{1}{8} \epsilon_{12} h_{12} \quad (5.15)$$

which is fully antisymmetric because o-shell two-dimensional kinematics implies that $h_{12} = h_{23} = h_{31}$.

The tree-level four-point o-shell ZM amplitude is

$$Z_{\text{M}} = \frac{2_{\text{B}=\text{B}}}{\text{B}} + \frac{2_{\text{C}=\text{C}}}{\text{C}} + \frac{2_{\text{D}=\text{D}}}{\text{D}} \quad (5.16)$$

where the kinematic numerators,

$$n_B = h_{12}h_{34} - \epsilon = h_{23}h_{14} - \phi = h_{31}h_{24} - \quad (5.17)$$

satisfy the on-shell kinematic Jacobi identity $n_B, n_C, n_D = 0$, on account of the Schouten identity. Applying the standard color decomposition [318], the color-ordered ZM amplitude is $M_{ZM} \gg 1234 \ll = \frac{n_B}{B} - \frac{n_C}{C}$.

For the alternating configuration described previously, $n_B, n_C = 0$, which implies that $M_{ZM} \gg 1234 \ll$ is free of collinear singularities. In this case $n_D = -n_C = h_{12}^2$, so $M_{ZM} \gg 1234 \ll = 0$, in accordance with the phenomenon of no-particle production described in [319]. For the split configurations $M_{ZM} \gg 1234 \ll$ is non-zero but must be evaluated with some choice of infrared regulator [315].

At loop level, integrands at arbitrary order are mechanically calculated using the Feynman vertex in Eq. (5.15). By construction, all loop-level kinematic Jacobi identities are automatically satisfied, even on-shell. While enforcing global color-kinematics constraints is a well-known difficulty in gauge theory starting at two-loops [320], we learn here that there is no obstacle to this for ZM theory at all orders in perturbation theory.

5.4.3 Special Galileon Theory

Eq. (5.7) maps the ZM Lagrangian in Eq. (5.12) to the action of the SG theory, whose Lagrangian is

$$L_{SG} = \frac{1}{2} m \dot{q}^2 - \frac{1}{6} m m_a \dot{q}^2 m^a \dot{q}^2 - \quad (5.18)$$

and whose equation of motion is

$$m \ddot{q} - \frac{1}{2} m m_a \dot{q}^2 m^a \dot{q}^2 = 0. \quad (5.19)$$

The three-point Feynman vertex is then

$$= -8h_{12}^2 - \quad (5.20)$$

which is fully permutation invariant. Applying either an on-shell or mass regulator for infrared singularities, the on-shell amplitude is

$$M_{SG} = \frac{n_B^2}{B} - \frac{n_C^2}{C} - \frac{n_D^2}{D} \quad B, C, D \neq 0 - \quad (5.21)$$

which is proportional to the Gram determinant and thus vanishes in two dimensions. This reflects the fact that the SG is field-redefinition equivalent to a two-dimensional free theory [321, 322].

5.5 Masses and Higher-Dimension Operators

Thus far we have only considered those theories which have historically appeared in the amplitudes-level double copy [79]. Our construction extends far more broadly, however. In particular, the color-kinematic replacement rules in Eq. (5.7) can be applied to any operator that does not have (i) a closed loop of color structure constants, nor (ii) multiple color traces. In both cases, the third line of Eq. (5.7) will induce ill-defined or nonlocal integrals over the volume of spacetime which enter into the Lagrangian. The mildness of the restrictions (i) and (ii) means that a very large class of operators manifestly obey color-kinematics duality, in sharp contrast to the typical intuition that almost all operators will fail the duality.

By these rules, mass terms are perfectly fine and trivially double copy via the same color-kinematic replacements as the kinetic terms. These mass terms serve only to change the propagator denominators.

Eq. (5.7) can also be implemented for an infinite class of higher-dimension operators. For example, consider the higher-dimension operator in BAS theory $O_{\text{BAS}} = \frac{5}{s_{14}} \frac{5}{s_{234}} \frac{5}{s_{014}} \frac{5}{s_{234}} q^{00} q^{1\bar{1}} q^{22} q^{3\bar{3}}$, where both the color and dual color structures are single trace. Applying Eq. (5.7) to dual color, we obtain the spacetime integral of $O_{\text{ZM}} = \frac{5}{s_{14}} \frac{5}{s_{234}} m^0 m^1 m^2 m^3$, which is the color-kinematic dual operator in ZM theory. Then applying Eq. (5.7) to the remaining color structures, we obtain the spacetime integral $O_{\text{SG}} = m^0 m^1 m^2 m^3$, which is the color-kinematic dual operator in the SG theory.

Now consider $O_{\text{BAS}}^0 = \frac{6}{s_{02}} \frac{6}{s_{13}} \frac{5}{s_{014}} \frac{5}{s_{234}} q^{00} q^{1\bar{1}} q^{22} q^{3\bar{3}}$, which is double trace in color and single trace in dual color. Applying Eq. (5.7) to the latter, we obtain $O_{\text{ZM}}^0 = m^0 m^1 m^2 m^3$. Since the resulting operator is double trace in color, it cannot be further double copied via Eq. (5.7) without generating an additional integral over all of spacetime.

5.6 Fundamental BCJ Relation

Our Lagrangian-level formulation of the double copy does not preserve the fundamental Bern-Carrasco-Johansson (BCJ) relation [77, 78] nor the so-called

minimal rank condition [323]. Ultimately, this is not so surprising because the fundamental BCJ relation is literally equivalent to the conservation equation for the kinematic current in theories with purely cubic interactions [292, 296], and our generalized double copy construction allows for quartic and higher interactions.

Crucially, failure of the minimal rank condition implies that our framework should be interpreted as a generalization of the color-kinematic dual formulation of the double copy [77, 78], which is built upon the kinematic Jacobi identities, rather than the Kawai-Lewellen-Tye (KLT) formulation [75], which relies on relations amongst color-ordered amplitudes.

As an example, consider BAS theory deformed by a mass and the higher-dimension operator defined earlier,

$$L = L_{\text{BAS}} - \frac{\leq^2}{2} q_{00} q^{00}, \frac{g}{16} O_{\text{BAS}} \bullet \quad (5.22)$$

For the moment, let us work in general dimensions, where infrared divergences are absent. The matrix of doubly color-ordered amplitudes is

$$\begin{aligned} {}^1\langle - | \mathcal{G} = & \begin{matrix} \gg 1234 | 1234 \ll & \gg 1234 | 1324 \ll \\ \gg 1324 | 1234 \ll & \gg 1324 | 1324 \ll \end{matrix} \\ = & \begin{matrix} \frac{1}{B <^2}, \frac{1}{C <^2} & g & \frac{1}{C <^2}, \frac{g}{2} \\ \frac{1}{C <^2}, \frac{g}{2} & \frac{1}{C <^2}, \frac{1}{D <^2} & g \end{matrix} \bullet \end{aligned} \quad (5.23)$$

The minimal rank condition holds for pure BAS theory in general dimensions since $\det {}^1\langle 0 | - \rangle^0 = 0$ on-shell. However, it fails in the presence of masses [324, 325] and higher-dimension operators [323],

$$\begin{aligned} \det {}^1\langle - | - \rangle^0 &= \frac{\leq^2}{1B <^{20} C <^{20} D <^{20}} \\ \det {}^1\langle 0 | - \rangle^0 &= g \frac{1}{B}, \frac{1}{C}, \frac{1}{D}, \frac{3g^2}{4} \bullet \end{aligned} \quad (5.24)$$

Evaluating these expressions for two-dimensional kinematics, we encounter the usual annoyances of infrared divergences, but irrespective of choice of regulator, the above determinants are still nonzero.

5.7 Integrable Models

Since ZM theory is classically equivalent to the PCM, it is similarly integrable [308, 316, 326]. Moreover, ZM theory maps to the SG under the double copy, so we will see that the latter is also integrable. Note that mapping the integrability

of one theory to another would not be possible with the standard amplitudes-level double copy because the integrability conditions are expressed in terms of currents and on-shell fields.

As a brief review, integrability is achieved by casting the equations of motion into the form of the Lax equation $\partial_t \Psi = \mathcal{M} \Psi - \mathcal{N} \Psi$ where the operators \mathcal{M} and \mathcal{N} constitute a Lax pair [327–331]. By virtue of this form of the equations of motion, the eigenvalues of \mathcal{M} are conserved charges. A familiar Lax pair is the Hamiltonian together with an observable in the Heisenberg picture. In two dimensions, integrability requires an infinite number of charges where the infinitude of Lax pairs is parameterized by a spectral parameter. The Lax pair comes from a Wilson line and a gauge field, the Lax connection where flatness of the gauge connection yields the Lax equation.

5.7.1 Integrability of Zakharov-Mikhailov Theory

Let us review the integrability properties of ZM theory [308, 316, 326]. To begin, we define the Lax connection [308, 326, 332, 333],

$$G_a = \frac{1}{1-\lambda^2} m_{ab} \lambda^b + \lambda^2 m_{ab} \lambda^b \quad (5.25)$$

whose corresponding field strength,

$$L_a = m_{ab} G_b - G_a = 0 \quad (5.26)$$

vanishes for all values of the parameter due to the ZM equation of motion in Eq. (5.13). Since the Lax connection is pure gauge, we can construct the Wilson line,

$$\begin{aligned} \mathcal{W}[\Gamma] &= \exp \int_{\Gamma} G_a dx^a \\ &= 1 + \int_{\Gamma} G_a dx^a + \frac{1}{2} \int_{\Gamma} \int_{\Gamma} G_a G_b dx^a dx^b + \dots \end{aligned} \quad (5.27)$$

which is path-independent and satisfies $\partial_a \mathcal{W} = m_a \mathcal{W}$, $G_a \mathcal{W} = 0$. Next, we define the Lax current [308, 316, 326]

$$P^{\alpha} = m_a \int_{-\infty}^{\infty} dx^a : P^{1:\alpha} : \quad (5.28)$$

which furnishes an infinite tower of currents, including

$$\begin{aligned} P^{1^0} &= m_5 - P^{1^2} = m_5 + m_5 \\ P^{1^3} &= m_5 + m_5 + m_5 + \int_{\Gamma} G_a m_5 + m_5 + \int_{\Gamma} G_a m_5 \end{aligned} \quad (5.29)$$

which become increasingly nonlocal at higher orders. On the support of the equations of motion in Eq. (5.13), these currents are conserved, $\dot{P}^{1,0} = 0$.

5.7.2 Integrability of Special Galileon Theory

Applying the color-kinematics replacement in Eq. (5.7) to Eq. (5.25) and Eq. (5.26) we obtain the Lax connection for SG theory,

$$\mathcal{L} = \frac{1}{1-\lambda^2} \mathcal{M} \mathcal{Q} \mathcal{L} - \mathcal{M} \mathcal{Q}^0 \quad (5.30)$$

whose corresponding field strength is also vanishing,

$$\mathcal{F}_a = \mathcal{M}^a \mathcal{M}^a, \mathcal{M}^a \mathcal{M}^a = 0 \quad (5.31)$$

Meanwhile, the Wilson line maps from a color matrix to a diffeomorphism via

$$\begin{aligned} \mathcal{W}^G &= \exp \int \mathcal{L}^G \mathcal{M}^a \mathcal{M}^a \\ &= 1 + \int \mathcal{L}^G \mathcal{M}^a \mathcal{M}^a + \frac{1}{2} \int \int \mathcal{L}^G \mathcal{M}^a \mathcal{M}^a \mathcal{L}^G \mathcal{M}^a \mathcal{M}^a, \\ &= \mathcal{L}^G \mathcal{M}^a \mathcal{M}^a \text{ where } \mathcal{L}^G = 1 \times \mathcal{L}^G \mathcal{M}^a \mathcal{M}^a. \end{aligned} \quad (5.32)$$

As per Eq. (5.28), the Lax current for the SG theory is

$$P = n_a \mathcal{M}^a \mathcal{M}^a \quad (5.33)$$

which is conserved since

$$\dot{P} = \mathcal{M}^a \mathcal{M}^a \mathcal{M}^a \mathcal{M}^a = \mathcal{M}^a \mathcal{M}^a \mathcal{M}^a \mathcal{M}^a = 0 \quad (5.34)$$

where $\mathcal{M}^a \mathcal{M}^a = \mathcal{M}^a \mathcal{M}^a$ follows directly from Eq. (5.31). The series expansion of Eq. (5.33) yields an infinite tower of conserved currents in the SG theory which include

$$P^{1,0} = \mathcal{M}^a \mathcal{M}^a \mathcal{M}^a \quad P^{2,0} = \mathcal{M}^a \mathcal{M}^a \mathcal{M}^a \mathcal{M}^a \mathcal{M}^a \mathcal{M}^a \quad (5.35)$$

and can also be obtained trivially from the currents of ZM theory in Eq. (5.29) by applying the color-kinematic replacement rules in Eq. (5.7).

5.8 Nonperturbative Solutions

Eq. (5.2) implies a nonperturbative map between the classical solutions of the equations of motion of BAS, ZM, and SG theory.

Since the SG theory is field redefinition equivalent to a two-dimensional free theory [321, 322, 334, 335], any arbitrary configuration of left- and right-moving wave packets will pass through each other unscathed even though the collision itself will be highly nonlinear and nonperturbative. Thus if we restrict to scattering on a spatial circle of circumference $2\pi c$, then the time evolution will be similarly periodic. Since every classical solution of the SG theory effectively resides on a spacetime torus, it can be expressed as a double discrete Fourier transform,

$$q^1 \mathcal{G} = \tilde{\mathcal{O}}_{ZZ} \mathcal{G} = \tilde{\mathcal{O}}_{ZZ\#} \mathcal{G}, \quad \mathcal{O}^1_{\#} \quad (5.36)$$

where the corrections to the right-hand side are negligible as long as the field does not vary on distances shorter than $\frac{1}{\#}$, which is always true for sufficiently large $\#$.

We now construct a dual field configuration in ZM theory defined for $\#^0$,

$$q^{01} \mathcal{G}_{Z_0} = \tilde{\mathcal{O}}_{ZZ\#} \mathcal{G}_{Z_0} \quad (5.37)$$

which is literally the SG solution under the replacement $\mathcal{G} \rightarrow \mathcal{G}_{Z_0}$. It is straightforward to see that Eq. (5.37) automatically satisfies the ZM equations of motion in Eq. (5.13) up to $\frac{1}{\#}$ corrections, since the commutator in Eq. (5.3) and Eq. (5.4) yields a color structure constant that exactly transforms the interaction vertex of ZM into that of SG theory. Repeating this procedure, we obtain

$$q^{001} \mathcal{G}_{Z_0} = \tilde{\mathcal{O}}_{ZZ\#} \mathcal{G}_{Z_0} \quad (5.38)$$

which is a classical solution of BAS theory.

Remarkably, the above analytic construction can be verified numerically as described in Fig. 5.1. Using the double copy replacement, we map a numerical solution of SG theory onto a corresponding matrix-valued field configuration of ZM theory, which is then shown to satisfy the ZM equations of motion to high precision.

Note that every solution of the SG theory maps to a dual solution in ZM theory but the converse is not true. This is not actually surprising given what is known from scattering: every gravity amplitude maps to a gauge theory amplitude with very specific color structures which are precisely chosen to be certain kinematic numerators. On the other hand, a generic gauge theory amplitude with arbitrary color structures will not have any interpretation as a gravity amplitude.

Figure 5.1: We numerically solve the SG equations of motion in Eq. (5.19) for a pair of colliding Gaussian wave packets. The discrete Fourier transform of this solution, defined in Eq. (5.36), is inserted into Eq. (5.37) to obtain a putative matrix-valued solution of ZM theory. The above density plots characterize this ZM configuration, where the horizontal (vertical) axes denote space (time) and lighter (darker) colors denote positive (negative) field values. Each panel depicts a different matrix-valued, spacetime-dependent operator $\mathcal{O}_{\alpha\beta\gamma\delta}$ etc., where the subscripts denote derivatives. Each operator is visualized by plotting its projection onto a single component, $\text{tr} \mathcal{O} Z_0^0$, where $Z_0 = \sum_i Z_i$. Each term in the ZM equations of motion in Eq. (5.13) is nonzero, but they nevertheless cancel to high precision in the final panel. These results were obtained for $\hbar = 1$ with $\# = 499$. See <https://bit.ly/3OdGlo4> for an animation of this scattering process.

That the SG is secretly free certainly detracts from the miracle of a nonperturbative mapping in this context. However, recall that very general deformations of BAS and ZM theory for example including masses or higher-dimension operators also double copy mechanically into analogous deformations of the SG theory. Nonperturbative solutions of this much larger class of nonfree theories will also exhibit the nonperturbative double copy defined in Eq. (5.36), Eq. (5.37), and Eq. (5.38).

5.9 Generalization Using the Moyal Algebra

We observed in Eq. (5.2) that the $\hbar \rightarrow 0$ limit of \star yields the deformed Moyal algebra. What about the $\hbar \rightarrow \infty$ limit? In this case the continuum version of Eq. (5.4) is the Moyal algebra [336],

$$f \star g = fg + \frac{i\hbar}{2} \{f, g\} + \mathcal{O}(\hbar^2) \quad (5.39)$$

which is the unique deformation of the Poisson algebra [337] encoding an infinite tower of higher-dimension corrections to the original kinematic structure constant in Eq. (5.8). Here we have defined a new coupling constant $\frac{2c}{\hbar}$. At the level of fields, the generalized color-kinematic replacement rule is

$$F_{\mu\nu} \rightarrow F_{\mu\nu} + \frac{i\hbar}{2} \{F_{\mu\nu}, \dots\} \quad (5.40)$$

where the subscripts denote which fields the derivatives act upon. Under this substitution, BAS theory maps to

$$L_{\text{ZM-}\mathcal{G}} = \frac{1}{2} m^{\mu\nu} q^{\rho} q^{\sigma} F_{\mu\nu} F_{\rho\sigma} + \frac{1}{6\hbar} \epsilon^{\mu\nu\rho\sigma} F_{\mu\nu} F_{\rho\sigma} q^1 q^2 \quad (5.41)$$

a Moyal-deformed variation of ZM theory which has also appeared in the context of SDYM [314].

The corresponding three-point Feynman vertex is

$$= \frac{8}{\hbar} \epsilon^{\mu\nu\rho\sigma} F_{\mu\nu} F_{\rho\sigma} \quad (5.42)$$

which is totally antisymmetric because of two-dimensional kinematics. The resulting four-point amplitude is given by Eq. (5.16) with the numerators

$$\begin{aligned} \Rightarrow_B &= \frac{1}{\hbar^2} \epsilon^{\mu\nu\rho\sigma} F_{\mu\nu} F_{\rho\sigma} F_{\alpha\beta} F_{\gamma\delta} \\ \Rightarrow_C &= \frac{1}{\hbar^2} \epsilon^{\mu\nu\rho\sigma} F_{\mu\nu} F_{\rho\sigma} F_{\alpha\beta} F_{\gamma\delta} \\ \Rightarrow_D &= \frac{1}{\hbar^2} \epsilon^{\mu\nu\rho\sigma} F_{\mu\nu} F_{\rho\sigma} F_{\alpha\beta} F_{\gamma\delta} \end{aligned} \quad (5.43)$$

Remarkably, these satisfy the kinematic Jacobi identity for any value of \hbar , for example

$$\epsilon^{\mu\nu\rho\sigma} F_{\mu\nu} F_{\rho\sigma} F_{\alpha\beta} F_{\gamma\delta} = 0 \quad (5.44)$$

for arbitrary on-shell two-dimensional kinematics.

The generalized replacement rule in Eq. (5.40) can be reapplied to ZM to generate a deformation of SG theory that includes a fixed tower of higher-dimension corrections, analogous to the infinite tower of corrections to self-dual gravity in Ref. [314].

5.10 Future Directions

The double copy is an extremely potent computational tool but it is fundamentally unclear why it works. Our results mark a radical departure from the status quo of the double copy in several ways. Typical theories that admit color-kinematics duality have a single coupling constant, massless particles, square in any spacetime dimension, only double copy on-shell, and all of this is only provable at tree level [79]. On the other hand we have presented an enormous class of scalar theories with arbitrary Wilson coefficients and masses that square on-shell (to all orders in perturbation theory) in two dimensions. A Lagrangian formulation coupled with an understanding of the algebra mapping also broadens the scope of the double copy to include Wilson lines, currents, and nonperturbative (non-Abelian) classical solutions.

The present Letter leaves several avenues for further inquiry. In general dimensions, the kinematic algebra for the NLSM is that of volume-preserving diffeomorphisms [292]. Generalizing this tree-level observation to the full loop-level action is an open problem. The two-dimensional results presented here suggest that this generalization may be possible, at least in principle. While we have found an enormous class of operators that double copy, it may be possible to enlarge the space even further by overcoming the restrictions (i) and (ii) given above.

Finally, it would also be interesting to apply our approach to gauge theory and gravity in two dimensions and beyond. The kinematic algebra for gauge theory [292], even at tree level, is not as well understood as for the NLSM. However, the self-dual sector of Yang-Mills theory has a simple kinematic algebra so it may be possible to systematically perturb away from the self-dual sector [289, 290].

Appendix A

DERIVATION OF EQ. (2.19)

The replacement in Eq. (2.19) eliminates all dependence on the angular momentum in favor of powers of ℓ and A . Its derivation is straightforward. To begin, consider the expression

$$\frac{\ell^2 A^{2\ell} |^{1=-\ell} \ell^2 A^2}{A^\ell} \quad (A.1)$$

where $|^{1=-\ell}$ is precisely chosen so that the Fourier transform of Eq. (A.1) is zero at leading order in the classical limit. Our aim will be to derive $|^{1=-\ell}$.

The Fourier transform of the tensor $A_{\alpha_1 \alpha_2} \dots A_{\alpha_{\ell-1} \alpha_\ell}$ is trivially obtained by taking derivatives of the Fourier transform of the scalar A ,

$$\begin{aligned} \frac{A_{\alpha_1 \alpha_2} \dots A_{\alpha_{\ell-1} \alpha_\ell}}{A^\ell} &= \frac{\ell!}{\ell!} \frac{\ell!}{\ell!} \frac{1}{A^{\ell-1}} \frac{1}{A} \\ &= \frac{\ell!}{\ell!} \frac{1}{A^{\ell-1}} \frac{1}{A} \\ &= \frac{\ell!}{\ell!} \frac{1}{A^{\ell-1}} \frac{1}{A} \end{aligned} \quad (A.2)$$

where the number of permutations in each summand is $\frac{\ell!}{\ell!}$. Truncating all but leading order classical contribution of Eq. (A.1) effectively sets ℓ to zero. In the Fourier transform of Eq. (A.2), each derivative brings down a factor of ℓ . Therefore, the first term vanishes when all free indices are contracted into the momentum ℓ . Inserting Eq. (A.1) we find that

$$\begin{aligned} |^{1=-\ell} &= \frac{1}{\ell!} \frac{\ell!}{\ell!} \frac{1}{A^{\ell-1}} \frac{1}{A} \\ &= \frac{1}{\ell!} \frac{\ell!}{\ell!} \frac{1}{A^{\ell-1}} \frac{1}{A} \end{aligned} \quad (A.3)$$

The solution to this equation is

$$|^{1=-\ell} = \frac{\ell!}{\ell!} \frac{1}{A^{\ell-1}} \frac{1}{A} \quad (A.4)$$

which is shown simply by plugging into both sides of Eq. (A.3). Starting from the left-hand-side of Eq. (2.19) and eliminating all factors of A^0 via Eq. (A.1) given

Eq. (A.4), we obtain

$$\frac{2: \tilde{Q}}{A} = \sum_{g=0}^{\infty} \frac{1}{9} \frac{10^{9+g} \Gamma(2g+1)}{\Gamma(2g+1)} \frac{\Gamma(2g+1)}{\Gamma(2g+1)} \frac{\text{Poch} \frac{\frac{1}{2}}{2}}{\text{Poch} \frac{\frac{1}{2}}{2}} - \quad (\text{A.5})$$

which correctly reproduces the right-hand-side of Eq. (2.19) with $\text{Poch} = \frac{\Gamma(x)}{\Gamma(x-1)}$ being a ratio of Gamma functions.

Appendix B

ELECTRIC AND MAGNETIC WEYL TENSORS

Here we summarize the electric and magnetic Weyl tensors in isotropic coordinates at all orders in the PM expansion. The expressions below are written in terms of $\epsilon = 1 - \frac{2M}{r}$. The electric Weyl tensor is

$$E^U_V = \frac{1}{2A^3} \begin{pmatrix} \frac{r^2}{2A^2} \frac{p}{5^{10}} & 0 & 0 & 0 \\ \frac{r}{2A^2} \frac{p}{5^{13}} & \frac{r^2}{2A^2} \frac{p}{5^{10}} & 0 & 0 \\ 0 & 0 & \frac{r^2}{2A^2} \frac{p}{5^{10}} & 0 \\ \frac{p}{2A^2 5^{13}} & 0 & 0 & \frac{p}{2A^2 5^{10}} \end{pmatrix} \quad (B.1)$$

and its eigenvalues are

$$\text{eig } E^U_V = 0, \frac{r^2}{2A^2 5^6}, \frac{r^2}{2A^2 5^{10}}, \frac{r^2}{2A^2 5^{10}} \quad (B.2)$$

The magnetic Weyl tensor is

$$B^U_V = \frac{1}{2A^3} \begin{pmatrix} 0 & 0 & \frac{3}{25} \frac{q}{5^{10}} & 0 \\ 0 & 0 & \frac{3}{25} \frac{q}{5^{10}} & 0 \\ \frac{3}{2A^2 5^{13}} \frac{q}{5^{10}} & \frac{3}{2A^2 5^{10}} \frac{p}{5^{10}} & 0 & 0 \\ 0 & 0 & 0 & 0 \end{pmatrix} \quad (B.3)$$

and its eigenvalues are

$$\text{eig } B^U_V = 0, 0, \frac{3}{2A^2 5^{10}} \frac{q}{5^{10}}, \frac{3}{2A^2 5^{10}} \frac{q}{5^{10}} \quad (B.4)$$

Appendix C

FEYNMAN RULES

In this section we summarize the Feynman rules for the EFT defined in Eq. (3.10), which describes a light particle worldline coupled to fluctuating gravitons in a Schwarzschild background with the addition of the recoil operator. Interpreted as a background-eld action, Eq. (3.10) has a corresponding set of background-eld Feynman diagrams that can be used to compute the 1SF radial action, e.g. as depicted in Fig. 3.1. To compute in the PM expansion, however, it is natural to further expand these background-eld Feynman diagrams order by order in Newton's constant. In this picture the fundamental perturbation theory is in flat space, and the difference of the Schwarzschild metric and particle geodesics from flat space and straight lines, respectively, are considered PM corrections.

To begin, let us define the background-eld effective action governing the light particle worldline and the fluctuation graviton in a curved background,

$$\begin{aligned}
 (S_{\text{B}})_{\text{G}} &= S_{\text{G}} - \frac{1}{2} \int_{\text{G}} \dot{x}^\mu \dot{x}^\nu G_{\mu\nu} - \frac{1}{2} \int_{\text{G}} \dot{x}^\mu \dot{x}^\nu G_{\mu\nu} + \dots \\
 &+ \frac{1}{2} \int_{\text{G}} \dot{x}^\mu \dot{x}^\nu G_{\mu\nu} + \dots \\
 &+ \frac{1}{2} \int_{\text{G}} \dot{x}^\mu \dot{x}^\nu G_{\mu\nu} + \dots \\
 &+ \frac{1}{2} \int_{\text{G}} \dot{x}^\mu \dot{x}^\nu G_{\mu\nu} + \dots
 \end{aligned} \tag{C.1}$$

where we have added a Lorenz gauge fixing term $\int_{\text{G}} \frac{1}{32c} \dot{x}^\mu \dot{x}^\nu G_{\mu\nu}$ with $\dot{x}^\mu = r^a \dot{x}^a - \frac{1}{2} \dot{r} \cdot \dot{x}$. In the first line of Eq. (C.1), the quantity S_{G} is just the probe radial action, which as usual is computed by plugging in the background metric and light geodesic in Eq. (3.4). Starting at the second line of Eq. (C.1), we show the terms needed to compute 1SF corrections, where the ellipses denote the higher order corrections.

Here $T_{\mu\nu}$ is the stress-energy tensor for the geodesic trajectory of the light particle, corresponding to a source term which implies the momentum-space Feynman rule,

$$\begin{aligned}
 \text{!} \text{---} &= \frac{1}{2} \int_{\text{G}} \dot{x}^\mu \dot{x}^\nu G_{\mu\nu} = \dots \\
 &= \dots \\
 &= \dots
 \end{aligned} \tag{C.2}$$

where the ellipsis denotes higher PM orders and where we have defined

$$O^{\mu\nu\alpha} D_{\mu\nu} = \frac{1}{2} D_{\mu\nu}^{\alpha} D_{\mu\nu}^{\alpha} + \dots \quad (C.3)$$

together with the frequency-domain trajectory $\dot{G}_{\mu\nu}^{(1)} = -3g^{\mu\nu} \dot{G}_{\mu\nu}^{(0)}$, and we have also explicitly expanded to subleading order. Case in point, we can trivially recast the trajectories in Eq. (3.9) into the form of perturbative Feynman diagrams. Concretely, using identities such as

$$\operatorname{arcsinh} \frac{Eg}{1} = \frac{1}{m_g} \frac{E}{11^2, E^2 g^{201 \cdot 2}} \quad (C.4)$$

we can write the 1PM time-domain trajectory as

$$\dot{G}_{\mu\nu} = \frac{A}{2E^2} 12E^2, 10^1, 11^2, E^2 g^{201 \cdot 2} + \frac{A}{2E^2} f 12E^2, 10^D, D_1 \frac{1}{m_g} \frac{1}{11^2, E^2 g^{201 \cdot 2}} \quad (C.5)$$

Powers of the spatial distance $d^2, E^2 g^{201 \cdot 2}$ can be rewritten as simple Fourier integrals. In the frequency domain, the trajectory then has a simple form

$$\dot{G}_{\mu\nu}^{(1)} = \frac{8^2 c^3 A}{E^2} \frac{3^4}{12c^4} 4^{8:G} X^{\mu\nu} D_1 :^0 X^{\mu\nu} :^0 + \frac{8^1 2E^2, 10^a :^a}{1^2 :^1 : 203} \frac{1 f 12E^2, 10^D, D_1 :^0}{: 2^1 D_1 :^0} \quad (C.6)$$

where $\delta^a = [\delta^a E^2 f D, D_1^0 D^a E^2 f D, D^0 D^a]$ projects onto directions orthogonal to the four-velocities. Note that factor of f^2 which one would expect from perturbatively solving the geodesic equation has been reduced in power to in one term, and entirely eliminated in the other.

The full background-field propagator can be expanded perturbatively around at space as

$$\text{wavy line} = \text{wavy line}, \text{wavy line} \otimes \text{wavy line}, \text{wavy line} \otimes \text{wavy line} \otimes \text{wavy line}, \quad (C.7)$$

where the circles denote background field insertions and the leading term is the at-space graviton propagator,

$$\text{wavy line} = \frac{16c^8}{?^2} [\delta^d \delta^a f, f \delta^a d, \delta^a \delta^d] \quad (C.8)$$

which is in de Donder gauge on account of our choosing Lorenz gauge the original background-eld action defined in Eq. (C.1).

Of course, the true background is the Schwarzschild metric, but in the PM expansion we can treat these effects as order by order corrections to the flat space graviton two-point function. These contributions are obtained by taking the difference of the isotropic gauge Schwarzschild metric from the flat space metric and expanding in PM, which is simply the momentum-space version of Eq. (4.96),

$$W_a^{1\mu\nu} = \frac{8c}{\ell^2} \left[\eta_{\mu\nu} \partial_a \partial_\rho \partial^\rho \partial^\mu \partial^\nu + \dots \right] \quad (C.9)$$

$$\frac{8c^2}{\ell^2} \left[\eta_{\mu\nu} \partial_a \partial_\rho \partial^\rho \partial^\mu \partial^\nu + \dots \right] \bullet$$

The corresponding insertion is just the three-point vertex, from standard graviton perturbation theory in flat space, connecting two graviton lines to a linearized background metric. Note the appearance of non-zero curvatures in Eq. (C.1), which also appear as insertions. These arise because the metric is not a vacuum solution but is sourced by the heavy particle.

At low PM orders, we only need the background and geodesics to linear order and hence the background-eld method is not more efficient than performing a flat space perturbative calculation. However, at higher orders one sees considerable simplification, since in isotropic gauge the background metric insertions are simple powers in the radius whose Fourier transforms yield very simple dependencies on the momentum transfer induced by the insertion. In particular, the resulting Feynman rules are the same as for simple loop integrands with numerator structures that depend solely of $\eta_{\mu\nu}$ and $\partial_a \partial_b$ and are thus effectively scalar. Hence, the background-eld method effectively performs tensor reduction on subdiagrams within multiloop Feynman diagrams.

Finally, as explained in the main text, the background-eld action must be supplemented by the recoil operator in Eq. (3.2). It is trivial to compute the corresponding two-point vertex, which is

$$\text{Diagram: a circle with wavy lines on both sides} \quad (C.10)$$

$$= \frac{8c}{2} \frac{\partial_a \partial_b \partial_c \partial_d}{\ell^2} \left[\eta^{ab} \eta^{cd} - \eta^{ac} \eta^{bd} - \eta^{ad} \eta^{bc} \right] \bullet$$

The above Feynman rules are sufficient to compute the 1SF radial action for point-like compact bodies order by order in the PM expansion.

Appendix D

TIME-DOMAIN TRAJECTORIES

In this appendix, we provide details on the mechanical approach to efficiently solving the probe particle equations of motion in the time domain and then extracting from it a Feynman loop integral. We cover the cases of both electromagnetism and gravity. The general strategy involves: (i) using the integrability of the probe system to write simple first-order ordinary differential equations for the motion, (ii) integrating these equations in the time domain, (iii) expressing the solutions completely in terms of the zeroth order radial trajectory,

$$\dot{r} = \sqrt{1 - g^2 - \frac{p^2}{12c^2 r^2}} \quad (D.1)$$

and finally, (iv) using the following integral as the basic building block to unpack the time domain solutions into momentum space integrals,

$$r^{2U+1} = \frac{1}{2} \frac{4^U c^{2U-1} U^0}{1 - \frac{1}{2}} \frac{3}{12c^0} 4^{8^{11, D, g^0}} \frac{\chi^1 D^0}{1 - 20U} \quad (D.2)$$

and

$$r^{2U+1} = 8 \frac{1}{2} \frac{4^U c^{2U-1} U^0}{1 - \frac{3}{2}} \frac{3}{12c^0} 4^{8^{11, D, g^0}} \frac{\chi^1 D^0}{1 - 20U} \quad (D.3)$$

when U is a positive integer, and where

$$\chi^a = \left[\chi^a - \frac{1}{f^2} \frac{1}{10} \frac{1}{11fD} \right] \frac{D^0 D^a}{1 - f^2} \frac{1}{10} \frac{1}{11fD} \quad (D.4)$$

is the projector orthogonal to both four-velocities.

D.1 Electromagnetism

Let us review the solution for a relativistic charged probe trajectory in a Coulomb potential. In $d = 4$ dimensions, this can be done exactly (see [268, 272]). However, to maintain a consistent dimensional regularization and renormalization scheme for applications within effective field theory, we present here the computation in general d where we no longer have a closed form solution. We show how to

¹Since $D^0 = 0$ in the integrand, χ^a as written has redundant terms.

mechanically compute the solution to a desired order in the PL expansion in terms of iterated integrals involving ${}_2F_1$ hypergeometric functions. While the latter may sound cumbersome, we then demonstrate how corresponding loop integrands in dimensions are readily extracted. The resulting expressions, especially in the later presented gravitational case, are considerably more compact than those generated by standard Feynman diagrammatics. Moreover, from the final expressions one can see that the detour through position space effectively performs integration-by-parts reduction automatically.

Consider the einbein action for the charged probed particle in a Coulomb potential,

$$S_{EM} = \int d\tau \left[\frac{1}{2} \dot{x}^2 - \frac{1}{2} \frac{1}{r} - q \dot{\phi} \right] \quad (D.5)$$

where, to reduce notational clutter, we will drop subscripts denoting this to be the light particle action. The einbein equation of motion gives $\dot{x}^2 = \frac{1}{r}$. Let us define the components $\dot{x}^i = \frac{1}{r} \frac{dx^i}{d\tau}$, where $\dot{x} = c \cdot 2$ for scattering in the equatorial plane. Next, we gauge $\dot{x} = 1$, which imposes the on-shell condition, $\dot{x}^2 = \frac{1}{r} - A^2 \dot{\phi}^2 = 1$, on the space of solutions. Assuming describes the time-independent and spherically symmetric Coulomb potential, we have the conserved energy and angular momentum,

$$E = \frac{1}{2} \dot{x}^2 + \frac{1}{r} \quad \text{and} \quad L = A^2 \dot{\phi} \quad (D.6)$$

More convenient variables for scattering processes are

$$f = \frac{1}{r} \quad \text{and} \quad 1 = \frac{1}{2} \left(\dot{x}^2 + \frac{1}{r} \right) - \frac{1}{2} A^2 \dot{\phi}^2 \quad (D.7)$$

which are readily defined in a Lorentz invariant manner from the asymptotic inertial trajectories of the two interacting masses.

Eliminating $\dot{\phi}$ and \dot{x}^2 via Eq. (D.7), the on-shell condition becomes

$$1 = f - \frac{A^2}{2} \left(\frac{1}{r} - A^2 \dot{\phi}^2 \right) \quad (D.8)$$

In dimensions, in the rest frame of the heavy source, the Lorenz gauge solution for the gauge potential is

$$\frac{1}{r} = \frac{A^2}{2} \left(\frac{1}{r} - A^2 \dot{\phi}^2 \right) = \frac{A^2}{2} \frac{1}{r} - \frac{A^2}{2} A^2 \dot{\phi}^2 \quad (D.9)$$

with the charge radius A_2 , defined in Eq. (4.53), and notation introduced to condense upcoming expressions. The quantity in parentheses is unity. On the outward branch of the scattering trajectory $\theta = 0^\circ$, we then have

$$\begin{aligned} \mathcal{E} &= f \left(\frac{\dot{\theta}}{A} \right)^3 - \\ \mathcal{P} &= \frac{1}{s} \frac{1 - f^2 \frac{1}{A^2}}{1 - f^2 \frac{1}{A^2}} - \\ \mathcal{A} &= f \left(\frac{\dot{\theta}}{A} \right)^3 - \frac{1 - f^2 \frac{1}{A^2}}{A^2} \cdot \end{aligned} \quad (\text{D.10})$$

By the integrability of the probe motion, the equations of motion have reduced to three first-order differential equations. As mentioned above, we do not have a general solution valid for all θ , however these equations are very simple to integrate perturbatively. We will find it more convenient to combine the equations of motion for $\mathcal{A} - \mathcal{P}$ into equations of motion for the Cartesian components \mathcal{G}_i ,

$$\begin{aligned} \mathcal{H} &= \frac{H}{A} \left(\frac{\dot{\theta}}{A} \right)^3 - \frac{G}{A^2} \frac{1 - f^2 \frac{1}{A^2}}{1 - f^2 \frac{1}{A^2}} - \\ \mathcal{G} &= \frac{G}{A} \left(\frac{\dot{\theta}}{A} \right)^3 - \frac{H}{A^2} \frac{1 - f^2 \frac{1}{A^2}}{1 - f^2 \frac{1}{A^2}} - \end{aligned} \quad (\text{D.11})$$

where here and in the equation above we understand \mathcal{A} as a function of $\mathcal{G} - \mathcal{H}$.

We now expand the trajectory in PL,

$${}^1\mathcal{C}g^0 - \mathcal{C}g^0 - \mathcal{H}g^{00} = \tilde{O} \quad {}^1\mathcal{C}^1g^0 - \mathcal{C}^1g^0 - \mathcal{H}^1g^{00} - \quad (\text{D.12}) \\ = 0$$

where the \tilde{O}^{th} terms are $\mathcal{O}^1: = 0$, and solve Eq. (D.11) order by order in ϵ . From this the Lorentz covariant solution is trivially obtained,

$$\mathcal{G}^1g^0 = \mathcal{C}g^0 \frac{D}{1}, \quad \mathcal{G}g^0 \frac{1}{1}, \quad \mathcal{H}g^0 \frac{D}{1} \frac{fD}{1^{01 \cdot 2}} \cdot \quad (\text{D.13})$$

The leading order solution is, of course,

$$\mathcal{G} = fg - \quad \mathcal{G}^0 = 1 - \quad \mathcal{H}^0 = 1f^2 - 1^{01 \cdot 2}g \cdot \quad (\text{D.14})$$

For all $\epsilon = 1$, the structure of the equations of motion is as follows,

$$\begin{aligned} \frac{3}{3g} \mathcal{C}^1g^0 &= \cdot^1g^0 - \\ \frac{3}{3g} \frac{\mathcal{G}^1g^0}{g} &= \frac{-}{g} \cdot^1g^0 - \\ \frac{3}{3g} \mathcal{H}^1g^0 &= \cdot^1g^0 - \end{aligned} \quad (\text{D.15})$$

²The word radius is inaccurate here since the parameter generally has mass dimension

where the functions $\mathcal{G}^{(1)}, \mathcal{H}^{(1)}$ depend only through the lower order solutions, $\mathcal{G}^{(0)}, \mathcal{H}^{(0)}$ for $\dot{\gamma} = 0$. As written, these equations are now exact differentials and the solutions can be immediately written down as integrals of the functions $\mathcal{G}^{(1)}, \mathcal{H}^{(1)}$, can be straightforwardly computed by expanding Eq. (D.11) to the desired order, and the solutions on which they depend can be straightforwardly written as integrals of the lower order $\mathcal{G}^{(0)}, \mathcal{H}^{(0)}$. The structure of the solutions at a given order is then just iterated integrals of various functions of proper time.

At 1PL order, which is all that is needed to compute the 1SF-3PM radial action, these expressions take the form,

$$\begin{aligned} \mathcal{G}^{(1)} &= \frac{1}{m_g} \dot{\gamma}^3 - \\ \mathcal{H}^{(1)} &= \frac{1}{f} \frac{\dot{\gamma}^3}{2} - \frac{1}{f} \frac{\dot{\gamma}}{2} \\ \mathcal{H}^{(1)} &= \frac{1}{f} \frac{\dot{\gamma}^3}{2} - \frac{1}{f} \frac{\dot{\gamma}}{2} \end{aligned} \quad (D.16)$$

We will not write the higher order equations here, just the solutions, however they are straightforwardly derived.

The first order solutions follow immediately,

$$\begin{aligned} \mathcal{G} &= \frac{1}{m_g} \dot{\gamma}^3 - \\ \mathcal{G} &= \frac{1}{m_g} \dot{\gamma}^3 - \frac{1}{m_g} \dot{\gamma} \\ \mathcal{H} &= \frac{1}{f} \frac{\dot{\gamma}^3}{2} - \frac{1}{f} \frac{\dot{\gamma}}{2} \end{aligned} \quad (D.17)$$

The explicit expressions are

$$\begin{aligned} 3g^{(1)} &= \frac{1}{m_g} \dot{\gamma}^3 - \frac{1}{m_g} \dot{\gamma} \\ 3g^{(0)} &= \frac{1}{m_g} \dot{\gamma}^3 - \frac{1}{m_g} \dot{\gamma} \end{aligned} \quad (D.18)$$

In $\dot{\gamma} = 4$, these reduce to trigonometric and algebraic functions and the iterated integrals required to build the higher order solutions are expressible in closed form. In general, however, one is left with iterated integrals involving hypergeometric

³In practice, we found it convenient in intermediate steps to work with the equivalent equation, $\mathcal{G} = \frac{1}{m_g} \dot{\gamma}^3 - \frac{1}{m_g} \dot{\gamma}$, from which the solution for \mathcal{G} still follows immediately from integration.

functions and it is more notationally economical to leave the expressions in terms of formal integrals over powers of $\dot{\phi}$.

In $d = 4$, there are simplifications which occur trivially when manipulating the time domain expressions which may have appeared nontrivial had the expressions been written in momentum space. One example of this is, of course, the relationship between products on one side, and convolutions on the other. Other examples include relationships between integrals of different loop orders. Given our interest in working in general d , and that we no longer have closed form expressions in the time domain, one may worry whether the same simplifications are still manifest. Fortunately the answer is yes. Using elementary relationships between $\dot{\phi}$ and its time derivatives, there is a mechanical way to solve Eq. (D.15) in terms of iterated integrals of powers of $\dot{\phi}$ and g , simplify the resulting expression, and unpack the result in momentum space in terms of Feynman loop integrals. The explicit dependence appearing in the resulting numerators is suggestive of the relationship between this method and integration-by-parts reduction.

The general strategy for solving the equations of motion and extracting loop integrals is the following. Have the solutions $\dot{\phi}(\tau) = \mathcal{G}^{-1} \mathcal{H}^0$ for $\tau < \check{Y} = 0$ in terms of integrals of powers of $\dot{\phi}$, use them to compute the RHS of Eq. (D.15) at order τ^0 . The resulting expressions will have various powers of $\dot{\phi}$ in both the numerator and denominator. We want to eliminate explicit appearance of $\dot{\phi}$ and its derivatives so that we may readily map to momentum space. g appears in the combination, $\dot{\phi}^2, \dot{\phi}^4, \dots, \dot{\phi}^{2n}$, simply replace it with g^2 . If g appears alone in the denominator, that is, if there are terms with a common factor g^i , for $i > 0$, just take the coefficient of g^i and write all of the factors of $\dot{\phi}$ explicitly in terms of g and then simplify the expression there will be overall factors of g^i in the numerator which cancel the the g^i factor in the denominator. This leaves only positive powers of g to be dealt with. For even-positive powers write $g^{2i} = \int_0^1 dx (1-x)^{2i-1} x^{2i-1} g^{2i}$, and for odd-positive powers write $g^{2i+1} = \int_0^1 dx (1-x)^{2i} x^{2i} g^{2i+1}$. Finally, the only explicit g dependence will be linear, and moreover, it will necessarily be in the form of a factor g^{α} , for some α . Simply rewrite this as

$$g^{\alpha} = \frac{m^{\alpha} g^{\alpha/2}}{\int_0^1 dx (1-x)^{\alpha/2} x^{\alpha/2}} \quad (D.19)$$

The expression is now expressed as a string of iterated integrals and derivatives, with respect to proper time, of various powers of

While the above prescription succeeds in expressing the solutions solely in terms of g^0 , there may still be another manipulation to perform in order to extract a loop integral. For the PL order solution, neglecting the various integrals and derivatives, the powers of g^0 that appear in each term will be in the form,

$$g^0 \cdot 2^l U_l \dots U^0 = 1 \quad (D.20)$$

However, some terms may have some to be non-positive integers, precluding the use of Eq. (D.2), because of the singular U^0 factor. There is a simple fix for all such terms, simply replace the g^0 ending factors using the formula,

$$g^0 = \frac{g^3}{12^2 g^2} = \frac{1}{12^2 g^2} g^3 \quad (D.21)$$

which will raise the power of the g^0 ending until it is a positive integer.

With this strategy, one can systematically compute solutions to a desired PL order. For example, to compute the radial action to 4PL order, one needs only 0SF and 1SF contributions. To compute the 1SF contribution one needs only the 1PL and 2PL trajectories, with the former given above and the latter given by,

$$\begin{aligned}
 G_2 = & \frac{2^1}{f^2} \frac{4^0 f \frac{1}{m_g} \cdot 6 \cdot 2}{1} + \frac{1}{f^2} \frac{5^0 f^3 \frac{1}{m_g} \cdot 3}{1} - \\
 G_3 = & \frac{1^1}{f^2} \frac{3^0 f^2 \frac{1}{m_g} \cdot 3 \frac{1}{m_g} \cdot 1}{1} \\
 & + \frac{1^1}{f^2} \frac{5^0 f^2 \frac{1}{m_g} \cdot 1 \frac{1}{m_g} \cdot 3}{1} \\
 & + \frac{1^1}{f^2} \frac{3^0 f^2 \frac{1}{m_g} \cdot 4 \cdot 2}{1} - \\
 H_2 = & \frac{1}{f^2} \frac{5^0 f^2 \frac{1}{m_g} \cdot 3}{1^{3 \cdot 2}} \\
 & + \frac{1^1}{21^2} \frac{3^0 f^2 \frac{1}{m_g} \cdot 8 \cdot 2}{5^0 f^2} + \frac{1}{12^2} \frac{4^0 f^2 \frac{1}{m_g} \cdot 3}{5^0 f^2} \\
 & + \frac{1}{12^2} \frac{4^0 f^2 \frac{1}{m_g} \cdot 3 \frac{1}{m_g} \cdot 3}{f^2} + \frac{1^1}{2} \frac{15^0 f^2 \frac{1}{m_g} \cdot 6 \cdot 2}{f^2} \cdot
 \end{aligned} \quad (D.22)$$

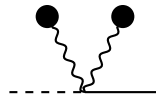


Figure D.1: Diagram topology corresponding to Eq. (D.23)

This expression is readily covariantized using Eq. (D.13) and expressed as loop integrals using Eq. (D.3). The corresponding Feynman diagram topologies can be read off the time-domain expressions by noting that \dot{g}_1 and \dot{g}_2 have straightforward interpretations as background field insertions and matter propagators. For example,

$$\dot{g}_2 \frac{1}{m_g} \delta^2 = \frac{8c^2 A_2^2}{12} \frac{4^{8A_1, 2^0} \dot{X}^1 D_1^0 \dot{X}^1 D_2^0}{2^1 2^{20} 2^1 D_1^1, D_1^2} \quad (D.23)$$

corresponds to the diagram topology shown in Fig. D.1. The explicit factors of \dot{g}_1 in the expressions in Eq. (D.22), together with doubled propagators such as the factor of $2^0 2^2$, are both structures which do not arise in a standard Feynman diagrammatic computation and suggest that integral reduction has, at least partially, been automatically performed by passing through the time domain.

Covariantizing these expressions, and Fourier transforming, we find for the 1PL trajectory,

$$\dot{G}_1 = \frac{8cA_2}{f^2 - 1} \frac{4^{8A_1} \dot{X}^1 D_1^0}{4^1 D_1^0 \dot{D}_1^0 f D_1^0 - 1 \quad \frac{5^0 1 \quad 3^0 f \quad f^2 - 1}{2^1 D_1^0 2} \quad a_a} \quad (D.24)$$

To keep the expressions concise, we present only the leading-order contribution to the 2PL trajectory integrand,

$$\dot{G}_2 = \frac{84c^2 A_2^2}{12 f^2 - 10^2} \frac{4^{8A_1, 2^0} \dot{X}^1 D_1^0 \dot{X}^1 D_2^0}{1^{-2} \frac{2^1 2^{20} 2^1 D_1^1, D_1^2}{2^1 D_1^0} \frac{2^1 D_1^0}{2^2 f^1 D_1^0} f D_1^0} \quad (D.25)$$

$$\frac{4^1 2^1 D_1^1, D_1^2 2^2 f^1 D_1^0}{, 1^1 D_1^1, D_1^2 2^0 1^2 \frac{2}{2} f^2 - 1 f^2 - 1 a_1 a_2} \quad (D.25)$$

$$\frac{, 2^1 D_1^2 2^0 1^2 \frac{2}{2} f^2 - 1 \quad 2f^2 - 1 f D_1^0}{, 1^2 \frac{2}{2} f^2 - 1 \quad 2^1 D_1^2 2^0 a_2 a_1} \quad (D.25)$$

The procedure continues straightforwardly to higher PL orders.

D.2 Gravity

The strategy for solving probe equations of motion and mining them for loop integrands is nearly identical between gravity and electromagnetism. Indeed this highlights a nice feature of the approach, the gravitational results are very similar in form and complexity to the electromagnetic results despite gravity being a nonlinear field theory.

We start from the worldline action for the light particle, again dropping the subscript,

$$S = \int d\tau \left[\frac{1}{2} g_{\mu\nu} \dot{x}^\mu \dot{x}^\nu - \frac{1}{2} \kappa^2 \right] \quad (D.26)$$

where the background metric sourced by the heavy (spinless) particle is just the Schwarzschild-Tangherlini solution,

$$g_{00} = \frac{5}{5} \frac{1}{A^2} \quad \text{and} \quad g_{89} = - \frac{1}{5} \frac{1}{A^2} \quad (D.27)$$

presented here in isotropic coordinates. We have defined the function,

$$\frac{1}{A^2} = 1 - \frac{4M}{r} \quad (D.28)$$

in terms of a generalization of the mass parameter,

$$M = \frac{4c^2}{1} \frac{1}{2^{10} c^{10} 1^{10} 2} \quad (D.29)$$

which is not to be confused with a renormalization scheme subtraction scale.

Again, we gauge fix the einbein to $e = 1$, which imposes the curved space on-shell condition, $g_{\mu\nu} \dot{x}^\mu \dot{x}^\nu = 1$, on the space of solutions.

The background is static and isotropic so we can restrict to motion in the equatorial plane, with dynamics constrained by the conserved energy and angular momentum. We will, again, prefer to label trajectories by (E, L) using Eq. (D.7), in terms of which we have equations of motion,

$$E = \frac{1}{A} \dot{t} \quad \text{and} \quad L = \frac{1}{A^2} \dot{\phi} \quad (D.30)$$

with the radial equation of motion coming from the on-shell condition,

$$1 = \frac{1}{A^2} \dot{r}^2 + \frac{1}{A^2} \dot{\phi}^2 + \frac{1}{A^2} \dot{t}^2 \quad (D.31)$$

As before, we will prefer to write equation of motion for the Cartesian components, now of the form,

$$\begin{aligned} \ddot{H} &= \frac{H}{A} - \frac{G}{A^2} \left(5 \frac{1}{A^0} - \frac{4}{3} f^2 - 10^{1 \cdot 2} \right) - \\ \ddot{G} &= \frac{G}{A} - \frac{H}{A^2} \left(5 \frac{1}{A^0} - \frac{4}{3} f^2 - 10^{1 \cdot 2} \right) \bullet \end{aligned} \quad (D.32)$$

Expanding the solutions in f^0 , where the n^{th} order trajectory is $O(f^n)$, we again find the leading solution, Eq. (D.14),

$$G^0 = fg - \quad G^{0^0} = 1 - \quad H^{0^0} = \frac{1}{2} f^2 - 10^{1 \cdot 2} g - \quad (D.33)$$

and all higher order equations of motion are of the form,

$$\begin{aligned} \frac{3}{3g} G^1 g^0 &= - \frac{1}{g} g^0 - \\ \frac{3}{3g} \frac{G^1 g^0}{g} &= - \frac{1}{g} g^0 - \\ \frac{3}{3g} H^1 g^0 &= - \frac{1}{g} g^0 \bullet \end{aligned} \quad (D.34)$$

The strategy outlined in the previous section on electromagnetism is used identically to solve the equations in gravity and is completely mechanical. For example, the trajectories through 2PM order,

$$\begin{aligned} G &= \frac{1}{m_g} \left(1 - \frac{4}{3} f^2 - 10^{1 \cdot 2} \right) - \\ G &= \left(\frac{1}{2} 1 - \frac{2}{3} f^2 - 10^{1 \cdot 2} \right) \frac{1}{m_g} - \\ H &= \frac{1}{2} \left(\frac{4}{3} f^2 - 10^{1 \cdot 2} \right) \frac{1}{m_g} - \end{aligned} \quad (D.35)$$

and

$$\begin{aligned}
 \mathcal{G} &= \left[\frac{f^1}{2 f^2} \right]_{1,3} \frac{4 f^2}{1} \left[\frac{1}{m_g} \right]_{1,3} \\
 &\quad \left[\frac{f^{12}}{2 f^2} \right]_{1,6,2} \frac{5 f^2}{1} \frac{3}{m_g} \\
 \mathcal{G}_2 &= \left[\frac{1^1}{4^1} \right]_{1,3} \frac{4 f^2}{3^0 f^2} \frac{1^1}{1} \frac{2 f^2}{1} \frac{1}{m_g} \left[\frac{1}{m_g} \right]_{1,1} \\
 &\quad \left[\frac{1^1}{4 f^2} \right]_{1,1} \frac{4 f^2}{4 f^2} \frac{1^1}{1} \frac{2 f^2}{1} \frac{1}{m_g} \left[\frac{1}{m_g} \right]_{1,3} \\
 &\quad \left[\frac{1^{12}}{8 f^2} \right]_{1,4,2} \frac{5 f^2}{8 f^2} \frac{1^2}{1} \frac{3 f^2}{1} \frac{6}{3} \frac{1}{m_g^2} \\
 \mathcal{H}_2 &= \left[\frac{1}{41^{21}} \right]_{1,3} \frac{4^{02}}{3^{02}} \frac{1^2}{f^2} \frac{1}{m_g^2} \left[\frac{1}{m_g} \right]_{1,3} \\
 &\quad \left[\frac{1^3}{81^{21}} \right]_{1,8,2} \frac{1^3}{5^{01}} \frac{1^3}{3^{02} f^2} \frac{1^2}{1^{3 \cdot 2}} \frac{1}{m_g} \\
 &\quad \left[\frac{1^1}{4^1} \right]_{1,3} \frac{4^{02} f^4}{3^0 f^2} \frac{1}{1^{3 \cdot 2}} \left[\frac{1}{m_g} \right]_{1,3} \\
 &\quad \left[\frac{1}{41^{21}} \right]_{1,5} \frac{4^0}{5^{01}} \frac{1^2}{3^{02} f^2} \frac{1^2}{1^{3 \cdot 2}} \left[\frac{1}{m_g} \right]_{1,3} \\
 &\quad \left[\frac{8^2}{16^1} \right]_{1,6,2} \frac{76}{3^{02} f^2} \frac{241}{1^{3 \cdot 2}} \frac{251 f^4}{1}{m_g} \\
 &\quad \left[\frac{2^1}{16^1} \right]_{1,6,2} \frac{12}{3^{02} f^2} \frac{15^0}{1^{3 \cdot 2}} \frac{31 f^2}{1^{3 \cdot 2}} \frac{7}{1} \frac{25}{m_g}
 \end{aligned} \tag{D.36}$$

are all that is needed to compute the radial action through 4PM order. Note that we obtain the same diagram topologies as in electromagnetism, without additional structures describing graviton self-interactions.

The mapping to Fourier space was already outlined in the previous section. Here,

we present the n -dimensional 1PM trajectory,

$$\dot{G}_1 = \frac{28c <}{1 \quad 2^0 f^2 \quad 1} \frac{4 \text{ }^8 A \text{ }^1 D \text{ }^0}{2^1 D_1 \text{ }^0 2}$$

$$1 \quad 5^0 1 \quad 3^0 f^2 \quad 1 \quad 1 \quad 2^0 f^2 \quad 1 \quad \text{`a} \text{ }_a$$

$$, 4f \text{ }^1 D_1 \text{ }^0 1 \quad 2^0 f^2 \quad 2 \quad , 5 \text{ } D \text{ }^1$$

$$, 4^1 D_1 \text{ }^0 1 \quad 4^0 f^2 \quad , 1 \text{ } D_1 \text{ }^1 \bullet$$

(D.37)

Again, since the n -dependent coefficients in the numerator are lengthy, we will give just the 4-dimensional integrand for the 2PM trajectory,

$$\dot{G}_2 = \frac{28c^2 \text{ }^2 <^2}{1^2 f^2 \quad 1^2} \frac{4 \text{ }^8 A_{1, 2^0} \text{ }^1 D_1 \text{ }^0 \text{ }^1 D_2 \text{ }^0}{2^1 \text{ }^2 2^0 2^1 D_1 \text{ }^0 2^0 1 D_1 \text{ }^1, D_1 \text{ }^2 0^2}$$

$$31^2 \text{ }^2_2 f^2 \quad 1^2 \quad 5f^2 \quad 1 \text{ }^1 D_1 \text{ }^2 0 \quad \text{`a} \text{ }_{2a}$$

$$81^2 \text{ }^2_2 \text{ }^1 D_1 \text{ }^1, D_1 \text{ }^2 0^2 f \quad 2f^2 \quad 3 \text{ } D \text{ }^1, D_1 \text{ }^1$$

$$, 21^2 \text{ }^2_2 \quad 2f^4 \quad 3f^2, 1 \text{ }^1 D_1 \text{ }^1, D_1 \text{ }^2 0 \quad \text{`a} \text{ }_{1a}, \text{ }_{2a^0}$$

$$8 \text{ }^1 \quad 2f^2 \text{ }^2 \text{ }^1 D_1 \text{ }^2 0^1 D_1 \text{ }^1, D_1 \text{ }^2 0^1 f D \text{ }^1 \quad D_1 \text{ }^0$$

$$61^2 \text{ }^2_2 f^2 \quad 1 \text{ }^1 D_1 \text{ }^2 0^1 D_1 \text{ }^1, D_1 \text{ }^2 0 f \quad 5f^2 \quad 9 \text{ } D \text{ }^1, 3f D_1 \text{ }^1, D_1 \text{ }^1$$

$$, O^1 \quad 4^0 \bullet$$

(D.38)

Appendix E

PROBE RADIAL ACTIONS

E.1 On-shell Action and Radial Action

Here, let us review some classical mechanics. Consider the generally covariant action for a massive charged particle,

$$S = -m \int \sqrt{-g_{\mu\nu} \dot{x}^\mu \dot{x}^\nu} d\tau - q \int A_\mu \dot{x}^\mu d\tau \quad (\text{E.1})$$

where we have included the worldline einbein¹, for manifest reparameterization invariance. If we define the conjugate momentum,

$$p_\mu = \frac{m \dot{x}_\mu}{\sqrt{-g_{\alpha\beta} \dot{x}^\alpha \dot{x}^\beta}} - q A_\mu \quad (\text{E.2})$$

we can write the action in a first-order form,

$$S = \int d\tau \left(p_\mu \dot{x}^\mu - H \right) \quad (\text{E.3})$$

where the reparameterization generator for this problem is

$$H = \frac{1}{2} \left(g^{\mu\nu} p_\mu p_\nu + m^2 \right) + q \dot{x}^\mu A_\mu \quad (\text{E.4})$$

As written, the action has a good variational principle if we would like to prescribe Dirichlet boundary conditions for the x^μ , but not for the p_μ . If we were to change basis and desire an action suitable for Dirichlet conditions on the momenta, we could simply add the boundary counter term,

$$S_{\text{boundary}} = \frac{3}{2} \int d\tau \dot{x}^\mu p_\mu \quad (\text{E.5})$$

This does not change the equations of motion, but it allows for a well defined variational principle and will certainly change the value of the on-shell action. Since we are interested in scattering dynamics, we certainly want to fix the asymptotic momenta. The upshot of this is that the correct action for the problem of scattering from a static isotropic source is

$$S = \int d\tau \left(p_\mu \dot{x}^\mu - H \right) + \frac{3}{2} \int d\tau \dot{x}^\mu p_\mu \quad (\text{E.6})$$

¹One could also consider problems with a more general $g_{\mu\nu}$ and what follows will continue to hold.

On-shell this simplifies considerably because the energy and angular momentum are conserved, and the einbein is a Lagrange multiplier forcing the reparameterization generator (on-shell condition) to vanish on physical solutions. This leaves the on-shell OSF action,

$$I = \int_{A_{\min}}^{A_{\max}} 3g_A^{-1} \dot{A}^0 - \dot{A} \cdot \quad (E.7)$$

Integrating by parts, and using the time reflection symmetry of the problem, this may be written as

$$I = \lim_{A_{\max} \rightarrow 1} \left[2A_{\max} \dot{A}^0 - 2 \int_{A_{\min}}^{A_{\max}} 3A \dot{A}^0 - \dot{A} \right] \quad (E.8)$$

with

$$\dot{A} = 4 \sqrt{6A} \dot{\varphi}, \quad \varphi|_{A_{\min}} \quad (E.9)$$

which is nothing but the radial action (suitably subtracted to be finite as $A_{\max} \rightarrow 1$). This subtraction will affect only the free-particle contribution to the radial action, and leaves scattering contributions unaffected. We will omit it in what follows.

The total change in azimuthal angle follows straightforwardly by Hamilton's equation. Since $\varphi = \varphi_q$ is a constant of motion, we have

$$\frac{3\langle \varphi \rangle}{3} = \int_{A_{\min}}^{A_{\max}} \frac{3}{3\varphi_q} H_{\text{on-shell}} = \int_{A_{\min}}^{A_{\max}} 3g_A^{-1} \dot{A}^0 = \varphi_q \quad (E.10)$$

E.2 General Perturbative Radial Action Integral

For a general d -dimensional theory, the on-shell radial action for a scattering solution is

$$I = 2 \int_{A_{\min}}^1 3A_j \dot{A}^0 - \dot{A}^j \quad (E.11)$$

where \dot{A}^0 is the radial momentum, and A_{\min} its largest real zero. In this work, we are only interested in scattering from static, spherically symmetric backgrounds. To solve for \dot{A}^0 , we may then first define the relativistic momentum,

$$q = \sqrt{1 - \frac{2}{\varphi^2} \dot{\varphi}^2} \dot{\varphi} \quad (E.12)$$

with φ being the asymptotic spatial momentum, and then impose the on-shell condition.

We are primarily interested in perturbative expansions of the radial action, particularly for theories where the particle's on-shell condition implies the following

form for the spatial momentum (in suitable coordinates),

$$\tilde{O} = \sum_{l=0}^{\infty} \frac{c_l}{A^{l+3/2}} n^{2l+1} \quad (E.13)$$

However, computing Eq. (E.11) perturbatively requires a little care. Since the radial momentum is solved for from the quadratic equation, Eq. (E.13), it is singular at the turning point A_{\min} , and a naive expansion yields divergent integrals. A careful treatment of this is given in [338], and the upshot is that one should: (i) integrate to the unperturbed turning point $A_{\min} = 0$, (ii) Taylor expand \tilde{O} in n , and (iii) take the Hadamard partie finie (Pf) of the resulting divergent integrals.

Following this prescription yields the well defined series expansion for the radial action,

$$S = \sum_{l=0}^{\infty} \frac{c_l}{A^{l+3/2}} \text{Pf} \int_1^{\infty} \frac{3A^{l+2} - 1}{A^{2l+3}} \quad (E.14)$$

where $l = 0, 1, \dots$ is the conserved angular momentum, and the c_l are simple monomials in the n^{2l+1} . Through $O(n^3)$, the non-zero coefficients are

$$\begin{aligned} c_{00} &= 2 - & c_{11} &= \frac{1}{2} \#_1 - & c_{22} &= \frac{1}{4} \#_1^2 - & c_{33} &= \frac{1}{8} \#_1^3 - \\ c_{20} &= \frac{1}{2} \#_1 - & c_{32} &= \frac{1}{2} \#_1 \#_2 - & c_{41} &= \frac{1}{2} \#_1 \end{aligned}$$

Evaluating the integral yields the general result,

$$S = \frac{1}{2} \sum_{l=0}^{\infty} \frac{c_l}{A^{l+3/2}} \frac{\Gamma(1/2) \Gamma(l+1)}{\Gamma(l+3/2)} \quad (E.15)$$

where Γ is the Euler beta function.

E.3 Electromagnetism

For electromagnetism, the on-shell condition is

$$1 - \frac{Q^2}{4} = \frac{1}{4} \quad (E.16)$$

The d -dimensional attractive Coulomb potential is

$$\frac{Q}{4} = \frac{1}{c} \frac{A_2}{A^{3/2}} \quad (E.17)$$

²Equivalently, impose a hard cut-off scheme $A_{\min} = 1/X$, and simply discard power-law divergences in $1/X$.

where U is the fine structure constant. Inserting Eq. (E.12) and Eq. (E.13) and solving for α , we obtain the α . Plugging back into the general probe radial action, Eq. (E.15), under the identification $\alpha = A_2$, and writing $\alpha = \frac{1}{2} \frac{c^2}{f^2} \frac{1}{10^{1/2}}$ to conform with our notation throughout the main text, we obtain

$$\begin{aligned} \frac{10^0}{EM} &= c \frac{1}{f^2} \frac{1}{1}, < A_2^4 & \frac{c^2 \frac{2}{f^2} \frac{2}{1}}{\frac{1}{f^2} \frac{1}{1}} \\ & < A_2^2 \frac{12c^4}{2 f^2} \frac{7f^2}{1} \frac{1}{3^2} \frac{1}{3^0} \frac{7}{2} \frac{3}{2} \\ & < A_2^3 \frac{c^5 \frac{3}{2} f^3}{3 f^2} \frac{10f^2}{1} \frac{3}{5^2} \frac{3}{2} \frac{11}{2} \end{aligned}$$

expanded up to 3PL order. Note that these expressions apply in general spacetime dimension, d .

E.4 Gravity

For gravity, the on-shell condition is

$$\alpha \alpha \delta^a = \frac{2}{1} - \quad (E.18)$$

where δ_a is the background metric in isotropic coordinates. For example, the d -dimensional Schwarzschild metric in isotropic coordinates is

$$\delta_{00} = \frac{1}{1 + \frac{2}{4A^3}} \quad \text{and} \quad \delta_{89} = \frac{1}{4A^3} \frac{1}{3} \quad (E.19)$$

where we have defined the mass parameter,

$$\frac{1}{4A^3} = \frac{4c^2}{2^0 c^2} \frac{1}{10^2} \quad (E.20)$$

Bibliography

- [1] D. P. A. Maurice, The quantum theory of the emission and absorption of radiation, Proc. R. Soc. Lond. A14(1927) 243 265.
- [2] A. Luna, R. Monteiro, I. Nicholson, D. O'Connell, and C. D. White, The double copy: Bremsstrahlung and accelerating black holes, JHEP 06(2016) 023, arXiv:1603.05737 [hep-th] .
- [3] W. D. Goldberger and A. K. Ridgway, Radiation and the classical double copy for color charges, Phys. Rev. D95 no. 12, (2017) 125010, arXiv:1611.03493 [hep-th] .
- [4] W. D. Goldberger, S. G. Prabhu, and J. O. Thompson, Classical gluon and graviton radiation from the bi-adjoint scalar double copy, Phys. Rev. D 96 (Sep, 2017) 065009.
- [5] F. Cachazo and A. Guevara, Leading singularities and classical gravitational scattering, JHEP 02 (2020) 181, arXiv:1705.10262 [hep-th] .
- [6] W. D. Goldberger, J. Li, and S. G. Prabhu, Spinning particles, axion radiation, and the classical double copy, Phys. Rev. D97 no. 10, (2018) 105018, arXiv:1712.09250 [hep-th] .
- [7] D. Chester, Radiative double copy for Einstein-Yang-Mills theory, Phys. Rev. D97 (Apr, 2018) 084025.
- [8] W. D. Goldberger and A. K. Ridgway, Bound states and the classical double copy, Phys. Rev. D97 no. 8, (2018) 085019, arXiv:1711.09493 [hep-th] .
- [9] J. Li and S. G. Prabhu, Gravitational radiation from the classical spinning double copy, Phys. Rev. D97 (May, 2018) 105019.
- [10] A. Laddha and A. Sen, Observational signature of the logarithmic terms in the soft-graviton theorem, Phys. Rev. D100 (Jul, 2019) 024009.
- [11] N. E. J. Bjerrum-Bohr, P. H. Damgaard, G. Festuccia, L. Planté, and P. Vanhove, General relativity from scattering amplitudes, Phys. Rev. Lett. 121 (Oct, 2018) 171601.
- [12] C.-H. Shen, Gravitational radiation from color-kinematics duality, JHEP11 (2018) 162, arXiv:1806.07388 [hep-th] .
- [13] J. Plefka, J. Steinhard, and W. Wormsbecher, Effective action of dilaton gravity as the classical double copy of Yang-Mills theory, Phys. Rev. D 99 (Jan, 2019) 024021.

- [14] B. Sahoo and A. Sen, Classical and quantum results on logarithmic terms in the soft theorem in four dimensions, *JHEP* 02 (2019) 086, arXiv:1808.03288 [hep-th] .
- [15] D. A. Kosower, B. Maybee, and D. O'Connell, Amplitudes, observables, and classical scattering, *JHEP* 02 (2019) 137, arXiv:1811.10950 [hep-th] .
- [16] M. Ciafaloni, D. Colferai, and G. Veneziano, Infrared features of gravitational scattering and radiation in the eikonal approach, *Phys. Rev. D* 99 (Mar, 2019) 066008.
- [17] A. Koemans Collado, P. Di Vecchia, and R. Russo, Revisiting the second post-Minkowskian eikonal and the dynamics of binary black holes, *Phys. Rev. D* 100 (Sep, 2019) 066028.
- [18] A. Cristofoli, P. H. Damgaard, P. Di Vecchia, and C. Heissenberg, Second-order post-Minkowskian scattering in arbitrary dimensions, *JHEP* 07 (2020) 122, arXiv:2003.10274 [hep-th] .
- [19] L. de la Cruz, B. Maybee, D. O'Connell, and A. Ross, Classical Yang-Mills observables from amplitudes, *JHEP* 12 (2020) 076, arXiv:2009.03842 [hep-th] .
- [20] G. Mogull, J. Plefka, and J. Steinhard, Classical black hole scattering from a worldline quantum field theory, *JHEP* 02 (2021) 048, arXiv:2010.02865 [hep-th] .
- [21] P. H. Damgaard, K. Haddad, and A. Helset, Heavy black hole effective theory, *JHEP* 11 (2019) 070, arXiv:1908.10308 [hep-ph] .
- [22] R. Aoude, K. Haddad, and A. Helset, On-shell heavy particle effective theories, *JHEP* 05 (2020) 051, arXiv:2001.09164 [hep-th] .
- [23] K. Haddad and A. Helset, The double copy for heavy particles, *Phys. Rev. Lett.* 125 (2020) 181603, arXiv:2005.13897 [hep-th] .
- [24] S. Caron-Huot and Z. Zahraee, Integrability of black hole orbits in maximal supergravity, *JHEP* 07 (2019) 179, arXiv:1810.04694 [hep-th] .
- [25] J. Parra-Martinez, M. S. Ruf, and M. Zeng, Extremal black hole scattering at \mathcal{O}^1 : Graviton dominance, eikonal exponentiation, and differential equations, *JHEP* 11 (2020) 023, arXiv:2005.04236 [hep-th] .
- [26] J. M. Henn and B. Mistlberger, Four-graviton scattering to three loops in $N = 8$ supergravity, *JHEP* 05 (2019) 023, arXiv:1902.07221 [hep-th] .

- [27] P. Di Vecchia, S. G. Naculich, R. Russo, G. Veneziano, and C. D. White, A tale of two exponentiations in $D = 8$ supergravity at subleading level, *JHEP*03(2020)173, arXiv:1911.11716 [hep-th] .
- [28] Z. Bern, H. Ita, J. Parra-Martinez, and M. S. Ruf, Universality in the classical limit of massless gravitational scattering, *Phys. Rev. Lett.*125 no. 3, (2020) 031601, arXiv:2002.02459 [hep-th] .
- [29] S. Abreu, F. Febres Cordero, H. Ita, M. Jaquier, B. Page, M. S. Ruf, and V. Sotnikov, Two-loop four-graviton scattering amplitude, *Phys. Rev. Lett.*124 no. 21, (2020) 211601, arXiv:2002.12374 [hep-th] .
- [30] B. Bertotti, On gravitational motion, *Nuovo Cim*4 no. 4, (1956) 898 906.
- [31] R. P. Kerr, The Lorentz-covariant approximation method in general relativity I, *Nuovo Cim*.13 no. 3, (1959) 469 491.
- [32] B. Bertotti and J. Plebanski, Theory of gravitational perturbations in the fast motion approximation, *Annals Phys*11 no. 2, (1960) 169 200.
- [33] M. Portilla, Momentum and angular momentum of two gravitating particles, *J. Phys. A*12 (1979) 1075 1090.
- [34] K. Westpfahl and M. Goller, Gravitational scattering of two relativistic particles in postlinear approximation, *Lett. Nuovo Cim*26 (1979) 573 576.
- [35] M. Portilla, Scattering of two gravitating particles: Classical approach, *J. Phys. A*13 (1980) 3677 3683.
- [36] L. Bel, T. Damour, N. Deruelle, J. Ibanez, and J. Martin, Poincaré invariant gravitational field and equations of motion of two pointlike objects: The postlinear approximation of general relativity, *General Relativity and Gravitation*13 no. 10, (Oct., 1981) 963 1004.
- [37] K. Westpfahl, High-speed scattering of charged and uncharged particles in general relativity, *Fortsch. Phys*33 no. 8, (1985) 417 493.
- [38] T. Ledvinka, G. Schaefer, and J. Bicak, Relativistic closed-form Hamiltonian for many-body gravitating systems in the post-Minkowskian approximation, *Phys. Rev. Lett.*100(2008)251101, arXiv:0807.0214 [gr-qc] .
- [39] T. Damour, Gravitational scattering, post-Minkowskian approximation and effective one-body theory, *Phys. Rev. D*94 no. 10, (2016) 104015, arXiv:1609.00354 [gr-qc] .

- [40] T. Damour, High-energy gravitational scattering and the general relativistic two-body problem, *Phys. Rev. D* **97** no. 4, (2018) 044038, arXiv:1710.10599 [gr-qc] .
- [41] A. Antonelli, A. Buonanno, J. Steinhilber, M. van de Meent, and J. Vines, Energetics of two-body Hamiltonians in post-Minkowskian gravity, *Phys. Rev. D* **99** no. 10, (2019) 104004, arXiv:1901.07102 [gr-qc] .
- [42] G. Kälin, Z. Liu, and R. A. Porto, Conservative dynamics of binary systems to third post-Minkowskian order from the effective field theory approach, *Phys. Rev. Lett.* **125** no. 26, (2020) 261103, arXiv:2007.04977 [hep-th] .
- [43] J. Droste, The field of moving centres in Einstein's theory of gravitation, *Proc. Acad. Sci. Amst.* **91** (1917) 447-455.
- [44] A. Einstein, L. Infeld, and B. Hoffmann, The gravitational equations and the problem of motion *Annals Math.* **39** (1938) 65-100.
- [45] T. Ohta, H. Okamura, T. Kimura, and K. Hiida, Physically acceptable solution of Einstein's equation for many-body system, *Progress of Theoretical Physics* **50** no. 2, (Aug., 1973) 492-514.
- [46] P. Jaranowski and G. Schaefer, Third post-Newtonian higher order ADM Hamilton dynamics for two-body point-mass system, *Phys. Rev. D* **57** (1998) 7274-7291, arXiv:gr-qc/9712075 . [Erratum: *Phys. Rev. D* **63**, 029902 (2001)].
- [47] T. Damour, P. Jaranowski, and G. Schaefer, Dynamical invariants for general relativistic two-body systems at the third post-Newtonian approximation, *Phys. Rev. D* **62** (2000) 044024, arXiv:gr-qc/9912092 .
- [48] L. Blanchet and G. Faye, Equations of motion of point particle binaries at the third post-Newtonian order, *Phys. Lett. A* **271** (2000) 58, arXiv:gr-qc/0004009 .
- [49] T. Damour, P. Jaranowski, and G. Schaefer, Dimensional regularization of the gravitational interaction of point masses, *Phys. Lett. B* **513** (2001) 147-155, arXiv:gr-qc/0105038 .
- [50] T. Damour, P. Jaranowski, and G. Schäfer, Nonlocal-in-time action for the fourth post-Newtonian conservative dynamics of two-body systems, *Phys. Rev. D* **89** no. 6, (2014) 064058, arXiv:1401.4548 [gr-qc] .
- [51] P. Jaranowski and G. Schäfer, Derivation of local-in-time fourth post-Newtonian ADM Hamiltonian for spinless compact binaries, *Phys. Rev. D* **92** (Dec, 2015) 124043.

- [52] L. Bernard, L. Blanchet, A. Bohé, G. Faye, and S. Marsat, Fokker action of nonspinning compact binaries at the fourth post-Newtonian approximation, *Phys. Rev. D* **93** no. 8, (2016) 084037, arXiv:1512.02876 [gr-qc] .
- [53] L. Bernard, L. Blanchet, A. Bohé, G. Faye, and S. Marsat, Energy and periastron advance of compact binaries on circular orbits at the fourth post-Newtonian order, *Phys. Rev. D* **95** no. 4, (2017) 044026, arXiv:1610.07934 [gr-qc] .
- [54] D. Bini and T. Damour, Gravitational scattering of two black holes at the fourth post-Newtonian approximation, *Phys. Rev. D* **96** no. 6, (2017) 064021, arXiv:1706.06877 [gr-qc] .
- [55] L. Bernard, L. Blanchet, A. Bohé, G. Faye, and S. Marsat, Dimensional regularization of the IR divergences in the Fokker action of point-particle binaries at the fourth post-Newtonian order, *Phys. Rev. D* **96** (Nov, 2017) 104043.
- [56] T. Marchand, L. Bernard, L. Blanchet, and G. Faye, Ambiguity-free completion of the equations of motion of compact binary systems at the fourth post-Newtonian order, *Phys. Rev. D* **97** no. 4, (2018) 044023, arXiv:1707.09289 [gr-qc] .
- [57] L. Bernard, L. Blanchet, G. Faye, and T. Marchand, Center-of-mass equations of motion and conserved integrals of compact binary systems at the fourth post-Newtonian order, *Phys. Rev. D* **97** no. 4, (2018) 044037, arXiv:1711.00283 [gr-qc] .
- [58] Y. Mino, M. Sasaki, and T. Tanaka, Gravitational radiation reaction to a particle motion, *Phys. Rev. D* **55** (Mar, 1997) 3457 3476.
- [59] T. C. Quinn and R. M. Wald, Axiomatic approach to electromagnetic and gravitational radiation reaction of particles in curved spacetime, *Phys. Rev. D* **56** (Sep, 1997) 3381 3394.
- [60] A. Buonanno and T. Damour, Effective one-body approach to general relativistic two-body dynamics, *Phys. Rev. D* **59** (1999) 084006, arXiv:gr-qc/9811091 .
- [61] A. Buonanno and T. Damour, Transition from inspiral to plunge in binary black hole coalescences, *Phys. Rev. D* **62** (2000) 064015, arXiv:gr-qc/0001013 .
- [62] F. Pretorius, Evolution of binary black hole spacetime, *Phys. Rev. Lett.* **95** (2005) 121101, arXiv:gr-qc/0507014 .

- [63] M. Campanelli, C. O. Lousto, P. Marronetti, and Y. Zlochower, Accurate evolutions of orbiting black-hole binaries without excision, *Phys. Rev. Lett.* **96** (2006) 111101, arXiv:gr-qc/0511048 .
- [64] J. G. Baker, J. Centrella, D.-I. Choi, M. Koppitz, and J. van Meter, Gravitational wave extraction from an inspiraling configuration of merging black holes, *Phys. Rev. Lett.* **96** (2006) 111102, arXiv:gr-qc/0511103 .
- [65] W. D. Goldberger and I. Z. Rothstein, Effective field theory of gravity for extended objects, *Phys. Rev. D* **73** (May, 2006) 104029.
- [66] J. B. Gilmore and A. Ross, Effective field theory calculation of second post-Newtonian binary dynamics, *Phys. Rev. D* **78** (Dec, 2008) 124021.
- [67] S. Foffa and R. Sturani, Effective field theory calculation of conservative binary dynamics at third post-Newtonian order, *Phys. Rev. D* **84** (2011) 044031, arXiv:1104.1122 [gr-qc] .
- [68] S. Foffa, P. Mastrolia, R. Sturani, and C. Sturm, Effective field theory approach to the gravitational two-body dynamics at fourth post-Newtonian order and quintic in the Newton constant, *Phys. Rev. D* **95** (May, 2017) 104009.
- [69] R. A. Porto and I. Z. Rothstein, Apparent ambiguities in the post-Newtonian expansion for binary systems, *Phys. Rev. D* **96** (Jul, 2017) 024062.
- [70] S. Foffa, P. Mastrolia, R. Sturani, C. Sturm, and W. J. Torres Bobadilla, Static two-body potential at fifth post-Newtonian order, *Phys. Rev. Lett.* **122** no. 24, (2019) 241605, arXiv:1902.10571 [gr-qc] .
- [71] J. Blümlein, A. Maier, and P. Marquard, Five-loop static contribution to the gravitational interaction potential of two point masses, *Phys. Lett. B* **800** (2020) 135100, arXiv:1902.11180 [gr-qc] .
- [72] S. Foffa, R. A. Porto, I. Rothstein, and R. Sturani, Conservative dynamics of binary systems to fourth post-Newtonian order in the EFT approach. II. Renormalized Lagrangian, *Phys. Rev. D* **100** (Jul, 2019) 024048.
- [73] J. Blümlein, A. Maier, P. Marquard, and G. Schäfer, Fourth post-Newtonian Hamiltonian dynamics of two-body systems from an effective field theory approach, *Nucl. Phys. B* **955** (2020) 115041, arXiv:2003.01692 [gr-qc] .
- [74] J. Blümlein, A. Maier, P. Marquard, and G. Schäfer, Testing binary dynamics in gravity at the sixth post-Newtonian level, *Phys. Lett. B* **807** (2020) 135496, arXiv:2003.07145 [gr-qc] .

- [75] H. Kawai, D. C. Lewellen, and S. H. H. Tye, A relation between tree amplitudes of closed and open strings, *Nucl. Phys. B* **269**(1986) 1-23.
- [76] Z. Bern, L. J. Dixon, M. Perelstein, and J. S. Rozowsky, Multileg one loop gravity amplitudes from gauge theory, *Nucl. Phys. B* **546** (1999) 423-479, arXiv:hep-th/9811140 .
- [77] Z. Bern, J. Carrasco, and H. Johansson, New relations for gauge-theory amplitudes, *Phys. Rev. D* **78**(2008) 085011, arXiv:0805.3993 [hep-ph] .
- [78] Z. Bern, J. J. M. Carrasco, and H. Johansson, Perturbative quantum gravity as a double copy of gauge theory, *Phys. Rev. Lett* **105** (2010) 061602, arXiv:1004.0476 [hep-th] .
- [79] Z. Bern, J. J. Carrasco, M. Chiodaroli, H. Johansson, and R. Roiban, The duality between color and kinematics and its applications, arXiv:1909.01358 [hep-th] .
- [80] Z. Bern, L. J. Dixon, D. C. Dunbar, and D. A. Kosower, One loop point gauge theory amplitudes, unitarity and collinear limits, *Nucl. Phys. B* **425**(1994) 217-260, arXiv:hep-ph/9403226 .
- [81] Z. Bern, L. J. Dixon, D. C. Dunbar, and D. A. Kosower, Fusing gauge theory tree amplitudes into loop amplitudes, *Nucl. Phys. B* **435**(1995) 59-101, arXiv:hep-ph/9409265 .
- [82] Z. Bern, L. J. Dixon, and D. A. Kosower, One loop amplitudes for e+ e- to four partons, *Nucl. Phys. B* **513**(1998) 3-86, arXiv:hep-ph/9708239 .
- [83] R. Britto, F. Cachazo, and B. Feng, Generalized unitarity and one-loop amplitudes in $\mathcal{N} = 4$ super-Yang-Mills, *Nucl. Phys. B* **725**(2005) 275-305, arXiv:hep-th/0412103 .
- [84] Z. Bern, J. J. M. Carrasco, H. Johansson, and D. A. Kosower, Maximally supersymmetric planar Yang-Mills amplitudes at ve loop, *Phys. Rev. D* **76**(2007) 125020, arXiv:0705.1864 [hep-th] .
- [85] Y. Iwasaki, Quantum theory of gravitation vs. classical theory. - fourth-order potential, *Prog. Theor. Phys* **46**(1971) 1587-1609.
- [86] Y. Iwasaki, Fourth-order gravitational potential based on quantum field theory, *Lett. Nuovo Cim* **15**(1971) 783-786.
- [87] H. Okamura, T. Ohta, T. Kimura, and K. Hiida, Perturbation calculation of gravitational potentials, *Prog. Theor. Phys* **50**(1973) 2066-2079.
- [88] D. Amati, M. Ciafaloni, and G. Veneziano, Higher order gravitational deflection and soft Bremsstrahlung in Planckian energy superstring collisions, *Nucl. Phys. B* **347**(1990) 550-580.

- [89] J. F. Donoghue, Leading quantum correction to the Newtonian potential, *Phys. Rev. Lett.* 72 (1994) 2996–2999, arXiv:gr-qc/9310024 .
- [90] J. F. Donoghue, General relativity as an effective field theory: the leading quantum corrections, *Phys. Rev. D* 50 (1994) 3874–3888, arXiv:gr-qc/9405057 .
- [91] N. E. J. Bjerrum-Bohr, J. F. Donoghue, and B. R. Holstein, Quantum gravitational corrections to the nonrelativistic scattering potential of two masses, *Phys. Rev. D* 67 (2003) 084033, arXiv:hep-th/0211072 . [Erratum: *Phys. Rev. D* 71, 069903 (2005)].
- [92] B. R. Holstein and A. Ross, Spin effects in long range electromagnetic scattering, arXiv:0802.0715 [hep-ph] .
- [93] N. E. J. Bjerrum-Bohr, J. F. Donoghue, and P. Vanhove, On-shell techniques and universal results in quantum gravity, *JHEP* 02 (2014) 111, arXiv:1309.0804 [hep-th] .
- [94] D. Neill and I. Z. Rothstein, Classical space-times from the S matrix, *Nucl. Phys. B* 777 (2013) 177–189, arXiv:1304.7263 [hep-th] .
- [95] C. Cheung, I. Z. Rothstein, and M. P. Solon, From scattering amplitudes to classical potentials in the post-Minkowskian expansion, *Phys. Rev. Lett.* 121 no. 25, (2018) 251110, arXiv:1808.02489 [hep-th] .
- [96] Z. Bern, C. Cheung, R. Roiban, C.-H. Shen, M. P. Solon, and M. Zeng, Scattering amplitudes and the conservative Hamiltonian for binary systems at third post-Minkowskian order, *Phys. Rev. Lett.* 122 no. 20, (2019) 201603, arXiv:1901.04424 [hep-th] .
- [97] Z. Bern, C. Cheung, R. Roiban, C.-H. Shen, M. P. Solon, and M. Zeng, Black hole binary dynamics from the double copy and effective theory, *JHEP* 10 (2019) 206, arXiv:1908.01493 [hep-th] .
- [98] G. Kälin and R. A. Porto, From boundary data to bound states, *JHEP* 01 (2020) 072, arXiv:1910.03008 [hep-th] .
- [99] G. Kälin and R. A. Porto, From boundary data to bound states. Part II. Scattering angle to dynamical invariants (with twist), *JHEP* 02 (2020) 120, arXiv:1911.09130 [hep-th] .
- [100] LIGO Scientific, Virgo Collaboration, B. P. Abbott et al., Observation of Gravitational Waves from a Binary Black Hole Merger, *Phys. Rev. Lett.* 116 no. 6, (2016) 061102, arXiv:1602.03837 [gr-qc] .

- [101] P. Amaro-Seoane, H. Audley, S. Babak, J. Baker, E. Barausse, P. Bender, E. Berti, P. Binetruy, M. Born, D. Bortoluzzi, J. Camp, C. Caprini, V. Cardoso, M. Colpi, J. Conklin, N. Cornish, C. Cutler, K. Danzmann, R. Dolesi, L. Ferraioli, V. Ferroni, E. Fitzsimons, J. Gair, L. G. Bote, D. Giardini, F. Gibert, C. Grimani, H. Halloin, G. Heinzl, T. Hertog, M. Hewitson, K. Holley-Bockelmann, D. Hollington, M. Hueller, H. Inchauspe, P. Jetzer, N. Karnesis, C. Killow, A. Klein, B. Klipstein, N. Korsakova, S. L. Larson, J. Livas, I. Lloro, N. Man, D. Mance, J. Martino, I. Mateos, K. McKenzie, S. T. McWilliams, C. Miller, G. Mueller, G. Nardini, G. Nelemans, M. Nofrarias, A. Petiteau, P. Pivato, E. Plagnol, E. Porter, J. Reiche, D. Robertson, N. Robertson, E. Rossi, G. Russano, B. Schutz, A. Sesana, D. Shoemaker, J. Slutsky, C. F. Sopuerta, T. Sumner, N. Tamanini, I. Thorpe, M. Troebs, M. Vallisneri, A. Vecchio, D. Vetrugno, S. Vitale, M. Volonteri, G. Wanner, H. Ward, P. Wass, W. Weber, J. Ziemer, and P. Zweifel, *Laser Interferometer Space Antenna*, 2017.
- [102] P. Amaro-Seoane, J. R. Gair, M. Freitag, M. C. Miller, I. Mandel, C. J. Cutler, and S. Babak, Intermediate and extreme mass-ratio inspirals astrophysics, science applications and detection using LISA, *Classical and Quantum Gravity* 24 no. 17, (Aug, 2007) R113.
- [103] J. R. Gair, L. Barack, T. Creighton, C. Cutler, S. L. Larson, E. S. Phinney, and M. Vallisneri, Event rate estimates for LISA extreme mass ratio capture sources *Classical and Quantum Gravity* 21 (2004) s1595.
- [104] J. Gair, I. Mandel, and L. Wen, Improved time frequency analysis of extreme-mass-ratio inspiral signals in mock LISA data, *Classical and Quantum Gravity* 25 no. 18, (Sept., 2008) 184031.
- [105] M. J. Du , Quantum tree graphs and the Schwarzschild solution, *Phys. Rev. D* 7 (1973) 2317 2326.
- [106] P. H. Damgaard and K. Lee, The Schwarzschild black hole from perturbation theory to all orders, [arXiv:2403.13216 \[hep-th\]](https://arxiv.org/abs/2403.13216) .
- [107] B. S. DeWitt, Quantum theory of gravity. III. Applications of the covariant theory, *Phys. Rev.* 162 (Oct, 1967) 1239 1256.
- [108] N. E. J. Bjerrum-Bohr, A. Cristofoli, and P. H. Damgaard, Post-Minkowskian scattering angle in Einstein gravity, *JHEP* 08 (2020) 038, [arXiv:1910.09366 \[hep-th\]](https://arxiv.org/abs/1910.09366) .
- [109] S. J. Parke and T. R. Taylor, Amplitude for gluon scattering, *Phys. Rev. Lett.* 56 (Jun, 1986) 2459 2460.
- [110] C. Cheung and M. P. Solon, Classical gravitational scattering $\mathcal{O}(G^3)$ from Feynman diagrams, *JHEP* 06 (2020) 144, [arXiv:2003.08351 \[hep-th\]](https://arxiv.org/abs/2003.08351) .

- [111] LIGO Scientific, Virgo Collaboration, B. P. Abbott et al., GW170817: Observation of gravitational waves from a binary neutron star inspiral, *Phys. Rev. Lett.* 119 no. 16, (2017) 161101, arXiv:1710.05832 [gr-qc] .
- [112] V. Vaidya, Gravitational spin Hamiltonians from the S matrix, *Phys. Rev. D* 91 no. 2, (2015) 024017, arXiv:1410.5348 [hep-th] .
- [113] A. Guevara, Holomorphic classical limit for spin effects in gravitational and electromagnetic scattering, *JHEP* 04 (2019) 033, arXiv:1706.02314 [hep-th] .
- [114] N. Arkani-Hamed, T.-C. Huang, and Y.-t. Huang, Scattering amplitudes for all masses and spins, *JHEP* 11 (2021) 070, arXiv:1709.04891 [hep-th] .
- [115] J. Vines, Scattering of two spinning black holes in post-Minkowskian gravity, to all orders in spin, and effective-one-body mapping, *Class. Quant. Grav.* 35 no. 8, (2018) 084002, arXiv:1709.06016 [gr-qc] .
- [116] A. Guevara, A. Ochirov, and J. Vines, Scattering of spinning black holes from exponentiated soft factors, *JHEP* 09 (2019) 056, arXiv:1812.06895 [hep-th] .
- [117] M.-Z. Chung, Y.-T. Huang, J.-W. Kim, and S. Lee, The simplest massive S-matrix: from minimal coupling to black holes, *JHEP* 04 (2019) 156, arXiv:1812.08752 [hep-th] .
- [118] Y. F. Bautista and A. Guevara, From scattering amplitudes to classical physics: Universality, double copy and soft theorems, arXiv:1903.12419 [hep-th] .
- [119] B. Maybee, D. O'Connell, and J. Vines, Observables and amplitudes for spinning particles and black holes, *JHEP* 12 (2019) 156, arXiv:1906.09260 [hep-th] .
- [120] A. Guevara, A. Ochirov, and J. Vines, Black-hole scattering with general spin directions from minimal-coupling amplitudes, *Phys. Rev. D* 100 no. 10, (2019) 104024, arXiv:1906.10071 [hep-th] .
- [121] N. Arkani-Hamed, Y.-t. Huang, and D. O'Connell, Kerr black holes as elementary particles, *JHEP* 01 (2020) 046, arXiv:1906.10100 [hep-th] .
- [122] M.-Z. Chung, Y.-T. Huang, and J.-W. Kim, Classical potential for general spinning bodies, *JHEP* 09 (2020) 074, arXiv:1908.08463 [hep-th] .

- [123] M.-Z. Chung, Y.-T. Huang, and J.-W. Kim, Kerr-Newman stress-tensor from minimal coupling, JHEP 12 (2020) 103, arXiv:1911.12775 [hep-th] .
- [124] M. Levi, A. J. Mcleod, and M. Von Hippel, \mathcal{N}^{LO} gravitational spin-orbit coupling at order \mathcal{G} JHEP 07 (2021) 115, arXiv:2003.02827 [hep-th] .
- [125] M.-Z. Chung, Y.-t. Huang, J.-W. Kim, and S. Lee, Complete Hamiltonian for spinning binary systems at first post-Minkowskian order, JHEP 05 (2020) 105, arXiv:2003.06600 [hep-th] .
- [126] M. Levi, A. J. Mcleod, and M. Von Hippel, \mathcal{N}^{LO} gravitational quadratic-in-spin interactions at $4\mathcal{G}$ JHEP 07 (2021) 116, arXiv:2003.07890 [hep-th] .
- [127] J. Vines, J. Steinhof, and A. Buonanno, Spinning-black-hole scattering and the test-black-hole limit at second post-Minkowskian order, Phys. Rev. D 99 no. 6, (2019) 064054, arXiv:1812.00956 [gr-qc] .
- [128] Z. Bern, A. Luna, R. Roiban, C.-H. Shen, and M. Zeng, Spinning black hole binary dynamics, scattering amplitudes, and effective field theory, Phys. Rev. D 104 no. 6, (2021) 065014, arXiv:2005.03071 [hep-th] .
- [129] A. Cristofoli, N. E. J. Bjerrum-Bohr, P. H. Damgaard, and P. Vanhove, Post-Minkowskian Hamiltonians in general relativity, Phys. Rev. D 100 no. 8, (2019) 084040, arXiv:1906.01579 [hep-th] .
- [130] P. Di Vecchia, C. Heissenberg, R. Russo, and G. Veneziano, Universality of ultra-relativistic gravitational scattering, Phys. Lett. B 811 (2020) 135924, arXiv:2008.12743 [hep-th] .
- [131] T. Damour, Radiative contribution to classical gravitational scattering at the third order in v , Phys. Rev. D 102 no. 12, (2020) 124008, arXiv:2010.01641 [gr-qc] .
- [132] A. Buonanno and B. S. Sathyaprakash, Sources of Gravitational Waves: Theory and Observations, 10, 2014, arXiv:1410.7832 [gr-qc] .
- [133] T. Dietrich, T. Hinderer, and A. Samajdar, Interpreting binary neutron star mergers: Describing the binary neutron star dynamics, modelling gravitational waveforms, and analyzing detections, Gen. Rel. Grav 53 no. 3, (2021) 27, arXiv:2004.02527 [gr-qc] .
- [134] LIGO Scientific, Virgo Collaboration, B. P. Abbott et al., GW190425: Observation of a compact binary coalescence with total mass $3.4 M_{\odot}$, Astrophys. J. Lett 892 no. 1, (2020) L3, arXiv:2001.01761 [astro-ph.HE] .

- [135] E. E. Flanagan and T. Hinderer, Constraining neutron star tidal Love numbers with gravitational wave detectors, *Phys. Rev. D* **77** (2008) 021502, arXiv:0709.1915 [astro-ph] .
- [136] C. Cutler et al., The last three minutes: issues in gravitational wave measurements of coalescing compact binaries, *Phys. Rev. Lett.* **70** (1993) 2984–2987, arXiv:astro-ph/9208005 .
- [137] C. Cutler and E. E. Flanagan, Gravitational waves from merging compact binaries: How accurately can one extract the binary's parameters from the inspiral wave form?, *Phys. Rev. D* **49** (1994) 2658–2697, arXiv:gr-qc/9402014 .
- [138] T. Hinderer, B. D. Lackey, R. N. Lang, and J. S. Read, Tidal deformability of neutron stars with realistic equations of state and their gravitational wave signatures in binary inspirals, *Phys. Rev. D* **81** (2010) 123016, arXiv:0911.3535 [astro-ph.HE] .
- [139] F. Pannarale, L. Rezzolla, F. Ohme, and J. S. Read, Will black hole-neutron star binary inspirals tell us about the neutron star equation of state?, *Phys. Rev. D* **84** (2011) 104017, arXiv:1103.3526 [astro-ph.HE] .
- [140] T. Damour, A. Nagar, and L. Villain, Measurability of the tidal polarizability of neutron stars in late-inspiral gravitational-wave signals, *Phys. Rev. D* **85** (2012) 123007, arXiv:1203.4352 [gr-qc] .
- [141] M. Favata, Systematic parameter errors in inspiraling neutron star binaries, *Phys. Rev. Lett.* **112** (2014) 101101, arXiv:1310.8288 [gr-qc] .
- [142] K. Yagi and N. Yunes, Love can be tough to measure, *Phys. Rev. D* **89** no. 2, (2014) 021303, arXiv:1310.8358 [gr-qc] .
- [143] B. D. Lackey and L. Wade, Reconstructing the neutron-star equation of state with gravitational-wave detectors from a realistic population of inspiralling binary neutron stars, *Phys. Rev. D* **91** no. 4, (2015) 043002, arXiv:1410.8866 [gr-qc] .
- [144] L. Wade, J. D. E. Creighton, E. Ochsner, B. D. Lackey, B. F. Farr, T. B. Littenberg, and V. Raymond, Systematic and statistical errors in a bayesian approach to the estimation of the neutron-star equation of state using advanced gravitational wave detectors, *Phys. Rev. D* **89** no. 10, (2014) 103012, arXiv:1402.5156 [gr-qc] .
- [145] K. Yagi and N. Yunes, Approximate universal relations among tidal parameters for neutron star binaries, *Class. Quant. Grav.* **34** no. 1, (2017) 015006, arXiv:1608.06187 [gr-qc] .

- [146] S. E. Gralla, On the ambiguity in relativistic tidal deformability, *Class. Quant. Grav.* 35 no. 8, (2018) 085002, arXiv:1710.11096 [gr-qc] .
- [147] A. Samajdar and T. Dietrich, Waveform systematics for binary neutron star gravitational wave signals: Effects of the point-particle baseline and tidal descriptions, *Phys. Rev. D* 98 no. 12, (2018) 124030, arXiv:1810.03936 [gr-qc] .
- [148] E. Poisson, Gravitomagnetic tidal resonance in neutron-star binary inspirals, *Phys. Rev. D* 101 no. 10, (2020) 104028, arXiv:2003.10427 [gr-qc] .
- [149] A. Le Tiec and M. Casals, Spinning black holes fall in Love, *Phys. Rev. Lett.* 126 no. 13, (2021) 131102, arXiv:2007.00214 [gr-qc] .
- [150] H. S. Chia, Tidal deformation and dissipation of rotating black holes, *Phys. Rev. D* 104 no. 2, (2021) 024013, arXiv:2010.07300 [gr-qc] .
- [151] M. Shibata, Fully general relativistic simulation of coalescing binary neutron stars: Preparatory tests, *Phys. Rev. D* 60 (1999) 104052, arXiv:gr-qc/9908027 .
- [152] L. Baiotti, B. Giacomazzo, and L. Rezzolla, Accurate evolutions of inspiralling neutron-star binaries: Prompt and delayed collapse to black hole, *Phys. Rev. D* 78 (2008) 084033, arXiv:0804.0594 [gr-qc] .
- [153] S. Bernuzzi, A. Nagar, M. Thierfelder, and B. Bruggmann, Tidal effects in binary neutron star coalescence, *Phys. Rev. D* 86 (2012) 044030, arXiv:1205.3403 [gr-qc] .
- [154] S. Bernuzzi, A. Nagar, T. Dietrich, and T. Damour, Modeling the dynamics of tidally interacting binary neutron stars up to the merger, *Phys. Rev. Lett.* 114 no. 16, (2015) 161103, arXiv:1412.4553 [gr-qc] .
- [155] J. S. Read, C. Markakis, M. Shibata, K. Uryu, J. D. E. Creighton, and J. L. Friedman, Measuring the neutron star equation of state with gravitational wave observations, *Phys. Rev. D* 79 (2009) 124033, arXiv:0901.3258 [gr-qc] .
- [156] L. Baiotti, T. Damour, B. Giacomazzo, A. Nagar, and L. Rezzolla, Analytic modelling of tidal effects in the relativistic inspiral of binary neutron stars, *Phys. Rev. Lett.* 105 (2010) 261101, arXiv:1009.0521 [gr-qc] .
- [157] L. Baiotti, T. Damour, B. Giacomazzo, A. Nagar, and L. Rezzolla, Accurate numerical simulations of inspiralling binary neutron stars and their comparison with effective-one-body analytical models, *Phys. Rev. D* 84 (2011) 024017, arXiv:1103.3874 [gr-qc] .

- [158] B. D. Lackey, K. Kyutoku, M. Shibata, P. R. Brady, and J. L. Friedman, Extracting equation of state parameters from black hole-neutron star mergers. I. Nonspinning black holes, *Phys. Rev. D* **85** (2012) 044061, arXiv:1109.3402 [astro-ph.HE] .
- [159] T. Damour, M. Soel, and C.-M. Xu, General relativistic celestial mechanics. 3. Rotational equations of motion, *Phys. Rev. D* **47** (1993) 3124–3135.
- [160] T. Damour, M. Soel, and C.-M. Xu, General relativistic celestial mechanics. 4: Theory of satellite motion, *Phys. Rev. D* **49** (1994) 618–635.
- [161] T. Hinderer, Tidal Love numbers of neutron stars, *Astrophys. J.* **677** (2008) 1216–1220, arXiv:0711.2420 [astro-ph] . [Erratum: *Astrophys. J.* **697**, 964 (2009)].
- [162] T. Damour and A. Nagar, Relativistic tidal properties of neutron stars, *Phys. Rev. D* **80** (2009) 084035, arXiv:0906.0096 [gr-qc] .
- [163] T. Binnington and E. Poisson, Relativistic theory of tidal Love numbers, *Phys. Rev. D* **80** (2009) 084018, arXiv:0906.1366 [gr-qc] .
- [164] J. E. Vines and E. E. Flanagan, Post-1-Newtonian quadrupole tidal interactions in binary systems, *Phys. Rev. D* **88** (2013) 024046, arXiv:1009.4919 [gr-qc] .
- [165] J. Vines, E. E. Flanagan, and T. Hinderer, Post-1-Newtonian tidal effects in the gravitational waveform from binary inspirals, *Phys. Rev. D* **83** (2011) 084051, arXiv:1101.1673 [gr-qc] .
- [166] Q. Henry, G. Faye, and L. Blanchet, Tidal effects in the gravitational-wave phase evolution of compact binary systems to next-to-next-to-leading post-Newtonian order, *Phys. Rev. D* **102** no. 4, (2020) 044033, arXiv:2005.13367 [gr-qc] . [Erratum: *Phys. Rev. D* **108**, 089901 (2023)].
- [167] Q. Henry, G. Faye, and L. Blanchet, Hamiltonian for tidal interactions in compact binary systems to next-to-next-to-leading post-Newtonian order, *Phys. Rev. D* **102** no. 12, (2020) 124074, arXiv:2009.12332 [gr-qc] .
- [168] J. Steinhilber, T. Hinderer, A. Buonanno, and A. Taracchini, Dynamical tides in general relativity: Effective action and effective-one-body Hamiltonian, *Phys. Rev. D* **94** no. 10, (2016) 104028, arXiv:1608.01907 [gr-qc] .

- [169] Q. Henry, G. Faye, and L. Blanchet, Tidal effects in the equations of motion of compact binary systems to next-to-next-to-leading post-Newtonian order, *Phys. Rev. D* 101 no. 6, (2020) 064047, arXiv:1912.01920 [gr-qc] .
- [170] D. Bini and T. Damour, Gravitational self-force corrections to two-body tidal interactions and the effective one-body formalism, *Phys. Rev. D* 90 no. 12, (2014) 124037, arXiv:1409.6933 [gr-qc] .
- [171] C. Kavanagh, A. C. Ottewill, and B. Wardell, Analytical high-order post-Newtonian expansions for extreme mass ratio binaries, *Phys. Rev. D* 92 no. 8, (2015) 084025, arXiv:1503.02334 [gr-qc] .
- [172] P. Nolan, C. Kavanagh, S. R. Dolan, A. C. Ottewill, N. Warburton, and B. Wardell, Octupolar invariants for compact binaries on quasicircular orbits, *Phys. Rev. D* 92 no. 12, (2015) 123008, arXiv:1505.04447 [gr-qc] .
- [173] T. Damour and A. Nagar, Effective one body description of tidal effects in inspiralling compact binaries, *Phys. Rev. D* 81 (2010) 084016, arXiv:0911.5041 [gr-qc] .
- [174] D. Bini, T. Damour, and G. Faye, Effective action approach to higher-order relativistic tidal interactions in binary systems and their effective one body description, *Phys. Rev. D* 85 (2012) 124034, arXiv:1202.3565 [gr-qc] .
- [175] D. Bini, T. Damour, and A. Geralico, Scattering of tidally interacting bodies in post-Minkowskian gravity, *Phys. Rev. D* 101 no. 4, (2020) 044039, arXiv:2001.00352 [gr-qc] .
- [176] G. Kälin and R. A. Porto, Post-Minkowskian effective field theory for conservative binary dynamics, *JHEP* 11 (2020) 106, arXiv:2006.01184 [hep-th] .
- [177] C. Cheung and M. P. Solon, Tidal effects in the post-Minkowskian expansion, *Phys. Rev. Lett* 125 no. 19, (2020) 191601, arXiv:2006.06665 [hep-th] .
- [178] W. D. Goldberger and I. Z. Rothstein, Horizon radiation reaction forces, *JHEP* 10 (2020) 026, arXiv:2007.00731 [hep-th] .
- [179] K. Haddad and A. Helset, Tidal effects in quantum field theory, *JHEP* 12 (2020) 024, arXiv:2008.04920 [hep-th] .
- [180] G. Kälin, Z. Liu, and R. A. Porto, Conservative tidal effects in compact binary systems to next-to-leading post-Minkowskian order, *Phys. Rev. D* 102 (2020) 124025, arXiv:2008.06047 [hep-th] .

- [181] S. Endlich, V. Gorbenko, J. Huang, and L. Senatore, An effective formalism for testing extensions to general relativity with gravitational waves, *JHEP* 09 (2017) 122, arXiv:1704.01590 [gr-qc] .
- [182] V. Cardoso, M. Kimura, A. Maselli, and L. Senatore, Black holes in an effective field theory extension of general relativity, *Phys. Rev. Lett.* 121 no. 25, (2018) 251105, arXiv:1808.08962 [gr-qc] . [Erratum: *Phys. Rev. Lett.* 131, 109903 (2023)].
- [183] B. S. Sathyaprakash et al., Extreme Gravity and Fundamental Physics, arXiv:1903.09221 [astro-ph.HE] .
- [184] N. Sennett, R. Brito, A. Buonanno, V. Gorbenko, and L. Senatore, Gravitational-Wave Constraints on an Effective Field-Theory Extension of General Relativity, *Phys. Rev. D* 102 no. 4, (2020) 044056, arXiv:1912.09917 [gr-qc] .
- [185] A. Brandhuber and G. Travaglini, On higher-derivative effects on the gravitational potential and particle bending, *JHEP* 01 (2020) 010, arXiv:1905.05657 [hep-th] .
- [186] W. T. Emond and N. Moynihan, Scattering amplitudes, black holes and leading singularities in cubic theories of gravity, *JHEP* 12 (2019) 019, arXiv:1905.08213 [hep-th] .
- [187] A. Cristofoli, Post-Minkowskian Hamiltonians in modified theories of gravity, *Phys. Lett. B* 800 (2020) 135095, arXiv:1906.05209 [hep-th] .
- [188] S. Cai and K.-D. Wang, Non-vanishing of tidal Love numbers, arXiv:1906.06850 [hep-th] .
- [189] M. Accettulli Huber, A. Brandhuber, S. De Angelis, and G. Travaglini, Eikonal phase matrix, deflection angle and time delay in effective field theories of gravity, *Phys. Rev. D* 102 no. 4, (2020) 046014, arXiv:2006.02375 [hep-th] .
- [190] D. Bini, T. Damour, and A. Gericco, Novel approach to binary dynamics: application to the fifth post-Newtonian level, *Phys. Rev. Lett.* 123 no. 23, (2019) 231104, arXiv:1909.02375 [gr-qc] .
- [191] D. Bini, T. Damour, and A. Gericco, Binary dynamics at the fifth and fifth-and-a-half post-Newtonian orders, *Phys. Rev. D* 102 no. 2, (2020) 024062, arXiv:2003.11891 [gr-qc] .
- [192] D. Bini, T. Damour, and A. Gericco, Sixth post-Newtonian local-in-time dynamics of binary systems, *Phys. Rev. D* 102 no. 2, (2020) 024061, arXiv:2004.05407 [gr-qc] .

- [193] A. Antonelli, C. Kavanagh, M. Khalil, J. Steinho, and J. Vines, Gravitational spin-orbit coupling through third-subleading post-Newtonian order: from first-order self-force to arbitrary mass ratios, *Phys. Rev. Lett.* 125 no. 1, (2020) 011103, arXiv:2003.11391 [gr-qc] .
- [194] A. Antonelli, C. Kavanagh, M. Khalil, J. Steinho, and J. Vines, Gravitational spin-orbit and aligned spin-spin couplings through third-subleading post-Newtonian orders, *Phys. Rev. D* 102 (2020) 124024, arXiv:2010.02018 [gr-qc] .
- [195] T. Damour, Classical and quantum scattering in post-Minkowskian gravity, *Phys. Rev. D* 102 no. 2, (2020) 024060, arXiv:1912.02139 [gr-qc] .
- [196] N. Siemonsen and J. Vines, Test black holes, scattering amplitudes and perturbations of Kerr spacetime, *Phys. Rev. D* 101 no. 6, (2020) 064066, arXiv:1909.07361 [gr-qc] .
- [197] N. Wex and G. Schafer, Innermost stable orbits for coalescing binary systems of compact objects—a remark, *Classical and Quantum Gravity* 10 no. 12, (1993) 2729.
- [198] Z. Bern, J. Parra-Martinez, R. Roiban, E. Sawyer, and C.-H. Shen, Leading nonlinear tidal effects and scattering amplitudes, *HEP* 05 (2021) 188, arXiv:2010.08559 [hep-th] .
- [199] M. H. Goro and A. Sagnotti, Quantum gravity at two loops, *Phys. Lett. B* 160 (1985) 81–86.
- [200] M. H. Goro and A. Sagnotti, The ultraviolet behavior of Einstein gravity, *Nucl. Phys. B* 266 (1986) 709–736.
- [201] A. E. M. van de Ven, Two loop quantum gravity, *Nucl. Phys. B* 378 (1992) 309–366.
- [202] Z. Bern, C. Cheung, H.-H. Chi, S. Davies, L. Dixon, and J. Nohle, Evanescent effects can alter ultraviolet divergences in quantum gravity without physical consequences, *Phys. Rev. Lett.* 115 no. 21, (2015) 211301, arXiv:1507.06118 [hep-th] .
- [203] N. E. J. Bjerrum-Bohr, Leading quantum gravitational corrections to scalar QED, *Phys. Rev. D* 66 (2002) 084023, arXiv:hep-th/0206236 .
- [204] M. S. Butt, Leading quantum gravitational corrections to QED, *Phys. Rev. D* 74 (2006) 125007, arXiv:gr-qc/0605137 .
- [205] S. Faller, Effective field theory of gravity: leading quantum gravitational corrections to Newton's and Coulomb's Law, *Phys. Rev. D* 77 (2008) 124039, arXiv:0708.1701 [hep-th] .

- [206] B. R. Holstein and A. Ross, Long distance effects in mixed electromagnetic-gravitational scattering, *arXiv:0802.0717 [hep-ph]* .
- [207] N. Arkani-Hamed, L. Motl, A. Nicolis, and C. Vafa, The string landscape, black holes and gravity as the weakest force, *JHEP*06(2007) 060, *arXiv:hep-th/0601001* .
- [208] Y. Kats, L. Motl, and M. Padi, Higher-order corrections to mass-charge relation of extremal black holes, *JHEP* 12 (2007) 068, *arXiv:hep-th/0606100* .
- [209] C. Cheung, J. Liu, and G. N. Remmen, Proof of the weak gravity conjecture from black hole entropy, *JHEP* 10 (2018) 004, *arXiv:1801.08546 [hep-th]* .
- [210] C. Cheung, J. Liu, and G. N. Remmen, Entropy bounds on effective field theory from rotating dyonic black holes *Phys. Rev. D*100 no. 4, (2019) 046003, *arXiv:1903.09156 [hep-th]* .
- [211] M. Accettulli Huber, A. Brandhuber, S. De Angelis, and G. Travaglini, Note on the absence of d^2 corrections to Newton's potential, *Phys. Rev. D*101 no. 4, (2020) 046011, *arXiv:1911.10108 [hep-th]* .
- [212] G. Agazie et al., The NANOGrav 15 yr data set: Evidence for a gravitational-wave background, *The Astrophysical Journal Letters*151 no. 1, (2023) L8.
- [213] L. Lehner and F. Pretorius, Numerical relativity and astrophysics, *Annual Review of Astronomy and Astrophysics*52 no. 1, (2014) 661-694.
- [214] V. Cardoso, L. Gualtieri, C. Herdeiro, and U. Sperhake, Exploring new physics frontiers through numerical relativity, *Living Reviews in Relativity*18 no. 1, (2015) .
- [215] E. Poisson, A. Pound, and I. Vega, The motion of point particles in curved spacetime, *Living Reviews in Relativity*14 no. 1, (2011) .
- [216] A. Pound, Motion of small objects in curved spacetimes: An introduction to gravitational self-force, in *Fundamental Theories of Physics* pp. 399-486. Springer International Publishing, 2015.
- [217] L. Barack and A. Pound, Self-force and radiation reaction in general relativity, *Reports on Progress in Physics*82 no. 1, (2018) 016904.
- [218] L. Blanchet, Gravitational radiation from post-newtonian sources and inspiralling compact binaries, *Living Reviews in Relativity*17 no. 1, (2014) .

- [219] H. Elvang and Y.-t. Huang, Scattering amplitudes, arXiv:1308.1697 [hep-th] .
- [220] L. Dixon, A brief introduction to modern amplitude methods, arXiv:1310.5353 [hep-ph] .
- [221] C. Cheung, TASI lectures on scattering amplitudes, arXiv:1708.03872 [hep-ph] .
- [222] K. G. Chetyrkin and F. V. Tkachov, Integration by parts: The algorithm to calculate beta functions in 4 loops, Nucl. Phys. B192 (1981) 159 204.
- [223] J. M. Henn, Multiloop integrals in dimensional regularization made simple, Phys. Rev. Lett.110 (2013) 251601, arXiv:1304.1806 [hep-th] .
- [224] Z. Bern, J. Parra-Martinez, R. Roiban, M. S. Ruf, C.-H. Shen, M. P. Solon, and M. Zeng, Scattering amplitudes and conservative binary dynamics at $\mathcal{O}(\epsilon^4)$, Phys. Rev. Lett.126 no. 17, (2021) 171601, arXiv:2101.07254 [hep-th] .
- [225] Z. Bern, J. Parra-Martinez, R. Roiban, M. S. Ruf, C.-H. Shen, M. P. Solon, and M. Zeng, Scattering amplitudes, the tail effect, and conservative binary dynamics at $\mathcal{O}(\epsilon^4)$, Phys. Rev. Lett.128 no. 16, (2022) 161103, arXiv:2112.10750 [hep-th] .
- [226] E. Herrmann, J. Parra-Martinez, M. S. Ruf, and M. Zeng, Radiative classical gravitational observables $\mathcal{O}(\epsilon^3)$ from scattering amplitudes, JHEP10 (2021) 148, arXiv:2104.03957 [hep-th] .
- [227] P. Di Vecchia, C. Heissenberg, R. Russo, and G. Veneziano, The eikonal approach to gravitational scattering and radiation $\mathcal{O}(\epsilon^3)$, JHEP 07 (2021) 169, arXiv:2104.03256 [hep-th] .
- [228] E. Herrmann, J. Parra-Martinez, M. S. Ruf, and M. Zeng, Gravitational Bremsstrahlung from reverse unitarity, Phys. Rev. Lett.126 no. 20, (2021) 201602, arXiv:2101.07255 [hep-th] .
- [229] A. Brandhuber, G. Chen, G. Travaglini, and C. Wen, Classical gravitational scattering from a gauge-invariant double copy, JHEP 10 (2021) 118, arXiv:2108.04216 [hep-th] .
- [230] A. V. Manohar, A. K. Ridgway, and C.-H. Shen, Radiated angular momentum and dissipative effects in classical scattering, Phys. Rev. Lett. 129 no. 12, (2022) 121601, arXiv:2203.04283 [hep-th] .

- [231] N. E. J. Bjerrum-Bohr, P. H. Damgaard, L. Plante, and P. Vanhove, The SAGEX review on scattering amplitudes Chapter 13: Post-Minkowskian expansion from scattering amplitudes, *Phys. A55* no. 44, (2022) 443014, arXiv:2203.13024 [hep-th] .
- [232] C. Dlapa, G. Kälin, Z. Liu, and R. A. Porto, Dynamics of binary systems to fourth Post-Minkowskian order from the effective field theory approach, *Phys. Lett. B* 831 (2022) 137203, arXiv:2106.08276 [hep-th] .
- [233] C. Dlapa, G. Kälin, Z. Liu, and R. A. Porto, Conservative dynamics of binary systems at fourth post-Minkowskian order in the large-eccentricity expansion, *Phys. Rev. Lett* 128 no. 16, (2022) 161104, arXiv:2112.11296 [hep-th] .
- [234] C. Dlapa, G. Kälin, Z. Liu, J. Neef, and R. A. Porto, Radiation reaction and gravitational waves at fourth post-Minkowskian order, *Phys. Rev. Lett.* 130(2023) 101401.
- [235] G. U. Jakobsen, G. Mogull, J. Plefka, and B. Sauer, Dissipative scattering of spinning black holes at fourth post-Minkowskian order, *Phys. Rev. Lett* 131 (Dec, 2023) 241402.
- [236] P. Di Vecchia, C. Heissenberg, R. Russo, and G. Veneziano, The gravitational eikonal: From particle, string and brane collisions to black-hole encounters, arXiv:2306.16488 [hep-th] .
- [237] L. Barack, T. Damour, and N. Sago, Precession effect of the gravitational self-force in a Schwarzschild spacetime and the effective one-body formalism, *Phys. Rev. D* 82 (2010) 084036, arXiv:1008.0935 [gr-qc] .
- [238] A. Nagar and S. Albanesi, Toward a gravitational self-force-informed effective-one-body waveform model for nonprecessing, eccentric, large-mass-ratio inspirals, *Phys. Rev. D* 106 no. 6, (2022) 064049, arXiv:2207.14002 [gr-qc] .
- [239] S. L. Detweiler, A consequence of the gravitational self-force for circular orbits of the Schwarzschild geometry, *Phys. Rev. D* 77 (2008) 124026, arXiv:0804.3529 [gr-qc] .
- [240] L. Barack and N. Sago, Beyond the geodesic approximation: conservative effects of the gravitational self-force in eccentric orbits around a Schwarzschild black hole, *Phys. Rev. D* 83 (2011) 084023, arXiv:1101.3331 [gr-qc] .
- [241] D. Bini and T. Damour, Analytical determination of the two-body gravitational interaction potential at the fourth post-Newtonian

- approximation, *Phys. Rev. D* 87 no. 12, (2013) 121501, arXiv:1305.4884 [gr-qc] .
- [242] T. Damour, F. Guercilena, I. Hinder, S. Hopper, A. Nagar, and L. Rezzolla, Strong-field scattering of two black holes: Numerics versus analytics, *Phys. Rev. D* 89 no. 8, (2014) 081503, arXiv:1402.7307 [gr-qc] .
- [243] M. van de Meent, Self-force corrections to the periapsis advance around a spinning black hole, *Phys. Rev. Lett.* 118 no. 1, (2017) 011101, arXiv:1610.03497 [gr-qc] .
- [244] S. E. Gralla and K. Lobo, Self-force effects in post-Minkowskian scattering, *Class. Quant. Grav.* 39 no. 9, (2022) 095001, arXiv:2110.08681 [gr-qc] .
- [245] O. Long and L. Barack, Time-domain metric reconstruction for hyperbolic scattering, *Phys. Rev. D* 104 no. 2, (2021) 024014, arXiv:2105.05630 [gr-qc] .
- [246] M. Khalil, A. Buonanno, J. Steinhof, and J. Vines, Energetics and scattering of gravitational two-body systems at fourth post-Minkowskian order, *Phys. Rev. D* 106 (Jul, 2022) 024042.
- [247] L. Barack and O. Long, Self-force correction to the deflection angle in black-hole scattering: A scalar charge toy model, *Phys. Rev. D* 106 no. 10, (2022) 104034, arXiv:2209.03740 [gr-qc] .
- [248] L. Barack, Z. Bern, E. Herrmann, O. Long, J. Parra-Martinez, R. Roiban, M. S. Ruf, C.-H. Shen, M. P. Solon, F. Teng, and M. Zeng, Comparison of post-minkowskian and self-force expansions: Scattering in a scalar charge toy model, *Phys. Rev. D* 108 (Jul, 2023) 024025, arXiv:2304.09200 [hep-th] .
- [249] C. Whittall and L. Barack, Frequency-domain approach to self-force in hyperbolic scattering, *Phys. Rev. D* 108 (Sep, 2023) 064017.
- [250] T. Adamo, A. Cristofoli, A. Ilderton, and S. Klisch, Scattering amplitudes for self-force, arXiv:2307.00431 [hep-th] .
- [251] C. R. Galley and B. L. Hu, Self-force on extreme mass ratio inspirals via curved spacetime effective field theory, *Physical Review D* 79 no. 6, (2009) .
- [252] S. Babak, J. Gair, A. Sesana, E. Barausse, C. F. Sopuerta, C. P. Berry, E. Berti, P. Amaro-Seoane, A. Petiteau, and A. Klein, Science with the space-based interferometer LISA. V. Extreme mass-ratio inspirals, *Physical Review D* 95 no. 10, (2017) .

- [253] C. P. L. Berry, S. A. Hughes, C. F. Sopuerta, A. J. K. Chua, A. He ernan, K. Holley-Bockelmann, D. P. Mihaylov, M. C. Miller, and A. Sesana, The unique potential of extreme mass-ratio inspirals for gravitational-wave astronomy, arXiv:1903.03686 [astro-ph.HE] .
- [254] M. van de Meent, Gravitational self-force on eccentric equatorial orbits around a Kerr black hole, Phys. Rev. D **94** (2016) 044034.
- [255] M. van de Meent, Gravitational self-force on generic bound geodesics in Kerr spacetime, Phys. Rev. D **97** (2018) 104033.
- [256] A. Pound, B. Wardell, N. Warburton, and J. Miller, Second-order self-force calculation of gravitational binding energy in compact binaries, Physical Review Letters **124** no. 2, (2020) .
- [257] N. Warburton, A. Pound, B. Wardell, J. Miller, and L. Durkan, Gravitational-wave energy flux for compact binaries through second order in the mass ratio, Physical Review Letters **127** no. 15, (2021) .
- [258] B. Wardell, A. Pound, N. Warburton, J. Miller, L. Durkan, and A. L. Tiec, Gravitational waveforms for compact binaries from second-order self-force theory, Physical Review Letters **130** no. 24, (2023) .
- [259] S. Mougiakakos and P. Vanhove, Schwarzschild-Tangherlini metric from scattering amplitudes in various dimension, Phys. Rev. D **103** no. 2, (2021) 026001, arXiv:2010.08882 [hep-th] .
- [260] T. Damour and G. Esposito-Farese, Testing gravity to second post-Newtonian order: A field theory approach, Phys. Rev. D **53** (1996) 5541–5578, arXiv:gr-qc/9506063 .
- [261] S. Chandrasekhar, The mathematical theory of black holes, vol. 69. Oxford university press, 1998.
- [262] F. J. Zerilli, Gravitational field of a particle falling in a Schwarzschild geometry analyzed in tensor harmonic, Phys. Rev. D **2** (1970) 2141–2160.
- [263] S. Detweiler and E. Poisson, Low multipole contributions to the gravitational self-force, Physical Review D **69** no. 8, (2004) .
- [264] L. M. Burko, Self-force on a particle in orbit around a black hole, Phys. Rev. Lett **84** (2000) 4529–4532.
- [265] M. J. Pfenning and E. Poisson, Scalar, electromagnetic, and gravitational self-forces in weakly curved spacetime, Phys. Rev. D **65** (Mar, 2002) 084001.

- [266] D. Kosmopoulos and M. P. Solon, Gravitational self force from scattering amplitudes in curved space, *JHEP* 03 (2024) 125, arXiv:2308.15304 [hep-th] .
- [267] D. G. Boulware and L. S. Brown, Tree graphs and classical electrodynamics, *Phys. Rev.* 172 (Aug, 1968) 1628–1631 <https://link.aps.org/doi/10.1103/PhysRev.172.1628>.
- [268] L. D. Landau and E. M. Lifschits, *The Classical Theory of Fields*, vol. 2 of *Course of Theoretical Physics*, Pergamon Press, Oxford, 1975.
- [269] P. H. Damgaard, L. Plante, and P. Vanhove, On an exponential representation of the gravitational S-matrix, *JHEP* 11 (2021) 213, arXiv:2107.12891 [hep-th] .
- [270] M. V. S. Saketh, J. Vines, J. Steinhilber, and A. Buonanno, Conservative and radiative dynamics in classical relativistic scattering and bound systems, *Phys. Rev. Res.* 4, no. 1, (2022) 013127, arXiv:2109.05994 [gr-qc] .
- [271] Z. Bern, J. P. Gatica, E. Herrmann, A. Luna, and M. Zeng, Scalar QED as a toy model for higher-order effects in classical gravitational scattering, *JHEP* 08 (2022) 131, arXiv:2112.12243 [hep-th] .
- [272] A. Sommerfeld, The fine structure of Hydrogen and Hydrogen-like lines, *The European Physical Journal* 39 (1916) 179–204.
- [273] C. Dlapa, G. Kälin, Z. Liu, and R. A. Porto, Bootstrapping the relativistic two-body problem, *JHEP* 08 (2023) 109, arXiv:2304.01275 [hep-th] .
- [274] D. Zwanziger, Local-Lagrangian quantum field theory of electric and magnetic charges, *Phys. Rev. D* 3 (Feb, 1971) 880–891.
- [275] U. Kol, D. O'Connell, and O. Telem, The radial action from probe amplitudes to all orders, *JHEP* 03 (2022) 141, arXiv:2109.12092 [hep-th] .
- [276] C. Cheung, N. Shah, and M. P. Solon, Mining the geodesic equation for scattering data, *Phys. Rev. D* 103 (Jan, 2021) 024030.
- [277] A. I. Janis, D. C. Robinson, and J. Winicour, Comments on Einstein scalar solutions, *Phys. Rev.* 186 (Oct, 1969) 1729–1731.
- [278] J. D. Bekenstein, Exact solutions of Einstein conformal scalar equations, *Annals Phys.* 82 (1974) 535–547.
- [279] J. D. Bekenstein, Black holes with scalar charge, *Annals Phys.* 91 (1975) 75–82.

- [280] Z. Bern, J. J. Carrasco, W.-M. Chen, A. Edison, H. Johansson, J. Parra-Martinez, R. Roiban, and M. Zeng, Ultraviolet properties of $N = 8$ supergravity at two loops, *Phys. Rev. D* **98** no. 8, (2018) 086021, arXiv:1804.09311 [hep-th] .
- [281] Z. Bern, J. J. M. Carrasco, W.-M. Chen, H. Johansson, R. Roiban, and M. Zeng, Five-loop four-point integrand of $N = 8$ supergravity as a generalized double copy, *Phys. Rev. D* **96** no. 12, (2017) 126012, arXiv:1708.06807 [hep-th] .
- [282] Z. Bern, S. Davies, and T. Dennen, Enhanced ultraviolet cancellations in $N = 5$ supergravity at four loops, *Phys. Rev. D* **90** no. 10, (2014) 105011, arXiv:1409.3089 [hep-th] .
- [283] Z. Bern, S. Davies, T. Dennen, A. V. Smirnov, and V. A. Smirnov, Ultraviolet properties of $N = 4$ supergravity at four loops, *Phys. Rev. Lett.* **111** no. 23, (2013) 231302, arXiv:1309.2498 [hep-th] .
- [284] Z. Bern, S. Davies, T. Dennen, and Y.-t. Huang, Ultraviolet cancellations in half-maximal supergravity as a consequence of the double-copy structure, *Phys. Rev. D* **86** (2012) 105014, arXiv:1209.2472 [hep-th] .
- [285] Z. Bern, S. Davies, T. Dennen, and Y.-t. Huang, Absence of three-loop four-point divergences in $N = 4$ supergravity, *Phys. Rev. Lett.* **108** (2012) 201301, arXiv:1202.3423 [hep-th] .
- [286] Z. Bern, J. J. M. Carrasco, L. J. Dixon, H. Johansson, and R. Roiban, Simplifying multiloop integrands and ultraviolet divergences of gauge theory and gravity amplitudes, *Phys. Rev. D* **85** (2012) 105014, arXiv:1201.5366 [hep-th] .
- [287] Z. Bern, J. J. Carrasco, L. J. Dixon, H. Johansson, and R. Roiban, Amplitudes and Ultraviolet Behavior of $N = 8$ Supergravity, *Fortsch. Phys.* **59** (2011) 561–578, arXiv:1103.1848 [hep-th] .
- [288] J. J. M. Carrasco, Gauge and gravity amplitude relations, *Theoretical Advanced Study Institute in Elementary Particle Physics: Journeys Through the Precision Frontier: Amplitudes for Colliders*, pp. 477–557. WSP, 2015, arXiv:1506.00974 [hep-th] .
- [289] R. Monteiro and D. O'Connell, The kinematic algebra from the self-dual sector, *JHEP* **07** (2011) 007, arXiv:1105.2565 [hep-th] .
- [290] N. E. J. Bjerrum-Bohr, P. H. Damgaard, R. Monteiro, and D. O'Connell, Algebras for amplitudes, *JHEP* **06** (2012) 061, arXiv:1203.0944 [hep-th] .

- [291] C. Cheung and C.-H. Shen, Symmetry for flavor-kinematics duality from an action, *Phys. Rev. Lett.* 118 no. 12, (2017) 121601, arXiv:1612.00868 [hep-th] .
- [292] C. Cheung and J. Mangan, Covariant color-kinematics duality, *JHEP* 11 (2021) 069, arXiv:2108.02276 [hep-th] .
- [293] M. Ben-Shahar and H. Johansson, O-shell color-kinematics duality for Chern-Simons, *JHEP* 08 (2022) 035, arXiv:2112.11452 [hep-th] .
- [294] N. Moynihan, Massive covariant colour-kinematics in 3D, arXiv:2110.02209 [hep-th] .
- [295] C. Cheung and J. Mangan, Scattering amplitudes and the Navier-Stokes equation, arXiv:2010.15970 [hep-th] .
- [296] C. Cheung, J. Parra-Martinez, and A. Sivaramakrishnan, On-shell correlators and color-kinematics duality in curved symmetric spacetimes, arXiv:2201.05147 [hep-th] .
- [297] A. Herderschee, R. Roiban, and F. Teng, On the differential representation and color-kinematics duality of AdS boundary correlators, *JHEP* 05 (2022) 026, arXiv:2201.05067 [hep-th] .
- [298] A. Sivaramakrishnan, Towards color-kinematics duality in generic spacetimes, *JHEP* 04 (2022) 036, arXiv:2110.15356 [hep-th] .
- [299] P. Diwakar, A. Herderschee, R. Roiban, and F. Teng, BCJ amplitude relations for Anti-de Sitter boundary correlators in embedding space, *JHEP* 10 (2021) 141, arXiv:2106.10822 [hep-th] .
- [300] J. A. Farrow, A. E. Lipstein, and P. McFadden, Double copy structure of CFT correlators, *JHEP* 02 (2019) 130, arXiv:1812.11129 [hep-th] .
- [301] A. E. Lipstein and P. McFadden, Double copy structure and the flat space limit of conformal correlators in even dimensions, *Phys. Rev. D* 101 no. 12, (2020) 125006, arXiv:1912.10046 [hep-th] .
- [302] X. Zhou, Double copy relation in AdS space, *Phys. Rev. Lett.* 127 no. 14, (2021) 141601, arXiv:2106.07651 [hep-th] .
- [303] L. F. Alday, C. Behan, P. Ferrero, and X. Zhou, Gluon scattering in AdS from CFT, *JHEP* 06 (2021) 020, arXiv:2103.15830 [hep-th] .
- [304] S. Albayrak, S. Kharel, and D. Meltzer, On duality of color and kinematics in (A)dS momentum space, *JHEP* 03 (2021) 249, arXiv:2012.10460 [hep-th] .

- [305] C. Armstrong, A. E. Lipstein, and J. Mei, Color/kinematics duality in AdS_4 , *JHEP*02(2021)194,arXiv:2012.02059 [hep-th] .
- [306] L. F. Alday, V. Gonçalves, and X. Zhou, Supersymmetric ve-point gluon amplitudes in AdS space, *Phys. Rev. Lett*128 no. 16, (2022) 161601,arXiv:2201.04422 [hep-th] .
- [307] J. Hoppe, Di eomorphism groups, quantization a f d $^{11^0}$, *Int. J. Mod. Phys. A* (1989) 5235.
- [308] V. E. Zakharov and A. V. Mikhailov, Relativistically invariant two-dimensional models in eld theory integrable by the inverse problem technique. (In Russian)*Sov. Phys. JETP*7 (1978) 1017 1027.
- [309] C. Cheung, K. Kampf, J. Novotny, and J. Trnka, E ective eld theories from soft limits of scattering amplitudes, *Phys. Rev. Lett*114 no. 22, (2015) 221602,arXiv:1412.4095 [hep-th] .
- [310] C. Cheung, K. Kampf, J. Novotny, C.-H. Shen, and J. Trnka, On-shell recursion relations for e ective eld theories, *Phys. Rev. Lett*116 no. 4, (2016) 041601,arXiv:1509.03309 [hep-th] .
- [311] K. Hinterbichler and A. Joyce, Hidden symmetry of the Galileon, *Phys. Rev. D*92 no. 2, (2015) 023503,arXiv:1501.07600 [hep-th] .
- [312] N. Seiberg and E. Witten, String theory and noncommutative geometry, *JHEP*09(1999)032,arXiv:hep-th/9908142 .
- [313] E. G. Floratos and J. Iliopoulos, Gauge theories and non-commutative geometry, *Phys. Lett. B* 632 (2006) 566 570, arXiv:hep-th/0509055 .
- [314] E. Chacón, H. García-Compeán, A. Luna, R. Monteiro, and C. D. White, New heavenly double copies, *JHEP* 03 (2021) 247, arXiv:2008.09603 [hep-th] .
- [315] B. Hoare, N. Levine, and A. A. Tseytlin, On the massless tree-level S-matrix in 2d sigma models, *J. Phys. A*52 no. 14, (2019) 144005, arXiv:1812.02549 [hep-th] .
- [316] A. M. Polyakov, Gauge elds as rings of glues, *Nucl. Phys. B*164(1980) 171 188.
- [317] C. R. Nappi, Some properties of an analog of the nonlinear sigma model, *Phys. Rev. D*21 (1980) 418.
- [318] V. Del Duca, L. J. Dixon, and F. Maltoni, New color decompositions for gauge amplitudes at tree and loop level, *Nucl. Phys. B*571 (2000) 51 70, arXiv:hep-ph/9910563 .

- [319] B. Gabai, D. Mazáuc, A. Shieber, P. Vieira, and Y. Zhou, No particle production in two dimensions: recursion relations and multi-Regge limit, *JHEP*02(2019) 094,arXiv:1803.03578 [hep-th] .
- [320] Z. Bern, S. Davies, and J. Nohle, Double-copy constructions and unitarity cuts, *Phys. Rev. D*93 no. 10, (2016) 105015, arXiv:1510.03448 [hep-th] .
- [321] C. de Rham, M. Fasiello, and A. J. Tolley, Galileon duality, *Phys. Lett. B* 733(2014) 46 51,arXiv:1308.2702 [hep-th] .
- [322] C. De Rham, L. Keltner, and A. J. Tolley, Generalized Galileon duality, *Phys. Rev. D*90 no. 2, (2014) 024050,arXiv:1403.3690 [hep-th] .
- [323] H.-H. Chi, H. Elvang, A. Herderschee, C. R. T. Jones, and S. Paranjape, Generalizations of the double-copy: The KLT bootstrap, *JHEP* 03(2022) 077,arXiv:2106.12600 [hep-th] .
- [324] L. A. Johnson, C. R. T. Jones, and S. Paranjape, Constraints on a massive double-copy and applications to massive gravity, *JHEP*02(2021) 148, arXiv:2004.12948 [hep-th] .
- [325] A. Momeni, J. Rumbutis, and A. J. Tolley, Massive gravity from double copy, *JHEP*12(2020) 030,arXiv:2004.07853 [hep-th] .
- [326] T. Curtright and C. K. Zachos, Currents, charges, and canonical structure of pseudodual chiral models, *Phys. Rev. D*49 (1994) 5408 5421, arXiv:hep-th/9401006 .
- [327] P. D. Lax, Integrals of nonlinear equations of evolution and solitary waves, *Commun. Pure Appl. Math*21 (1968) 467 490.
- [328] N. Beisert, Introduction to integrability. <https://people.phys.ethz.ch/~nbeisert/lectures/Int-16HS-1/Notes.pdf> .
- [329] A. Torrielli, Lectures on classical integrability, *J. Phys. A*49 no. 32, (2016) 323001,arXiv:1606.02946 [hep-th] .
- [330] A. V. Mikhailov, ed., *Integrability*. Springer Heidelberg, Heidelberg, 2009.
- [331] V. E. Zakharov, ed., *What Is Integrability?* Springer Heidelberg, Heidelberg, 1991.
- [332] J. M. Evans, M. Hassan, N. J. MacKay, and A. J. Mountain, Local conserved charges in principal chiral models, *Nucl. Phys. B*561 (1999) 385 412, arXiv:hep-th/9902008 .

- [333] C. Devchand and J. Schiff, “Hidden symmetries of the principal chiral model unveiled,” *Commun. Math. Phys.* **190** (1998) 675–695, arXiv: hep-th/9611081.
- [334] P. Millington, F. Niedermann, and A. Padilla, “Non-perturbative aspects of Galileon duality,” *Eur. Phys. J. C* **78** no. 7, (2018) 546, arXiv: 1707.06931 [hep-th].
- [335] K. Kampf and J. Novotny, “Unification of Galileon dualities,” *JHEP* **10** (2014) 006, arXiv: 1403.6813 [hep-th].
- [336] J. E. Moyal, “Quantum mechanics as a statistical theory,” *Proc. Cambridge Phil. Soc.* **45** (1949) 99–124.
- [337] P. Fletcher, “The uniqueness of the Moyal algebra,” *Phys. Lett. B* **248** (1990) 323–328.
- [338] T. Damour and G. Schaefer, “Higher order relativistic periastron advances and binary pulsars,” *Nuovo Cim. B* **101** (1988) 127.